PLATELET ACTIVATION IN TRAUMA AND OTHER INFLAMMATORY CONDITIONS

By

Samantha J. Montague

A thesis submitted to the University of Birmingham for the degree of DOCTOR OF PHILOSOPHY

Institute of Cardiovascular Sciences

College of Medical and Dental Sciences

University of Birmingham

September 2016

Abstract

Platelets play critical roles in thrombosis, inflammation, and wound healing, which are essential in response to trauma. These processes are primarily driven through the immunoreceptor tyrosine-based activation motif (ITAM)-containing receptors, glycoprotein VI (GPVI) and C-type lectin-like receptor 2 (CLEC-2). This study aimed to investigate; (i) the effects of Alarmins released following trauma on platelet reactivity and the mechanisms involved; (ii) establish whether soluble GPVI (sGPVI), a platelet activation marker is elevated in trauma and other inflammatory conditions; (iii) determine whether the CLEC-2 ligand, podoplanin, is elevated in inflammatory conditions and (iv) establishing the role of GPVI and platelets in cutaneous wound healing.

The nuclear-related Alarmin, histones, induced robust platelet activation both *in vitro* and *in vivo*. Histone-induced platelet activation was mediated through GPVI *in vitro* However, this pathway was found not to underlie histone-induced lowering of platelet count *in vivo* and is most likely to result from mediators released following vascular damage. GPVI shedding was shown to be induced following activation by thrombin, through a pathway dependent on fibrin generation. sGPVI was found to be a marker for platelet activation during a variety of inflammatory disorders, notably in association with sepsis. Furthermore, GPVI shedding reflects platelet activation by collagen and potentially thrombin-induced fibrin generation.

Publications arising from this thesis

Alshehri OM, Hughes CE, **Montague S,** Watson SK, Frampton J, Bender M, Watson SP (2015). Fibrin activates GPVI in human and mouse platelets. *Blood*. Sept 24;126(13):1601-8.

Alshehri OM, **Montague S**, Watson S, Carter P, Sarker N, Manne BK, Miller JL, Herr AB, Pollitt AY, O'Callaghan CA, Kunapuli S, Arman M, Hughes CE, Watson SP (2015). Activation of glycoprotein VI (GPVI) and C-type lectin-like receptor-2 (CLEC-2) underlies platelet activation by diesel exhaust particles and other charged/hydrophobic ligands. *Biochem J.* Jun 15;468(3):459-73.

Gitz E, Pollitt AY, Gitz-Francois JJ, Alshehri O, Mori J, **Montague S,** Nash GB, Douglas MR, Gardiner EE, Andrews RK, Buckley CD, Harrison P, Watson SP (2014) CLEC-2 expression is maintained on activated platelets and on platelet microparticles. *Blood.* Oct 2;124(14):2262-70.

Book chapter

Rayes J, Hardy AT, Lombard SE, **Montague SJ**, Watson SP and Lowe KL (2015). The role of CLEC-2 in and beyond the vasculature. *Platelets in Thrombotic and Non-thrombotic Disorders- Pathophysiology, Pharmacology and Therapeutics***.** (Book chapter - in press).

Acknowledgements

I would firstly like to thank my supervisor Steve Watson for allowing me to complete this PhD and for all the support and research opportunities given over the four years. Thanks also goes to the National institute for Health Research Surgical Reconstruction and Microbiology Research Centre (NIHR SRMRC) for funding my PhD. I would like to thank Paul Harrison, Elizabeth Gardiner and my second supervisor Gerrard Nash for valuable discussions, advice and support given throughout the PhD. I would to thank all external collaborators for helpful discussions advice and reagents given. A special thanks is for Johan Heemskerk at Maastricht University for allowing me to complete three valuable months of research in his lab and to all his lab members who were welcoming and supportive during my stay. I would also like to thank all of the clinicians that have helped in patient requirement and access to samples, including everyone involved with the Healing Foundation and David Thickett's group at the Queen Elizabeth Hospital. I would like to thank Tariq Iqbal for all his help in patient recruitment and valuable discussions. Thanks also needs to go to the [redacted] Biomedical Services Unit for all their guidance and support with animal work.

I would particularly like to give a great deal of thanks to all members of the Watson group and Birmingham platelet group over the four years, for providing great levels of support, kindness, laughter and cake. In particular I would like to thank Julie, Kate and Natalie for super helpful discussions, advice, support and being amazing people to look up to. I would like to give a great deal of thanks to Stef, Beata and Gayle for all their help over the years. I would like to thank Craig, Neil and Steve T for their help and great lunch time discussions. To all my fellow students, I would like to give a great deal of thanks for making the lab such a fun place to work and for all the fun had outside of the lab as well, in particular Steph and Ben for putting up with me for the whole four years and Alex, Kieran and Rob for keeping me sane (ish) in the final year.

Outside of the lab, I would like to thank all my friends for letting me escape from Birmingham now and then and providing me with tea or cider and listening to PhD chat. Most importantly, I would like to thank all my family, especially my parents for all the support over the years. I could not have done it without you all.

TABLE OF CONTENTS

LIST OF FIGURES

CHAPTER 1

CHAPTER 3

CHAPTER 4

CHAPTER 5

CHAPTER 6

LIST OF Tables

CHAPTER 1

CHAPTER 2

CHAPTER 3

CHAPTER 4

Abbreviations

ACD	Acid citrate dextrose
ADAM	A disintegrin and metalloproteinases
ADP	Adenosine diphosphate
AGE	Advanced Glycation Endproducts
ARDS	Acute respiratory distress syndrome
ATP	Adenosine triphosphate
BSA	Bovine serum albumin
cAMP	cyclic adenosine monophosphate
cGMP	Cyclic guanosine monophosphate
CLEC-2	C-type lectin-like receptor 2
CRD	C-terminal carbohydrate-like recognition domain
CRP	Collagen-related peptide
CRP	C-reactive protein
Csk	c-Src kinase
CTH	Calf thymus histones
CTLD	C-type lectin-like domain
DAMPs	Danger associated molecular pattern molecules
DCs	Dendritic cells
DC-SIGN	Dendritic Cell-Specific Intercellular adhesion molecule-3-Grabbing Non-integrin
DNA	Deoxyribonucleic acid
DVT	Deep vein thrombosis
ECM	Extracellular matrix
EDF	Epidermal growth factor
EDTA	Ethylenediaminetetraacetic acid
ELISA	Enzyme-linked immunosorbent assay
EMMPRIN	Extracellular matrix metalloproteinase inducer
ETOH	Ethanol
FBS	Fetal bovine serum

FcRγ-chain	Fc receptor common γ-chain
FPR1	Formyl peptide receptor
FRCs	Fibroblastic reticular cells
GM-CSF	Granulocyte-macrophage colony-stimulating factor
GPCRs	G protein-coupled receptors
GPO	Glycine-proline-hydroxyproline
GPRP	Gly-Pro-Arg-Pro
GPV	Glycoprotein V
GPVI	Glycoprotein VI
H&E	Hematoxylin and eosin
HC	Healthy controls
HSC	Haematopoietic stem cell
HEK-293T	Human embryonic kidney cells
HIT	Heparin induced thrombocytopenia
HIV	Human immunodeficiency virus
HMGB-1	High-mobility-group-box-1
HRP	Horseradish peroxidase
HSPR	Heat shock protein receptors
IBD	Inflammatory bowel disease
IDA	Iron deficiency anaemia
Ig	Immunoglobulin
IHC	Immunohistochemistry
IP	Immunoprecipitation
IP3	Inositol-1,4,5-trisphosphate
IRAG	IP3R-associated cGMP kinase substrate
Iso	Isotype
ITAM	Immunoreceptor tyrosine-based activation
ITIM	Immunoreceptor tyrosine-based inhibitory motif
ITU	Intensive care unit
kD/ kDa	Kilodalton
LAT	Linker for activation of T-cells

LECs	Lymphatic endothelial cells
LPS	Lipopolysaccharide
mAb	Monoclonal antibody
M-CSF	Macrophage colony-stimulating factor
MMPS	Matrix metalloproteinases
MOF	Multi-organ failure
MS	Multiple sclerosis
MtDNA	Mitochondrial DNA
NEM	N-ethylmaleimide
NETs	Neutrophil Extracellular Traps
NHEKs	Normal human epidermal keratinocytes
NO	Nitric Oxide
OCS	Open canalicular system
OxLDL	Oxidised low density lipoprotein
PAMPs	Pathogen associated molecular pattern molecules
PARs	Protease-activated receptors
PAS	Protein A Sepharose
PBMC	Peripheral blood mononuclear cells
PBS	Phosphate-buffered saline
PDGF	Platelet-derived growth factor
PECAM-1	Platelet endothelial adhesion molecule-1
PF4	Platelet factor-4
PFA	Paraformaldehyde
PGI_2	Prostacyclin
PGS	Protein G Sepharose
PIP2	PLCγ2 hydrolyses phosphatidylinositol-4,5 bisphosphate
PKA	Protein kinase A
PKC	Protein kinase C
PLAG domain	Platelet-aggregation stimulating domain
PLCγ2	Phospholipase Cγ2
PPP	Platelet Poor Plasma

PRP	Platelet-Rich-Plasma
PRRs	Pattern recognition receptors
PS	Phosphatidylserine
RA	Rheumatoid arthritis
RAGE	Receptor for Advanced Glycation Endproducts
RBCs	Red blood cells
Rho	Rhodocytin
rpA	Reverse passive Arthus reaction
rPdpn	Recombinant human podoplanin
RT	Room temperature
sCLEC-2	Soluble CLEC-2
SDF-1	Stromal cell-derived factor-1
SFKs	Src family kinases
sGPVI	Soluble GPVI
SHIP	Src homology 2 (SH2) domain–containing inositol-5-phosphatase-1
SIRS	Systemic inflammatory response syndrome
SLP-76	SH2 domain containing leukocyte protein of 76
sP-selectin	Soluble P-selectin
sRAGE	Soluble RAGE
TGF-β	Transforming-growth factor-β
TLRs	Toll-like Receptors
TLT-1	TREM-like transcript 1
TPO	Thrombopoietin
TxA_2	Thromboxane
UC	Ulcerative colitis
VASP	Vasodilator stimulated phosphoprotein
VEGF	Vascular endothelial growth factor (VEGF
vWF	von Willebrand Factor
WB	Western Blot
WT	Wild-type

CHAPTER 1

GENERAL INTRODUCTION

1.1 Platelet physiology

1.1.1 The physiological role of platelets

Platelets are small anucleate cells with a primary role in haemostasis. Under physiological conditions, platelets circulate in the vascular system in a resting state unable to interact with the endothelium. Their small size (1-3μm) and margination by red blood cells (RBCs), allows platelets to make continual contact with vascular endothelial cells and thereby detect any injury that occurs. Following endothelial injury, platelets respond quickly to form a haemostatic plug. Platelets contain numerous surface receptors, signalling proteins and granule contents which mediate robust activation through contact and interactions with sub-endothelial matrix proteins exposed after vascular damage (Li et al., 2010).

Platelet aggregation leads to vascular plug formation at injury sites in blood vessels. However, pathological platelet activation, such as at sites of diseased endothelium, can result in a range of thrombotic disorders, including atherosclerosis, sepsis, myocardial infarction and stroke (Lindemann et al., 2007, Claushuis et al., 2016, Nieswandt et al., 2005). In recent years, platelets have also been shown to have important roles in inflammation (Engelmann and Massberg, 2013) and maintenance of vascular integrity (Lee et al., 2007, Gros et al., 2014, Gros et al., 2015b). An overview of platelet function, activation and roles in thrombosis and inflammation will be discussed in the following sections.

1.1.2 Platelet production

The life-span of human platelets is approximately 8-10 days, unless they undergo activation when they are removed by the reticuloendothelial system (Fritz et al., 1986). There is a constant requirement for platelets to maintain a circulating level of 150-450x10^9 platelets per litre.

Platelets, along with all other circulating blood cells, arise from haematopoietic stem cells (HSC) located in the bone marrow. Figure 1.1 shows the origin of the various of blood cells. Platelets result from megakaryocyte maturation, differentiated from common myeloid progenitor cells (Patel et al., 2005). The cytokine, thrombopoietin (TPO) and its receptor c-Mpl play a critical role in megakaryocyte differentiation, with a variety of other transcription factors also having regulatory roles (Johnson et al., 2016, Kaushansky, 2005). Megakaryocytes form pro-platelets processes that extend into the vasculature and release platelets into the circulation (Kaushansky, 2005) .

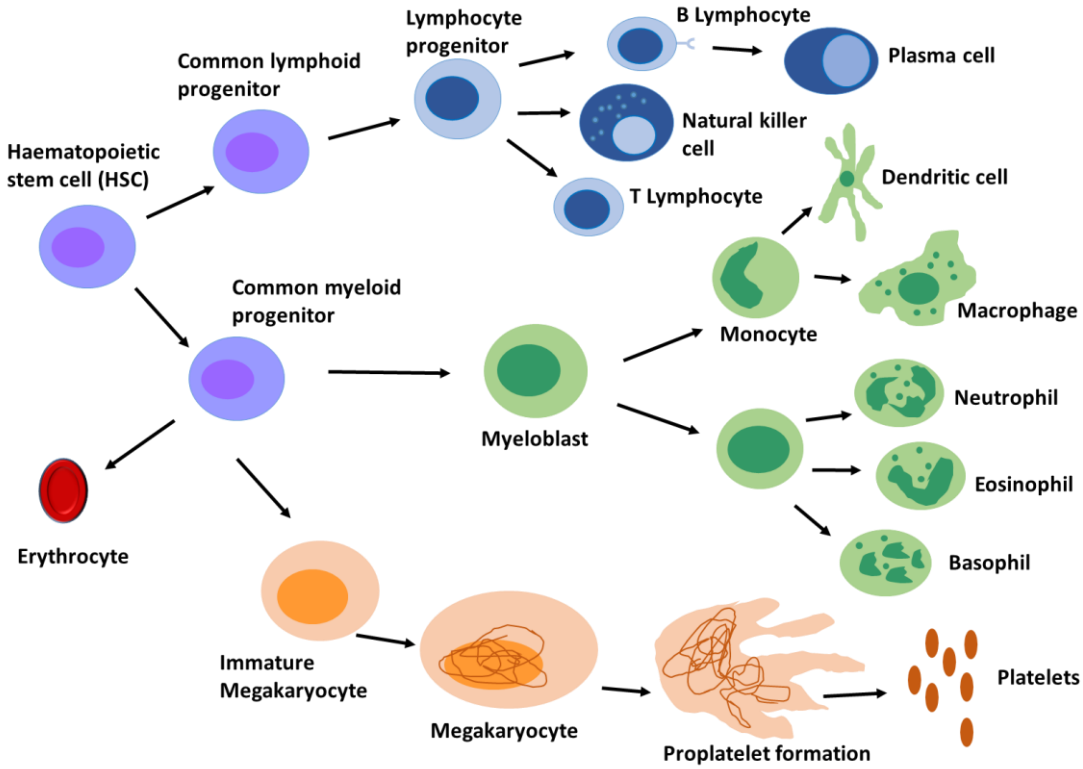

Figure 1.1. Haematopoietic stem cell lineages. Lineages of different derived blood cells arising from the haematopoietic stem cells (HSC) in the bone marrow. Figure based on (Kondo et al., 2003, Johnson et al., 2016).

1.1.3 Platelet anatomy

Because platelets are anucleate, they have a very limited ability to undergo *de novo* protein synthesis and consequently nearly all organelles, proteins and protein granule contents are synthesised in the precursor megakaryocyte. Platelets do however have the ability to uptake plasma proteins, such as fibrinogen. Platelets have actin cytoskeleton and microtubule systems supporting the plasma membrane and undergo marked structural changes during platelet activation and spreading (Calaminus et al., 2008, Hartwig, 1992). The platelet membrane contains the open canalicular system (OCS), which is a network of invaginations, important for increasing platelet surface area available for granule content release. The dense tubular system is also contained in the OCS, which is involved in Ca^{2+} storage and is the location of cyclooxygenase-1 (Cox-1), an important enzyme involved in thromboxane A_2 (TxA_2) production. Another important component of the plasma membrane is phosphatidylserine (PS). This is held on the cytosolic side of the membrane by flippases until periods of activation and apoptosis, where it is exposed on the extracellular side. Once exposed, PS provides a procoagulant surface for thrombin generation to occur, facilitating fibrin generation through the coagulation cascade.

Platelets contain secretory vesicles in the cytoplasm including α-granules, lysosomes and dense granules. Once platelets are activated, the granular contents are rapidly released. These granular contents include a variety of proteins, which have various functional roles, from promoting platelet activation feedback; recruiting new platelets and helping with thrombus generation, attracting leukocytes and facilitating repair at areas of damage. Table 1.1 shows the various contents of α-granules and dense granules

and their functional roles. Deficiencies in granule number, contents or ability to release their contents result in mild to severe abnormalities leading to bleeding disorders, such as grey-platelet syndrome (Raccuglia, 1971, Deppermann et al., 2013), Hermansky-Pudlak syndrome (Hermansky and Pudlak, 1959) and platelet storage pool deficiencies (Bolton-Maggs et al., 2006). A wide variety of receptors and other proteins are located at the platelet membrane, which will be discussed in Section 1.3-1.4.

Table 1.1. Example contents of platelet α- and dense granules and their functional roles. Main contents of α- and dense granules, including their function and roles.

α-granules			dense granules		
Function	**Contents**	**Role**	**Function**	**Contents**	**Role**
Adhesion proteins	Fibrinogen von Willebrand Factor (vWF)	Platelet aggregation and thrombus formation	**Feedback mediators**	ADP ATP Ca^{2+} 5-HT (serotonin)	Feedback mediators involved in platelet aggregation and thrombus growth
Chemokines	Platelet factor-4 (PF4) SDF-1	Leukocyte recruitment	**Polyphosphates**	Poly-P	
Growth factors	PDGF EGF VEGF	Wound repair and angiogenesis			
Membrane protein	P-selectin	Leukocyte binding			

1.2 Thrombus formation

1.2.1 Platelet activation and thrombus formation

Thrombus formation involves multiple processes and signalling events after platelet adhesion and activation at damaged areas. Upon endothelium damage collagen fibres in the sub-endothelial matrix become exposed. Platelets then adhere to the exposed sub-endothelial matrix and undergo activation. This leads to further platelet recruitment, thrombus formation and wound occlusion (Li et al., 2010). Several stages leading to thrombus formation are detailed below and in Figure 2.1

1) **Collagen exposure and tethering**

Under conditions of low shear stress, the platelet integrin α2β1 binds to exposed collagen fibres with a low rate of association. It remains unclear as to what extent this requires platelet activation and inside-out activation of the integrin. At high stress this association is not adequate to tether the platelets to the endothelial surface. However, upon vascular damage exposed collagen fibres become coated with von Willebrand factor (vWF), which allows interactions to occur with the GPIb-IX-V receptor on the platelet surface, leading to initial platelet capture, known as tethering. The fast on-off rate of association and dissociation of GPIb-IX-V receptor to vWF is however, not sufficient for stable adhesion, therefore platelets roll along the endothelium in the direction of blood flow (Offermanns, 2006).

2) **Stable adhesion**

Stable platelet adhesion is required for the initiation of thrombus formation. Platelet tethering to vWF allows the collagen fibres to become in close proximity to the major

collagen receptor glycoprotein VI (GPVI), resulting in platelet activation. The integrins αIIbβ3 and α2β1 are then converted into their active form, leading to greater interactions with vWF and collagen, respectively, establishing stable adhesion.

3) **Spreading and secretion**

Once platelets become activated their morphology changes from discoid to fully spread. Actin polymerisation following activation results in formation of filopodia and lamellipodia, which in turn leads to stronger platelet attachment to exposed collagen and vWF, as the platelet surface area is increased. Consequently, actin stress fibres are formed providing support for aggregate formation (Calaminus et al., 2008). GPVI and integrin activation leads to secretion of α- and dense granule contents, including the feedback messengers, adenosine diphosphate (ADP) and thromboxane (TxA_2), which mediate further activation and aggregation (Watson and Harrison, 2007). Release of α-granule contents, including the adhesion proteins, fibrinogen and vWF, further supports platelet capture supporting aggregation.

4) **Thrombus growth**

For thrombus growth, circulating platelets are recruited after pronounced platelet activation and secretion, promoting the growth of the thrombus. Platelet activation is further reinforced through thrombin generation through activation of the coagulation cascade. Platelets provide a pro-coagulant surface for thrombin generation, in turn leading to more platelet activation. Moreover, the thrombin generated converts fibrinogen into fibrin, which provides a network for thrombus stabilisation leading to effective wound occlusion at the site of injury (Renne et al., 2005).

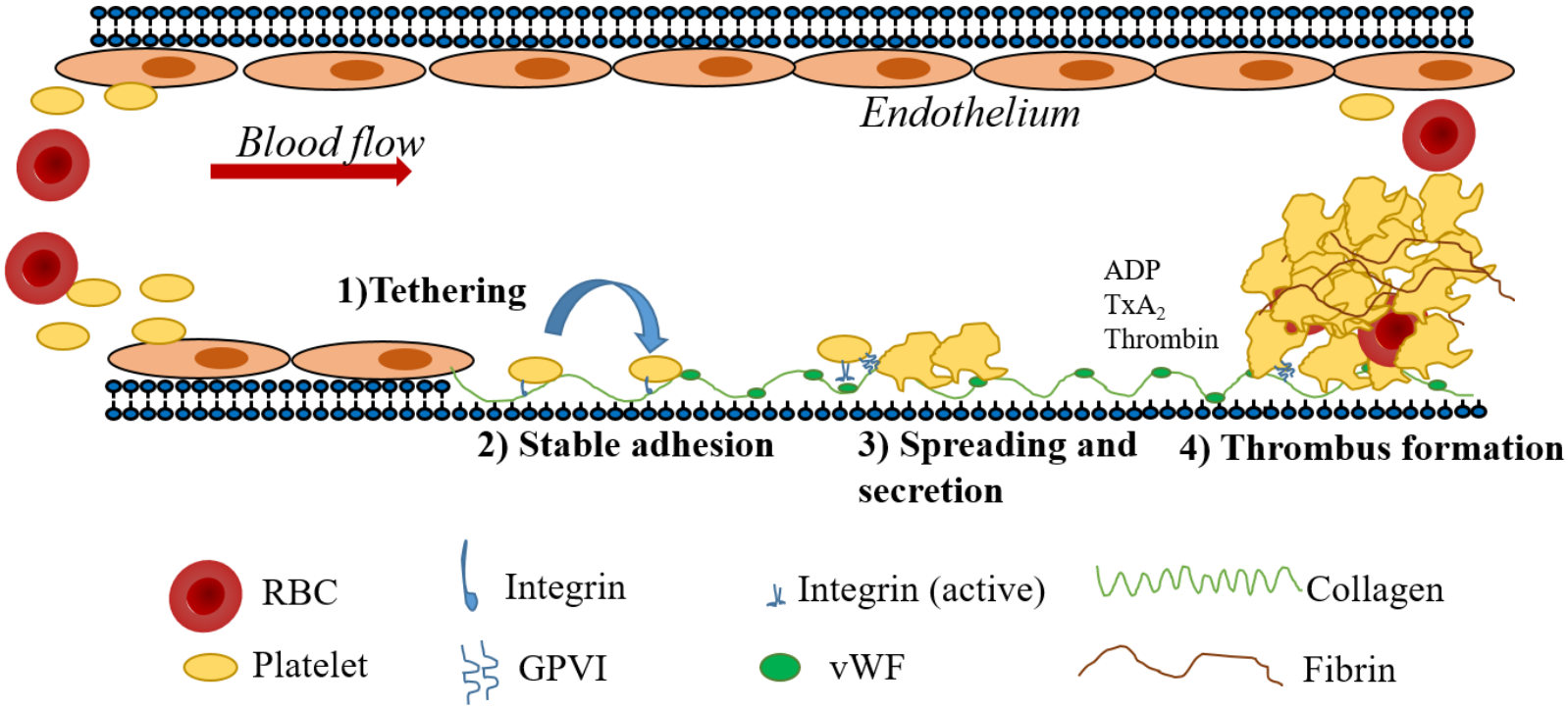

Figure 1.2. Processes of thrombus formation. 1) Platelets are marginated to blood vessel walls by red blood cells (RBCs) in the direction of blood flow. Platelets tether to vessel wall through weak interactions of GPIb-IX-V and von Willebrand factor (vWF). 2) Tethering of platelets allows GPVI and exposed collagen to become close and lead to stable adhesion through integrin activation. 3) Platelets are active and spread, releasing granule contents. 4) Released mediators promote thrombus growth, by recruiting more platelets. Thrombin converts fibrinogen to fibrin which stabilises the thrombus.

1.3 Platelet activation and signalling

Platelet receptors signal through various mechanisms leading to Ca^{2+} mobilisation and functional effects, such as secretion of granule contents. Platelet receptor activation can also result in the initiation of positive feedback mechanisms and inhibitory mechanisms to regulate platelet function. The next sections will describe the different platelet receptors and signalling mechanisms that are essential for platelet function and activation, including feedback mechanisms.

1.3.1 G protein-coupled receptors (GPCRs)

G protein-coupled receptors (GPCRs) are a family of seven transmembrane domain receptors that couple with heterotrimeric G proteins (α, β and γ) and have major roles in enhancing platelet activation through positive feedback mechanisms. GPCRs can bind a number of agonists released from platelet granules and endothelial cells in response to endothelial damage to enhance platelet activation. ADP is released both from damaged endothelial cells and platelet granules after activation and binds to $P2Y_1$ and $P2Y_{12}$, which are G_q- and $G_{i/z}$-coupled receptors. $P2Y_1$ and $P2Y_{12}$ receptors, give synergy with other receptors leading to enhancement of secretion and results in powerful aggregation (Dawood et al., 2007). $P2Y_1$ receptor interactions are implicated in Ca^{2+} mobilisation leading to shape change. Furthermore, ADP activation of $P2Y_{12}$ inhibits cyclic adenosine monophosphate (cAMP) formation. This blocks the cAMP inhibitory action and allows platelet activation to proceed (see section 1.3.4). ADP also can bind to $P2X_1$, an ATP-gated Ca^{2+} ion channel. Although activation is sufficient to cause only weak aggregation, it can enhance platelet response to other agonists (Murugappa and Kunapuli, 2006). TxA_2 is released from stimulated platelets (it is made *de novo* by the

action of Cox-1) and induces platelet activation through G_q-and $G_{12/13}$ coupled thromboxane receptors, TPα and TPβ (Li et al., 2010).

1.3.2 Protease-activated receptors (PARs)

Protease-activated receptors (PARs) are GPCRs. Unlike other GPCR receptors, in which activation is mediated through direct ligand binding, PAR activation occurs by proteinases that cleave the amino terminus of the receptor to unmask the N-terminal 'tethered ligand'. This remains attached and leads to activation and signalling (Adams et al., 2011, Gieseler et al., 2013). PAR-1 and PAR-4 are the PAR receptors in human platelets, whereas PAR-3 and PAR-4 are the important ones in mice platelets. Thrombin cleaves PAR1 and 4 at specific extracellular N-terminus recognition sites inducing activation (Gieseler et al., 2013).

1.3.3 Integrins

Integrins are important for allowing stable platelet adhesion and aggregation for thrombus formation. Integrin $\alpha_{IIb}\beta_3$ is highly expressed with a copy number of approximately 80,000 per human platelet. $\alpha_{IIb}\beta_3$ is a heterodimer formed of α and β subunits. The extracellular domain of the β3 subunit contains an RGD sequence and a second binding site for fibrinogen (Bennett, 2005). Src family kinases (SFKs) associate constitutively with the β3 cytosolic tail (Arias-Salgado et al., 2005). Following platelet activation by ligand binding to other receptors, 'inside-out' signalling occurs. This, results in conformational changes of $\alpha_{IIb}\beta_3$, increasing its affinity for ligands such as fibrinogen and vWF. Binding of its ligands then mediates 'outside-in' signalling. This signalling mechanism involves proteins that are also involved in platelet activation by immunoreceptor tyrosine-based activation motif (ITAM) receptors (Zhi et al., 2013).

1.3.4 Inhibition of platelet activation

Inhibitory mechanisms are in place to prevent platelet activation on the intact endothelium. An important inhibitory mechanism is through generation of the membrane permeable gas, nitric oxide (NO); which has a short half-life and is continuously synthesised by endothelial cells through nitric oxide synthase (NOS) (Pacher et al., 2007, Naseem and Riba, 2008). Guanylyl cyclase is activated by NO resulting in formation of cyclic guanosine monophosphate (cGMP) which inhibits platelet activation (Feil et al., 2003). Platelets are also inhibited when endothelial cells release prostaglandin I_2 (PGI_2). PGI_2 interacts with the platelet G protein-coupled PGI_2 receptor coupled to Gαs, causing activation, and accumulation of cAMP (Raslan and Naseem, 2015). cAMP and cGMP activates protein kinase A (PKA) and protein kinase G (PKG) respectively, leading to further phosphorylation of targeted platelet proteins, such as Rap1b and vasodilator stimulated phosphoprotein (VASP) (Francis et al., 2010, Wentworth et al., 2006). PKG also phosphorylates the IP_3 receptor-associated cGMP kinase substrate (IRAG), which is in complex with PGK-1 and the IP_3 receptor (Schlossmann et al., 2000). IP_3- induced Ca^{2+} release is inhibited by the phosphorylation of IRAG and PKG-1. Another inhibitory mechanism by action of endothelial cells is through CD39. This is an enzyme which hydrolyses adenosine triphosphate (ATP) and ADP, which in turn prevents them from activating platelets through the feedback mechanisms (Glenn et al., 2008).

Platelets also express inhibitory receptors that contain an immunoreceptor tyrosine-based inhibitory motif (ITIM). These include platelet endothelial adhesion molecule-1 (PECAM-1) (Dhanjal et al., 2007), G6b-B (Mori et al., 2008, Mazharian et al., 2012),

TREM-like transcript 1 (TLT-1) (Washington et al., 2002) and carcinoembryonic antigen-related cell adhesion molecule (CEACAM-1) (Wong et al., 2009). Proteins containing ITIMs provide docking sites for Src homology 2 (SH2) domain–containing inositol-5-phosphatase-1 (SHIP-1), SH2 domain–containing protein-tyrosine phosphatases 1 and 2 (SHP1 and SHP2) and c-Src kinase (Csk). The two inhibitory phosphatases SHP1 and SHP2 dephosphorylate key proteins in platelet activation pathways (Senis, 2013). G6b-B is constitutively phosphorylated and inhibits constitutive tyrosine kinase signalling by the ITAM-containing receptors, GPVI and CLEC-2 (Mori et al., 2008).

1.4 ITAM signalling

An ITAM is a conserved sequence of amino acids, Yxx(L/I)x6-12Yxx(L/I), important for signal transduction in a range of immune and platelet receptors. ITAMs are found in T- cells and B-cell antigen receptors, and various Fc receptors, including FcγRI and FcγRIIA (Daeron, 1997). ITAMs play a critical role in the activation of Syk family kinases, Syk and Zap-70 (Mócsai et al., 2010).

1.4.1 The GPVI -Fc receptor γ-chain complex

GPVI is a type 1 transmembrane receptor of the immunoglobulin (Ig) superfamily (Clemetson et al., 1999). GPVI is expressed on megakaryocytes and platelets and is recognised as the major signalling receptor for collagen on platelets. There are between 3700-9300 GPVI copies on the platelet surface (Burkhart et al., 2012, Best et al., 2003). On resting platelets, GPVI is predominately in the monomeric form, with the dimeric form increasing after activation (Jung et al., 2012, Loyau et al., 2012). GPVI is found in

association with the Fc receptor common γ-chain (FcRγ-chain), which contains one copy of an ITAM. The GPVI and FcRγ-chain complex was first identified by Gibbins *et al.* (1997) with further studies confirming its role as a collagen receptor in transfected cell lines using a NFAT-reporter assay (Tomlinson et al., 2007, Gibbins et al., 1997).

GPVI activation and clustering leads to tyrosine phosphorylation of the FcRγ-chain by SFKs, including Fyn, Lyn and Src (Severin et al., 2012). Fyn and Lyn associate through their SH3 domains to a poly-proline region of the GPVI cytoplasmic tail (Suzuki-Inoue et al., 2002). SFK phosphorylation of FcRγ chain provides a docking site for the SH2 domains of spleen tyrosine kinase (Syk). Syk binds to the phosphorylated ITAM and leads to a signalling cascade through proteins including adaptor proteins, such as the linker for activation of T-cells (LAT) as shown in Figure 1.3. LAT phosphorylation leads to the formation of a signalosome, which binds adaptor proteins Grb2 (growth factor receptor bound protein 2) and Gads (Grb2 related adaptor protein downstream of Shc), along with phospholipase C (PLC)γ2. The binding of these proteins allows the recruitment of SLP-76 (SH2 domain containing leukocyte protein of 76 kD), leading to PLCγ2 activation and Ca^{2+} mobilisation (Nieswandt and Watson, 2003). Once activated PLCγ2 hydrolyses phosphatidylinositol-4,5 bisphosphate (PIP2). Two second messengers, inositol-1,4,5-trisphosphate (IP3) and 1,2-diacylglycerol (DAG) mediate Ca^{2+} release from intracellular stores and activation of protein kinase C (PKC), respectively.

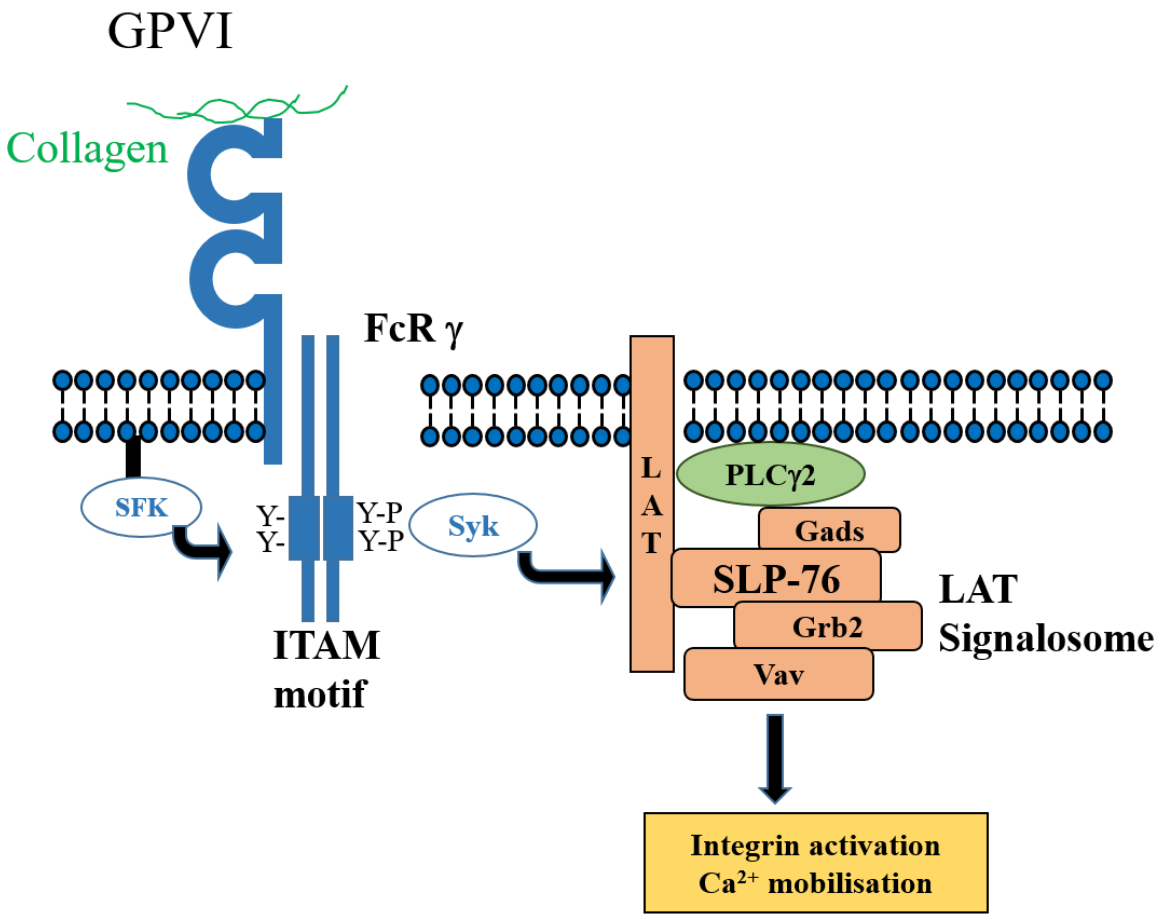

Figure 1.3. Schematic of GPVI signalling mechanism. GPVI signalling cascade after stimulation with collagen, involving ITAM FcRγ-chain and the formation of the LAT signalosome leading to integrin activation, Ca^{2+} mobilisation and platelet activation. SFK: Src family kinases, ITAM: immunoreceptor tyrosine-based activation motif.

1.4.1.1 GPVI agonists

GPVI is the major platelet receptor for collagen. Collagen contains glycine-proline-hydroxyproline (GPO) helical peptide chains that activate GPVI (Knight et al., 1999). Synthetic peptides, including collagen-related peptide (CRP) have been developed which mimic collagen activity by containing GPO repeats (Smethurst et al., 2007). GPVI is activated by a number of different endogenous ligands, including laminin and extracellular matrix metalloproteinase inducer (EMMPRIN) and other synthetic/exogenous ligands (Inoue et al., 2006, Seizer et al., 2009, Alshehri et al., 2015b). GPVI can also be activated by antibodies, including JAQ1 (Nieswandt et al., 2001) and snake venom toxins such as alborhagin, convulxin and crotarhagin (Jandrot-Perrus et al., 1997, Polgar et al., 1997).

Activation of GPVI by collagen or other GPVI agonists mentioned above is an important process in platelet adhesion and aggregation and can also lead to metalloproteolytic shedding. Deficiencies in GPVI, such as mice lacking GPVI and the FcRγ chain leads to defects in both adhesion and aggregation (Poole et al., 1997). Furthermore, mice treated with an anti-GPVI antibody to deplete GPVI display reduced thrombus formation *in vivo* using the ferric chloride injury model and with low laser injury (Nieswandt et al., 2001, Dubois et al., 2007). Patients with either partial or full GPVI deficiency are extremely rare, usually presenting with mild mucous membrane and skin bleeding. In addition, their platelets show no aggregation response to collagen or CRP (Matus et al., 2013, Arthur et al., 2007). GPVI is also critical for maintenance of vessel wall integrity at sites of inflammation by sealing areas of neutrophil-mediated vascular damage, to reduce blood leakage (Boulaftali et al., 2013, Gros et al., 2015a).

1.4.2 FcγRIIa

Another important platelet ITAM receptor, lacking in the rodent genome, is FcγRIIA (also known as CD32A). FcγRIIA a low affinity IgG receptor, belonging to the Fc family of receptors, which interact with IgGs. Human platelets express between 1000-4000 copies per platelet. It contains an ITAM, similar to the FcRγ-chain with 12 amino acids separating the tandem YxxL sequences. FcγRIIA phosphorylation results from receptor clustering after binding of immune complexes, leading to platelet aggregation (Chacko et al., 1996, Arman et al., 2014). The association and binding of Syk leads to autophosphorylation and activation (Chacko et al., 1994). The main role of FcγRIIA is in the immune response, through bacterial-induced platelet activation and binding of antibody coated pathogens (Cox et al., 2011, Arman et al., 2014). FcγRIIA is also implicated in the pathogenesis of heparin-induced thrombocytopenia, through platelet activation mediated by antibodies clustering (Carlsson et al., 1998).

1.4.3 CLEC-2

C-type lectin-like receptor 2 (CLEC-2) is type II membrane receptor with a hemi immunoreceptor tyrosine-based activation motif (HemITAM). CLEC-2 is highly expressed on platelets with around 2000 copies per platelet (Gitz et al., 2014). CLEC-2 was initially thought to be expressed on dendritic cells (DCs) and subsets of murine myeloid cells in resting conditions and increasingly expressed seen in various leukocyte subsets in response to inflammatory stimuli (Kerrigan et al., 2009, Acton et al., 2012b). However recent work has described a more restricted expression profile to just platelets and a subset of circulating inflammatory myeloid cells (Lowe et al., 2015b).

CLEC-2 contains a N-terminal cytoplasmic tail, a stalk region, single transmembrane domain and a C-terminal carbohydrate-like recognition domain (CRD), also known as a C-type lectin-like domain (CTLD) (Weis et al., 1998, Drickamer, 1999). The CTLD does not contain key residues needed for carbohydrate binding, suggesting its ligands are required to bind through protein-protein interactions. CLEC-2 signals through a hemITAM rather than a full ITAM as it only signals by tyrosine phosphorylation of a single YXXL motif in the cytoplasmic tail (Suzuki-Inoue et al., 2006). Some aspects of CLEC-2 and GPVI signalling are similar, with signalling occurring through Src and Syk dependent tyrosine kinases (Hughes et al., 2010). However, activation of Syk requires cross linking of two CLEC-2 receptors due to the hemITAM. A difference between CLEC-2 signalling and other ITAM signalling is the hemITAM is reliant more on Syk rather than SFKs for the initial phosphorylation (Spalton et al., 2009, Severin et al., 2011). Upon CLEC-2 activation with its ligand, the hemITAM is phosphorylated, allowing the SH2 domain-containing Syk to be recruited. Syk then undergoes a conformational change, from an auto-inhibited form to an activate confirmation, before undergoing auto-and trans-phosphorylation by itself and SFKs. This leads to full activation of Syk and phosphorylation of downstream signalling proteins, resulting in the formation of the LAT signalosome, PLCγ2 activation and Ca^{2+} mobilisation, culminating in granule release and integrin activation (Figure 1.4).

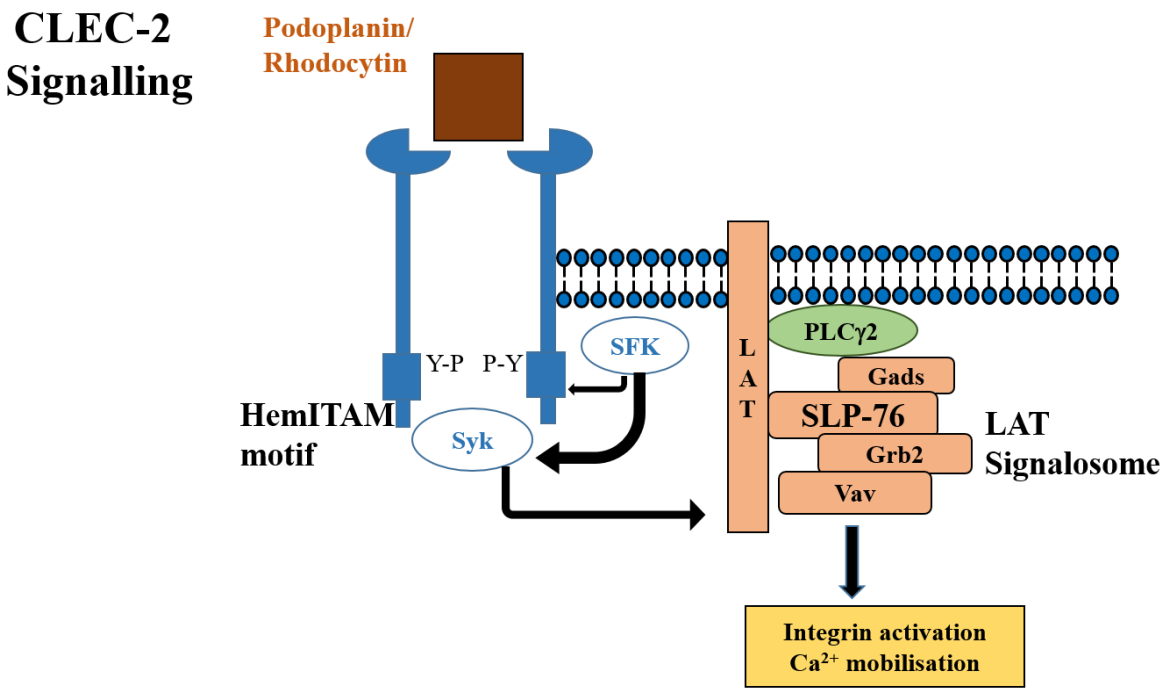

Figure 1.4. Schematic of CLEC-2 signalling pathway. Upon receptor activation by the snake toxin rhodocytin or podoplanin, the hemITAM becomes phosphorylated by Syk and Src family kinases (SFK). Syk recruitment and phosphorylation leads to downstream signalling events at the formation of the LAT signalosome, resulting in activation of PLCγ2, integrin activation and Ca^{2+} mobilisation.

Multiple studies over the years have shown that mice deficient in any of the signalling proteins downstream of CLEC-2, including Syk, SLP-76 and PLCγ2 exhibit haemorrhaging, oedema and blood-filled lymphatics during mid-gestation (Turner et al., 1995, Bertozzi et al., 2010, Clements et al., 1999, Finney et al., 2012). There have however been no descriptions of CLEC-2-deficient human patients to date, potentially due to lethality of CLEC-2 defects in development.

1.4.2.1 CLEC-2 agonists

CLEC-2 was first identified as a platelet receptor through activation by the snake venom toxin, rhodocytin (Suzuki-Inoue et al., 2006). Initially it was proposed that rhodocytin-mediated platelet activation was through integrin $\alpha_2\beta_1$; however, later studies showed rhodocytin activation was independent of $\alpha_2\beta_1$ as activation was still seen in the presence of a blocking antibody (Suzuki-Inoue et al., 2006). The sulphated sugar fucoidan and dextran sulphate can also lead to platelet activation through CLEC-2 in humans and mice (Manne et al., 2013, Alshehri et al., 2015b).

CLEC-2 was first proposed to have an endogenous ligand through studies of platelet binding to HIV-1 viral particles (Chaipan et al., 2006). Chaipan *et al.*'s study described how platelets bound and internalised viral particles through a CLEC-2 and Dendritic Cell-Specific Intercellular adhesion molecule-3-Grabbing Non-integrin (DC-SIGN)-dependent pathway (Chaipan et al., 2006). DC-SIGN, is another C-type lectin receptor and was shown to bind to the viral envelope protein Env by binding to mannose sugars (Geijtenbeek et al., 2000). However, CLEC-2 binding was independent of Env, suggesting involvement of another host cell protein. Platelet aggregation occurred when

platelets were added to human embryonic kidney cells (HEK-293T) cells incorporated with HIV, suggesting the cells expressed an endogenous ligand for CLEC-2 to mediate aggregation (Christou et al., 2008).

Podoplanin was identified as the endogenous ligand for CLEC-2 in 2007 by Suzuki-Inoue (Suzuki-Inoue et al., 2007). Podoplanin had been shown to be expressed on tumour cells and was able to induce platelet aggregation when added with platelets (Kato et al., 2003). Suzuki-Inoue *et al*.'s studies went on to show podoplanin was the ligand for CLEC-2 following the observation that the podoplanin-expressing tumour cell mediated platelet aggregation with similar kinetics to rhodocytin (Suzuki-Inoue et al., 2007). The CLEC-2 and podoplanin interaction was confirmed using podoplanin-expressing Chinese hamster ovary (CHO) cells and lymphatic endothelial cells (LECs) which also induce platelet aggregation in a CLEC-2 dependent manner (Suzuki-Inoue et al., 2007). The interaction between recombinant-CLEC-2 and podoplanin was shown to have a binding affinity (K_D) of 25 μM after surface plasmon resonance was performed (Christou et al., 2008).

Podoplanin, also known as gp38, aggrus, T1α and E11 antigen, is a 36-43 kDa type-1 transmembrane sialoglycoprotein containing a large, heavily glycosylated extracellular domain, a single transmembrane domain and a short cytoplasmic tail (RKMSGRYSP sequence). Podoplanin consists of a transmembrane domain and an *O*-glycosylated platelet-aggregation stimulating domain (PLAG domain), which interacts with the CLEC-2 receptor. It has also been proposed to interact with the family of ERM (ezrin, radixin, moesin) proteins, through three basic amino acids in its cytoplasmic tail

(Martin-Villar et al., 2006). These interactions forming associations with the ERM proteins which increase RhoA activity demonstrating that podoplanin is also a signalling receptor (Martin-Villar et al., 2006). Podoplanin was identified as the E11 antigen on LECS in 1996 (Wetterwald et al., 1996), with the podoplanin structure being described on kidney podocytes in 1997 (Breiteneder-Geleff et al., 1997). Podoplanin is widely expressed on cells outside the vasculature including, alveolar type-1 epithelial cells, LECs (Schacht et al., 2003), kidney podocytes and fibroblastic reticular cells (FRCs) (Astarita et al., 2015). It is also upregulated under pathological conditions on T-helper 17 (T_H17 cells) (Peters et al., 2015), tumour cells (Kato et al., 2003) and inflammatory macrophages (Kerrigan et al., 2012). The consequences of podoplanin upregulation will be discussed further in Section 1.8.

1.5 Platelet receptor shedding

As previously discussed, there are multiple ways of regulating platelet receptor activation. Proteolytic cleavage of receptors can also regulate receptor expression and consequent activation. Extracellular proteolysis of receptors results in irreversible inactivation of receptors and can also release soluble receptor fragments into the plasma. Approximately 10% of all platelet receptors can be regulated by proteolytic cleavage, including GP1b, GPV and GPVI (Bender et al., 2016).

1.5.1 GPVI shedding

GPVI is one of the most intensively studied receptor that undergoes proteolytic cleavage. A principle mechanism for GPVI shedding in humans is through ligand-mediated shedding. GPVI signalling has been shown to lead to proteolytic inactivation

of GPVI through ectodomain shedding (Qiao et al., 2010, Gardiner et al., 2004, Bergmeier et al., 2004, Stephens et al., 2005). GPVI shedding can occur between minutes and hours, depending on the conditions involved, with more powerful agonists, such as convulxin, inducing quicker shedding (Andrews et al., 2007). Ligand-mediated shedding reduces platelet reactivity in areas where there is extensive collagen exposure and may serve to prevent occlusive thrombus formation (Bender et al., 2016). Downregulation or reduced expression of GPVI has been shown to reduce the platelet activation response to GPVI ligands, including collagen (Snell et al., 2002, Stephens et al., 2005).

Several non-physiological agents, including calcium ionophore, N-ethylmaleimide (NEM) and calmodulin inhibitors also induce GPVI shedding. NEM directly activates sheddases and calmodulin inhibitors, such as W7, allowing calmodulin dissociation from the cytoplasmic tail, thereby leading to GPVI shedding. Carbonyl cyanide m-chlorophenylhydrazone (CCCP) can also induce GPVI shedding in mice though activation of sheddases (Bergmeier et al., 2004).

Pathological shear stress can also induce GPVI shedding independent of platelet activation, also suggesting a regulatory role of shedding in preventing excessive thrombus formation (Al-Tamimi et al., 2012). Coagulation mediated shedding of GPVI through FXa activity has also been described, resulting in GPVI downregulation in procoagulant conditions. Furthermore, antibody-induced GPVI shedding by FcγRIIA leads to shedding of GPVI (Rabie et al., 2007, Takayama et al., 2008), with GPVI

downregulation reported through shedding after treatment with anti-GPVI antibodies in mice (Nieswandt et al., 2001).

GPVI shedding is mainly metalloproteinase-dependent. The sheddase ADAM10 plays a major role in GPVI shedding, with ADAM 17 also contributing (Facey et al., 2016, Bender et al., 2016). ADAM10 and ADAM17 are endogenous sheddases, which are part of the family of a disintegrin and metalloproteinases (ADAM family) and are closely related to the family of matrix metalloproteinases (MMPS) (Facey et al., 2016). They contain a metalloproteinase domain that cleaves the receptor. In basal conditions, ADAMs contain an unpaired cysteine in their pro-domain, which inhibits the metalloproteinase domain. When ADAMs become activated, the pro-domain is proteolytically removed. NEM and other thiol-modifying agents can also directly activate the sheddases (Andrews et al., 2007). Multiple studies have shown ADAM10 to be the key sheddases involved in GPVI shedding. Gardiner *et al*. mapped the site of GPVI cleavage by ADAM10 and introduced mutations that prevent GPVI shedding (Gardiner et al., 2007). Other studies confirmed this, showing platelet ADAM10-deficient mice do not undergo GPVI shedding after stimulation. However, these studies also suggested that shedding is reduced when ADAM17 is absent (Bender et al., 2010). ADAM17 is the main sheddase involved in GP1b shedding and plays a minor role in GPVI shedding in mice.

Proteolytic cleavage of GPVI by the sheddases ADAM10 and ADAM17 and other mechanisms described, results in the release of a soluble GPVI fragment (55 kDa) into the plasma, leaving a remnant 10 kDa membrane bound fragment. As GPVI is only

found on megakaryocytes and platelets the soluble GPVI (sGPVI) fragment detected in the plasma can be used as a biomarker of platelet activation. To this end, sGPVI is a specific platelet activation marker, which has been detected in a range of thrombotic disorders and is also elevated in other conditions such as Alzheimer's disease, thrombotic microangiopathy and ischaemic stroke (Laske et al., 2008, Yamashita et al., 2014b, Wurster et al., 2013).

1.5.2 Other ITAM receptor shedding

FcγRIIA is another ITAM receptor that can undergo cleavage. Binding of ligands such as antibody complexes to FcγRIIA activates calpain resulting in intracellular proteolytic cleavage (Gardiner et al., 2008b). Activation of FcγRIIA or GPVI can lead to shedding of both receptors (Gardiner et al., 2008b). This has also been described *in vivo*, as patients with heparin induced thrombocytopenia (HIT) associated with activation of FcγRIIA results in elevated sGPVI levels (Qiao et al 2015). The hemITAM, CLEC-2, can also mediate GPVI shedding (Gitz et al., 2014), however GPVI activation cannot induce CLEC-2 shedding. In mice, it is proposed that CLEC-2 is internalised (May et al., 2009).

1.6 Platelet roles

The major role of platelets is considered to be in haemostasis and thrombosis, and more recently, in maintaining vascular integrity. Over the last few years, other functional roles in numerous processes have been proposed including in embryonic development, angiogenesis and in wound healing (Bertozzi et al., 2010, Kisucka et al., 2006, Nurden et al., 2008). In addition, platelets play a critical role in infection and in inflammation (Morrell et al., 2014, Engelmann and Massberg, 2013). This section will examine the

different role of platelets, in particular looking at the roles associated with the podoplanin/CLEC-2 axis and GPVI pathways.

1.6.1 Role of platelets in cancer

Platelets have also been shown to contribute to cancer metastasis and facilitating tumour growth. Interactions between platelet receptors and ligands on tumour cells, predominately podoplanin and CLEC-2. Podoplanin is upregulated in a wide range of cancers, including colorectal adenocarcinomas (Kato et al., 2003), lung carcinomas and central nervous system related tumours (Kato et al., 2005, Shibahara et al., 2006a). The implications of podoplanin upregulation on cancer cells have yet to be fully established; however, roles in cell migration and presence at the tumour invasive edge have been proposed (Wicki and Christofori, 2006). Platelet coating of tumour cells allows formation of platelet/tumour aggregates, protecting tumour cells from shear stress and help in evasion from the immune system (Gay and Felding-Habermann, 2011, Jain et al., 2009). Studies using an anti-podoplanin antibody (MS-1 mAb) has given rise to reductions in platelet aggregation *in vitro* and reductions in pulmonary metastasis *in vivo*, making podoplanin a potential anti-metastatic drug target (Takagi et al., 2013).

1.6.2 Role of platelets in infection

Many studies have described the interactions between platelets and bacteria. Both Gram-negative and Gram-positive species of bacteria induce activation through a shared pathway that is critically dependent on FcγRIIA (Watson et al., 2016, Arman et al., 2014). Several additional platelet receptors have been implicated in platelet-pathogen interactions, including Toll-like receptors (TLRs). Platelets can also limit bacterial dissemination by capturing pathogens after thrombus formation (Engelmann and

Massberg, 2013, Morrell et al., 2014). In addition, platelets interact with viruses, facilitating viral capture through interactions with different receptors including TLR-9 and CLEC-2 (Zhang et al., 2010, McCarthy et al., 2015) and mediating viral transmission, such as HIV (Chaipan et al., 2006). Furthermore, CLEC-2 has recently been shown to be involved in bacterial-driven thrombus formation. Hitchcock *et al*. reported that the upregulation of podoplanin in livers of mice infected with *Salmonella* resulted in an inflammation-driven occlusive thrombosis, with the absence of platelet CLEC-2 negated thrombus formation (Hitchcock et al., 2015).

1.6.3 Role of platelets in inflammation

The role of platelets in the inflammatory response has been extensively studied, and in particular in regard to platelet adhesion to activated endothelium and to circulating leukocytes (Gros et al., 2015a). Platelets interact with a variety of immune cells to release pro-inflammatory cytokines. Platelets also have pathological roles in various inflammatory conditions, such as atherosclerosis and deep vein thrombosis, where they contribute to the initial damage to the vessel. Moreover, platelet activation is linked to chronic inflammatory disorders, such as rheumatoid arthritis (RA), inflammatory bowel disease (IBD) and in response to thermal injury and sepsis. The next section will assess whether platelet activation is associated with these inflammatory conditions.

1.6.3.1 Rheumatoid Arthritis

Rheumatoid arthritis (RA) is a chronic systemic inflammation affecting joints which leads to progressive destruction of articular cartilage (Del Rey et al., 2014). Platelets have been implicated in this underlying damaged. Specifically, it is proposed that there are abundant levels of platelet microvesicles in synovial fluid which mediate pro-

inflammatory effects (Del Rey et al., 2014, Boilard et al., 2010). GPVI signalling has been implicated in increasing platelet microvesicle production in RA, leading to a pro-inflammatory response as a result of microvesicle interactions with synovial fibroblasts (Boilard et al., 2010). Increased CLEC-2 expression has also been observed in synovial arthroscopic tissue biopsies taken from RA patients (Del Rey et al., 2014). Platelet-CLEC-2 interacts with synovial fibroblasts resulting in increased production of the pro-inflammatory cytokines IL-6 and IL-8 (Del Rey et al., 2014). Podoplanin expression is also markedly increased in inflamed areas, notably on synovial fibroblast, and therefore may play a role in driving the inflammation (Miyamoto et al., 2013, Ekwall et al., 2011, Del Rey et al., 2014).

1.6.3.2 Inflammatory Bowel Disease

Inflammatory bowel disease (IBD) is another chronic inflammatory condition associated with platelet activation. IBD is a collective term for inflammatory conditions primarily affecting the gastrointestinal tract. The two main predominant forms of IBD are Crohn's disease and ulcerative colitis (UC). Crohn's disease is a chronic inflammation of the gut, mostly commonly associated with inflammation of distal end of the ileum in the small intestine and the colon (Pedersen et al., 2014). UC is an inflammatory condition mainly affecting the rectum, colon and large bowel. Both conditions exhibit chronic inflammation with active and non-active phases, where the patient experiences flare ups and times of remission. It is not established fully the direct cause of IBD cases or reasons for flare ups, but both genetic and environmental causes have been proposed (Ponder and Long, 2013). Platelets have been shown to have roles in IBD as many patients present with several abnormalities in platelet dysfunction,

including smaller mean corpuscular volume and increased chronic activation (Giannotta et al., 2015, Jaremo and Sandberg-Gertzen, 1996)

Iron deficiency anaemia is common clinical complication arising in IBD, with around 15-20% of IBD patients developing iron deficiency anaemia with increasing prevalence (up to 60%) when taking into account hospitalised patients (Guagnozzi and Lucendo, 2014, Bergamaschi et al., 2010). Iron deficiency can also affect disease severity in IBD patients. Chronic intestinal bleeding often occurs at inflamed sites and is a potential explanation for the iron-deficiency that develops, with platelet activation and thrombocytosis described during periods of intestinal inflammation (Voudoukis et al., 2014). Platelet activation may occur to maintain haemostasis and vascular integrity in inflamed areas.

1.6.3.3 Thermal injury

A major inflammatory response is observed in patients with thermal burn injuries. Platelet activation is commonly seen due to the excessive tissue damage. In a study of 244 patients with thermal injuries, Marck *et al*. reported a substantial drop in platelet count at day 3 post injury with rebound thrombocytosis at day 15. Interestingly, lower platelet counts observed at day 3 and 15 were associated with poor patient outcomes (Marck et al., 2013). It is currently unknown if this drop in platelet count results from platelet consumption or reduced platelet formation. Measurement of a platelet activation marker at these early time points could indicate the degree of platelet activation and potentially disease prognosis.

1.6.3.4 Sepsis

Sepsis is described as a majorly exaggerated systemic immune response in the response to pathogens, mainly bacterial infections such as *Klebsiella pneumoniae*. Sepsis is a devastating condition which can often result in mortality, even with aggressive antibiotic treatment (Angus and van der Poll, 2013). Sepsis has an estimated incidence of 19 million cases worldwide per year (Adhikari et al., 2010, Proudfoot and Summers, 2014). Sepsis development can result from many conditions including acute lung injury and is a critical complication of thermal injury due to the vast amounts of tissue damage causing increased susceptibility to bacterial infection. Although advancements in the treatment of initial thermal injury have been greatly improved, sepsis development and associated mortality remains a major challenge for recovery (Mann et al., 2012). Clinical diagnosis of sepsis is very difficult and prolonged with many criteria needing to be met. The diagnosis of the causative pathogen can also become difficult with positive blood cultures being required. Sepsis diagnosis criteria can also be masked by the systemic inflammatory response syndrome (SIRS) that can also develop in these patients (Levy et al., 2003). An effective biomarker with a strong predictive value would enable rapid treatment and thus lead to a reduction in mortality.

Sepsis is also strongly associated with thrombocytopenia (Sharma et al., 2007). Thrombocytopenia is a common clinical presentation in critically ill patients who go onto develop sepsis and can impair the patient's response to infection and lead to increased mortality (Claushuis et al., 2016). This has also been shown in mice, for example where thrombocytopenia impaired the host response to *Klebsiella pneumoniae* infection, leading to enhanced bacterial growth in the blood and lungs (de Stoppelaar et

al., 2014). These studies illustrate that platelets have a potential role in host defence against pathogens and sepsis development.

1.6.4.5 Other inflammatory conditions

Platelets are also implicated in multiple sclerosis (MS); an auto-immune inflammatory disorder affecting the brain and central nervous system as a result of demyelination. Studies have shown the interaction of CLEC-2 and podoplanin can have a positive effect on the resolution of inflammation (Peters et al., 2015). Platelets have also described to contribute to the initial damage to the vascular wall that leads to the onset of atherosclerosis and in deep vein thrombosis (Huo et al., 2003, Lindemann et al., 2007, Nieswandt et al., 2005, Brill et al., 2012). The CLEC-2 ligand is expressed in atherosclerotic plaques with the level of expression correlating with plaque severity (Hatakeyama et al., 2012).

1.7 Role of platelets in trauma

Trauma is the leading cause of death in people under 40 in the UK (NCEPOD, 2007). The leading cause of mortality in trauma is through excessive bleeding, although a large number of other factors are also associated, including coagulation defects and severe inflammation. Together these lead to multi-organ failure (MOF). Trauma research over recent years has produced several acute treatment therapies to prevent excessive blood loss and thereby save lives. However, there is now a focus on therapeutic developments targeting a wide range of secondary complications resulting from different severity and types of trauma, including amplified inflammation and MOF. Platelets have been described to have a role in activating the innate immune response through antigen

recognition and presentation to immune cells. Platelets may also play a role in the increased immune response, resulting in the initiation of SIRS and increased mortality.

1.7.1 Systemic inflammatory response syndrome (SIRs)

SIRS is a substantially amplified inflammatory response that can lead to tissue damage, MOF and mortality. A dynamic inflammatory response after trauma is usually required for tissue repair and regeneration (Hirsiger et al., 2012). However, after severe trauma, the release of inflammatory mediators and cytokine production is exaggerated causing an excessive, tissue-damaging inflammatory response and SIRS (Hirsiger et al., 2012). The causes of the amplified inflammatory are now being studied extensively, with danger associated molecular pattern molecules (DAMPs) and Alarmins proposed to be key players.

1.7.2 Alarmins and DAMPs

Danger Associated Molecular Pattern molecules (DAMPs) are danger signals released from stressed or damaged cells. Mazinger (1994) was the first to describe the danger theory where host cells recognise and respond to danger signals released from the body's own cells, and it is now believed that this may give rise to its own cells and has become the basis of how SIRS may develop (Matzinger, 1994). DAMPs are proposed as the host's version of Pathogen Associated Molecular Pattern molecules (PAMPs). PAMPs are microbial-derived molecules that are recognised by pattern recognition receptors (PRRs), such as TLRs, which upon binding their ligands, cause activation of the innate immune response in order to destroy the pathogen. DAMPs are believed to initiate the immune response in a similar way but without the presence of a pathogenic/microbial agent. SIRS therefore develops after release of DAMPs resulting

in enhancement of cytokine production and immune system activation under sterile conditions. Alarmins are a subset of endogenous DAMPs that are elevated in response to trauma. They can remain at high levels for days after initial trauma. Alarmins bind to corresponding Alarmin receptors inducing intracellular signalling pathways eliciting the pro-inflammatory response described above (Manson et al., 2012).

1.7.3 Nuclear-related Alarmins

Nuclear-related Alarmins are nuclear protein and material released after damage to the nucleus. These include DNA, high-mobility-group-box-1 protein (HMGB-1), nucleosomes and histones.

1.7.3.1 Histones

Histones are highly positively charged nuclear proteins with an important role in DNA organisation and chromatin formation (Doenecke and Albig, 2001).They are a main component of Neutrophil Extracellular Traps (NETs; discussed in Section 1.7.3.3), and can be released into the circulation having been released after nucleosomes breakdown. Histones can be elevated 200 fold in trauma patients, reaching levels in the order of 250 μg/ml. There are four main histone proteins, H2A, H2B, H3 and H4, with H3 and H4 having the greatest effect on cells. Histones have multiple effects on many cell types, including vascular endothelial cells, resulting in cytokine activation and thrombin generation (Semeraro et al., 2011). Histones are extremely cytotoxic and elevated histones levels have been reported to induce acute lung injury (Abrams et al., 2013).

1.7.3.2 High-mobility-group-box-1 (HMGB-1)

Another nuclear related Alarmin, HMGB-1 interacts with other nuclear proteins to regulate DNA organisation and gene transcription. HMGB-1 levels have been measured in a range of inflammatory conditions, including sepsis (Klune et al., 2008) and has

been shown to be elevated 30 fold after trauma (Park et al., 2004). HMGB-1 has been described to signal through a variety of receptors from TLRs to Receptor for Advanced Glycation Endproducts (RAGE) to activate immune cells. Interactions between HMGB-1 and TLR-4 have also been shown to promote NET formation (Tadie et al., 2013). HMGB-1 has been described to promote inflammatory cell recruitment to damaged areas via forming complexes with CXCL12, which change the conformation of CXCR4 leading to signalling and recruitment (Schiraldi et al., 2012). HMGB-1 has been described to have many inflammatory roles through a variety of mechanisms, however the role of HMGB-1 in platelet activation has yet to be established.

1.7.3.3 DNA

Released after cell damage, cell free-DNA is present in the plasma of patients and is a marker of disease, including sepsis (Hampson et al., 2016). Although DNA can be released from different immune cells, neutrophils have been the predominate source of DNA studied due to the release of NETS through a process known as NETosis (Yipp et al., 2012) NETs are made up of extracellular DNA, serine proteases and anti-microbial molecules which play a critical role in trapping and elimination of bacteria (Brinkmann et al., 2004). Long extracellular extrusions are the main structure of NETs giving the possibility for platelets to adhere to the NETs and undergo activation (Fuchs et al., 2010). Platelets have been shown to be activated by NETs (Fuchs et al. 2010), but the underlying mechanism remains unclear.

1.7.3.4 Mitochondrial DNA (MtDNA)

DNA released from mitochondria following damage has been shown to be elevated in the plasma of trauma patients and to remain elevated for up to 24 hours (Zhang et al., 2010). MtDNA has been shown to increase endothelial permeability during systemic

inflammation (Sun et al., 2013) and to be associated with acute lung injury (Hauser et al., 2010). The effect of MtDNA is believed to be due to its close evolutionary relationship with bacterial DNA, with similar CpG DNA repeats (Zhang et al., 2010). MtDNA activates many of the same receptors as bacterial DNA, including TLR-9, which is expressed in platelets.

1.7.4 Oxidised low density lipoprotein (OxLDL) and Advanced Glycation End Products (AGE)

AGE are glycated proteins that have undergone protein modifications and are implicated in conditions such as diabetes and atherosclerosis (Goldin et al., 2006). Studies by *Zhu et al*. suggested AGE gives a prothrombotic phenotype, enhancing platelet reactivity through CD36 signalling (Zhu et al., 2012). OxLDL, a lipid-based DAMP, has been associated with hyperlipidaemia and site of atherosclerotic lesions (Matsuura et al., 2008). OxLDL forms after lipids and apolipoprotein B (apoB) components undergo lipid per oxidation (Stewart et al., 2005). It has been proposed that Alarmins, such as AGE and OxLDL, may not induce platelet aggregation directly but may modulate platelet responses to other agonists.

1.7.5 Alarmin receptors

A large number of Alarmin receptors have been characterised, including TLRs, formyl peptide receptor (FPR1), heat shock protein receptors (HSPR) and the ATP receptor, P2RX7. Platelets express a number of Alarmin/DAMP receptors which support a pro-inflammatory response. The direct signalling mechanisms behind Alarmin-induced platelet activation however have yet to be fully established. The main Alarmin receptor type recognised as potential platelet Alarmin receptors are TLRs.

1.7.5.1 TLRs

TLRs are a family of receptors involved in host defence against pathogens, which recognise PAMPs, activating the immune response (Cognasse et al., 2005) . Eleven TLRs have characterised with functional roles, with TLR2, TLR4 and TLR9 having been described on the platelet surface (Cognasse et al., 2005). TLR2 and TLR4 have been shown to have roles in recognition of bacterial-derived molecules. Platelet TLR4 is also associated with platelet-neutrophil interactions (Clark et al., 2007) and with NET formation. As discussed above, TLR9 has been shown to recognise bacteria DNA and MtDNA. TLR signalling in platelets has been proposed to involve NF-kB/TRIF/Myd88 signalling cascades but a full understanding of the mechanisms between TLR activity and platelet activation has yet to be fully established, in part because of their low levels and that of their signalling proteins (Garraud and Cognasse, 2010).

1.7.5.2 CD36 (GPIIIb)

The class B scavenger receptor CD36 has been proposed as a potential DAMP receptor. CD36 is expressed on the platelet surface with a copy number of 20,000 per platelet (Saboor et al., 2013). It is the major receptor involved in OxLDL signalling and has also been shown to bind microparticles (Ghosh et al., 2008). CD36 also supports long-chain fatty acid transport (Su and Abumrad, 2009) CD36 has been implicated in atherosclerosis, hyperlipidaemia, and insulin insensitivity in diabetes mellitus (Podrez et al., 2007). CD36 may also play a role in sterile inflammation through formation of a CD36-TLR4-TLR6 heterotrimer (Stewart et al., 2005). However, the CD36 signalling mechanism has yet to be fully established.

1.7.5.3 Receptor for Advanced Glycation Endproducts (RAGE)

The 35kDa scavenger receptor, RAGE, is expressed at low levels on endothelial cells and leucocytes cells but upregulated at sites of inflammation sites RAGE has been shown to interact with AGE and to contribute to persistent NF-κB activation potentially leading to hyperglycaemia in patients with diabetes (Bierhaus and Nawroth, 2009). RAGE is located on platelets and is proposed to be a receptor for HMGB-1 in inflammation and cancer (Sims et al., 2010).

1.8 The role of platelets in vascular integrity

1.8.1 Other cell interactions in inflammation and vascular integrity

Platelets play a critical role in the maintenance of vascular integrity during development and at sites of inflammation. Vascular integrity is maintained through the interactions with endothelial cells. As previously mentioned (section 1.4.2), CLEC-2 has been shown to maintain integrity of the cerebrovasculature in mid-gestation through association with podoplanin (Lowe et al., 2015a). The GPVI/ FcRγ-chain complex has been shown to maintain vascular integrity in inflamed blood vessels by opposing the action of neutrophils (Gros et al., 2015a). This extends an earlier study that reported critical roles for CLEC-2 and GPVI-FcR γ-chain in prevention of bleeding at sites of inflammatory challenge (Boulaftali et al., 2013).

Podoplanin undergoes marked up-regulation at sites of inflammation (Ekwall et al., 2011, Astarita et al., 2012b) . The consequences of podoplanin upregulation however, seems to vary depending on the type of inflammation and cell types that are involved,

with the podoplanin/CLEC-2 interaction sometimes being beneficial and on other occasions promoting inflammation. Podoplanin upregulation has been observed on fibroblastic reticular cells (FRCs), with the interaction between CLEC-2 on platelets and podoplanin on FRCs being shown to underlie lymph node expansion (Astarita et al., 2015). In addition, maintenance of lymph node high-endothelial venule (HEV) integrity requires platelet-expressed CLEC-2 and podoplanin-expressed FRCs; absence of either leads to the appearance of blood-filled lymph nodes (Herzog et al., 2013). In a mouse model of autoimmune encephalomyelitis, upregulation of podoplanin on T_H17 cells is associated with their inhibition, leading to improved recovery (Miyamoto et al., 2013). Likewise, podoplanin expressed on fibroblastic macrophages, a $F4/80^+$ subtype macrophage found in the red pulp of the spleen, is upregulated in response to zymosan induced peritonitis and this upregulation leads to increased phagocytosis (Hou et al., 2010). On the other hand, upregulation of podoplanin on inflammatory macrophages or upregulation on tumour cells can lead to platelet aggregation and thrombosis (Kerrigan et al., 2012, Jain et al., 2009). Upregulation of podoplanin on liver macrophages ($F4/80^+$ cells) of *Salmonella*-infected mice triggers CLEC-2-mediated thrombosis (Hitchcock et al., 2015). The consequence of podoplanin upregulation on human cells however is not known.

1.8.2 Role of platelets in wound healing

Platelets have been shown to play critical roles in wound healing, most notably during the immediate response to injury through formation of a vascular plug and prevention of excessive blood loss. The formation of the thrombus also provides a matrix scaffold for recruited cells to infiltrate the damaged area (Li et al., 2007). Platelets release a number of chemo-attractants and growth factors, including both pro-angiogenic and anti-

angiogenic proteins, various growth factors including, platelet-derived growth factor (PDGF), transforming-growth factor-β (TGF-β), and chemo-attractants such as platelet factor 4 (PF4) which act to recruit immune cells (Li et al., 2007). The platelet releasate has been shown to increase the rate of granulation and to promote tissue granulation; involving fibroblast proliferation, deposition of extracellular matrix (ECM) proteins and new blood vessel formation (Li et al., 2007). The range of cytokines and growth factors released help to increase the rate of granulation and promote tissue granulation (Ksander et al., 1990a, Li et al., 2007).

Relatively few studies however have investigated the effect of platelet depletion immediately following wound injury because of their critical role in the haemostatic process. This question can be addressed through the targeted deletion of platelet proteins implicated in wound repair but not the haemostatic process such as CLEC-2. For example, the critical role of CLEC-2 in maintenance of vascular integrity as shown in the reverse passive Arthus (rpA) reaction model (Boulaftali et al., 2013) may also translate to a role in wound repair. Additionally, platelet CLEC-2 has also been shown to regulate migration of keratinocytes *in vitro* and this may be important at all stages of wound healing (Asai et al., 2016). The role of platelets in wound healing may play a critical role in the context of trauma which leads to a reduction in platelet count as described above.

1.9 Aims of the thesis

Platelet activation is associated with many aspects of trauma and inflammation, from initial damage and associated bleeding and the resulting release of Alarmins and platelet-activating mediators, to platelet activation occurring post injury during a recovery phase and development of secondary complications. Furthermore, platelets also play a role in the maintenance of vascular integrity that may also be important in the wound healing process. While, many of these roles have been described, we still have a rudimentary understanding of the role of platelets in trauma and other inflammatory conditions, and also in wound repair, as well as the underlying mechanisms of platelet activation and interactions with other cells in these processes. In this thesis, the overall aim is to further our understanding of the regulation and role of platelets in trauma and in inflammation and to identify a soluble marker of platelet activation that correlates with disease progression. The specific aims are:

1) To investigate the effect and underlying mechanisms of DAMPs and nuclear-related Alarmins on platelet function and activation *in vitro* and *in vivo*.
2) To investigate whether the product of the proteolytic cleaving of GPVI in the plasma, known as soluble GPVI, as a marker of platelet activation and disease pathogenesis in trauma and other inflammatory disorders.
3) To study the functional consequence of upregulation of podoplanin on inflammatory macrophages and to measure the levels of podoplanin and in trauma and in inflammatory diseases.
4) To investigate the role of GPVI and CLEC-2 on platelets and podoplanin on wound repair.

CHAPTER 2

MATERIALS AND METHODS

2.1. Materials

2.1.1. Antibodies and reagents

Details of the agonists, antagonists and inhibitors and cytokines used in the course of this thesis ae listed in Tables 2.1, 2.2 and 2.3, respectively. Table 2.4 lists the antibodies used. If unstated, materials used were from Sigma (Poole, UK).

Table 2.1 Agonists

Reagents used	**Source**
Advanced Glycation End Product (AGE)-BSA	Biovision (San Franciso, USA)
Calf thymus histones (CTH)	Worthington Biochemical Corporation (Reading, UK)
Collagen (Kollagen Reagens HORM suspension)	Takeda (Linz, Austria)
Collagen related peptide (CRP)	Dr R.W. Farndale (Cambridge University, UK)
Glycoaldehyde-AGE-BSA	Cell Biolabs, INC (San Diego, USA)
Oxidised Low Density Lipoprotein (OxLDL)	Source Bioscience LifeSciences (Nottingham, UK)
PAR-1 Peptide (SFLLRN)	AltaBioscience (Birmingham UK)
PAR-4 Peptide (AYPGKF)	AltaBioscience (Birmingham UK)
Rhodocytin	Dr. J.A. Eble (University of Münster

Table 2.2 Antagonists and inhibitors

Reagents used	**Use**	**Source**
DAPT	γ-secretase inhibitor	Sigma (Poole, UK)
Dasatinib	Src and Bcr/Abl inhibitor	LC Laboratories (Woburn, MA).

GI254023	ADAM10 inhibitor	Sigma (Poole, UK)
GM6001	Broad MMP inhibitor	Calbiochem (San Diego, USA)
Hirudin	Thrombin inhibitor	Sigma (Poole, UK)
Prostacyclin (PGI_2)	Platelet inhibitor	Cayman Chemicals (Cambridge, UK)
PRT060318	Syk inhibitor	Portola Pharmaceuticals Inc (San Francisco, CA).

Table 2.3. Recombinant Cytokines (human)

Reagents used	Use	Concentration	Source
GM-CSF	Pro-inflammatory	50 ng/ml	PeproTech (New Jersey, USA)
M-CSF	Anti-inflammatory	100 ng/ml	

Table 2.4. Antibodies

Antibody	Host species	Use*	Source
PRIMARY			
204-11 Fab (GPVI dimer monoclonal antibody)	Mouse	FC: 1/20 25 µg/ml	Dr S. Jung (Cambridge, UK)
β-Tubulin (human)	Mouse	WB: 1/2000	Sigma (Poole, UK)
CLEC-2 (human)	Goat	IP: 2 µg/ml	R+D Systems (Abingdon, UK)
CLEC-2 (human) AYP1	Mouse	IP: 2 µg/ml	Dr A. Pollitt (Reading, UK)
CD62-P (P-selectin: human)	Mouse	FC: 1/100	BD Biosciences (Oxford, UK)
CD45- APC (human)	Mouse	FC: 1/100	Beckman Coulter (California, USA)
CD38- FITC	Mouse	FC: 1/100	EBioscience (Hatfield, UK)

CD66b-PerCP	Mouse	FC: 1/100	EBioscience (Hatfield, UK)
CD41-PE	Mouse	FC: 1/100	EBioscience (Hatfield, UK)
GPVI (human) polyclonal Ab -	Rabbit	ELISA: 1 µg/ml	Dr E. Gardiner (Canberra, Australia)
1A12 (human: GPVI monoclonal Ab)	Mouse	ELISA: 1 µg/ml	Dr E. Gardiner (Canberra, Australia
PLCγ2 sc-407	Rabbit	IP: 1/500 WB: 1/1000	Santa Cruz Biotechnology (Heidelberg, Germany)
Phosphotyrosine (4G10)	Mouse	WB: 1/1000	Millipore (Bucks, UK)
Podoplanin NZ-1.3 (human) – PE and Unconjugated	Rat	FC: 1/100 ELISA: 1& 5 µg/ml WB: 5 µg/ml	EBioscience (Hatfield, UK)
IgG2a κ Isotype control) – PE and Unconjugated	Rat	FC: 1/100 ELISA: 1& 5 µg/ml WB: 5 µg/ml	EBioscience (Hatfield, UK)
Podoplanin 18H5	Mouse	FC: 1/100 ELISA: 1& 5 µg/ml WB: 5 µg/ml	Santa Cruz Biotechnology (Heidelberg, Germany) Novus Biologicals (Colorado, USA)
Podoplanin/gp36 (ab109059)	Rabbit	FC: 1/400	Abcam (Cambridge, UK)
Podoplanin 8.1.1 - mouse	Syrian hamster	IH: 1/500	M.Goodall (Birmingham, UK)
Podoplanin (mouse – monoclonal)	Syrian hamster	IH: 1/500	EBioscience (Hatfield, UK)
Rabbit IgG – polyclonal - isotype control		FC: 1/400	Abcam (Cambridge, UK)
Syk	Rabbit	IP: 1/500	Dr M.G. Tomlinson

			(Birmingham, UK)
Syk-sc1077	Rabbit	WB: 1/200	Santa Cruz Biotechnology (Heidelberg, Germany)
Syk-sc-573	Rabbit	IP: 1/500	Santa Cruz Biotechnology (Heidelberg, Germany)
SECONDARY			
Hamster IgG HRP conjugated - sc-2905	Goat	IHC: 1/500	Santa Cruz Biotechnology (Heidelberg, Germany)
Mouse IgG, F(ab')2 Fragment Specific -AF647	Goat	FC: 75 µg/ml	Stratech Scientific Ltd (Newmarket, UK)
Mouse IgG HRP conjugate	Sheep	WB:1/1000	Amersham Bioscience (Bucks, UK)
Mouse IgG HRP conjugate	Rabbit	ELISA: 2.6 µg/ml	Dako (Denmark)
Rabbit IgG HRP conjugate	Donkey	WB: 1/10000	Amersham Bioscience (Bucks, UK)
Rat IgG HRP conjugate	Goat	ELISA: 2.6 µg/ml WB: 1/10000	Dako (Denmark)

*IP: Immunoprecipitation, WB: Western Blot, FC: Flow cytometry, ELISA: Enzyme-linked immunosorbent assay, AF: Alexa Fluor®, IHC: Immunohistochemistry

2.1.2. Constructs and plasmids

The following constructs and plasmids were used for CLEC-2 and GPVI transfections into cells for NFAT-luciferase assays as previously described (Tomlinson et al., 2007). Human CLEC-2 sub-cloned into pEF6 vector with a C-terminal Myc tag, human GPVI in pcDNA3 with a C-terminal Myc tag and human FcRγ (untagged) in pEF6 were made in the lab (Fuller et al., 2007, Berlanga et al., 2007). The nuclear factor of activated T-cells (NFAT)-luciferase reporter containing three copies of the distal NFAT site from

the IL-2 promoter as described in (Shapiro et al., 1997) was donated from Prof A. Weiss (UCSF School of Medicine, USA).

2.1.3. Recombinant proteins

Recombinant human GPVI was obtained from Dr Andrew Herr (Cincinnati Children's Hospital Medical Center, USA). The dimeric form of GPVI was fused with human Fc immunoglobulin (GPVI-Fc_2), as described (Miura et al., 2002).

Recombinant human Pdpn (rPdpn) was obtained with a non-cleavable C-terminal His-tag from M. Hoellerer (Oxford, UK).

2.1.4. Transgenic mice

All animal experimentation was performed in accordance to licenses PPL30/2721, PPL 70/8359 and PPL 70/8286. *Gp6*$^{-/-}$ mice and C*lec1b*$^{fl/fl;PF4\text{-}Cre}$ used in Chapter 3 have been previously been described (Kato et al., 2003, Finney et al., 2012). GPVI and CLEC-2 double deficient mice (*Gp6*$^{-/-}$*;Clec1b*$^{fl/fl;PF4\text{-}Cre}$*)* were produced by crossbreeding the two strained. *Clec1b*$^{fl/fl}$ or C57BI/6 were used as wild type (WT) controls. For wound healing studies in chapter 5, *Gp6*$^{-/-,}$ *Clec1b*$^{fl/fl;PF4\text{-}Cre}$, *Gp6*$^{-/-}$;*Clec1b*$^{fl/fl;PF4\text{-}Cre}$, *Pdpn*$^{fl/fl}$*VAV-1*$^{\text{-}Cre}$ were used and compared to C57BI/6, WT1F- ER$^{T2Cre\text{-}}$ and ROSA$^{\text{-}EYFP}$, as WT controls.

2.2. Blood Collection

2.2.1. Human blood collection

Healthy control (HC) donors: Ethical approval for blood donation from healthy volunteers was granted by Birmingham University Internal Ethical Review (ERN_11-

0175). Venous blood was collected from consenting, healthy drug free volunteers. Blood was drawn in to sodium citrate (4% citrate 1:9 ratio) or in 3.2% trisodium citrate BD vacutainers (Becton Dickinson, Oxford, UK) depending on corresponding patient group tested. For some experiments blood was drawn into EDTA, Hirudin or Lithium Heparin BD Vacutainers or S-Monovettte hirudin vacutainers (SARSTEDT, Germany). On occasions blood was drawn into hirudin (50 µg/ml, REVASC) or sodium heparin (10 U/ml, Heparin (mucous) injection BP).

Rheumatoid arthritis (RA) patients: Blood was collected into 3.2% trisodium citrate BD vacutainers (Becton Dickinson, Oxford, UK), obtained from patients with rheumatoid arthritis under informed consent approved by the local ethics committee (071Q270612) (Gitz et al., 2014). All patients with rheumatoid arthritis satisfied the 1987 American College of Rheumatology criteria for rheumatoid arthritis and clinical details are stated in Gitz et al. (2014) and Arnett FC (1988)(Arnett et al., 1988, Gitz et al., 2014).

Inflammatory Bowel Disease (IBD) patients: Blood was collected into 3.2% trisodium citrate BD Vacutainers from 42 patients with inactive or active Crohn's disease and/or ulcerative colitis. IBD disease activity state was based on specialist diagnosis, determined by clinical records, endoscopy results and C-reactive protein levels. Clinical parameters and full blood counts were collected from routine hospital measurements and with the Sysmex XN-1000-Hematology Analyzer (Sysmex UK, Milton Keynes, UK).

Thermal injury patients: Patients with thermal injury were admitted to the Queen Elizabeth Hospital Birmingham Burns Centre and recruited to the Scientific Investigation of the Biological Pathways Following Thermal Injury Study (SIFTI - REC:12/EM/0432). For patient recruitment details and parameters see Table 4.2 and

(Hampson et al., 2016). Blood samples were collected into 3.2% trisodium citrate BD Vacutainers at intervals following injury (day 1 [< 24 h post-injury], day 3 [+/- 1 day], day 7 [+/- 1 day], day 14 [+/- 3 days], day 21 [+/- 3 days], day 28 [+/- 3 days], month 2 [+/- 3 days], month 3 [+/- 7 days], month 6 [+/- 7 days] and month 12 [+/- 7 days]. Patients were categorised into septic or non-septic groups based on fulfilling at least three American Burn Association sepsis criteria (Greenhalgh et al., 2007) with a positive culture or response to antibiotics as stated in Hampson *et al*. (2016). Platelet counts were initially measured using the Beckman Coulter UniCel DxH 800 Cellular Analysis System followed by the Sysmex XN-1000-Hematology Analyzer (introduced mid-way through the study). Both analyzers measured platelet impedance.

Sepsis patients: Blood was collected into 3.2% trisodium citrate or Lithium Heparin BD Vacutainers from patients from the intensive care unit (ITU) and respiratory wards at the Queen Elizabeth Hospital Birmingham. Samples were donated by Dr D. Thickett (University of Birmingham, UK) under the ethics of different septic studies including BALTI (β-Agonist Lung Injury Trial: see (Perkins et al., 2006)) and SNOOPI (Simvastatin to modify neutrophil function in older patients with septic pneumonia: see (Greenwood et al., 2014)). 62 septic patients with different sepsis forms, including severe sepsis, patients with acute respiratory syndrome (ARDS) and 22 aged matched HCs were obtained.

2.2.2. Mouse blood collection

For basal blood counts, samples were taken from the tail vein 100 µl EDTA (20 mM). Platelet counts were measured by the ABX Pentra60 haematology counter (HORIBA Scientific, UK). For platelet studies, blood was obtained by terminal cardiac puncture.

Blood was taken from the vena cava of CO_2-asphyxiated mice anaesthetised with isoflurane and collected into 1:9 (v:v) acid citrate dextrose (ACD – 120 mM sodium citrate, 110 mM glucose, 80 mM citric acid), 4% citrate (1 in 9) in Modified Tyrode's buffer (134 mM NaCl, 0.34 mM Na_2HPO_4, 2.9 mM KCl, 12 mM $NaHCO_3$, 20 mM HEPES(4-(2-hydroxyethyl)-1-piperazineethanesulfonic acid), 5 mM glucose, and 1 mM $MgCl_2$; pH 7.3) or where stated, hirudin (50 µg/ml). 200 µl of Modified Tyrode's buffer was added to samples post collection before further processing.

2.3. Human Platelet preparation

2.3.1. Platelet Rich Plasma

Anti-coagulated blood was centrifuged for 20 min at 200 *g* at room temperature (RT) using a Sanyo Harrier 18/80 centrifuge. Blood was separated and the top layer of platelet-rich-plasma (PRP) was extracted, avoiding the buffy coat layer. Platelet-Poor-Plasma (PPP) was obtained following a 10 min centrifugation spin of remaining blood at 1000 *g* to use as a blank for light transmission aggregometry (LTA). Collected platelet concentrations were determined by the Coulter Zcs counter (Beckman Coulter Ltd, High Wycombe, UK).

2.3.2. Washed platelet preparation

Washed platelets were prepared by adding 10% acid citrate dextrose (ACD) to citrated blood before centrifugation at 200 g for 20 min. The top layer of PRP was removed, avoiding the buffy coat layer. Prostacyclin (PGI_2; 1 µg/ml) was added to PRP before centrifugation at 1000 g for 10 min. The supernatant was discarded and the platelet pellet was resuspended in Modified Tyrode's buffer (with 5 mM glucose, and 1 mM

$MgCl_2$; pH 7.3). The pellet was then washed in Modified Tyrode's buffer containing ACD and PGI_2 (1 µg/ml) and again centrifuged at 1000 g for 10 min. The washed platelets were then resuspended to the required platelet concentration; $2x10^7$/ml for flow cytometry and platelet spreading, $2x10^8$- $5x10^8$ platelets/ml for aggregation and $5x10^8$-$1x10^9$ platelet/ml for lysate preparation (unless otherwise stated). Washed platelets were rested for 30 min before experiments.

2.3.3. Plasma preparation

Platelet-free-plasma was obtained from anti-coagulated blood of patients and HCs after two centrifugation steps. For the thermal injury patients, blood was centrifuged at 2000 g for 20 min. The supernatant isolated was centrifuged again at 13 000 g for 20 min (Hampson et al. 2016). For all other patient cohorts and HCs, blood was centrifuged twice at 2500 g for 15 min at RT with no brake. The supernatant from the first centrifugation step was isolated and placed into a new tube before the second centrifugation step. Supernatants were used for experiments or frozen in aliquots for storage at -80^{o}C. Plasma from septic patients and HC cohort were obtained after centrifugation at 560 g for 10 min at RT. To compare the different centrifugation protocols, HC plasma was also obtained in this manner.

2.3.4. Microvesicle preparation

Microvesicles were isolated from double centrifuged plasma (double spun plasma) after whole blood (taken in either citrate or EDTA) was centrifuged twice at 2500 g for 15 min at RT (no brake). Supernatants from the first centrifugation were extracted into a new tube before the second centrifugation step.

2.4. Cell isolation from blood

2.4.1. Peripheral blood mononuclear cells (PBMC) isolation

Isolation of PBMCs and other blood cells were performed in a laminar flow *ho*od under sterile conditions and cells were incubated in Sanyo MCO-17AIC CO_2 incubators. Citrated blood was centrifuged at 200 g for 20 min to deplete platelets. The remaining blood was diluted 1/5 in complete media (RPMI; Gibco life technologies, supplemented with 10% foetal bovine serum (FBS; 100 U/mL penicillin, 100 μg/mL streptomycin and 2 mM L-glutamine) and placed on a ficoll-paque PLUS (GE Healthcare, Bucks, UK) gradient and centrifuged for 400 g for 30 min RT. The top plasma layer was removed to access the PBMC ring. PBMCs were extracted and washed twice in complete RPMI by centrifugation for 10 min at 300 g. RPMI was removed to leave cell pellet. Cells were resuspended in 1 ml of complete RPMI, counted and diluted to required concentrations.

2.4.2. Monocyte isolation and monocyte-derived macrophage differentiation

Where stated, isolated PBMCs were cultured in flasks or in 6-well plates for 1-3 h. Monocytes readily adhere to surfaces and remained on the surface once media was removed. Ice cold PBS was added to detach non-adherent monocytes. Cells were collected, washed in PBS for 5 min at 300 g and resuspended in media before counting and diluting to required concentrations. Where stated, monocytes were isolated by negative selection to avoid activation with the PAN monocyte isolation kit and separation columns (MACS miltenyi biotec, Woking, UK) following manufacturer's instructions. Monocytes contained in the blocking buffer (BSA 1% in PBS) used for isolation, were collected into 10% FBS, washed and counted. Cells were diluted in complete media to the required concentrations. CD14/CD38 staining of cells was

measured by flow cytometry using the BD Accuri C6 flow cytometer (BD Biosciences, Oxford, UK) to confirm monocyte isolation.

THP-1 cells (a human monocytic leukaemia cell line; (Auwerx, 1991)) were also used. THP-1 cells were cultured in complete RPMI, supplemented with 50 µM 2-mercaptoethanol.

Monocyte derived macrophage differentiation: isolated monocytes were treated with GM-CSF (50 ng/ml) or M-CSF (100 ng/ml) for 5/6 days for differentiation to M1 and M2 cells before LPS (100ng/ml) stimulation for 16 h for macrophage differentiation. CD68 staining confirmed the percentage of macrophage differentiation.

2.5. Mouse platelet preparation

2.5.1. Platelet-rich-plasma (PRP)

Anti-coagulated blood was centrifuged at 2000 rpm for 5 min in a microcentrifuge (ThermoScientific, Paisley, UK). PRP with the top third of erythrocytes were extracted before centrifugation at 200 g for 6 min (Sanyo Harrier) and PRP retained. To increase platelet yield, 200 µl of Modified Tyrode's buffer was added to the remaining sample, mixed and centrifuged at 200 g for 6 min and top layer extracted again. Samples were before pooled and platelet counts measured using the Coulter Zcs counter (Beckman Coulter Ltd, High Wycombe, UK).

2.5.2. Washed platelet preparation

Modified Tyrode's buffer was added to PRP to give a total volume of 1 ml. PGI_2 (1 µg/ml) was added to the sample before centrifugation at 1000 g for 6 min. The supernatant was removed, and the platelet pellet was resuspended with Modified

Tyrode's buffer. Platelets were counted, resuspended in Modified Tyrode's buffer to required concentration and rested for 30 min before experimentation.

2.6. Platelet function testing

2.6.1. Light transmission aggregometry (LTA)

Platelet aggregation and granule secretion was monitored using a Lumi-Dual channel aggregometer (Chrono-log Model 460VS; Chronolog, Labmedics, Manchester, UK). Aggregometer tubes (with stirrer bars) containing PRP or washed platelets were pre-warmed at 37^{o}C for 2 min, and stirred at 1200 rpm for 1 min before agonist stimulation. Where stated, $CaCl_2$ (1 mM) or inhibitors were added at least 5 min before stimulation. For AGE experiments, PRP was incubated with AGE-BSA 30 min before LTA was performed. Modified Tyrode's buffer or PPP were used as blanks to measure platelet optical density against. Aggregation traces were usually recorded for 5 min. For measuring dense granule secretion, Chronolume, a luciferin/luciferase reagent, (Chronolog, Manchester, UK) was added during sample warming. ATP secreted in response to agonist stimulation catalyesd the luciferase reaction. An ATP standard (1.6 nmol) was added at the end of each aggregation, to allow ATP secretion to be calculated.

2.6.2. Lysate preparation.

Washed platelets were prepared to the required concentrations. Where stated, integrilin (9 μM; an αIIbβ3 inhibitor), apyrase (2 U/ml) and indomethacin (10 μM) were added before stimulation. Stimulations were performed in aggregometer tubes as described above. After agonist stimulation, 2X ice cold lysis buffer containing protease inhibitors

(300 mM NaCl, 20 mM Tris, 2 mM EGTA, 2 mM EDTA, and 2% IGEPAL CA-630 [NP-40 equivalent], pH 7.4, plus 2 mM Na_3VO_4, 100 µg/mL AEBSF (4-(2-aminoethyl) benzenesulfonyl fluoride hydrochloride), 5 µg/mL leupeptin, 5 µg/mL aprotinin, and 0.5 µg/mL pepstatin) was added for 30 s to terminate reactions. Lysates were placed on ice or stored at -20^{o}C for Western blotting or immunoprecipitations. Whole cell lysates (WCLs) were prepared by adding equal volume of lysate to 2X Laemmli sample buffer (20% glycerol, 10% β-mercaptoethanol, 4% SDS, 50 mM Tris, trace of Brilliant Blue).

2.6.3. GPVI shedding experiments

400 µl of washed platelets were pre-incubated with $CaCl_2$ (1 mM) for 5 min in aggregometer tubes. Where stated, inhibitors (GI254023 2 µM, GM6001 10 µg/ml, DAPT 10 µM, PRT060318 10 µM or dasatinib 10 µM) were added. Tubes were warmed at 37^{o}C for 1 min before addition of integrilin (9 µM). Platelet suspensions were stirred at 1200 rpm for 1 min before agonist addition. Aggregation traces were monitored for 5 min and samples left to stir for 1 h. For fibrin treatment conditions, fibrinogen (100 µg/ml) was added prior to the pre-incubation step. After 3 min of fibrinogen treatment, thrombin (1 U/ml) was added and aggregation recorded for a further 5-8 min. To produce monomeric fibrin, GPRP (10 mM) was added with the fibrinogen, before thrombin stimulation. After 1 h under stirring conditions, 400 µl of 2X ice cold lysis buffer containing protease inhibitors was added for 30 s. Lysates were extracted and placed in tubes on ice or stored in the freezer (-20^{o}C).

2.6.4. Immunoprecipitations (IPs).

Lysates were pre-cleared by adding 10 µl of Protein A Sepharose (PAS) or Protein G Sepharose (PGS) beads (Pierce, Rockfield, IL) and placed on a rotator at 4^{o}C for 30 min. Samples were centrifuged at 8600 g for 15 min in a microcentrifuge at 4 ^{o}C (Eppendorf 5477 centrifuge, Germany). Supernatants were transferred to tubes containing primary antibodies against the proteins of interest and PAS or PGS beads and left to incubate for 1 h or overnight at 4^{o}C depending on antibody used. Samples were centrifuged at 8600 g for 1 min at 4 ^{o}C. The supernatant was aspirated and discarded before the pellet was washed three times with 1X lysis buffer. Samples were centrifuged once more at 8600 g for 1 min at 4 ^{o}C. Supernatant was extracted for future IP preparations or eluted in 2X Laemmli sample buffer for Western blotting.

2.6.5. Platelet spreading

Coverslips (13 mm) were coated with 200 µl of agonists (CTH (10-50 µg/ml), HMGB-1 (10-50 µg/ml), OxLDL (10-50 µg/ml), Collagen (10 µg/ml) or PBS-BSA as a control) overnight at 4^{o}C. Protein coated coverslips were washed 3 times with PBS and blocked with heat inactivated BSA (5 mg/ml) blocking buffer for 1h at room temperature. After blocking, coverslips were washed with PBS before addition of 200 µl washed platelets ($2x10^{7}$/ml). Where stated platelets were pre-incubated with inhibitors such as dasatinib (10 µM), PRT (10 µM) or PP2 (10 µM). Platelets were allowed to spread for 45 min at 37^{o}C. Non-adherent platelets were removed by gently washing coverslips with Modified Tyrode's buffer before extraction. 300 µl of formalin was then added to each well for 10 min at RT. PBS washes were performed before mounting onto glass slides with Hydromount (National Diagnostics, Atlanta, USA). Platelets were imaged using a

differential interference contrast (DIC) microscope (Zeiss Axiovert 200, 63x oil immersion). Adherent platelets were counted and platelet surface area was measured using Image J software (NIH, Bethesda, USA). At least 7 fields of view were taken per condition.

2.6.6. Monolayer phosphorylation samples

Plates (10 cm diameter) were coated with agonists overnight at 4^{o}C, washed and blocked with heat-inactivated BSA (5%) blocking buffer. Washed platelets (5x10^{8}/ml) were pre-treated with apyrase (2 U) and indomethacin (10 μM) before being added to immobilised protein-coated plates for 45 min at 37^{o}C. Non-adherent platelets (basal samples) were removed and lysed in ice cold 2X lysis buffer. Adherent cells were lysed for 15 min on ice with 1X lysis buffer (1 ml). Protein concentration of the lysates was measured to adjust for equal protein levels for Western blotting.

2.6.7. SDS-PAGE and Western blotting

WCLs and IPs containing sample buffer were heated to 100^{o}C for 5 min, and centrifuged at 8600 g for 5 min, before being run on either; pre-cast sodium dodecyl sulphate polyacrylamide gels (4-12%), NuPage gel (Novex, Life Technologies) or a 4-12% gradient BOLT gel (Invitrogen, UK). Pre-stained molecular weight markers (Bio-Rad, Hemel Hempstead, UK) were run alongside samples to determine molecular weights of proteins of interest. Samples were separated by SDS-polyacrylamide gel electrophoresis and transferred onto a polyvinylidene difluoride (PVDF) membrane. Membranes were blocked in 3% BSA in TBS-T (Tris-buffered saline (200 mM Tris, 1.37 M NaCl; pH 7.6) with 0.2% Tween20 and 0.1% w/v sodium azide) for 1 h at RT or

overnight at 4^{o}C depending on antibody used. Membranes were then incubating with primary antibody diluted in 3% BSA-TBS-T (primary antibody concentration dependent on experiment) for 1 h at RT or overnight at 4^{o}C. Membranes were washed 4 times for 10 min in TBS-T incubation with HRP-conjugated secondary antibody (GE Healthcare, UK) in TBS-T for 1 h at RT. Enhanced chemiluminescence reagent (ThermoScientific Paisley, UK) was added to the blots before imaging on autoradiographic film or imaged with the Licor Odyssey-FC imager (Chemiluminescence channel; Cambridge, UK) for band quantitation.

In experiments where membranes required reprobing, membranes were incubated with stripping buffer (TBST-T containing 2% SDS) containing 1% β-mercaptoethanol for 20 min at 80˚C. The stripping buffer was removed and stripping buffer without β-mercaptoethanol was added for a further 20 min at 80˚C. After 4 washes of 10 min in TBS-T, membranes were processed again for Western blotting. Li-cor Image Studio software was used for protein band quantitation. A blank area of the membrane was defined as background and densitometry measurements were made after the area was placed over the bands. The imaging software subtracted the background from the signal to give integrated intensity of each measured band.

2.6.8. NFAT luciferase reporter assays.

Jurkat T-cells were grown in complete RPMI media. 2×10^{7}cells were transfected in 0.4 ml of either 1% serum or serum-free RPMI by electroporation using a GenePulser II (Bio-Rad). GenePulserII was set at 350 V and 500 μF for DT40 cells and 250 V and 950 μF for Jurkat cells. DT40 cells were transfected with 15 μg of the NFAT-luciferase

reporter and 2 μg of both human GPVI and human FcRγ-chain. Where described 10 μg of human CLEC-2 was added (constructs detailed above). For Jurkat cell transfection, cells were transfected with 3.75 μg of the NFAT-luciferase reporter, 0.5 μg each of human GPVI and human FcRγ-chain and where stated 2.5 μg of human CLEC-2. Complete RPMI media was added to the transfect cells and cells were incubated at 37^{o}C overnight. After 20 h, cells were counted and diluted to 2×10^{6}cells/ml in complete RPMI media or serum-and antibiotic-free media as stated. Agonist were added to wells of a 96 well plate at 2X required concentration in a 50 μl volume. Phorbol 12-myristate-13-acetate (PMA: 50 ng/ml) and ionomycin (1 μM) were used as positive controls. 50 μl of cells were added to the agonist well. RPMI was used for basal samples. Cells were incubated with agonists for 6 h at 37^{o}C, before luciferase assays were performed in triplicate. Luciferin (1 mM) in dd$H_2$0 was add to wells and used also to prime the luminometer. 11 μl of luciferase harvest buffer (1M KPO_4, 12.5% Triton X-100 and 1 M dithiothreitol (DTT)) was added to each well and plate was left to incubate for 5 min at RT. 90 μl of luciferase assay buffer (1 M KPO4, 1 M $MgCl_2$, 0.1 M ATP and dd$H_2$0) was transferred to an opaque 96-well plate before measurements with the microplate luminometer (Berthold Technologies, Wildbad, Germany). The instrument was primed with luciferin (1 mM) followed by sequential injection into the wells (50 μl, counting time 10 s per well). Measured luminescence was averaged across triplicates and normalised relative to basal.

2.7. Animal Experimentation and *In vivo* models

Collagen and histone infusion work performed in collaboration with

2.7.1. Collagen infusion thrombosis model

WT and GP6$^{-/-}$ mice were injected into the tail veins with collagen (25 μg) and adrenaline (1 μg) to induce thrombocytopenia as described (Abrams et al., 2013). Decrease in platelet count was calculated by comparing the platelet count from a basal sample, collected from a tail bleed taken before injection and the platelet count taken by a terminal cardiac puncture taken 3 min after agonist injection.

2.7.2. Histone infusion thrombosis model

A histone infusion *in vivo* model was used to assess whether histones activate platelets through GPVI by injecting CTH (2.5-75 mg/kg) into tail veins of WT and Gp6 $^{-/-}$ mice. A basal platelet count (tail vein bleed) was measured before CTH infusion and 3 min post CTH injection (terminal cardiac puncture). The drop in platelet count from the basal level indicated the level of platelet aggregation through histone-induced thrombocytopenia. Where stated, hirudin (10 mg/kg) was injected by intraperitoneal injection 5 min before CTH injection (25 mg/kg).

2.7.3. Wound punch biopsies

helped with anaesthesia monitoring during surgery, restraining of mice for wound healing measurements and with staining of collected wounds.

Punch biopsies were taken from GP6$^{-/-}$, Pdpn$^{fl/fl}$ Vav-1-Cre, Clec1b$^{fl/fl}$ PF4-Cre mice and WT mice. Mice were given buprenorphine 30 min before surgery. Mice were anaesthetised using isoflurane and area undergoing biopsy was shaved before a small (4 mm) full-thickness punch biopsy was taken from the flank skin under sterile surgical conditions. Analgesia was given daily for two days post biopsy. Wound diameters were imaged and measured daily for 10 days to establish the rate of wound closure. Mice

were culled by Schedule-1 methods to collect skin biopsies for Hematoxylin and Eosin (H&E) staining to define structure (section 2.7.4) and collect blood for platelet count measurements (see section 2.2.2).

2.7.4. Immunohistochemistry

Paraffin embedding and sectioning

Skin wound biopsies collected were washed in PBS three times before being fixed in 4% paraformaldehyde (PFA) overnight. Samples were then dehydrated in increasing concentrations of ethanol (ETOH), 70% ETOH or 1 h, 2 x 95% ETOH for 30 min and 2 x 100% ETOH for 30 min, followed by Histoclear (National diagnostics, Hessle, UK) for 2 h. Samples were embedded in paraffin at 58^{o}C for 2 h. Paraffin embedded samples were oriented, mounted into blocks and stored at RT. Tissue sections of 4-8 µm thickness were collected onto polylysine adhesion slides (ThermoScientific Paisley, UK) for staining.

Staining

For H&E staining, paraffin was removed by dehydrating in Histoclear twice for 5 min and 3 min, followed by rehydration in concentrations of ETOH; 100% ETOH for 3 min, 90% ETOH for 1 min, 75% ETOH for 1 min, 55% ETOH for 1 min, 30% ETOH for 1 min. Samples were placed in H_20 for 3-5 min. Slides were stained for 2 min in Harris' Haematoxylin and washed three times with tap water before being dipped twice in 0.3% acid alcohol. Slides were rinsed in tap water, added briefly to Scott's tap water and then dipped 10 times in Eosin. Slides were rinsed further in water and dehydrated once more in 70% ETOH>90% ETOH >100% ETOH for 3 min each step. Slides were then placed in Xylene substrate overnight. The following day slides were mounted onto coverslips

using Hydromount (National Diagnostics, Hessle, UK) mounting media. Slides were imaged and analysed using the Zeiss Axio Scan.Z1 microscope.

For antibody staining, after rehydration, sections were boiled in citric acid buffer (pH 6.0) for 15 min. Sections were cooled to RT and washed in PBS-T (0.1% Tween20). Endogenous peroxidase was blocked with 3% H_2O_2 for 10 min, followed by blocking with 5% goat serum plus 1% BSA-PBS-T for 1 hour at RT. Sections were then incubated with the primary antibody (anti-podoplanin monoclonal antibody 1/500 in 3% BSA-PBS-T) overnight at 4°C. Slides were then washed in PBS-T before incubation with the secondary antibody (goat anti-hamster IgG HRP-conjugated 0.8 µg/ml) in PBS-T for 1 h at RT. After further washes in PBS-T, ImmPACT DAB® peroxidase substrate (SK-4105, Vectorlab) was added for 2.5 min. Tissue sections were counter stained for haematoxylin, dehydrated, mounted and analysed as above.

2.8. Flow cytometry

2.8.1. Microvesicle experiments

Podoplanin expression on microvesicles: 30 µl of double spun plasma (section 2.3.4) from patients and HCs were incubated in the dark at RT for 20 min with 20 µl of antibody mix of rat anti-human podoplanin–PE antibody (1/100) or the IgG2a κ control (1/100) and the anti- CD45- APC antibody (1/200). After incubation the sample was further diluted in Tyrode's buffer + 0.2% formaldehyde before analysis by flow cytometry (BD Accuri).

2.8.2. GPVI dimerisation studies

Washed platelets ($5x10^7$ cells/ml) were stimulated with agonists at concentrations used for platelet aggregation. 10 µl of stimulated platelets were incubated for 10 min with 10 µl of the 204-11 primary antibody (F.C. 25 µg/ml), that detects GPVI dimers, followed by incubation with the secondary antibody conjugated to AF-647 (F.C. 75 µg/ml), for 10 min. GPVI dimers on the platelet surface were measured by flow cytometry (BD Accuri) before and after stimulation. Resting controls containing both antibodies, no primary antibody and only were also analysed.

2.9. ELISAs

2.9.1. Soluble GPVI (sGPVI) ELISA

sGPVI levels in patient plasma and HCs were measured using a recognised sGPVI sandwich ELISA (Al-Tamimi et al., 2009). Nunc MaxiSorp® micro-titer 96 well plates (ThermoScientific, Paisley, UK) were coated overnight at 4^{o}C with a rabbit polyclonal anti-human GPVI antibody (1 µg/ml) that recognises the N-terminal extracellular portion of cleaved GPVI. Plates were washed 6 times in 0.2% v/v Tween20 in PBS before blocking in BSA (1%) in PBS for 1 h. After 6 washes in PBS-T, test samples or sGPVI standards generated by the serial dilution of GPVI ectodomain (prepared from N-ethylmaleimide [NEM]-treated platelet-rich plasma) into GPVI-depleted plasma (5% in PBS) were added to the plate and left to incubate for 1 h at RT. After 6 further PBS-T washes, samples were incubated with a mouse anti-human GPVI monoclonal antibody (IA12: 1 µg/ml) for 1 h. Samples were washed 6 times in PBS-T before incubation with a polyclonal rabbit anti-mouse immunoglobulins/HRP antibody (DAKO, Denmark; 2.6 µg/ml) for 1 h at RT. Plates were washed 6 times in PBS-T before. 100 µl of

SuperSignal ELISA Pico chemiluminescent substrate (Pierce, Rockford, IL, USA), was added for 1 min before detection of the chemiluminescence signal using the Wallac-Victor3 luminescence plate reader (PerkinElmer, Massachusetts, USA) for 10s/well. sGPVI concentrations for the patient samples were extrapolated from the standard curve generated.

2.9.2. GPVI binding to immobilised agonists

Binding of GPVI to immobilised agonists including fibrin/fibrinogen was measured using an adapted version of a sGPVI ELISA (section 2.9.1). Wells of Nunc MaxiSorp® micro-titer plates were coated with agonists overnight at 4^{o}C. Wells were washed six times with 100 µl of 0.2% v/v Tween20 in PBS before being blocked with 1% (w/v) BSA for 1 h at RT. After 6 washes in TBS-T, the GPVI ectodomain (again prepared from NEM treated plasma) was added to the wells and incubated for 1 h at RT. A standard curve was generated by a series dilution of GPVI ectodomain added into GPVI depleted plasma (5%) as in section 2.9.1. Primary and secondary antibody incubation steps and washes were performed as stated in section 2.9.1. Levels of GPVI bound were extrapolated from the standard curve generated.

2.9.3. Podoplanin (Pdpn) ELISAs

Sandwich ELISA: A Pdpn sandwich ELISA was developed to measure human recombinant podoplanin (rPdpn) and plasma Pdpn in septic patients and HCs. Nunc MaxiSorp® micro-titer 96 well plates (Thermo Scientific, Paisley, UK) were coated overnight at 4^{o}C with mouse anti-human Pdpn antibody (18H5: 0.5 µg/ml) that recognises the PLAG1/2 domain in the Pdpn extracellular tail. Plates were washed 6

times in 0.2% v/v Tween20 in PBS before blocking in BSA (1%) PBS for 1 h at RT. After 6 washes in PBS-T, a serial dilution of human rPdpn (0.3 µg/ml to 10 µg/ml) in ddH_20 was added to the plate and left to incubate at RT for 1 h. Samples were washed 6 times in PBS-T washes before incubation of a rat anti-human Pdpn antibody (NZ-1.3: 1 µg/ml) for 1 h at RT. Six more PBS-T washes occurred before incubation with a polyclonal goat anti-rat HRP antibody (DAKO, Denmark; 2.6 µg/ml) for 1 h at RT. Plates were washed 6 times in PBS-T before incubation in SuperSignal ELISA PICO chemiluminescence substrate added for bound antibody detection. Chemiluminescence signal (wavelength 425nm) was detected by the Wallac-Victor3 luminescence plate reader (PerkinElmer, Waltham, MA). Pdpn standard curve was generated using GraphPad Prism software (version 5).

Competitive ELISA: Nunc MaxiSorp® micro-titer 96 well plates (Thermo Scientific, Paisley, UK) were coated for 1 h at RT with human rPdpn (3 µg/ml). Plates were washed 6 times in PBS-T before blocking for 1 h in BSA-PBS (1%). Samples were washed again 6 times in PBS-T. Human rPdpn at various concentrations (0.3 µg/ml – 10 µg/ml) and rat anti-human Pdpn antibody (NZ-1.3: 1 µg/ml) were added to separate tubes for 1 h incubation. Samples from this tube were transferred to the ELISA plate coated in human rPdpn (3 µg/ml) and left to incubate for 1 h at RT. Wash steps, incubation step with the polyclonal goat anti-rat HRP antibody (DAKO, Denmark; 2.6 µg/ml) and chemiluminescence signal detection was performed as with the sandwich Pdpn ELISA above. Pdpn standard curve was also generated using GraphPad Prism software (version 5).

Commercial ELISA – A commercial Pdpn ELISA (Biomatik, Ontario, Canada) was used to detect rPdpn and Pdpn in plasma samples from septic patients and HCs, following manufacturer's instructions. A standard curve was generated using the manufacture's reagents. A series dilution of recombinant Pdpn was added to the plate to compare standard curves. Three HC plasma samples and four septic patient samples were tested for detection of plasma podoplanin.

2.10. Podoplanin (Pdpn) upregulation

2.10.1. Podoplanin upregulation after LPS stimulation

Whole blood (in 4% citrate) was stimulated by adding LPS 0111 (0.1, 1 µg/ml) in the presence of GPRP (10 µM) and integrilin (9 µM). Blood was diluted 1/5 in RPMI and left on a shaker at 37^{o}C for 4 h and 24 h. Unstimulated blood was used for compensation at corresponding time points. 100 µl of blood from each time point was incubated with antibody mix of CD45-APC or CD14-APC and CD41-FITC and Pdpn-PE or isotype or CD41-PE for 20 min at RT. RBCs were then lysed and samples fixed using the BD Cytofix kit (BD biosciences, Oxford, UK). Pdpn upregulation and neutrophil/monocyte platelet complexes were measured by flow cytometry.

2.10.2. Podoplanin upregulation on stimulated cells.

PBMCs: PBMCs isolated (in section 2.4.1) were on a 6-well plate at 1x10^{6}/ml and treated with staurosporine (1 µM) and cycloheximide (25 µg/ml) or LPS 0111 (100 ng/ml) for 16 h. Untreated cells were used as controls. Cells were blocked using 10% FBS-TBS buffer, washed and stained for CD38, Pdpn (Anti-Pdpn NZ-1.3 Antibody) and Annexin V (BD Biosciences; Oxford, UK) in 1% FBS-TBS buffer + $CaCl_2$ (1 mM)

for 20 min, before washing again in 1% FBS-TBS + $CaCl_2$ (1 mM) buffer. Pdpn upregulation was measured on Annexin V+ cells (activated/ dying cells) and Annexin V- cells.

Monocytes: Isolated monocytes isolated (see section 2.4.2) were incubated on 6-well plates at $1x10^6$/ml. THP-1 were also used for stimulations. Monocytes were treated with staurosporine (1 µM) and cycloheximide (25 µg/ml) or LPS (0111: 100 ng/ml) for 16 h. Untreated cells were used as controls. Cells were washed, blocked and stained for CD14, Pdpn (Anti-Pdpn NZ1.3 Antibody) and Annexin V as above. Pdpn upregulation was compared on Annexin V+ and Annexin V- cells.

Macrophages: Monocyte-derived macrophages were differentiated from GM-CSF (50 ng/ml) and M-CSF (100 ng/ml) treated monocytes (see section 2.4.2) and were then treated with staurosporine (1 µM) and cycloheximide (25 µg/ml) or LPS 0111 (100 ng/ml) for 16 h. Cells were washed, blocked and stained for CD68, Pdpn (Anti-Pdpn NZ1.3 Antibody) and Annexin V. Pdpn upregulation was compared on Annexin V+ and Annexin V- cells.

2.10.3. Platelet activation by cells with upregulated podoplanin

Isolated human monocytes were differentiated into macrophages using GM-CSF and M-CSF and stimulated with LPS (100 ng/ml) for 16 h. Macrophages (0.3 million cells/ml) were incubated with platelets ($2x10^7$/ml) from the same donor in the presence of integrilin (9 µM) and stirred at 1200 rpm for 10 min at 37^oC. PGI_2 (10 µg/ml) and FBS (10%) was added to prevent further interactions for 10 min before antibody

staining for 20 min. Cells were fixed in PFA (4%) and platelet activation was determined by flow cytometry. A P-selectin antibody (CD62P) was added used to determine if adhered platelets were activated. Stimulated washed platelets ($2x10^7$/ml) were stained for CD41 and P-selectin as positive controls. NZ-1.3 anti-Pdpn Ab (unconjugated; 10 µg/ml) was added to washed platelets and macrophages before stirring to block Pdpn and determine if platelet/macrophage interactions mediated platelet activation.

2.10.4. Trypsin cleavage of 293T cells

Human 293T cells (embryonic kidney cells) were grown in complete RPMI. When confluent cells were isolated from flasks and centrifuged at 300 g for 5 min and resuspended in RMPI to required concentrations. Trypsin (10%) was added to the cells for 15 min and 30 min and 1 h. Cells were centrifuged at 300 g for 5 min. Supernatant was removed and cell pellet resuspended in 1 ml of 10% FBS in TBS (FBS-TBS). 100 µl of supernatant was extracted for staining, whilst the rest was centrifuged at 2500 g for 15 min. Resuspended cells and supernatants were stained with Pdpn antibodies (NZ-1.3 and 18H5) and isotype controls for 20 min in 1% FBS-TBS buffer. Cells were washed and podoplanin expression measured by flow cytometry.

2.11. Statistical analysis

2.11.1. General statistical analysis

Results are shown as mean ± SD, unless stated otherwise. D'Agostino-Pearson normality tests were performed to determine normality. Student's T-tests were performed when there were two groups and data showed normal distribution. Mann-

Whitney tests were performed when the data was not normally distributed. One-way ANOVA with a Bonferroni post-test or Kruskal-Wallis tests with Dunn's post tests were performed when there were more than two groups for comparisons when the data was shown to be normally distributed or not normally distributed respectively. Statistical tests were performed using GraphPad Prism (version 5) software.

2.11.2. Logistic regression and longitudinal analyses of sGPVI in thermal injury patients

Analysis performed by Jonathan Bishop as part of the SIFTI study.

Categorical variables were compared using a Chi-squared test. Logistic regression analyses examined the relationships between sGPVI at pre-specified sample days (e.g. day 7) and sepsis presence. Discriminatory power was assessed through the area under the receiver operator characteristic curve (AUROC). Longitudinal analyses were performed using linear mixed-effects models. Sample day was included as a restricted cubic spline to allow for a flexible non-linear relationship between time and response variable. Analysis was performed using SPSS (IBM) and R version 3.0.1 (http://www.r-project.org) statistical software packages alongside lme4, effects, rms and pROC packages.

CHAPTER 3

ALARMIN-MEDIATED PLATELET ACTIVATION

3.1 Introduction

A major new focus of trauma research, alongside preventing extensive blood loss, is targeting a wide range of secondary complications that can occur post injury due to the complexity of different traumas, including amplified inflammation resulting in multiple organ failure (MOF). Alarmins is a term given to endogenous danger associated molecular pattern molecules (DAMPs) released from damaged cells (Harris and Raucci, 2006). Binding of Alarmins to corresponding Alarmin receptors on the surface of immune cells induces intracellular signalling pathways mediating a pro-inflammatory response (Manson et al., 2012). Several of the described Alarmin receptors are located on the platelet surface, providing a potential avenue for Alarmin-mediated platelet activation and further cytokine release (Clark et al., 2007, Zhang et al., 2010, Zhu et al., 2012).

The 'danger theory' behind the action of DAMPS was first described by Mazinger (1994). This was the theory that DAMPs are the host version of Pathogen Associated Molecular Pattern molecules (PAMPs), with PAMPs being microbial derived molecules which bind to pattern recognition receptors (PPRs), which include a number of toll-like receptors (TLRs) (Matzinger, 1994). PAMPs bind to PPRs, leading to activation of signalling mechanisms, antigen presentation or production of pro-inflammatory cytokine production (Kono and Rock, 2008, Manson et al., 2012). DAMPs are thought to work through a similar mechanism, which when released after damage will signal through PPRs and TLRs after binding, mediating a pro-inflammatory response resulting in increased cytokine production (Manson et al., 2012, Kono and Rock, 2008). In unchallenged conditions, DAMPs will remain hidden in the cell and not released. Figure

3.1 shows a schematic of the control of DAMPs. If the cell is programmed to die, the living cell will undergo apoptosis in a controlled manner, where the DAMPs will remain hidden as the cell is phagocytosed and removed, meaning that no inflammatory response will occur. When the cell undergoes severe damage, as observed with trauma, cells will become necrotic, releasing their contents and DAMPs. These DAMPs are then able to circulate and find their corresponding DAMP receptors eliciting the pro-inflammatory response, with increased production of cytokines, such as IL-1 (Srikrishna and Freeze, 2009, Chan et al., 2012). Cytokine levels remain elevated for several days after injury and can lead to development of systemic inflammatory response syndrome (SIRS) and increased MOF incidence and higher mortality rates (Jastrow et al., 2009, Hranjec et al., 2010).

3.1.1 Trauma Alarmins

Alarmins is the term give for DAMPs released in response to trauma. There are a wide range of Alarmins released from multiple cell types which have various effects leading to a pro-inflammatory phenotype. Table 3.1. lists a number of the most extensively studied Alarmins which are elevated after trauma, with the predominate group being nuclear-related Alarmins. These are nuclear material/proteins released after damage to the nucleus and include DNA, high-mobility-group-box-1 protein (HMGB-1) and histones.

HMGB-1 interacts with other nuclear proteins to regulate DNA organisation along with helping to support gene transcription. HMGB-1 levels have been measured in patients with sepsis and other inflammatory conditions (Klune et al., 2008) and can be elevated 30 fold after trauma (Park et al., 2004). HMGB-1 has been proposed to signal through

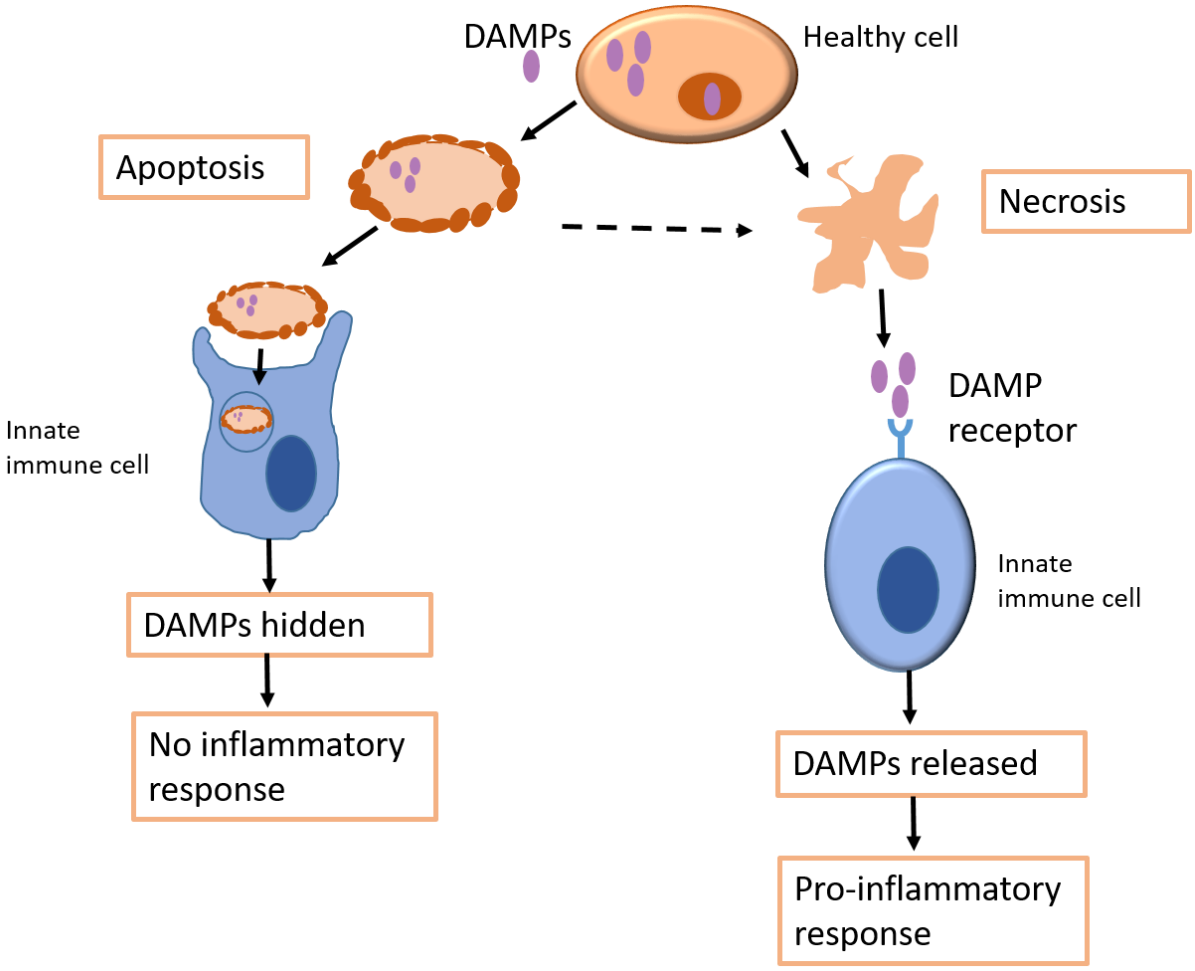

Figure 3.1 - Schematic of the control of DAMP release in controlled and inflammatory settings (based on (Kono and Rock, 2008)). In healthy cells DAMPs are kept inside the cell or located in the nucleus. With normal controlled cell death, cells undergo apoptosis, where the DAMPs remain hidden, as cells are phagocytosed by immune cells and DAMPs are never released. Under inflammatory challenge or damage, cells undergo necrosis, releasing DAMPS. These exposed DAMPs are then able to bind to innate immune cells and induce a pro-inflammatory response, increasing pro-inflammatory cytokine production.

TLRs and **R**eceptor for **A**dvanced **G**lycation **E**ndproducts (RAGE) to activate immune cells. HMGB-1 has been implicated in promoting neutrophil extracellular trap (NET) formation through interactions with TLR4 (Tadie et al., 2013). HMGB-1 has been described to have several inflammatory roles, including promoting pro-inflammatory cell recruitment to damaged areas through forming a complex with CXCL12 (Schiraldi et al., 2012). The role of HMGB-1 in platelet activation has yet to be established.

DNA is another nuclear-related Alarmin which can be measured in the plasma of patients. Cell-free DNA, is DNA released from cells and is a marker of disease severity and a strong predictive marker for sepsis in patients with thermal injury (Margraf et al., 2008, Hampson et al., 2016). DNA released from neutrophils in the form of NETs has been extensively studied. NETs are made up of extracellular DNA, serine proteases and anti-microbial molecules, involved in trapping and elimination of bacteria (Clark et al., 2007). Long extracellular extrusions of NETs have been show to provide surfaces for platelets to adhere and undergo activation (Fuchs et al., 2010).

Mitochondrial DNA (mtDNA), is DNA released from mitochondria after damage. MtDNA can also be measured in the plasma of trauma patients, remaining elevated for 24 hours (Zhang et al., 2010). MtDNA been shown to increase endothelial permeability during systemic inflammation (Sun et al., 2013) and is associated with acute lung injury and neutrophil activation (Hauser et al., 2010). MtDNA has been shown to bind to TLR9 and may potentially bind other pathogen recognition receptors, as mtDNA contains similar unmethylated CpG DNA repeats to those seen in the bacterial genome,

resulting from endosymbiosis, which suggests mtDNA can signal in a similar fashion to bacterial DNA (Fang et al., 2016, Zhang et al., 2010).

Histones are a major component of NETs and another type of nuclear-related Alarmins. Histones are highly positively charged with important roles in DNA organisation and chromatin formation. Histones have multiple effects on different cell types and can mediate cytokine activation and thrombin generation (Semeraro et al., 2011). Histones are also elevated in the circulation in response to lung injury and trauma (Abrams et al., 2013). Circulating histones can be cytotoxic to endothelial cells, causing substantial cell damage. Histones are proposed to activate platelets through TLR4 interaction (Fuchs et al., 2011b, Semeraro et al., 2011). However, the charge of histones could disrupt membranes allowing potential binding to other receptors. Several studies have shown that therapeutics prevent histones induced thrombocytopenia and increase survival after histone treatment, ranging from heparin treatment to active protein C (APC) (Fuchs et al., 2011b, Xu et al., 2009). Therefore, mechanisms of histone-induced platelet activation are yet to be fully established.

3.1.2 DAMPs implicated in inflammation

Oxidised low density lipoprotein (OxLDL) is a lipid-based DAMP, associated with hyperlipidaemia and has been shown to accumulate in atherosclerotic lesions (Matsuura et al., 2008). OxLDL is formed after lipid peroxidation of lipids and apolipoprotein B (apoB) components (Stewart et al., 2005). OxLDL has been shown to bind to the scavenger receptor CD36, which is abundantly expressed on platelet surfaces, with a copy number of 20, 000 per platelet (Saboor et al., 2013). OxLDL therefore has the potential to bind to platelets and affect platelet function. Advanced Glycation End

Products (AGE) are another type of DAMPs which have been implication in conditions such as diabetes and atherosclerosis (Goldin et al., 2006). AGE are glycated proteins that have undergone further protein modifications. Studies have shown AGE can elicit a prothrombotic phenotype by enhancing platelet reactivity through CD36 signalling.

3.1.3 Alarmin receptors

A number of Alarmin receptors identified on other cell types have been described (Figure 3.2). Some of these Alarmins shown such as TLRs are located on the platelet surface, therefore giving a potential mechanism for platelets to contribute to the pro-inflammatory response.

3.1.3.1 Toll-like receptors (TLRs)

TLRs are recognised Alarmin receptors on a range of immune cells. Signalling results in a pro-inflammatory response. TLRs are a family of receptors involved in host defence against pathogens, which recognise PAMPs and DAMPs, activating the immune response (Cognasse et al., 2005). Eleven TLRs have been characterised with functional roles, with TLR2, TLR4 and TLR9 having been described on the platelet surface (Cognasse et al., 2005). TLR signalling involves the NF-kB/TRIF/Myd88 signalling cascades (Garraud and Cognasse, 2010). TLR2 and TLR4 have been shown to have roles in recognition of bacterial-derived molecules. Platelet TLR4 is also associated with platelet-neutrophil interactions and implicated in NET formation (Clark et al., 2007). TLR9 recognises bacteria DNA and MtDNA. TLR9 recognises MtDNA as it contains bacterial-derived CpG DNA repeats, which entered the mitochondrial genome after the endosymbiosis event (Zhang et al., 2010) .

3.1.3.2 Scavenger receptors

RAGE is a 35kDa scavenger receptor, expressed at low levels in normal tissue, but is upregulated at inflammatory sites (Chavakis et al., 2004). RAGE has been shown to interact with ligands such as AGE to contribute to persistent NF-κB activation, which may result in hyperglycaemia (Bierhaus et al., 2001). RAGE has also been described as a receptor for HMGB-1 in different inflammatory settings and cancer (Sims et al., 2010).

CD36, also referred to as (GPIIIb) is a class B scavenger receptor. It is described as the major receptor implicated in OxLDL signalling, facilitating microparticle binding (Ghosh et al., 2008) and long-chain fatty acid transport (Su and Abumrad, 2009). CD36 has been implicated in atherosclerosis, hyperlipidaemia, and insulin insensitivity in diabetes mellitus (Podrez et al., 2007). CD36 has also been implicated in sterile inflammation, due to increased CD36-TLR4-TLR6 heterodimer complex assembly being observed (Stewart et al., 2010). The CD36 signalling mechanism has yet to be fully established.

Table 3.1. A range of Alarmins implicated with trauma – based on Alarmins reviewed in Manson et al. (2012). List of Alarmins, source they are released from after damage, proposed receptor to induce and elevated levels in response to trauma. HC = healthy controls.

Alarmin	Source	Proposed Receptor	Raised levels in trauma	Fold increase compared to HCs	References
ATP	Mitochondria	P2X7	-	-	(Schneider et al., 2006)
DNA	Nucleus	-	181 000 kilogenome-equivalents/l (Median)	**57-fold increase**	(Lo, 2000)
HMGB-1	Nucleus	TLR2/ TLR4 /RAGE	526 ng/ml (Median)	**30-fold increase**	(Bianchi and Manfredi, 2007) (Park et al., 2004) (Cohen et al., 2010) (Peltz et al., 2009)
Histones	Nucleus	-	10 – 230 µg/ml	**200-fold increase**	(Abrams et al., 2013) (Xu et al., 2009)
DNA	Nucleus	-	181 000 kilogenome-equivalents/l (Median)	**57-fold increase**	(Lo, 2000)
MtDNA	Mitochondria	TLR9	2.7 ± 0.94 µg/ml (Median)	**1000-fold increase**	(Zhang et al., 2010)
Nucleosomes	Nucleus	-	53 units/ml (Median)	-	(Zeerleder et al., 2003)
sRAGE	Extracellular	-	1500 pg/ml (Median)	-	(Cohen et al., 2010)
Uric acid	Cytoplasm	TLR2, TLR4, CD14,	-	-	(Rock et al., 2005) (Shi et al., 2006)

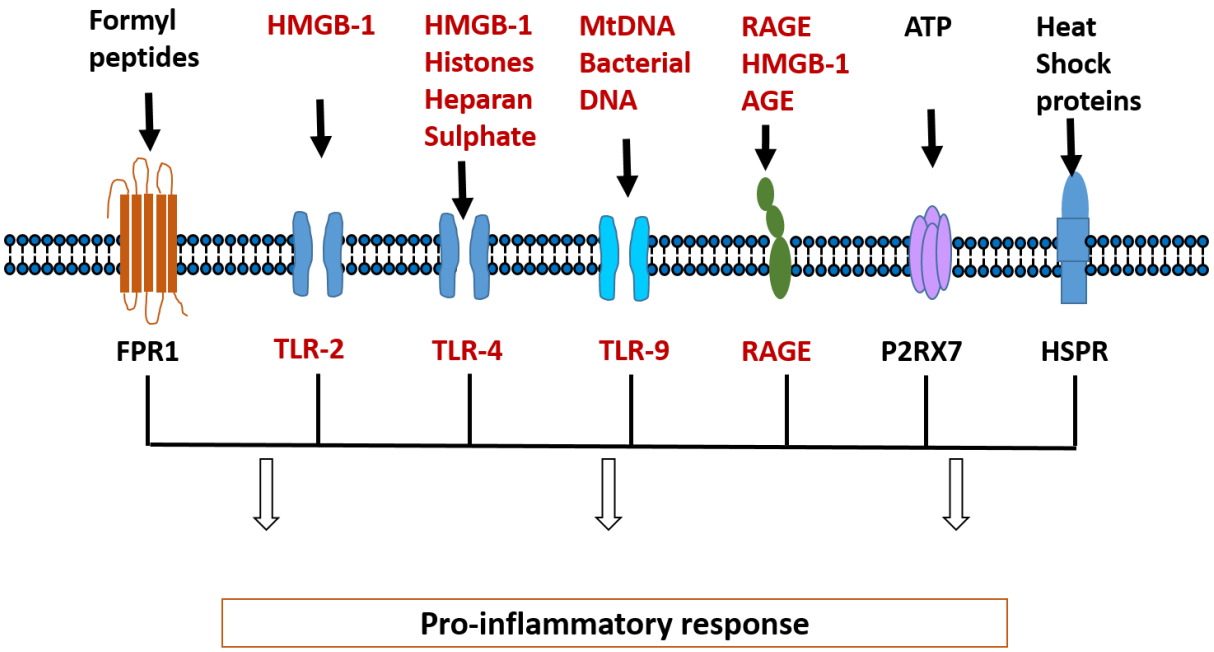

Figure 3.2. Alarmins and their corresponding receptors (Based on (Manson et al., 2012))**.** Trauma Alarmins released after damage bind to the corresponding Alarmin receptors on innate immune cells and potentially platelets **(red**), leading to intracellular signalling pathways and the production of inflammatory cytokines, resulting in the pro-inflammatory response. FPR: Formyl peptide receptor, HMGB: High-mobility-group box-protein-1, TLR: Toll-like receptor, MtDNA: Mitochondrial DNA, RAGE: Receptor for Advanced Glycation Endproducts, HSPR: Heat-shock protein receptor, P2RX7: Purinergic receptor

Alarmins released in response to cell damage have the potential to affect platelet function. TLR, RAGE and CD36 are potential Alarmin receptors proposed to be involved in platelet activation as well as enhancing the inflammatory response (Stewart et al., 2010, Fuchs et al., 2011b, Clark et al., 2007). The signalling mechanisms of these receptors after Alarmin activation are inconclusive, with multiple receptors being suggested to have an involvement. The potential of these receptors to also be involved clustering of other receptors, including ITAM receptors, leading to platelet activation has not been fully explored. The main aim of this chapter is to firstly determine which Alarmins induce platelet activation and which ones do not. Different categories of Alarmins, including nuclear-related Alarmins, lipid-based DAMPs and other DAMPs such as AGE will all be tested. The Alarmins which mediate platelet activation will then be studied further to uncover the mechanism behind the Alarmin response *in vitro* and *in vivo.*

Routine platelet function assays, such as flow cytometry and light transmission aggregometry (LTA), will be performed to test Alarmin effects on platelet function, and determine if they activate, inhibit or modulate platelet function. The ability of the Alarmins to affect platelet activation when they are immobilised on a surface will also be studied. The signalling mechanisms behind the Alarmin response on platelets will be assessed both when the Alarmin is in suspension and immobilised on a surface, using western blotting for analysis of key signalling proteins. Inhibitors and platelets deficient in certain receptors will be used to determine mechanism behind Alarmin mediated responses. The Alarmins which have the greatest effect on platelet function will be further analysed *in vivo* using infusion models to determine if the Alarmins mediate

platelet activation *in vivo*. Various inhibitors will be tested to see if activation can be prevented, in the hope of finding potential therapeutic targets.

3.2 Results

3.2.1 AGE does not induce platelet activation or increase response to ADP

AGE are formed after modifications of proteins produced from reactions between sugars and the amino groups (Hogan et al., 1992). AGE has been implicated as a mediator of inflammation in diabetes and atherosclerosis (Giacco and Brownlee, 2010, Ono et al., 1998). Previous studies have also suggested that AGE can amplify the response of platelets to other agonists, such as ADP, both in mice and humans (Zhu et al., 2012). AGE has been described to signal through the scavenger receptors RAGE and recently through CD36. Both are potential Alarmin receptors located on platelet surfaces; therefore, AGE is a potential Alarmin candidate inducing pro-inflammatory response through platelets. The effect of AGE on platelet function was examined by light transmission aggregometry (LTA). Stimulation of platelet-rich-plasma (PRP) with AGE complexed with bovine serum albumin (BSA, a carrier protein for AGE; 300 μg/ml) alone did not induce platelet aggregation, giving similar results to a PBS control. To determine if AGE-BSA could enhance platelet aggregation to other agonists, PRP was pre-treated with AGE-BSA (300 μg/ml) for 30 min before ADP (1, 3 and 10 μM) stimulation. AGE-BSA pre-treatment did not enhance the response of platelets to ADP at any of the classical ADP concentrations usually used to induce platelet aggregation (Figure 3.3A). A wide range of AGE-BSA concentrations were also tested, from 10 μg/ml to 300 μg/ml, however there was no enhancement of ADP induced platelet aggregation (results not shown), which is contradictory to results previously shown (Zhu et al., 2012).

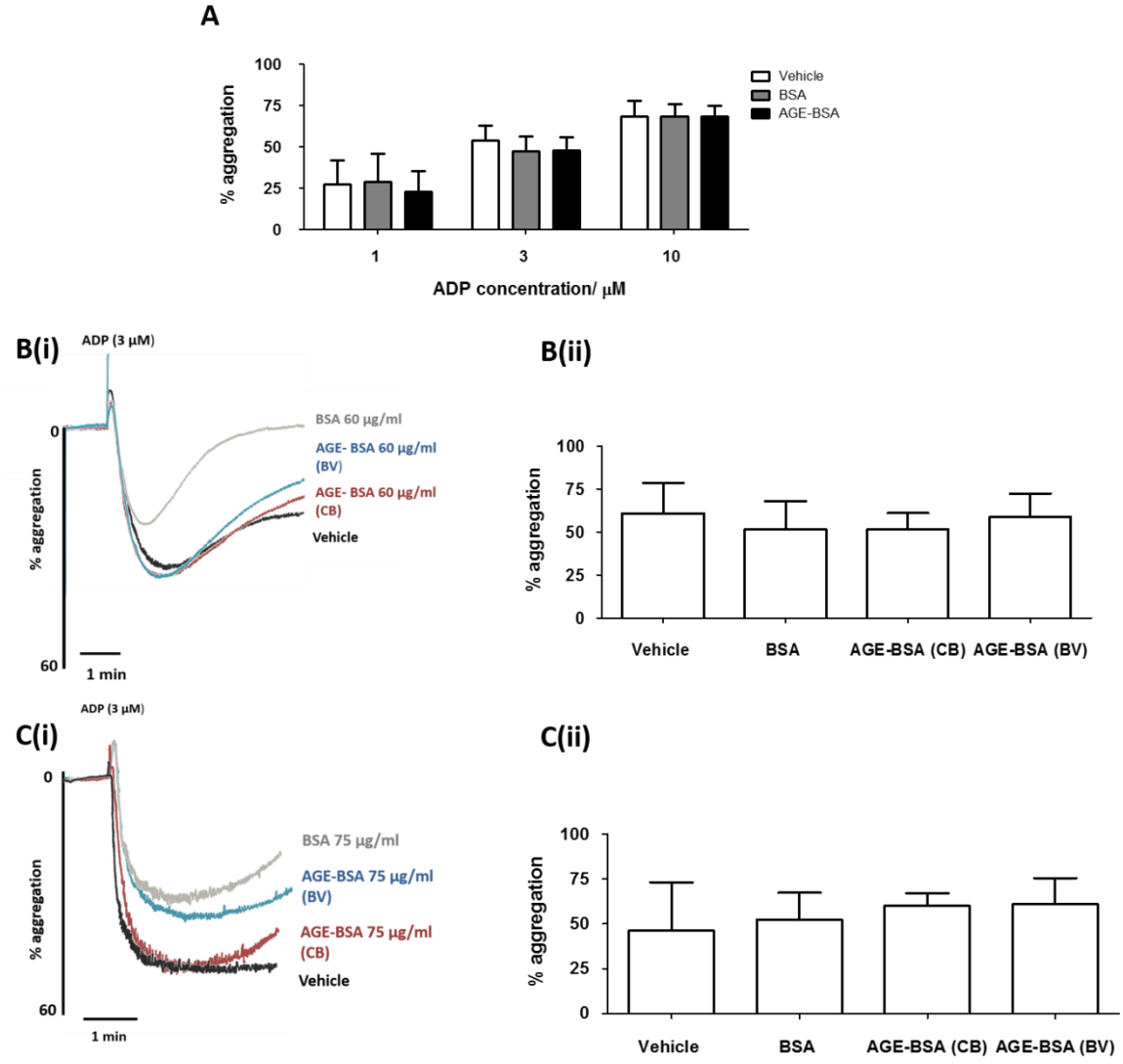

Figure 3.3 - No significant increase in ADP induced aggregation with AGE-BSA pre-treated human and mice platelets. A) Human platelet-rich-plasma (PRP) was pre-treated with AGE-BSA (300 µg/ml: Biovision (BV)) or BSA control (300 µg/ml) for 30 min before stimulation with ADP (vehicle) at different concentrations (1, 3 and 10 µM). Percentage aggregation measured by light transmission aggregometry (LTA). N=3 (per condition), mean ±SEM shown. Two-way ANOVA performed with Bonferroni post-test. No significance shown. B) Human PRP pre-treated with AGE-BSA (60 µg/ml) from Biovision (BV) and Cell Biolabs (CB) or BSA (60 µg/ml) for 30 min before stimulation of ADP (3 µM). (i) Representative trace of 3 separate experiments. (ii)

Average aggregation response for each condition from 3 separate experiments, mean ±SEM shown. One-way ANOVA performed with Bonferroni post-test; no significance shown C) Mouse PRP pre-treated with AGE-BSA (75 µg/ml) from BV and CB or BSA (75 µg/ml) for 30 min before stimulation of ADP (3 µM). (i) Representative trace of 3 separate experiments. (ii) Maximum aggregation response per condition from 3 experiments, mean ±SEM shown. One-way ANOVA performed with Bonferroni post-test; no significance shown.

To investigate whether this was due to the source of the AGE, two different commercial sources of AGE-BSA (Biovision and Cellbiolabs) were compared at similar concentrations used in the Zhu *et al.* (2012) study. However, neither source of AGE-BSA had an effect on platelet aggregation on its own or in response to ADP. Specifically, neither preparations of AGE-BSA at intermediate concentrations altered the time course or magnitude of response to intermediate concentrations of ADP (3 μM) in human PRP (Figure 3.3B; n=3). Similar findings were observed with AGE-BSA treated mouse PRP of mice, with no substantial enhancement of ADP-medicated aggregation (Figure 3.3C).

3.2.2 Oxidised Low Density Lipoprotein (OxLDL) induces minor aggregation of washed platelets

Platelets were stimulated with the lipid-based DAMP, OxLDL to determine effects on platelet aggregation. There was minor increase in platelet aggregation in response to OxLDL in washed platelets (compared to a PBS vehicle), which varied between donors and was all or nothing response (rather than dose-dependent). A wide range of OxLDL concentrations were initially tested based on established concentrations in the literature and previous work performed in our laboratory. The OxLDL concentration of 10 µg/ml gave the greatest response of 16.1 ± 14.7% aggregation (mean ±SD, n=4; Figure 3.4Ai&ii). There was no increase in aggregation response above the PBS vehicle control, with all concentrations of OxLDL tested (Figure 3.4Aiii). The degree of aggregation induced by OxLDL in washed platelets was substantially less than collagen (10 µg/ml), which caused 74.0 ± 13.8% aggregation (Figure 3.2Aii) A small shape change was induced in response to OxLDL. OxLDL has been shown to signal through a Src and Syk dependent pathway downstream of CD36 (Wraith et al., 2013). I used inhibitors of Src and Syk tyrosines to investigate the involvement of GPVI and other ITAM receptors in the OxLDL response. There was no significant reduction in the platelet response to OxLDL (10 µg/ml) observed in the presence of Src inhibitors, dasatinib (10 µM) and PP2 (10 µM) or with the Syk inhibitor PRT060318 (10 µM), when used at concentrations well characterised in our laboratory and in the literature, compared to PBS and DMSO vehicle controls, whereas all inhibitors at substantially reduced the collagen response (***$p<0.005$, n=4; Figure 3.4B), suggesting no major involvement of Src and Syk in the shape change and OxLDL aggregation response.

Interestingly, when the OxLDL-mediated tyrosine phosphorylation was examined through western blotting of whole cell lysates, it was observed that OxLDL induced a similar phosphorylation pattern to collagen-stimulated platelets (Figure 3.4C). The level of increase in whole cell phosphorylation over basal and phosphorylation of specific bands were both similar. There was reduced phosphorylation of signalling proteins mediated by OxLDL stimulated platelets in the presence of the Src and Syk inhibitors, which again was similar to the response to collagen in the presence of inhibitors (Figure 3.4Ci). Immunoprecipitates for the key signalling proteins Syk, FcRγ-chain and PLCγ2 were performed and showed increased phosphorylation above basal conditions, with Syk and PLCγ2 Figure 3.4Cii). There was however a reduced response compared to GPVI ligands, collagen and CRP, but similar levels observed with the CLEC-2 ligand, rhodocytin (Figure 3.4Cii). Increases in phosphorylation of the FcRγ-chain were not observed with OxLDL and rhodocytin stimulation (Figure 3.4Cii). There was also no phosphorylation of CLEC-2 seen after OxLDL stimulation (Figure 3.4Ciii), showing there is no involvement of CLEC-2 in the OxLDL response. Overall this suggests there is a Src and Syk dependent signalling mechanisms alternative to GPVI and CLEC-2 behind the OxLDL response.

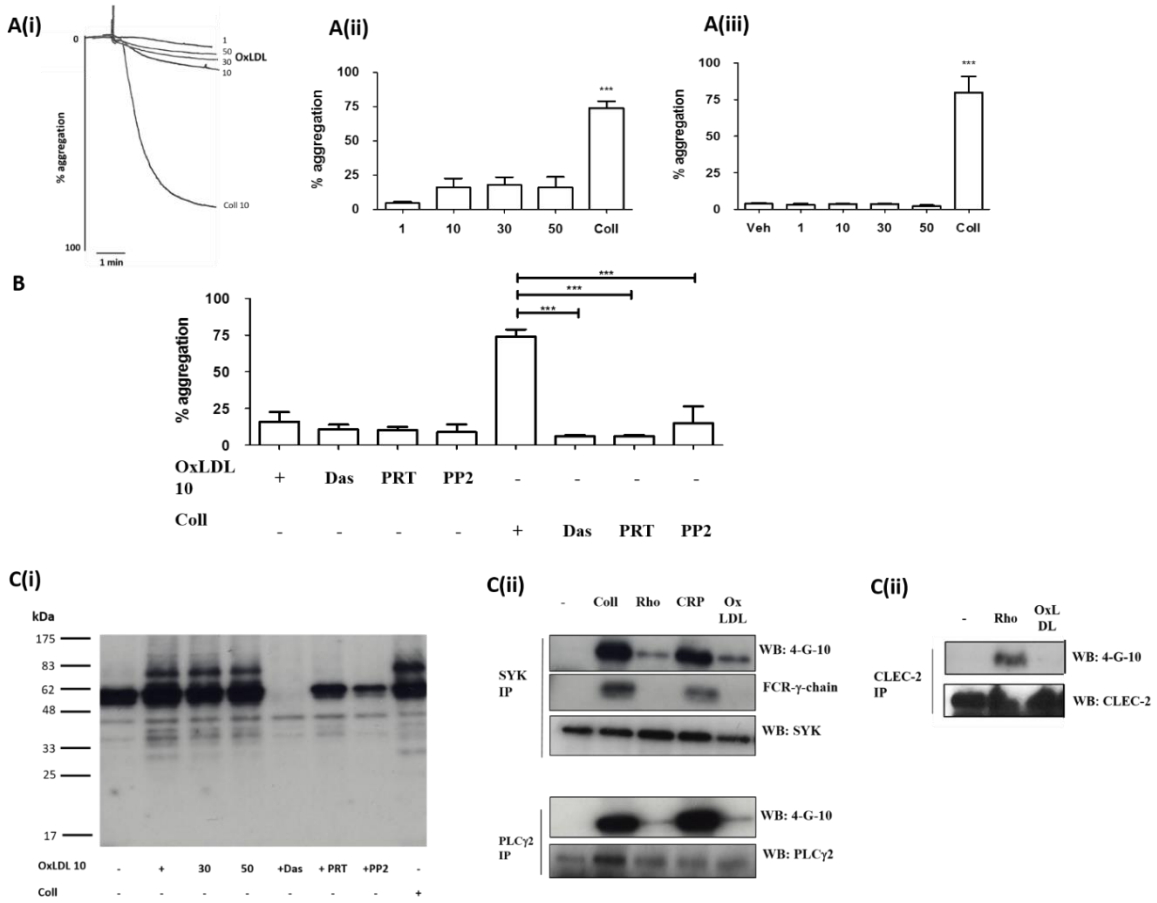

Figure 3.4 - OxLDL induces weak aggregation response in human washed platelets. A(i) Dose response curve after stimulation of human washed platelets ($2x10^8$/ml) with different concentrations of OxLDL (Source Biosciences; 1-50 µg/ml). Representative of trace of 4 experiments. A(ii) Mean aggregation ±SEM; n=4. One-way ANOVA with Bonferroni's post-hoc test performed to compare OxLDL concentrations with the collagen (10 µg/ml) control, ***p<0.005. A(iii) Dose response curve after stimulation of PRP with different concentrations of OxLDL (1-50 µg/ml). Mean aggregation shown as ±SEM; n=3. One-way ANOVA with Bonferroni's post-hoc test performed to compare OxLDL concentrations with the collagen (10 µg/ml) control, ***p<0.005. B) Washed platelets pre-incubated with dasatinib (10 µM), PRT (10 µM) and PP2 (10 µM) 1 min before OxLDL (10 µg/ml) or collagen (10 µg/ml) stimulation. Mean aggregation shown ±SEM; n=4. Unpaired T-test performed to compare

aggregation responses in the presence of inhibitors., ***p<0.005. C(i) Phosphorylation response to different concentrations of OxLDL (10, 30 and 50 µg/ml) and the OxLDL (10 µg/ml) response in the presence of inhibitors (dasatinib (10 µM), PRT (10 µM) and PP2 (10 µM) compared to collagen (10 µg/ml) controls after Western blotting with the monoclonal 4G10 antibody. C(ii) Syk and PLCγ2 were immunoprecipitated (IP) after washed platelets were stimulated with collagen (10 µg/ml), rhodocytin (300 nM), CRP (10 µg/ml) and OxLDL (10 µg/ml). IPs samples were Western blotted for phosphotyrosine. Proteins were re-probed using corresponding antibodies (anti-Syk-sc1077 and anti-PLCγ2 – sc407) for determining loading control. Image representative of 4 experiments. C(iii) CLEC-2 IP after washed platelets ($1x10^9$/ml) were stimulated with rhodocytin (300 nM) and OxLDL (10 µg/ml). IPs samples were Western blotted for phosphotyrosine. Proteins were re-probed with anti-CLEC-2 antibody to determining loading control. Image representative of 2 experiments.

3.2.3 Mitochondrial DNA (mtDNA) does not induce platelet activation

Nuclear-related Alarmins were also assessed to determine their effects on platelet function. To test mtDNA effects on platelet function, mtDNA was isolated from PBMCs of a healthy control (HC) and used to stimulate washed platelets in suspension at concentrations previously shown to affect other cells. MtDNA did not induce significant platelet aggregation above the PBS vehicle control at any of the MtDNA concentrations tested (12-60 μg/ml; Figure 3.5A), which were based on concentrations used in other studies and high levels observed in trauma patients (Zhang et al., 2010). MtDNA did not have an effect on modulating responses to other agonists, including ADP and collagen (results not shown). Due to the lack of effect with isolated mtDNA and the difficulties in the isolation process only giving a small yield of mtDNA for testing, other nuclear-related Alarmins were then tested.

3.2.4 High-Mobility-Group-Box-1 (HMGB-1) does not affect platelet aggregation in suspension

HMBG-1 is another nuclear-related Alarmin shown as a pro-inflammatory mediator (Hauser et al., 2010). HMGB-1 was used to stimulate washed platelets in suspension at concentrations shown to have effects in other cell types (Schiraldi et al., 2012, Tadie et al., 2013). HMGB-1 did not induce significant platelet aggregation at any of the concentrations used, based on concentrations shown to have effects on other cell types in other peer studies (Figure 3.5B). There was no visible shape change after stimulation nor was there a dose-dependent response (Figure 3.5Bii), HMGB-1 had no effect on modulating platelet responses to other agonists as no synergy or increased levels of aggregation were seen in response to collagen with pre-treatment of washed platelets

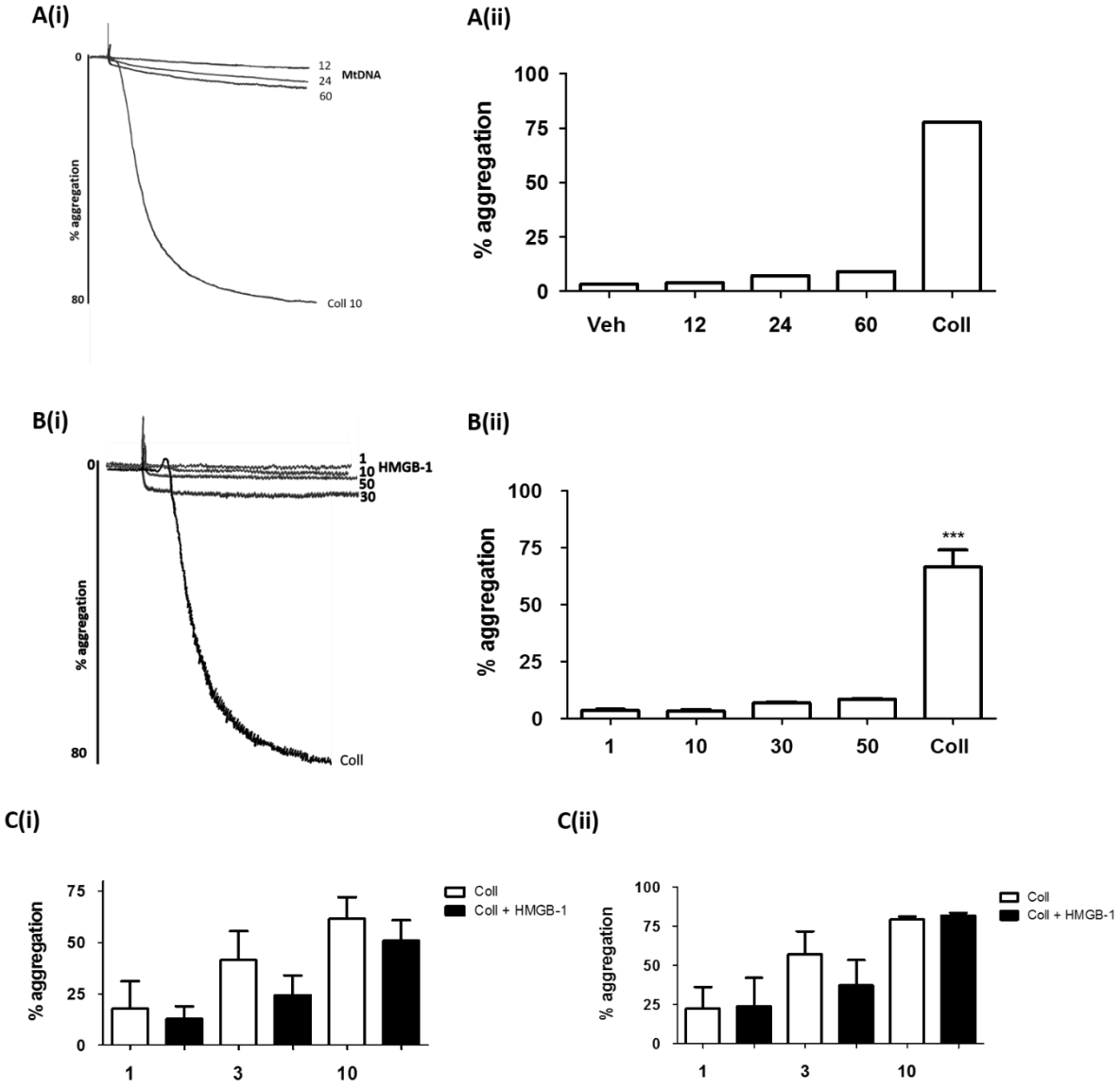

Figure 3.5 - MtDNA and HMGB-1 have no effect on platelet aggregation in human washed platelets. A) Human washed platelets ($2x10^8$/ml) were stimulated with isolated mtDNA. A(i) Dose response curve after stimulation with different mtDNA concentrations (12, 24 and 60 µg/ml). A(ii) Maximum aggregation in response to mtDNA compared to collagen (10 µg/ml) control. N=1. B) Human washed platelets ($2x10^8$/ml) were stimulated with HMGB-1 (1, 10, 30 and 50 µg/ml). B(i) Dose response cure of platelets stimulated with HMGB-1. Representative trace of 6 experiments. B(ii) Mean aggregation induced by HMGB-1. Mean ±SEM showed. One-way ANOVA

performed with Bonferroni post-hoc test to compare HMGB-1 responses with collagen (10 µg/ml) control (n=6); ***p<0.005. C(i) Human washed platelets ($2x10^8$/ml) were treated with HMGB-1 (10 µg/ml) before addition with collagen (1 -10 µg/ml). Aggregation of synergy shown as mean ±SEM; n=4. C(ii) Human PRP was treated with HMGB-1 (10 µg/ml) for 1 before collagen (1 -10 µg/ml) stimulation. Aggregation of synergy shown as mean ±SEM; n=3.

and PRP with HMGB-1 (Figure3.5Ci&ii). HMGB-1 therefore does not affect platelet aggregation.

3.2.5 Calf thymus histones (CTH) induces platelet aggregation in washed platelets and PRP

CTH experiments were in collaboration with two undergraduate students – Najiat Sarker and Paul Carter, who performed some experiments as stated in the Figures. Some experimental data for this section has been published (Alshehri et al., 2015b).

Histones are another extensively studied nuclear-related Alarmin released after nucleosome breakdown following damage (Abrams et al., 2013). Calf thymus histones (CTH) are a commercial source of histones, containing a heterogeneous mixture of histone fractions, including the most active ones in effecting other cells, H3 and H4 (Fuchs et al., 2011b). Histones have close sequence homology between species, therefore CTH was used as an agonist for stimulation of washed platelets and PRP. CTH induced a dose-dependent response causing shape change and full platelet aggregation after stimulation of human washed platelets and PRP (Figure 3.6A&B respectively). The dose response curve of CTH stimulation of washed platelets is approximately 10 times lower than in PRP, suggesting plasma protein binding to histones may reduce bioavailability to platelets in PRP. CTH aggregation in washed platelets is integrin αIIbβ3-dependent as aggregation is blocked in the presence of the αIIbβ3 inhibitor, integrilin (eptifibatide 9 μM; Figure 3.6Cii), at a concentration well recognised in our laboratory to block aggregation to other agonists, although secretion is still retained (Figure3.6Cii) The CTH dose response curve for aggregation and secretion are PRP sigmoidal (Figure 3.6Bii&iii).

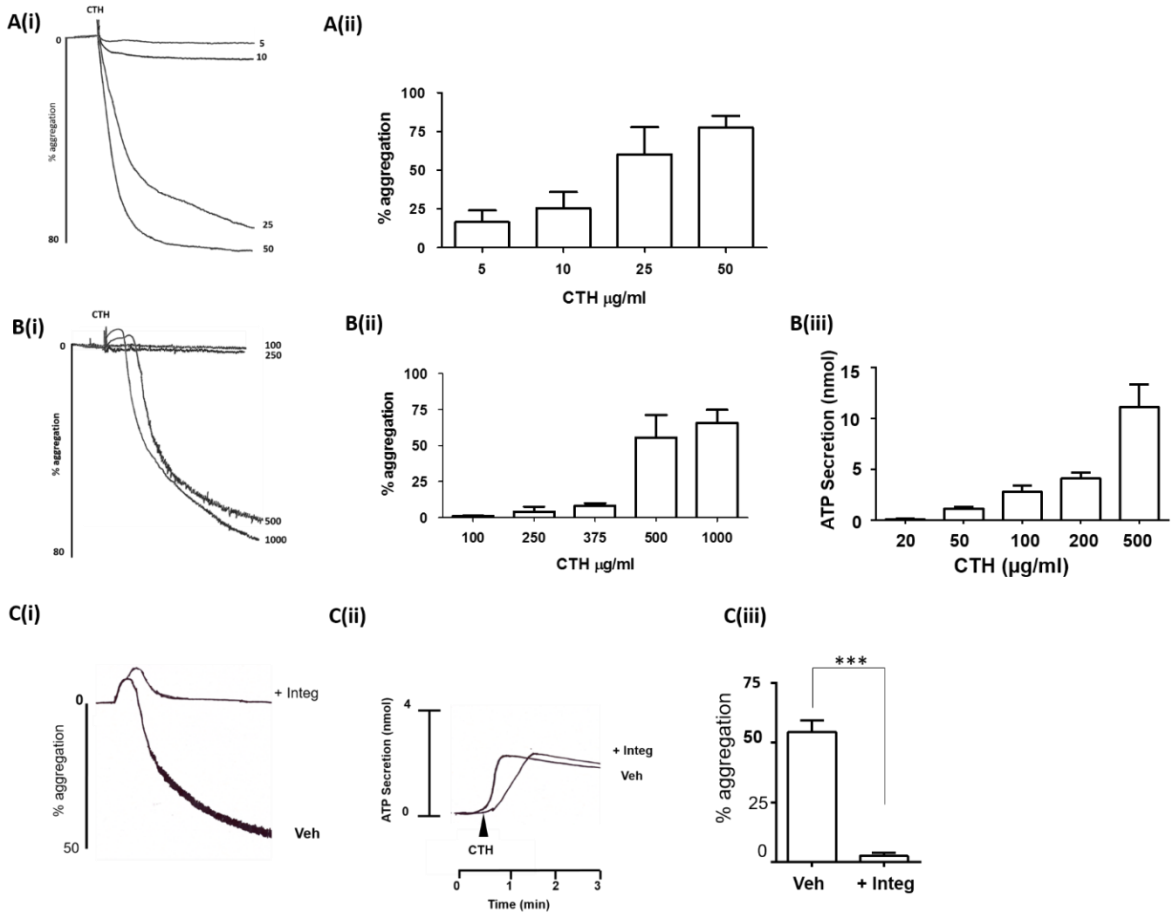

Figure 3.6 - Calf thymus histones (CTH) induce platelet aggregation in washed platelets and PRP. A) Human washed platelets ($2x10^8$/ml) were stimulated with CTH. A(i) Dose response curve after stimulation with different CTH concentrations (5, 24 and 60 µg/ml). A(ii) Aggregation in response to increasing concentrations of CTH shown as mean ±SEM. B) CTH does response in human PRP. B(i) Representative CTH dose response of 4 experiments. B(ii) Aggregation response to CTH in PRP. Mean ±SEM shown, n=4. B(iii) ATP secretion in response to CTH stimulation of human PRP at different concentrations, mean ± SEM shown (*secretion result of project student Najiat Sarker*). C) CTH (2 mg/ml) stimulation of human PRP pre-incubated with integrilin (9 µM). C(i) Representative aggregation trace of 3 separate experiments. C(ii) ATP secretion in response to CTH (2 mg/ml) in the presence of integrilin (9 µM). C(iii)

Aggregation response of CTH stimulation with and without integrilin (9 µM). Results are shown as mean ± SEM; n=3, ***p<0.005 (*Integrilin results of project student Paul Carter*).

3.2.6 CTH induced platelet activation is Src and Syk dependent

Histone induced aggregation was blocked by inhibitors of Src and Syk tyrosine kinases. Washed platelets were pre-treated with dasatinib (10 µM) and PRT060318 (10 µM) for 5 min before CTH stimulation. Both dasatinib and PRT060318 significantly inhibited histone-mediated aggregation (Figure3.7A). CTH stimulated strong phosphorylation in mouse washed platelets above the unstimulated basal levels (Figure 3.7B). PLCγ2 and Syk were among the predominant phosphorylated proteins, with phosphorylation of FcRγ-chain also observed (Figure 3.7Bi&ii). The increase in tyrosine phosphorylation was similarly observed in human washed platelets (Figure 3.7Biii). In the presence of dasatinib, phosphorylation of all these signalling proteins was blocked. In the presence of PRT060318, only PLCγ2 phosphorylation was completely blocked, with reduced phosphorylation of Syk being observed, consistent with Syk and FcRγ-chain phosphorylation lying downstream of Src kinases in mouse washed platelets (Figure3.7Bi&ii), which was also observed in human washed platelets. There was negligible phosphorylation of CLEC-2 after histone stimulation of mouse platelets (Figure 3.6Bii). No CLEC-2 phosphorylation was observed after CTH stimulation of human washed platelets (data not shown). These results suggest that histones stimulate phosphorylation through the GPVI- FcRγ-chain complex.

3.2.7 CTH mediated synergy with adrenaline is Src-dependent

CTH induced strong aggregation at concentrations of 50 µg/ml in washed platelets and 500 µg/ml in PRP. Although these concentrations fall in the range of levels measured in in trauma patients (10-230 µg/ml), histones have however, been shown to have cytotoxic affects at concentrations as low as 10 µg/ml (Abrams et al., 2013). Therefore,

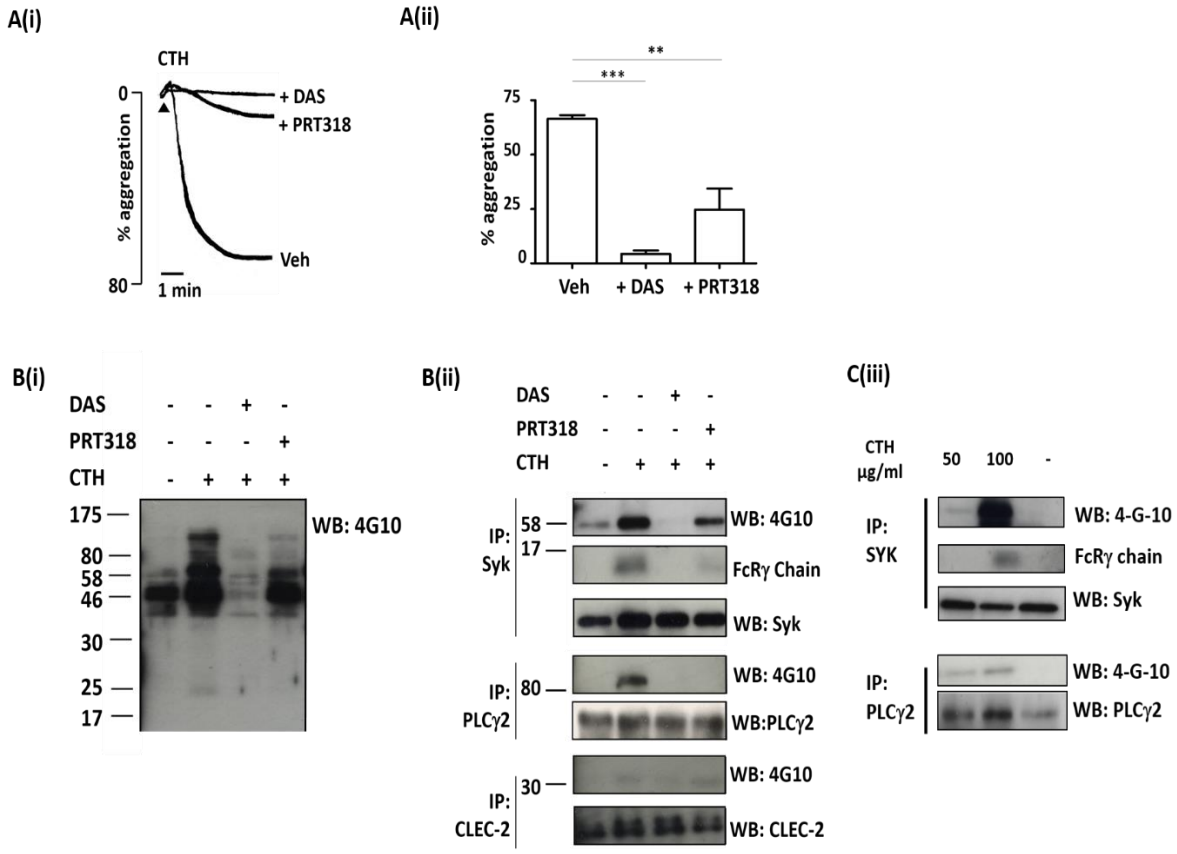

Figure 3.7 - CTH phosphorylation response is blocked with Src and Syk inhibitors in mice. A) Mouse PRP pre-incubated with dasatinib (10 µM), PRT060318 (10 µM) or vehicle were stimulated with CTH (1 mg/ml) A(i) Aggregation trace representative of 3 experiments. A(ii) Aggregation response to CTH in the presence of inhibitors. Results shown as mean ±SEM, n=3, unpaired T-test performed **p<0.01, ***p<0.005. B) Mouse washed platelets ($5x10^8$/ml) were stimulated with CTH (50 µg/ml) in the presence of dasatinib (10 µM), PRT060318 (10 µM) or vehicle and analysed for tyrosine phosphorylation. Lysates prepared in the presence of integrilin (9 µM), indomethacin (10 µM) and apyrase (2 U/ml). B(i) Whole cell lysate representative of 3 experiments, molecular mass (kDa) indicated as numbers on left-hand side. B(ii) IPs for Syk, PLCγ2 and CLEC-2 separated by SDS/PAGE and Western blotted for phosphotyrosine using mAb 4G10. Representative image of 4 experiments *(work*

completed by project student Najiat Sarker). B(iii) IPs for Syk, PLCγ2 and CLEC-2 at CTH stimulation of human washed platelets ($5x10^8$/ml) separated by SDS/PAGE and Western blotted for phosphotyrosine using mAb 4G10. Representative image of 4 experiments.

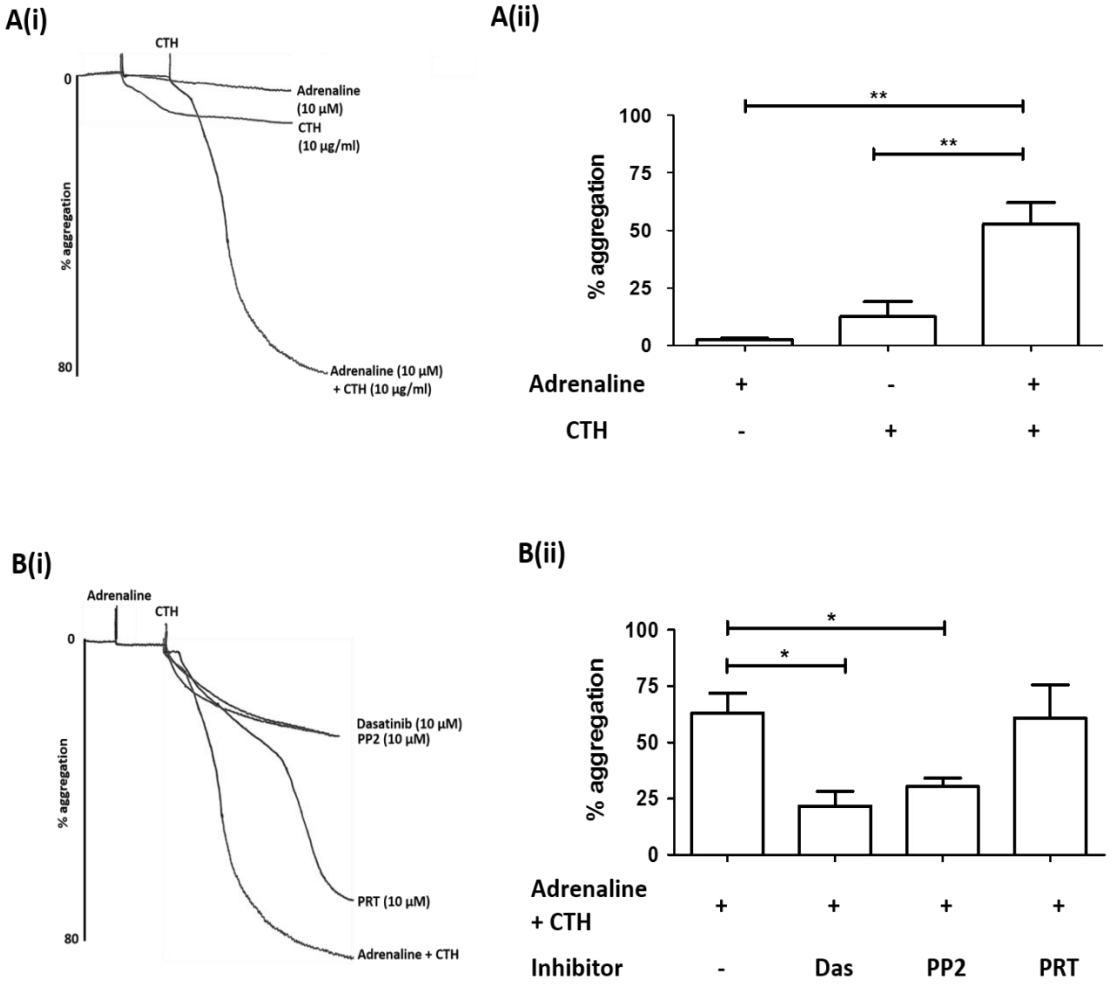

Figure 3.8 - Synergy seen between adrenaline and sub-threshold levels of CTH in human washed platelets, which is blocked with Src inhibitors. A) Human washed platelets ($2x10^8$/ml) were treated with adrenaline (10 µM) for 1 min before CTH (10 µg/ml) treatment. A(i) Aggregation trace of synergy with adrenaline and CTH, representative of 6 experiments. A(ii) Aggregation of synergy shown as mean ±SEM. Unpaired T-test performed. **$p<0.01$, n=6. B) Adrenaline and CTH synergy observed when washed platelets pre-incubated for 1 min with dasatinib (10 µM), PP2 (10 µM) and PRT060318 (10 µM). B(i) Aggregation trace representative of 3 experiments. B(ii) Aggregation of synergy in the presence of inhibitors shown as mean ±SEM, n=3. Unpaired T-test performed to assess synergy in presence of inhibitors, *$p<0.05$.

the ability of histones to modulate platelet function at lower concentrations was examined. During the preparation of washed platelets, platelets become desensitised to ADP and adrenaline due to loss of activation of the Gq-coupled $P2Y_1$ receptor and adrenaline α2-receptor. This allows the testing for synergy between CTH activation and the Gi-coupled $P2Y_{12}$ ADP or adrenaline α2-receptor. Washed platelets were stimulated with a strong dose of adrenaline (10 μM), at a concentration greater than found in physiological conditions, which gives minimal platelet aggregation in washed platelets alone but has been previously shown in our laboratory to induce robust platelet aggregation in PRP, before addition of sub-threshold levels of CTH (10 μg/ml), which alone induce minimal aggregation. In the presence of adrenaline, CTH gave robust platelet aggregation (Figure 3.8Ai), which was significantly greater than the sum of the responses to the individual agonist (**$p<0.01$; n=6; Figure 3.8Ai). When tested in the presence of Src inhibitors, dasatinib and PP2, the synergy in washed platelets was blocked (*$p<0.05$, n=3; Figure 3.8B). A slightly smaller effect in reducing the synergy response was observed with PRT060318, suggesting a great role for Src kinases in the CTH-adrenaline synergy.

3.2.8 Platelets bind and activate to immobilised CTH and OxLDL but not HMGB-1

Of the Alarmins and DAMPs tested, CTH was the most effective at inducing aggregation, with OxLDL and HMGB-1 only having a small response when used to stimulate platelets in suspension. To determine if the Alarmins and DAMPs can activate platelets when immobilised on a surface, platelets were added to agonist coated-coverslips and levels of adhesion and activation were assessed. Platelets adhered to

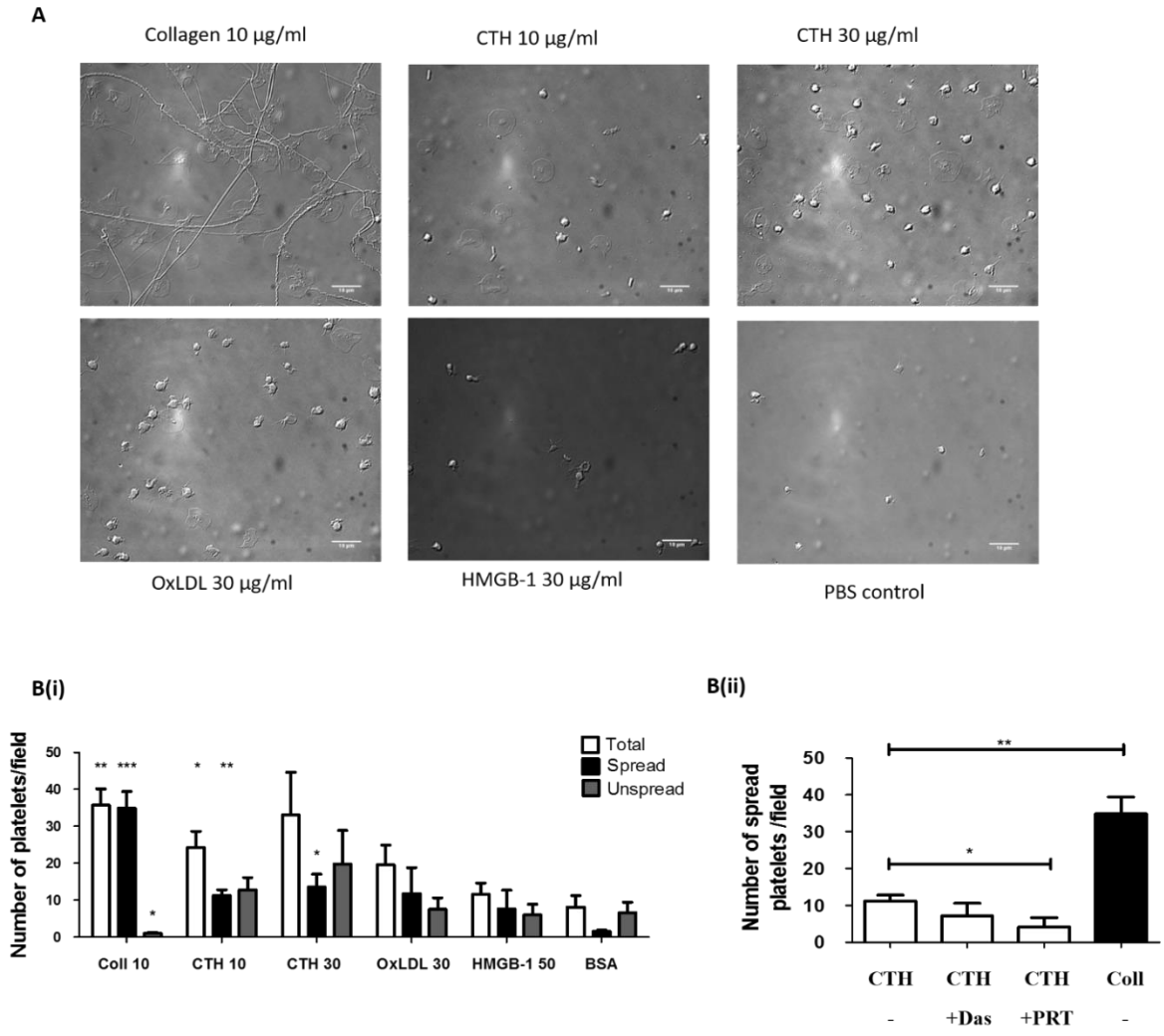

Figure 3.9 - Platelets bind and activate on immobilised CTH and OxLDL but not HMGB-1. Human washed platelets ($2x10^7$/ml) were incubated on pre-coated slides with immobilised agonists; collagen (10 µg/ml), CTH (10 & 30 µg/ml), OxLDL (30 µg/ml), HMGB-1 (30 µg/ml) and the BSA-PBS control. A) Images of spread platelets on different immobilised agonists. Representative images of 6 separate donors. Scale bar = 10 µm. B(i) Number of total platelets, spread and unspread platelets adhered on immobilised agonist, results shown as mean ±SEM. Unpaired T-test to compare number of platelets to BSA controls, n=6, *p<0.05, **p<0.01. ***p<0.005. B(ii) Number of spread platelets observed per field of view on immobilised CTH (10 µg/ml) with pre-treatment of platelets for 5 min with dasatinib (10 µM), PP2 (10 µM) and PRT060318

(10 µM) compared to collagen (10 µg/ml) control. Results shown as ±SEM, n=4. Unpaired T-test was performed to compare differences of spread platelets on immobilised CTH compared on collagen and compare difference in the number of spread platelets on CTH in the presence of inhibitors, *$p<0.05$ and **$p<0.01$.

immobilised CTH (10-30 µg/ml) to a similar level on collagen (10 µg/ml). Platelets did not significantly adhere to coated OxLDL (30 µg/ml), with even fewer platelets adhering to HMGB-1 (30-50 µg/ml) near to levels of the PBS-BSA control (Figure 3.9Aand Bi). Platelets adhered and spread on immobilised CTH at significantly higher levels than the BSA-PBS control (**$p<0.01$, n=6; Figure 3.9Bi), although the number of spread platelets was less with CTH compared to the collagen control coated surfaces. When platelets were pre-treated with dasatinib and PRT, platelets still adhered to CTH surfaces, but remained in an inactive state, as less spread platelets were observed (**$p<0.01$, n=4; Figure 3Bii). There was a significant reduction in number of platelets spreading on CTH when pre-treated with the Syk inhibitor, PRT (*$p<0.05$).

To determine whether tyrosine phosphorylation caused by CTH was similar when CTH was presented as a monolayer rather than in solution, lysates were prepared from platelets following adhesion to the immobilised agonists. Non-adhered cells were removed and lysis buffer was then added to the adhered platelets. Whole cell lysates of adhered samples showed there was an increase in tyrosine phosphorylation in platelets adhered to CTH (10 µg/ml), OxLDL (30 µg/ml) and collagen (10 µg/ml), compared to the non-adherent basal platelets (Figure 3.10A). There were very minimal increases in phosphorylation after HMGB-1 (30 µg/ml) stimulation of washed platelets. When immunoprecipitating samples for Syk, FcRγ-chain and PLCγ2, there was increased phosphorylation in platelets adhered to collagen, CTH and OxLDL, with minor phosphorylation of PLCγ2 seen after HMGB-1 stimulation (Figure 3.10B&C. However, collagen had a greater level of phosphorylation then the other agonists. Also, when comparing tyrosine phosphorylation of platelets after CTH stimulation at low concentrations, less tyrosine phosphorylation of key signalling proteins was observed

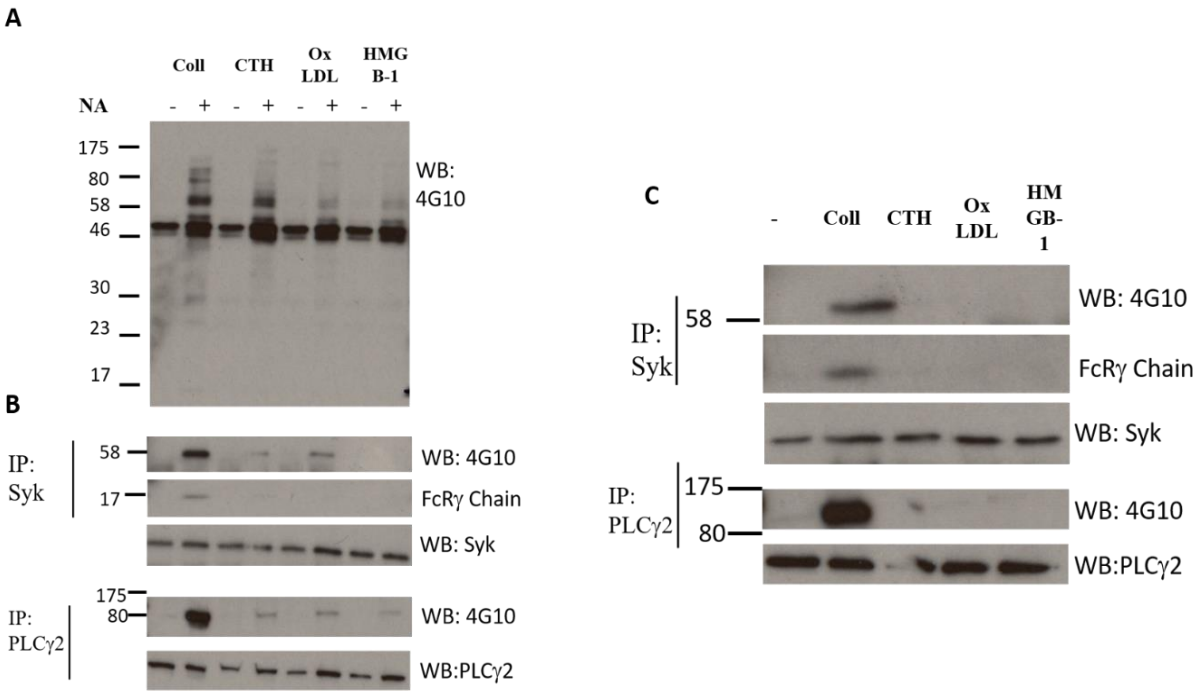

Figure 3.10 - Platelets bind and activate leading to phosphorylation of key signalling proteins when incubated on immobilised CTH and OxLDL but not HMGB-1. A) Washed platelets ($5x10^8$/ml) were added on to plates coated with immobilised agonists; collagen (10 µg/ml), CTH (10 µg/ml), OxLDL (30 µg/ml), HMGB-1 (30 µg/ml) for 45 min. Non-adherent (NA) cells were extracted and lysed. Adherent cells were also lysed. A) Whole cell lysate representative of 4 experiments. B) IPs for Syk and PLCγ2 separated by SDS/PAGE and Western blotted for phosphotyrosine using mAb 4G10. C) IPs of lysates prepared from washed platelets ($5x10^8$/ml) stimulated with agonists as above in suspension for 5 min at 1200 rpm.

after CTH stimulation in suspension compared to stimulation by immobilised CTH (Figure 3.10C), whereas there was phosphorylation when CTH was immobilised.

3.2.9 GPVI transfected cells do not signal after incubation on immobilised CTH

To confirm that immobilised CTH can activate and signal through GPVI, immobilised CTH was used to stimulate Jurkat cells (a human T-lymphocyte cell line) transfected with GPVI using a NFAT luciferase assay. Jurkat cells were transfected with vectors and GPVI and FcRγ constructs before being incubated on immobilised surfaces including collagen (100 µg/ml) and CTH (100 µg/ml) for 6 h. The readout of the NFAT luciferase reporter assay was the luciferase signal in response to cells binding and being activated by the immobilised agonists. The relative luciferase activity of GPVI transfected cells on immobilised histones and collagen were compared to basal (unstimulated) samples and cells transfected with a mock (empty) vector. Increases in relative luciferase activity of Jurkat cells transfected with GPVI above the basal samples and vector controls were only seen when cells were incubated on immobilised collagen surfaces (*$p<0.05$, $n=4$; Figure 3.11Ai). There was no increased luciferase activity when GPVI- transfected Jurkat cells were incubated on CTH coated surfaces (Figure 3.11Ai).

After the initial NFAT luciferase assays were performed with immobilised CTH and a range of other agonists tested (as described in (Alshehri et al., 2015b)), it was suggested that the serum and antibiotic added to the transfection media could interfere with the binding of the transfected cells to the immobilised agonists, which may have reduced the luciferase signal. The assay was then repeated after Jurkat cells were transfected with GPVI in transfection made that did not contain any antibiotic or serum, which

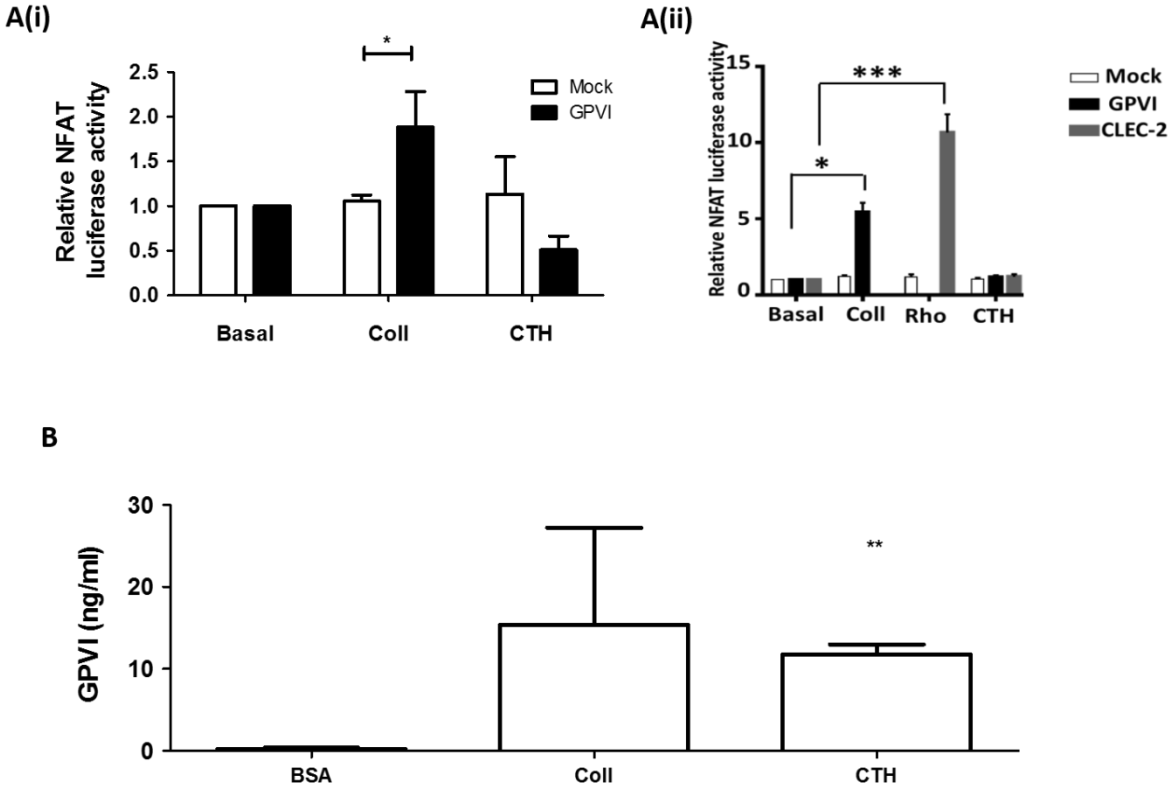

Figure 3.11 - GPVI binds to immobilised CTH *in vitro* but cannot confer signalling in a cell line. A) A NFAT luciferase reporter assay was performed to assess if Jurkat cells transfected with GPVI become activated when incubated with immobilised CTH (100 µg/ml) and collagen (100 µg/ml). Cells were transfected with a mock(empty) vector or GPVI-FcR-γ-chain and a NFAT-luciferase reporter. Cells were incubated on immobilised agonists for 6 h and luciferase activity measured. A(i) Results shown as relative NFAT luciferase activity above basal control. N=4, results shown as mean ±SEM. Unpaired T-test performed to assess luciferase activity above basal and empty vector, *p<0.05. A (ii) NFAT luciferase assay performed as before, however, no antibiotic was present in the transfection media during GPVI transfection into Jurkat cells. Cells were also transfected with CLEC-2 vector for which rhodocytin was used as a positive control agonist. Results representative of three experiments, and means shown ±SEM. *p<0.05, ***p<0.001. B) GPVI ectodomain ELISA binding assay. GPVI

ectodomain (80 ng/ml) from NEM-treated plasma was incubated on pre-coated microtiter plates with immobilised agonists, collagen (100 µg/ml) and CTH (100µg/ml) compared to BSA-PBS control. GPVI concertation bound was calculated using the ectodomain standard curve generated. Results shown as mean ±SEM, n=3. Unpaired T-test was performed to compare levels of binding to BSA control. **$p<0.01$

increased the luciferase signal to give a higher fold increase over basal with the positive control agonist, collagen (*p<0.05, n=3; Figure 3.11Aii). There was however, no difference in signalling of GPVI transfected cells after incubation with immobilised CTH. For the second set of NFAT luciferase reporter assays, Jurkat cells were also transfected with CLEC-2 constructs to see if immobilised CTH could induce CLEC-2 signalling. There were no increases in luciferase activity when transfected cells were incubated with immobilised CTH, whereas a large signal was seen when transfected cells were activated by the CLEC-2 ligand, rhodocytin (***p<0.005, n=3; Figure 3.11Aii). These results suggest that in a cell line, CTH was not able to activate GPVI or CLEC-2 signalling.

3.2.10 GPVI ectodomain binds to immobilised CTH

We next sought to measure direct GPVI binding to CTH, to determine if GPVI can directly bin to CTH. A GPVI ELISA binding assay was then developed based on an existing GPVI ELISA (Al-Tamimi et al., 2011a). GPVI ectodomain (80 ng/ml) produced from N-ethylmaleimide (NEM) treated plasma (which cleaves GPVI) was incubated with immobilised agonists on a 96 well plate before washing and addition of GPVI antibodies. Chemiluminescence signal was measured using a Wallac-Victor2 luminescence plate reader and concentrations of bound-GPVI were extrapolated from a generated standard curve. CTH bound to the GPVI ectodomain at similar levels to collagen (12 ± 1.7 ng/ml and 15 ± 20.6 ng/ml respectively) and were significantly higher than binding to the BSA-PBS control (0.19 ± 0.3 ng/ml; **p<0.01, n=3; Figure 3.11B).

3.2.11 CTH mediates platelet aggregation in mice through GPVI and not CLEC-2

CTH induced platelet aggregation is Src and Syk dependent. These are important proteins involved in ITAM signalling. To determine if GPVI is an important ITAM receptor predominantly involved in the histone response and not the hemITAM receptor, CLEC-2, platelets from GPVI knock out mice ($GPVI^{-/-}$) and mice deficient in platelet CLEC-2 ($CLEC\text{-}2^{-/-}$) were stimulated with CTH histones. CTH-induced aggregation and shape change were blocked in $GPVI^{-/-}$ mice (Figure 3.12A). There was no effect on the response to CTH in CLEC-2-deficient mice, with full aggregation and shape change occurring to similar levels as wild type (WT) mice (Figure 3.12A). When studying tyrosine phosphorylation, there was reduced phosphorylation after CTH stimulation of washed platelets from $GPVI^{-/-}$ mice, which was similar to the reduction in tyrosine phosphorylation observed in mice platelets deficient in both CLEC-2 and $GPVI^{-/-}$ mice (Figure 3.12Bi). There was a weak increase in tyrosine phosphorylation after CTH stimulation of GPVI/CLEC-2 double deficient platelets compared to basal (Figure 3.12Bi) The key signalling proteins, Syk, FcRγ-chain and PLCγ2 showed reduced phosphorylation in the GPVI/CLEC-2 double-deficient platelets (Figure 3.12Bii). There were no reductions in phosphorylation were observed after stimulation of CLEC-2 deficient platelets.

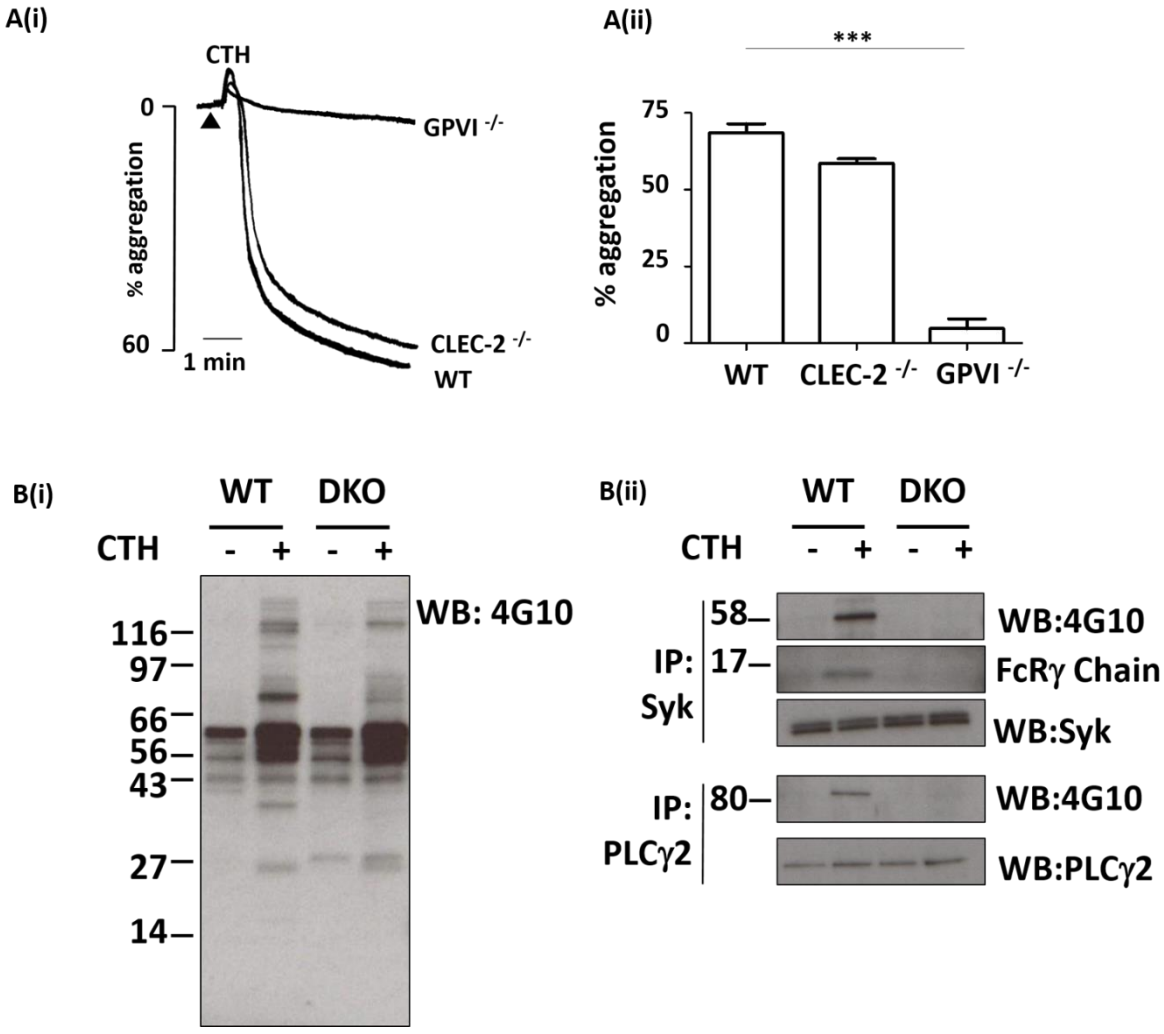

Figure - 3.12 CTH mediates platelet aggregation in mice through GPVI and not CLEC-2. A) PRP was stimulated with CTH (1 mg/ml) for 5 min from WT mice, GPVI$^{-/-}$ mice and mice deficient in platelet CLEC-2 (CLEC-2$^{-/-}$). A(i) Aggregation trace representative of 3 experiments. A(ii) Aggregation results shown as mean ±SEM, n=3, ***p<0.005 (*experiments from project student Najiat Sarker*). B) Lysates prepared after CTH (1 mg/ml) stimulation of PRP from WT mice and GPVI$^{-/-}$/CLEC-2$^{-/-}$ (DKO) mice in the presence of integrilin (9 µM), indomethacin (10 µM) and apyrase (2 U/ml). B(i) Whole cell lysate separated by SDS/PAGE and Western blotted for phosphotyrosine using mAb 4G10. B(ii) IPs for Syk and PLCγ2 of WT and DKO samples stimulated with CTH compared to basal.

3.2.12 GPVI$^{-/-}$ mice are not protected from CTH-induced thrombocytopenia

Histone-medicated aggregation and phosphorylation is GPVI dependent *in vitro*, as CTH response is lost after CTH stimulation of GPVI-deficient platelets. Histone infusion models in mice were used to determine if CTH activation *in vivo* is also GPVI dependent. CTH induced thrombocytopenia over a concentration range of 2.5-75 mg/kg (Figure 3.13A). Basal platelet counts were measured in blood taken from mice immediately prior to CTH injection. After 3 min mice were sacrificed and platelet count measured again. The drop in platelet count indicated platelet consumption. CTH injections of 7.5mg/kg and above significantly reduced platelet count in the mice, with 25 and 75 mg/kg injection inducing a severe level of thrombocytopenia, to approximately 20% of basal levels (Figure 3.13A).

CTH was injected into GPVI$^{-/-}$ mice to determine whether CTH-induced thrombocytopenia could be rescued in the absence of GPVI. A collagen-adrenaline infusion model was set up based previous studies to induce thrombocytopenia (Abrams et al., 2013), to establish the levels of rescue that could be expected in GPVI$^{-/-}$. Collagen and adrenaline (25 µg and 1 µg) were injected into WT and GPVI$^{-/-}$ for 3 min and the drop in platelet count was measured as before. The collagen and adrenaline infusion induced thrombocytopenia to similar levels as with CTH infusion, being significantly lower than the basal counts (Figure 3.13B). The reduction in platelet count was significantly reduce in GPVI $^{-/-}$ (n=3).

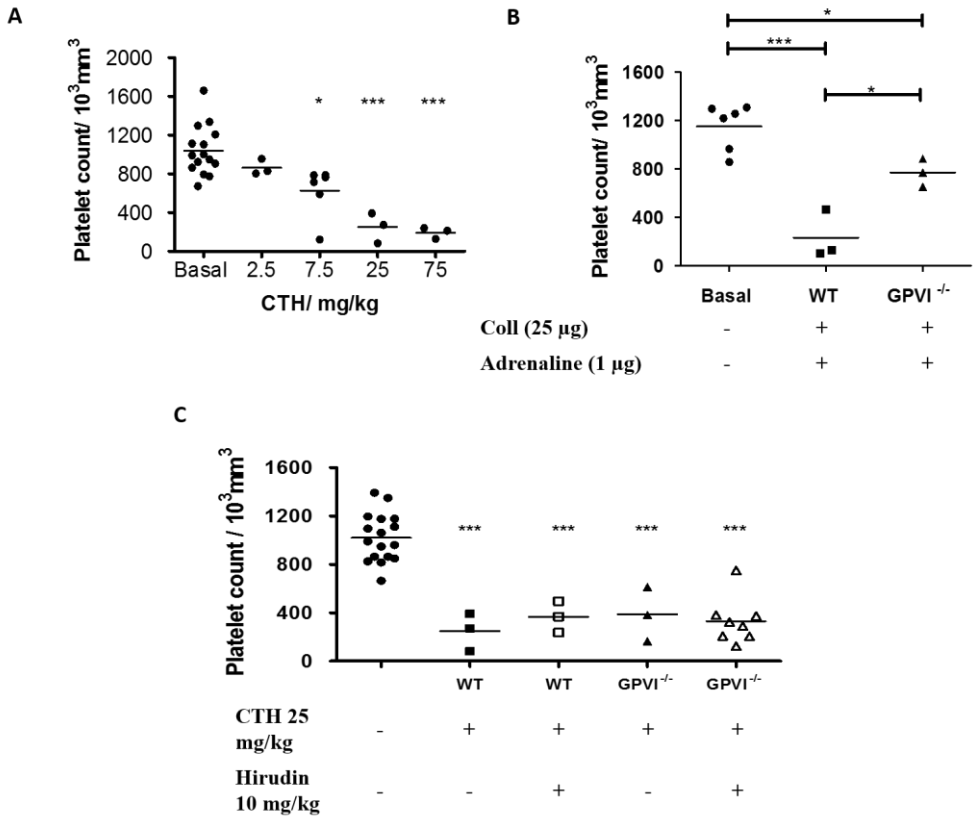

Figure 3.13-CTH induces thrombocytopenia in mice which is not rescued in GPVI$^{-/-}$ mice or with hirudin treatment. A) Platelet count drop measured after WT mice were injected with different doses of CTH (2.5-75mg/kg) for 3 min. Platelet counts were measured from samples taken before injection (basal) and after a terminal bleed. Mean shown, individual points represent one mouse. T-test was performed to compare counts after injection with basal levels, *p<0.05, ***p<0.005. B) Collagen and adrenaline infusion model. WT mice and GPVI$^{-/-}$ mice were injected with a mixture of collagen (25 µg) and adrenaline (1 µg). Platelet counts were measured from blood samples before and after injection. Mean shown. *p<0.05, **p<0.01 and ***p<0.005. C) CTH infusion model. WT mice and GPVI$^{-/-}$ mice were injected with 25 mg/kg CTH. In some experiments mice were injected subcutaneously with hirudin (10 mg/kg). Platelet counts were measured pre and post CTH infusion. Mean shown, ***p<0.005.

GPVI is the major platelet receptor for collagen. To establish if GPVI is also an important receptor for CTH in vivo, it would be expected that the degree of rescue in the platelet count after CTH infusion would be similar to that of collagen infusion in $GPVI^{-/-}$ mice. CTH (25 mg/kg) was injected into WT and $GPVI^{-/-}$ mice. There was no prevention of the reduction of platelet count in $GPVI^{-/-}$ mice as the levels of activation and thrombocytopenia induced were similar to WT and all significantly different to basal count (***$p<0.005$; Figure 3.13C). Therefore, CTH-induced aggregation in vivo is not GPVI dependent.

Histones have been shown to activate the coagulation cascade and to lead to thrombin generation (Fuchs et al., 2011b, Semeraro et al., 2011). To assess if the strong CTH-aggregation *in vivo* was a result of thrombin generation by histones leading to platelet activation observed, the direct thrombin inhibitor, hirudin (10 mg/kg) was injected 5 min before CTH infusion (Figure 3.13C). No rescue was seen with pre-treatment of hirudin in WT mice $GPVI^{-/-}$ mice, with levels of thrombocytopenia induced remaining the same (36%- and 35%- of basal count respectively) Therefore, CTH-mediated platelet activation was not dependent on GPVI or thrombin.

3.3 Discussion

Alarmins and DAMPs released in response to trauma have been proposed to lead to inflammation after interacting with Alarmin receptors located on immune cells and increasing production of pro-inflammatory cytokines (Manson et al., 2012). Alarmins have the potential to interact with and activate platelets, as some of the identified Alarmin receptors have been described on the platelet surface (Cognasse et al., 2005, Zhu et al., 2012). A number of Alarmins including DNA and histones have been shown to activate platelets. The aim of this chapter was to assess a several Alarmins and determine if they can activate or modulate platelets and establish any signalling mechanisms behind the Alarmin-mediated response.

One of the first Alarmins/DAMPs tested was AGE. AGE has been implicated in a range of conditions including diabetes and consequent cardiovascular events (Lapolla et al., 2007, Ono et al., 1998, Giacco and Brownlee, 2010). AGE has been shown to signal through RAGE and CD36, a scavenger receptor located on the platelet surface (Saboor et al., 2013, Zhu et al., 2012). AGE has been proposed to modulate ADP aggregation after stimulation of platelets pre-incubated with AGE-BSA through CD36 (Zhu et al., 2012). To confirm this finding, different concentrations of ADP were used to stimulate platelets pre-incubated with AGE-BSA for 30 min under the same conditions previously described (Zhu et al., 2012). However, the AGE-BSA tested was unable to induce aggregation after direct stimulation or be able to modulate the ADP response when platelets were pre-treated with AGE-BSA at a range of concentrations and different doses of ADP. This finding was confirmed in both mice and human platelets, even with different AGE-BSA sources being tested. AGE-BSA was found not to modulate ADP

response, which differs from the findings of the Zhu et al. (2012) studies. An explanation for this result is unclear, as the source and concentrations of AGE-BSA used, along with the experimental conditions described in Zhu et al. (2012) studies being the same. The previous study did however only show a weak potentiation of the ADP response, which along with these findings suggests AGE is not an important DAMP for mediating platelet activation or modulating platelet responses to other agonists.

Oxidised Low Density Lipoprotein (OxLDL) has been implicated in atherosclerosis (Matsuura et al., 2008, Jackson and Calkin, 2007, Ghosh et al., 2011). OxLDL is also a lipid based DAMP and was tested to see if OxLDL could induce platelet activation. OxLDL, along with AGE-BSA has been shown to interact with the scavenger receptor CD36, therefore giving a potential route for platelet activation. OxLDL was shown in this study to induce weak aggregation in washed platelets and no aggregation in platelet-rich-plasma (PRP). Other studies have shown a greater platelet aggregation response after OxLDL stimulation of washed platelets (Wraith et al., 2013). However, this response may depend on the oxidation process to produce the OxLDL. In this set of experiments I have used a commercial source of OxLDL, which may have given a reduced response compared to a self-produced OxLDL. Comparisons of the different oxidation process and consequent OxLDL products would be a future approach to establish fully the effects of OxLDL on platelet aggregation. Platelets did not however significantly adhere to immobilised OxLDL above the BSA-PBS control, with the level of adhesion also being much less than to other platelet agonists such as collagen. OxLDL induced a small shape change after stimulation of washed platelets, which was

not blocked with Src and Syk inhibitors, suggesting no major involvement of Src and Syk in OxLDL-induced aggregation.

An interesting finding with OxLDL however was observed when examining the tyrosine phosphorylation after OxLDL stimulation, with a similar increase in tyrosine phosphorylation above basal observed after OxLDL and collagen stimulation of washed platelets, suggesting a similar ITAM signalling mechanism. The level of increase in phosphorylation of key GPVI signalling proteins such as, Syk, FcRγ-chain and PLCγ2 were however much lower than observed with collagen. Other studies have since shown that OxLDL induces mild platelet activation and shape change through a Src and Syk kinase dependent mechanism downstream of CD36 and a Src/RhoA kinase (ROCK) dependent pathway, which overall lead to myosin light chain (MLC) phosphorylation and the OxLDL aggregation response (Wraith et al., 2013). It is therefore unclear why Src and Syk kinases had no effect on the aggregation and phosphorylation response to OxLDL in this present study. Further experiments looking at immunoprecipitates of different signalling proteins and the use of phospho-specific antibodies to other signalling proteins would allow further investigation of the OxLDL phosphorylation patterns and clarification of the signalling proteins involved in the OxLDL signalling pathway.

The DAMPs, OxLDL and AGE did not induce extensive platelet activation. Therefore the effects of a variety of nuclear-related Alarmins were also assessed. Alarmins are a term for DAMPs released after trauma. Mitochondrial DNA (mtDNA) can be released from mitochondria after cell damage and has been shown to mediate inflammatory

responses (Zhang et al., 2010). MtDNA are proposed to interact with TLR-9, which has been shown to be expressed on the platelet surface (Zhang et al., 2010) and therefore could potentially induce platelet activation. MtDNA was extracted from mitochondria from the blood of a healthy control donor and used to stimulate platelets at concentrations previously shown to affect other cells (Sun et al., 2013, Hauser et al., 2010). MtDNA failed to have a major effect on platelet aggregation at all concentrations tested. The MtDNA studies were limited as the isolation of mtDNA from donated blood did not give a high yield of mtDNA to perform an adequate number of experiments per donor. There were no further mtDNA experiments performed due to the limited aggregation response observed and the small yield produced. The use of a commercial or recombinant source of mtDNA would allow further experiments to be performed and useful in confirming whether mtDNA does not affect platelet function.

High-mobility-group-box 1 (HMGB-1) was an alternative nuclear-related Alarmin tested. HMGB-1 been shown to be elevated after trauma (Peltz et al., 2009) and is a potent inflammatory mediator (Schiraldi et al., 2012). HMGB-1 has been proposed to interact with TLR4 and therefore could induce platelet activation. A commercial source of HMGB-1 was used to stimulate washed platelets and PRP. There was minimal platelet aggregation in response to HMGB-1 stimulation at any of the concentrations tested, previously shown to have effects on other cells. Platelets did not significantly adhere and bind more to immobilised HMGB-1 above the BSA coated control. Recent studies have however shown that platelets can be activated and substantial aggregation can be induced with recombinant HMGB-1 (Yang et al., 2015). This suggests there is a potential issue with the isolation process of HMGB-1, which could affect reactivity.

HMGB-1 can also be released after platelet activation, therefore comparisons between isolated HMGB-1, recombinant HMGB-1 and different sources of HMGB-1 would be crucial to confirm whether HMGB-1 can mediate platelet activation.

Histones are the most extensively studied Alarmin. Histones are released in the plasma after nucleosome breakdown and are elevated after trauma and sepsis developed (Abrams et al., 2013, Xu et al., 2009). Histones are very reactive and can cause damage to endothelial cells (Abrams et al., 2013). Histones have been shown to activate platelets through TLR4 mechanisms (Semeraro et al., 2011, Fuchs et al., 2011b), however the signalling mechanisms have not been fully established, with multiple TLRs and other receptors such as TLR-2 have also been implicated in the histone-mediate aggregation (Xu et al., 2011). This study first set out to confirm that histones can mediate platelet activation in vitro and secondly to further investigate the signalling mechanisms behind the histone-mediated response.

CTH were used to stimulate platelets to examine the histone response. CTH are a heterogeneous mixture of different types of histones (H1-H4) and have been used in many previous histone studies (Fuchs et al., 2011b, Xu et al., 2009). CTH induced full platelet aggregation in both washed platelets and PRP in mice and humans, which was αIIbβ3 dependent, supporting the finding that histones-induced aggregation was the result of platelet agglutination only. The CTH concentrations used for stimulations were high in comparisons available plasma concentration, with histone concentrations as low as 10 µg/ml shown to have cytotoxic effects on endothelial cells (Abrams et al., 2013). The ability of histones to modulate the response to other agonists were therefore

studied. Sub-threshold levels of CTH were able to synergise with other agonists such as adrenaline in washed platelets to amplify the response and cause robust platelet activation, giving an explanation as to how histones can mediate effects at the lower concentrations. This along with platelets adhering and spreading on immobilised CTH at low concentrations supports the ability of histones to mediate platelet activation at physiological concentrations.

The signalling mechanisms behind the CTH-mediated activation were studied. CTH induced aggregation was Src and Syk dependent, with the CTH response being diminished in platelets pre-treatment with the Src inhibitor, dasatinib and the Syk inhibitor, PRT060318. Aggregation was reduced in the presence of the Src and Syk inhibitors and increases in tyrosine phosphorylation above basal of key signalling proteins such as Syk, FcRγ-chain and PLCγ2 was abolished. The synergy with adrenaline was significantly reduced in the presence of Src inhibitors, dasatinib and PP2, however there was no reduction observed in the presence of PRT060318, suggesting a Src dependent mechanism being involved in CTH/adrenaline synergy over a Syk dependent mechanism. Platelet spreading after adhesion to immobilised CTH was reduced in the presence of the Syk inhibitor. Overall, the aggregation, phosphorylation and spreading results in response to CTH stimulation suggests a Src and Syk dependent mechanism behind CTH mediated platelet activation.

Src and Syk are major signalling proteins involved in ITAM signalling (Senis et al., 2014). Therefore, to determine if CTH-induced aggregation was dependent on ITAM signalling, CTH was used to stimulate platelets from $GPVI^{-/-}$ and $CLEC\text{-}2^{-/-}$ mice.

Deficiencies in CLEC-2 did not affect CTH-induced aggregation and phosphorylation. CTH aggregation was reduced after CTH stimulation of platelets from GPVI$^{-/-}$ mice and there was no increase in phosphorylation of Syk, FcRγ-chain and PLCγ2 signifying a role of GPVI in CTH-induced platelet aggregation response.

To confirm if histones can induce GPVI signalling, Jurkat cells were transfected with GPVI and added to immobilised CTH before an NFAT luciferase reporter assay was performed. This assay measured the luciferase activity of the transfected cells, where increased luciferase signal represented signalling of GPVI in the transfected cells. There was no increase in NFAT-luciferase activity in the transfected GPVI cells incubated with immobilised CTH in contrast to the response to collagen. One explanation for this is due to the limitations of the NFAT assay and use of cell lines to transfect with GPVI. Activation by the positive control agonist collagen was lower than expected, suggesting the transfection efficacy may not be substantial enough to show activation by CTH. Other factors may have also interfered with binding and activation, such as antibiotics in the media, as in the absence of antibiotics the collagen response was increased. Another explanation is that activation of GPVI in platelets by CTH is indirect and requires other co-factors or receptors to be present to bind and active GPVI. A direct binding assay showing the binding of the GPVI ectodomain to immobilised histones was shown to be similar to that for collagen. Future experiments performing surface plasmon resonance would confirm whether there was direct binding of CTH to GPVI.

To determine if CTH could induce platelet aggregation *in vivo*, histone infusion assays were performed in mice. CTH infusion induced a rapid dose dependent reduction in

platelet count, with a CTH dose of 25-75 mg/kg causing thrombocytopenia to approximately 10% of basal count after 3 min. Interventions were tested to establish if any could improve the severe reduction in platelet count. A collagen-adrenaline infusion assay was performed as a proof of concept based on Abrams *et al.* studies (Abrams et al., 2013). WT mice experienced a severe drop in platelet count after infusion of collagen and adrenaline, with a less severe reduction in platelet count being observed in $GPVI^{-/-}$ mice. GPVI is a major signalling receptor on platelets; therefore the collagen-induced thrombocytopenia would be rescued because collagen would not be able to interact with GPVI to induce platelet activation and aggregation. A full recovery, representing no reduction in platelet count would not be observed as other minor collagen receptors on the platelet surface, including scavenger receptors wound be able to bind collagen and induce a small degree of platelet activation. If the CTH-induced aggregation *in vivo* was mediated through GPVI, then the same level of rescue of the platelet count to collagen would be expected. A CTH dose of 25 mg/kg was chosen for injection as it delivered a substantial level of thrombocytopenia in the mice. A CTH dose of 7.5 mg/kg only induced a moderate decrease in platelet count, therefore any further reduction in platelet count would be minimal. WT mice injected with CTH (25 mg/kg) experienced the substantial reduction in platelet count. There was no rescue in the reduction of platelet count after CTH infection in $GPVI^{-/-}$ mice, suggesting alternative mechanisms were involved in the CTH-induced thrombocytopenia.

Histones have been shown to enhance thrombin generation (Semeraro et al., 2011). Hirudin, a direct inhibitor of thrombin, was injected into the mice before CTH infusion to assess if it could neutralise the CTH-induced thrombocytopenia by reducing fibrin

formation through inhibiting thrombin's activity to convert fibrinogen to fibrin. There was however no rescue in the reduction of platelet count in WT mice pre-treated with hirudin or in GPVI$^{-/-}$ mice pre-treated with hirudin, suggesting that the CTH-induced aggregation and thrombocytopenia observed was independent of GPVI and thrombin, with alternative mechanisms being involved. The hirudin treatment may however, not been effective enough to inhibit the CTH-induced aggregation, with heparin treatment, another thrombin inhibitor, previously been shown to reduce the effects of histones (Fuchs et al., 2011b). Another explanation for the insufficient effect of hirudin and GPVI could result from other factors, such as the cytotoxic effect of histones on other cell types potentially leading to platelet activation. Histones have been shown to damage endothelial cells (Abrams et al., 2013), which could then release mediators causing platelet activation and aggregation. Staining for endothelial cell damage after histone injection or investigating for endothelial markers in the future would help show role for endothelial cells in the histone response. An alternative explanation may result from histones interacting with other receptors, such as the TLRs, resulting in platelet activation. Most therapeutic targets for preventing histone-mediated effects are with the use of anti-histone blocking antibodies or developing antibodies against multiple TLRs to give the most therapeutic value (Abrams et al., 2013, Semeraro et al., 2011, Fuchs et al., 2011b).

Histones are highly positively charged molecules, which could cause disruption to the membrane due to the charge affects. It is therefore proposed that the disruption of the membrane caused by the charged histones can lead to clustering of receptors, such as GPVI and result in the Src and Syk signalling mechanism mediating the platelet

aggregation. This new alternative GPVI signalling mechanism by charge interactions was also confirmed with other agonists such as diesel exhaust particles (Alshehri et al., 2015b). Histone-induced aggregation may also be mediated by a similar mechanism causing clustering of other receptors such as the TLRs that have previously been shown as receptors for histones. The histone charge effect would support the findings that heparin injections and treatment can reduce histone effects and increase survival of mice histone-induced thrombocytopenia and heparin-mediated cytotoxicity in a rat model (Fuchs et al., 2011b, Iba et al., 2015). Heparin is a heavily negatively charged molecule, which has been shown to bind to positively charged histones to neutralise the charge effect (Wildhagen et al., 2014). Therefore, this gives a potential explanation as to how heparin can have a more effective response against histones than hirudin and how survival is improved. Further studies investigation histone induced thrombocytopenia after pre-treatment of heparin would be useful to determine if the histone response is due to increased thrombin generation or whether the histone charge effect is a more important factor and if the *in vivo* histone-mediated aggregation could be rescued.

The aim of this study was to assess a variety of Alarmins to establish which Alarmins could activate platelets and determine the mechanism behind this. AGE and OxLDL are DAMPs implicated in a range of inflammatory conditions, but were unable to directly induce platelet activation or modulate responses to other agonists. Of the nuclear-related Alarmins, only histones effected platelet function. Histones were found to be powerful mediators of platelet activation in vitro and in vivo. More work is required to establish interventions that are sufficient to prevent histone-induced platelet activation. Direct

neutralisation of the histone charge, a crucial aspect of their action has the greatest potential to reduce histone-mediated activation.

CHAPTER 4

SOLUBLE GPVI (sGPVI) AS A MARKER OF PLATELET ACTIVATION IN INFLAMMATION

4.1 Introduction

Platelets have been implicated in the pathophysiology of a wide range of thrombotic and inflammatory conditions, including atherosclerosis, diabetes and inflammatory bowel disease (IBD) (Lindemann et al., 2007, Ponder and Long, 2013). Markers of platelet activation have been proposed to have clinical relevance as prognostic markers and relate to disease severity. Most markers proposed are based on detection of plasma protein levels, including various granule proteins released from α- and dense-granules after platelet activation, such as fibrinogen and ATP, respectively (Ang et al., 2013, Ghoshal and Bhattacharyya, 2014). Importantly these markers are not specific to platelets as they can originate from a number of other cells, such as endothelial cells (Gurney et al., 2002). Therefore, there is a requirement to identify and study a specific platelet activation marker.

Membrane glycoproteins on platelets, including P-selectin, the integrin αIIbβ3 and Glycoprotein V (GPV), are potential candidate markers. P-selectin is an extensively studied glycoprotein, which is a 140 kDa adhesion molecule that binds to P-selectin glycoprotein ligand-1 (PGSL-1) on leukocytes, allowing platelet-leukocyte interactions. P-selectin is predominately located on platelet α-granules, and upon activation, becomes exposed on the platelet surface. P-selectin surface expression can be measured by flow cytometry and increased expression is a marker of platelet activation. Soluble P-selectin (sP-selectin) is elevated in the plasma in patients with thrombotic conditions, such as atherosclerosis, myocardial infarction and stroke (Blann et al., 1997, Shimomura et al., 1998, Liu et al., 2005) and has been reported as a predictor of cardiovascular events (Ridker et al., 2001). Although sP-selectin has been proposed as a platelet activation

marker, questions surrounding its value have not been conclusive, with more sensitive markers being described (Naitoh et al., 2015, Gurbel et al., 2000). Endothelial cells express P-selectin on their surface so difficulties arise in discriminating between platelet and endothelial sP-selectin. Platelets internalise sP-selectin which will alter plasma measurements.

GPVI is the major signalling collagen receptor found on platelets. GPVI can be shed after activation through various mechanisms resulting inactivation (Gardiner et al., 2004). Cleavage of GPVI results in the release of a soluble 55-kDa GPVI fragment, which can be measured in plasma, leaving a 10-kDa remnant fragment membrane bound (Figure 4.1). Soluble GPVI (sGPVI) is a specific marker of platelet activation, as GPVI is restricted to platelets and megakaryocytes. Multiple groups have reported elevated levels of sGPVI in thrombotic conditions including microangiopathy and ischaemic stroke (Wurster et al., 2013, Al-Tamimi et al., 2011a).

The sheddase A disintegrin and metalloproteinase domain-containing protein 10 (ADAM10) has been shown to play the major role in GPVI shedding in humans, with ADAM17 also contributing to shedding in mice (Bender et al., 2010, Facey et al., 2016, Bergmeier et al., 2004). ADAM10 and ADAM17 are type 1 transmembrane proteases that are closely related to matrix metalloproteinases (MMPs) and which regulate levels of several surface receptors and ectoenzymes (Facey et al., 2016). The transmembrane of ADAM10 is thought to critical for regulation of ADAM10 activity. ADAM10 and ADAM17 are expressed on a wide variety of cells (Matthews et al., 2016, Facey et al., 2016).

GPVI shedding can be mediated by a range of mechanisms. Ligand-mediated shedding occurs when ligands such as collagen, collagen-related peptide (CRP), and the snake venom toxins alborhagin, crotarhagin and convulxin activate and signal through GPVI leading to ADAM10 activation (Gardiner et al., 2004, Wijeyewickrema et al., 2007, Stephens et al., 2005, Bergmeier et al., 2004). GPVI shedding can also be induced to be induced by activation of the other two platelet ITAM receptors, FcγRIIA and CLEC-2 (Gitz et al., 2014, Gardiner et al., 2008a). GPVI shedding can also be induced by shear stress and FX activation (Gardiner et al., 2008a, Al-Tamimi et al., 2011b).

An established sGPVI sandwich- ELISA method has been developed to measure sGPVI in the plasma of patients (Al-Tamimi et al., 2009) and used to show its elevation in thrombotic conditions (Wurster et al., 2013, Al-Tamimi et al., 2011a). The recent observation that GPVI is also activated by fibrin (Alshehri et al., 2015a, Mammadova-Bach et al., 2015) however makes it unclear whether the increase in GPVI is a reflection of activation by collagen or by fibrin, or by both ligands. Furthermore, platelets are now recognised as key players in inflammation and in a variety of thromboinflammatory disorders such as deep vein thrombosis and sepsis. Under these conditions, sGPVI may potentially be activated by exposure to fibrin or to other pathways of platelet activation alongside classical collagen activation.

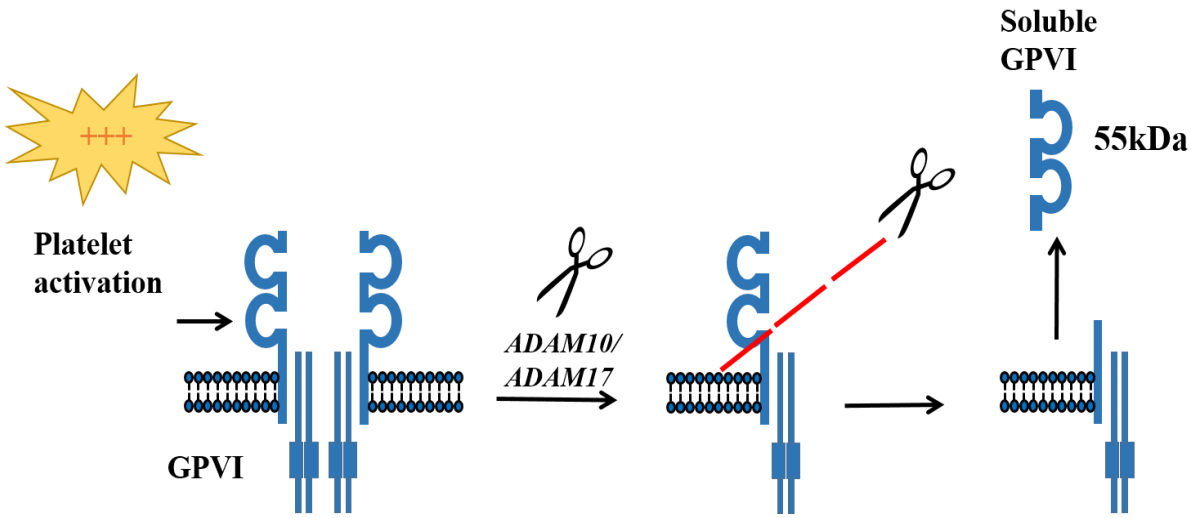

Figure 4.1 Schematic diagram of soluble GPVI (sGPVI) release into the plasma after GPVI cleavage by ADAM10. Activation of the sheddase ADAM10 (and ADAM17 in mice) leads to cleavage of GPVI leading to a 10-kDa membrane bound remnant and a 55-kDa fragment (sGPVI) that is released into the plasma and which can be measured by an established sGPVI ELISA.

The main aims of this chapter are (i) compare the level of shedding of GPVI ligands by collagen and CRP alongside activation by, G protein-coupled receptor (GPCR) agonists and fibrin; and (ii) the level of sGPVI in the plasma of patients with a variety of inflammatory conditions, namely rheumatoid arthritis (RA), thermal injury, clinically diagnosed sepsis or inflammatory bowel disease (IBD).

4.2 Results

4.2.1 GPVI is not detected in GPVI deficient patients

To confirm the validity of the anti-GPVI antibody, lysates were collected from unstimulated and fibrin stimulated samples of patients with GPVI deficiencies (Matus et al., 2013) and blotted for GPVI using an anti-GPVI antibody to the cytosolic tail, which recognises full length GPVI and the 10 kDa membrane remnant. Reductions in full length GPVI and the appearance of the remnant tail represent shedding of the glycoprotein receptor. As expected, no GPVI or tail remnant was recognised in the samples from the patients with GPVI deficiencies compared to healthy controls (HCs; Figure 4.2). GPVI shedding was observed in stimulated samples of HCs, supporting the finding that the anti-GPVI only detects GPVI and the tail remnant is also of GPVI origin.

4.2.2 Classical GPVI agonists induce GPVI shedding

This study initially set out to quantitate GPVI shedding by classical GPVI ligands. GPVI ligands, collagen and CRP, along with A23187, a potent GPVI shedding stimulus, were used to activate platelets under stirring conditions (1200 rpm) for 1 h in the presence of the αIIbβ3 blocker integrilin (eptifibatide; 9 μM) and $CaCl_2$ (1 mM). Lysates were prepared and blotted for GPVI using an anti-GPVI antibody to the cytosolic tail and again reductions in full length GPVI and the appearance of the remnant tail represent shedding of the glycoprotein receptor. Collagen, CRP and A23187 induced shedding of GPVI as shown by the reduction of full length protein and appearance of a doublet, with a major band of approximately 14 kDa and a smaller band below (Figure 4.3Ai).

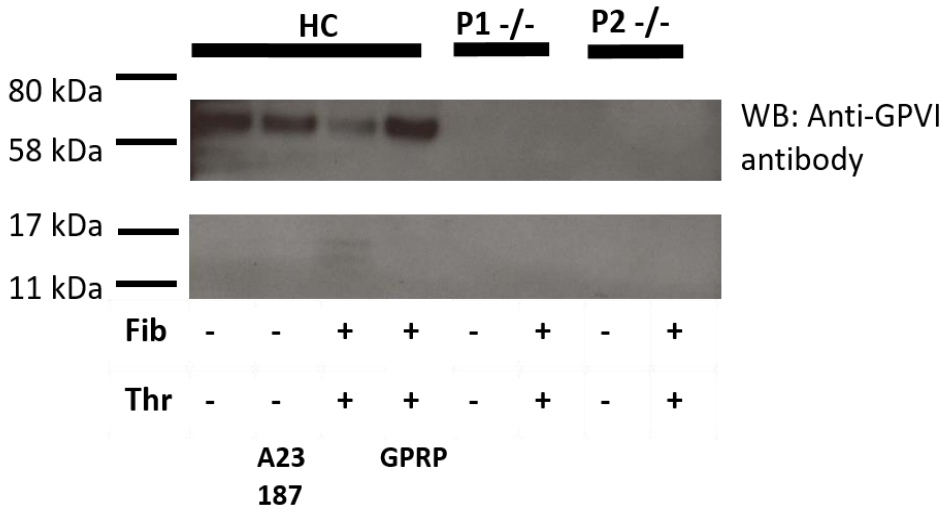

Figure 4.2 – GPVI is not detected in GPVI deficient patients. Washed platelets ($5x10^8$/ml) of patients with GPVI deficiencies (P1 and P2) were stimulated with thrombin (1 U/ml) in the presence of fibrinogen (100 µg/ml: polymerised fibrin) under stirring conditions in the presence of eptifibatide (9 µM) and blotted for GPVI using the anti-GPVI antibody. Washed platelets from healthy controls (HCs) were also stimulated with thrombin (1 U/ml) in the presence of fibrinogen (100 µg/ml), thrombin (1 U/ml) in the presence of fibrinogen (100 µg/ml) and GPRP (10 mM). This experiment was performed once experiment with two unrelated families.

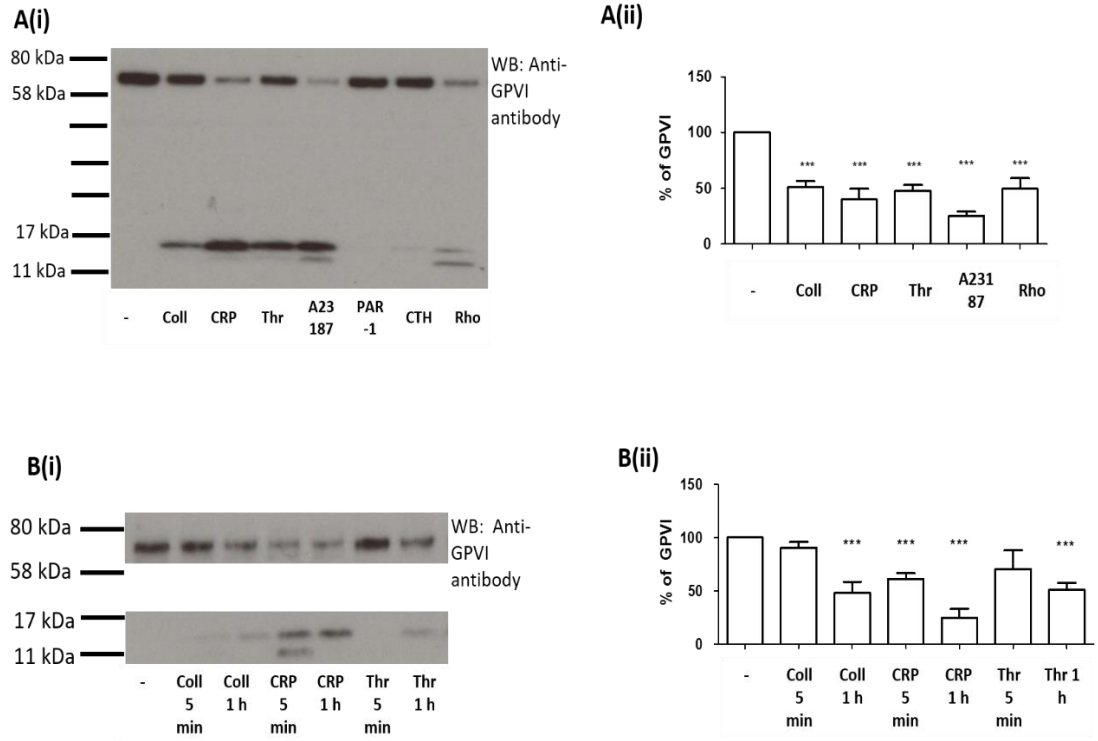

Figure 4.3 - Stimulation of platelets with GPVI and ITAM ligands induces GPVI shedding. A(i) Washed platelets ($5x10^8$/ml) were stimulated with collagen (30 µg/ml), CRP (30 µg/ml), thrombin (1 U/ml), rhodocytin (300 nM) and caclium ionophore (A23187: 10 µM), a potent shedding medaitor, in suspension under stirring conditions for 1 h at 37°C, in the presence of eptifibatide (9 µM) and $CaCl_2$ (1 mM). Membranes were blotted with an anti-GPVI antibody for GPVI (60-65-kDa) and the GPVI remnant band (10-17-kDa). Representative figure of stimulations from 8 separate donors. A(ii) Quantitation analysis of GPVI shedding after platelet stimulation with various GPVI and ITAM ligands. GPVI shedding represented as % of intact GPVI remaining after stimulation compared to unstimulated GPVI levels. Results are shown as mean ±SEM. One-way ANOVA performed with Bonferroni post-test, n=8, ***$p<0.005$. Bi) Western blot for GPVI after platelet treatment with collagen, CRP and thrombin for 5 min or 1 h stimulation. Representative figure of at least 6 donors. B(ii) Quantitation analysis of

GPVI shedding after 5 min and 1 h stimulation with GPVI ligands and thrombin. GPVI shedding represented as % of GPVI remaining compared to unstimulated GPVI levels. Results are shown as mean ±SEM. One-way ANOVA performed with Bonferroni post-test, n=6, ***$p<0.005$.

Shedding could be first observed after 5 min as illustrated by the increase in the remnant tail, but was more prominent after 60 min (Figure 4.3B). There was no evidence of shedding of GPVI in unstimulated samples as shown by the absence of the membrane remnant. There was minimal shedding observed with calf thymus histones (Figure 4.3Ai). The level of GPVI shedding was calculated using a Li-cor Odyssey-FC imager and Image Studio software based on the percentage of GPVI left after stimulation. Collagen (30 µg/ml), CRP (30 µg/ml), and A23187 (10 µM) reduced the level of GPVI on platelets to 51.0 ± 22.4%, 40.1 ± 25.3% and 29.5 ± 18.1% (± SD, n=7) relative to unstimulated controls (Figure 4.3A).

GPVI cleavage has also been shown to be mediated by the two platelet ITAM receptors, FcγRIIA and CLEC-2 (Gitz et al., 2014, Gardiner et al., 2008b). The CLEC-2 ligand, rhodocytin (300 nM) reduced the level of GPVI to 49.6 ± 27.0% of unstimulated GPVI samples (figure 4.3B). These results show that GPVI is shed by several mechanisms, namely by direct receptor activation, by the hemITAM receptor CLEC-2 and by the Ca^{2+} ionophore CLEC-2. The former all induce a similar level of shedding of GPVI after 1 h, namely approximately 50% of controls. A23187 induced a great degree of shedding in the order of 75% of control levels.

4.2.3 Activation of G protein-coupled receptors does not induce GPVI shedding

Studies were performed to investigate whether G protein-coupled receptors (GPCRs) could induce GPVI shedding. To address this, the GPCR agonists, ADP, a $P2Y_1$ and $P2Y_{12}$ ligand, PAR-1 peptide (SFLLN), a PAR-1 receptor ligand and thrombin, a PAR-1 and PAR-4 agonist, were used to activate platelets under stirring conditions for 1 h in

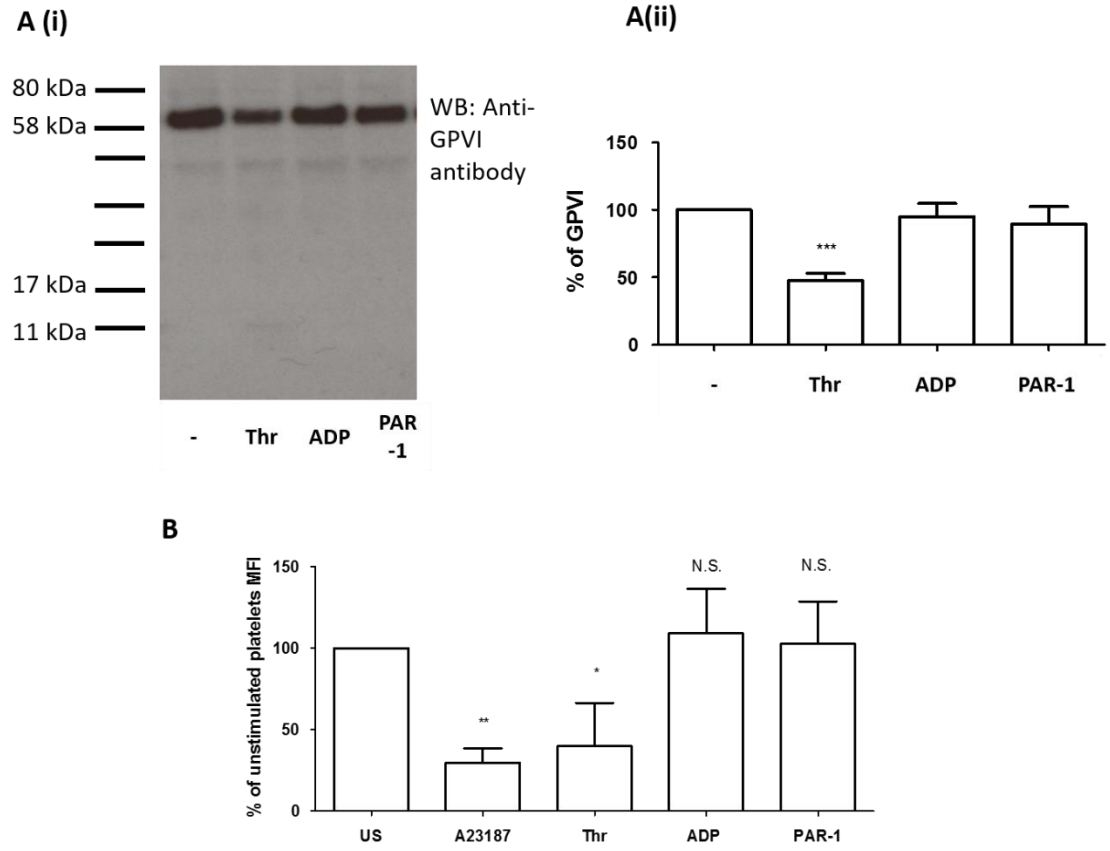

Figure 4.4 – Activation of GPCRs does not induce GPVI shedding. A(i) Western blot for GPVI after platelet stimulation with GPCR agonists, thrombin (1 U/ml), ADP (10 µM) and PAR-1 peptide (SFLLRN :100 µM) in the presence of eptifibatide (9 µM) and $CaCl_2$ (1 mM) under stirring conditions for 1 h at 37^{o}C. Representative figure of at least 8 donors. A(ii) Quantitation of GPVI shedding after platelet stimulation with GPCR agonists. % of GPVI represents levels of intact GPVI remaining compared to unstimulated GPVI levels. Results are shown as mean ±SEM. One way ANOVA with Bonferroni post-test was performed to compare shedding to unstimulated platelets, n=8-12, ***$p<0.05$ B) GPVI shedding measured by flow cytometry. Washed platelets ($2x10^8$/ml) were pre-incubated with IG5(Fab')$_2$-488 (8 µg/ml), an antibody that recognises GPVI, before stimulation (static) with A23187 (10 µM), thrombin (1 U/ml), ADP (10 µM) and PAR-1 peptide (SFLLRN :100 µM) in the presence of $CaCl_2$ (1 mM)

for 45 min at 37^{o}C. % of Median intensity fluorescence (MFI) of unstimulated samples were compared to stimulated samples. One-way ANOVA performed with Bonferroni post-test, n=4, mean shown ±SEM, *p<0.05, **<0.01.

the presence of the αIIbβ3 blocker eptifibatide (9 μM) and $CaCl_2$ (1 mM). The level of GPVI was measured using the antibody to the cytosolic tail of GPVI as described above and by flow cytometry using mAb 1G5 to the GPVI ectodomain. The GPCR agonists, ADP (10 μM) and PAR-1 peptide (SFLLRN; 100 μM), did not induce shedding as measured by western blotting (Figure 4.4A) and by flow cytometry (Figure 4.5B). A23187 was used as a control and shown to reduce the level of GPVI to 29.8 ± 8.6% of controls as measured by flow cytometry (Figure 4.4B).

In contrast to the above results for ADP and PAR-1 peptide, thrombin (1 U/ml) induced a similar level of GPVI shedding to that induced by collagen as measured by western blotting, 47.6 ± 20.6% and 51.0 ± 22.4% of unstimulated GPVI levels, respectively (± SD, n=8-12). The appearance of a band of an ~14 kDa major and 10 kDa minor band corresponding to the GPVI remnant was also seen in 50% of donors (Figure 4.4 and 4.5A). The basis for the variation between donors in formation of the GPVI tail remnant is not known, although this could be related to variation of donor responses to thrombin, but indicates that in some donors, it may undergo further cleavage. Thrombin (1 U/ml) also induced a similar level of shedding of GPVI when measured by flow cytometry to 40.0 ± 26.5% of controls (n = 4; Figure 4.4B). These results demonstrate that thrombin but neither ADP nor PAR-1 peptide induces shedding of GPVI indicating that shedding is not mediated by activation of the Gi- and Gq-coupled GPCRs.

4.2.4 Fibrin stimulation of platelets induces GPVI shedding

The mechanism of shedding of GPVI by thrombin was further investigated. Two possibilities for thrombin-induced shedding were considered, namely either that

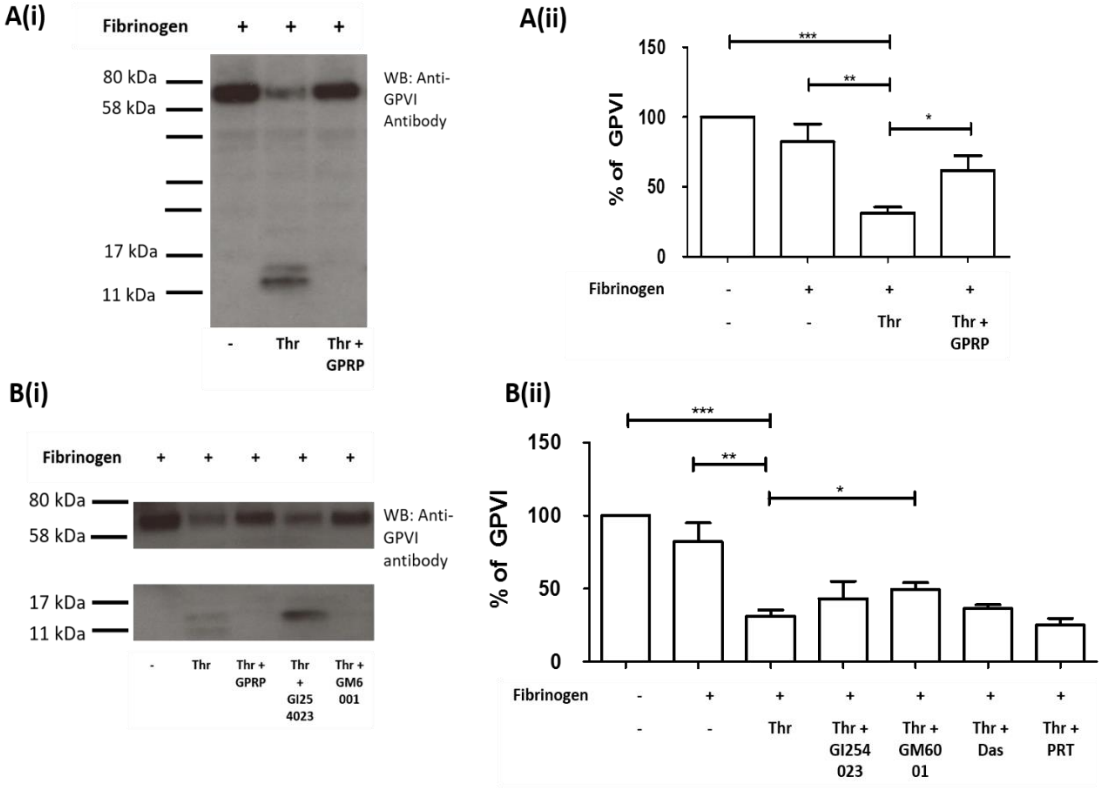

Figure 4.5 – Fibrin stimulation of platelets induces GPVI shedding. A(i) Western blot for GPVI after washed platelets ($5x10^8$/ml) were stimulated with fibrinogen (100 µg/ml), thrombin (1 U/ml) in the presence of fibrinogen (polymerised fibrin) and fibrin formed in the presence of GPRP (10 mM) and under stirring conditions for 1 h at 37^oC in the presence of eptifibatide (9 µM) and $CaCl_2$ (1 mM). GPRP was addded with fibrinogen 3 min before thrombin stimulation to prevent fibrin polymerisation. Representative figure of stimulations from 5 donors. A(ii) Quantitation analysis of GPVI shedding induced by different forms of fibrin. % of GPVI represents levels of intact GPVI remaining after stimulation compared to unstimulated GPVI levels. Results are shown as mean ±SEM. One-way ANOVA performed with Bonferroni post-test to compare fibrin-induced shedding in the presence of GPRP and fibrinogen alone to unstimulated samples, *$p<0.05$ **$p<0.01$ ***$p<0.005$, n=5 donors. B(i) Western blot for GPVI after stimulation with thrombin (1U/ml) in the presence of fibrinogen (100

µg/ml; polymerised fibrin) in the presence of inhibitors under same conditions as before. Representative figure of 5 separate donors. GI254023 (2 µM) and GM6001 (10 µg/ml) were added 5 min before fibrinogen and thrombin stimulation. B(ii) Quantitation GPVI shedding analysis of fibrin in the presence of sheaddase inhibitors (GI254023: 2 µM, GM6001: 10 µg/ml), GPRP (10 mM) and dasatinid (10 µM) and PRT (10 µM). % of GPVI represents levels of intact GPVI after stimulation compared to unstimulated GPVI levels. Results are shown as mean ±SEM. A two-tailed t-test was performed to show significant differnece between fibrin-induced shedding with and with out inhibitors. n=3; *$p<0.05$ **$p<0.01$ ***$p<0.005$.

thrombin can directly cleave GPVI or that cleavage results from activation of GPVI by fibrin. There is however no cleavage site in GPVI for thrombin. Therefore, this favours the latter option that fibrin, formed from cleavage of fibrinogen (released from platelets) by thrombin, mediated shedding.

To further investigate the mechanism of shedding of GPVI, platelets were stimulated with thrombin in the presence of fibrinogen (100 µg/ml) to ensure that a constant amount of fibrin was formed between experiments. In the presence of fibrinogen, thrombin induced a marked reduction in GPVI and stimulated formation of a doublet corresponding to the GPVI tail remnant, with the lower band being prominent in some studies (Figure 4.5Ai). Fibrinogen alone did not induce GPVI shedding (Figure 4.5Ai). In the presence of fibrinogen, thrombin induced a greater level of GPVI shedding than in the absence of fibrinogen and was similar to that induced by A23187 (31.4 ± 10.9%, 47.6 ± 20.6% and 29.5 ± 18.1% of unstimulated GPVI, respectively; Figure 4.5Aii).

Fibrin can be present in a monomeric form and polymerised form. To determine if thrombin induces cleavage of GPVI through monomeric or polymerised fibrin, polymerisation of fibrin was inhibited by addition of GPRP (10 mM). In the presence of GPRP, there was a marked reduction in the level of GPVI cleavage (Figure 4.5A&Bi) suggesting monomeric fibrin does not induce GPVI shedding in platelet suspensions.

4.2.5 D-dimers do not induce shedding of GPVI

Fibrin is degraded through activation of fibrinolytic pathways. D-dimers are a degradation product of fibrin breakdown and can be released into the circulation

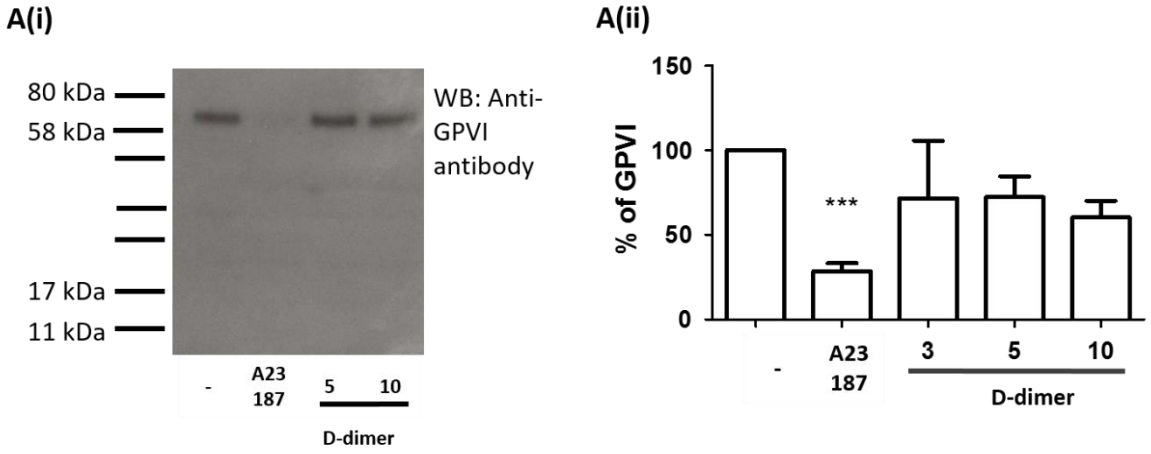

Figure 4.6 – Platelet stimulation with D-dimer does not induce GPVI shedding. A(i) Western blot for GPVI after washed platelets ($5x10^8$/ml) were stimulated with different concentrations of D-dimer (5-10 µg/ml) under stirring conditions for 1 h at 37^oC in the presence of eptifibatide (9 µM) and $CaCl_2$ (1 mM). A23187 (10 µM) used as positive control. Representative figure of 3 donors. A(ii) Quantitation analysis of GPVI shedding induced by D-dimers. % of GPVI represents levels of GPVI remaining after stimulation compared to unstimulated GPVI levels. Results are shown as mean ±SEM, n=3-5. One way ANOVA with Bonferroni post-test was performed to compare shedding to unstimulated platelets, ***$p<0.005$.

(Ohlmann et al., 2006). To determine if this fibrin degradation product can also induce GPVI shedding, platelets were stimulated with D-dimers (5-10 μg/ml) and blotted for GPVI. D-dimers had no effect on GPVI shedding. There was no reduction in GPVI and no appearance of the tail remnant (Figure 4.6A), demonstrating that D-dimers do not induce shedding of GPVI.

4.2.6 Multiple sheddases are involved in fibrin-induced GPVI shedding

Collagen-induced GPVI shedding has previously been shown to be predominately through the activity of the sheddase ADAM10 (Facey et al., 2016), with a partial role for ADAM17 in mice (Bergmeier et al., 2004). To determine if this was the case for fibrin-induced GPVI shedding various inhibitors known to reduce GPVI shedding, including collagen-mediated GPVI shedding were used. GM6001, a general metalloproteinase inhibitor, which inhibits ADAM10 and ADAM17, and the specific ADAM10 inhibitor, GI254023, were added to fibrinogen before thrombin stimulation. GM6001 reduced GPVI shedding by thrombin in the presence of fibrinogen, with less reduction in GPVI being observed and less tail remnant expressed (Figure 4.5Bi). To determine if ADAM10 was the major contributor to this reduction, GI254023, the ADAM10 inhibitor, was added before stimulation. In the presence of GI254023, only the upper band of the doublet GPVI tail was observed suggesting that the lower band is formed by the action of a second sheddases (Figure 4.5Bi). Fibrin-induced GPVI shedding was significantly reduced in the presence of GM6001 (*$p<0.05$), but there was no significant difference in fibrin-induced stimulation in the presence of GI24023 (Table 4.1 and Figure 4.5Bii). This suggests that other sheddases other than ADAM10 are involved in fibrin-induced GPVI shedding. DAPT (10μM), a γ-secretase inhibitor,

also had no effect on the degree of fibrin-induced GPVI shedding (42.0 ± 15.8% of unstimulated GPVI ± SD, data not shown). Overall these results suggest multiple sheddases and alternative mechanisms are involved in fibrin-induced shedding.

4.2.7 GPVI signalling does not mediate fibrin-induced GPVI shedding

Ligand-mediated shedding of GPVI, such as collagen-induced shedding, can be blocked in the presence of inhibitors of Src and Syk kinases (Stephens et al., 2005). To investigate if this was a similar result in the presence of thrombin and fibrin polymerisation, the Src and Syk inhibitors, dasatinib (10µM) and PRT060318 (10µM) were added before fibrinogen and thrombin stimulation. There was no difference was seen in the amount of GPVI shed by thrombin/fibrinogen in the presence of dasatinib and PRT060318 compared to fibrin alone (38.1 ± 12.1% and 21.6 ± 1.25% compared to 37.3 ± 13.7% respectively, Figure 4.5Bii and table 4.1). This demonstrates that GPVI signalling does not mediate shedding by fibrin.

4.2.8 Soluble GPVI is detectable in patients with chronic inflammation including rheumatoid arthritis and inflammatory bowel disease

The results above have shown GPVI shedding occurs after platelet stimulation with GPVI ligands including collagen and fibrin. The cleavage of GPVI results in a 55kDa soluble fragment, referred to as sGPVI being released into the plasma. An aim of this study was to show sGPVI can be detected by sGPVI ELISA (Al-Tamimi et al., 2009) in a range of inflammatory conditions, therefore, sGPVI was measured in patients with rheumatoid arthritis (RA), inflammatory bowel disease (IBD) and patients that have

Table 4.1 – Inhibitors effects on fibrin-induced GPVI shedding. Quantitation analysis of GPVI shedding induced by fibrin in the presence of sheaddase inhibitors (GI254023: 2 µM, GM6001: 10 µg/ml), GPRP (10 mM) and Src and Syk inhibitors (dasatinib: 10 µM, PRT: 10 µM). % of GPVI remaining compared to unstimulated samples, mean shown as ±SD. A two-tailed t-test was performed to compare fibrin-induced shedding with and without inhibitors to unstimulated platelets. T-test also performed to show significant differnece between fibrin-induced shedding with and with out inhibitors. *p<0.05 **p<0.01 ***p<0.005

Condition	% of GPVI of unstimulated samples Mean (± SD)	Significance to unstimulated samples		Significance to Fib + Thr samples	
Unstimulated	100	-	-	<0.0001	***p<0.001
Fibrinogen	82.2 (34.3)	0.1270	N.S.	0.0082	**p<0.001
Fibrinogen + Thrombin	31.4 (10.85)	<0.0001	***p<0.001	-	-
Fibrinogen Thrombin + GPRP	61.8 (23.6)	0.0223	*p<0.05	0.0422	*p<0.5
Fibrinogen Thrombin + GI254023	43.2 (32.13)	0.0030	**p<0.01	0.409	N.S.
Fibrinogen Thrombin + GM6001	49.4 (10.75)	0.0005	***p<0.001	0.040	*p<0.5
Fibrinogen Thrombin + Dasatinib	36.4 (4.59)	0.0020	**p<0.01	0.141	N.S.
Fibrinogen Thrombin + PRT060318	25.1 (6.51)	0.0020	**p<0.01	0.275	N.S.

undergone thermal injury and septic patients. RA is a chronic inflammatory condition, associated with platelet activation, predominately effecting and causing damage to joints (Del Rey et al., 2014). Plasma was obtained from 10 RA patients and compared to healthy controls. sGPVI levels were significantly in RA patients compared to HCs (***$p<0.005$; Figure 4.7A).

sGPVI was also measured in IBD patients, another chronic inflammatory condition linked with platelet activation. sGPVI was detected in the plasma of 42 IBD patients consisting of either active/inactive Crohn's disease and active/inactive ulcerative colitis (UC). sGPVI levels were not raised in patients with active/inactive Crohn's disease and inactive UC compared to HCs, with a similar distribution of sGPVI levels being observed (Figure 4.7B). sGPVI was only significantly elevated in patients with active UC, with higher levels then both inactive UC patients and HCs (*$p<0.05$ and **$p<0.01$ respectively; Figure 4.7B). Active UC patients also had a wider distribution range of sGPVI levels compared to controls.

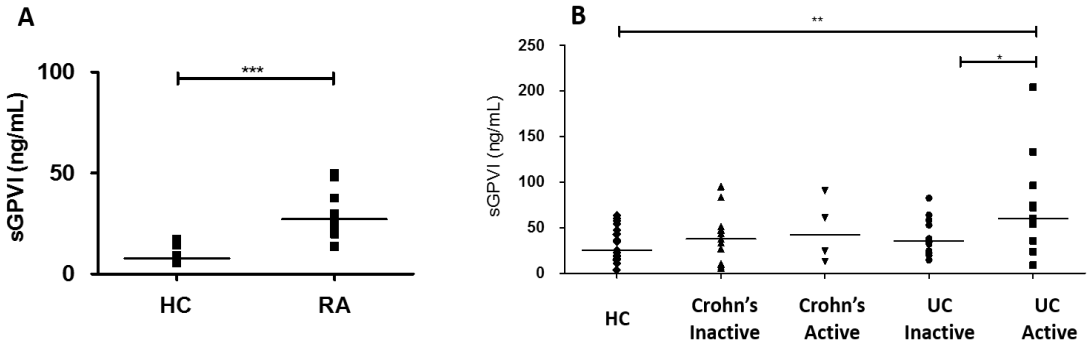

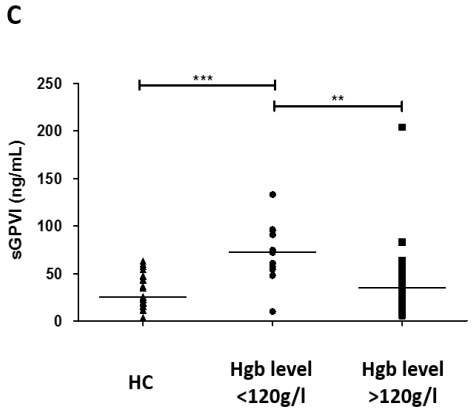

D

Conditions vs sGPVI	N number	Test value/ Spearmen's rank	P value	Correlation
Age	39	-0.220	0.184	N.S
Hgb	42	-0.300	0.028	Weak negative correlation
Platelet count	41	-0.252	0.110	N.S.
Ferritin	30	-0311	0.095	N.S.
Ferritin of patients with CRP>5	19	-0.530	0.020	Moderate negative correlation

Figure 4.7 - sGPVI is elevated in patients with chronic inflammatory conditions including rheumatiod arthritis (RA) and Ulcerative Colitisis (UC). A) sGPVI levels measured by sGPVI ELISA in 10 RA patients compared to 10 HCs. Mann-Whitney statistical test was performed to compare sGPVI levels of RA patients and HCs, ***p<0.005: median shown. B) sGPVI levels of inflammatory bowel disease (IBD) patients with inactive, active Crohn's disease (n=13, n=4), inactive and active UC (n=12, n=13), compared to HCs (n=20). Mann-Whitney statistical test was performed to compare sGPVI levels of different IBD patient groups and HCs, *p<0.05, **p<0.01: median shown. C) sGPVI levels of IBD patients with haemoglobin (Hgb) levels of above or below 120 g/l (n=28, 13 respectively) compared to HCs (n=20). A Kruskal-Wallis statistical test with Dunn's multiple comparisons was performed to compare the

three patient groups (**p<0.01, ***p<0.005). D) Table of statistical values after Spearman's rank correlation performed to examine correlations between sGPVI levels and clinical parameters, including age, Hgb levels, platelet count, ferritin levels (CRP represents C-Reactive protein levels). Significant correlation is observed when p<0.05. A Spearman's rank value of 0.3 gives weak correlation, 0.5 moderate and above 0.7 represents strong correlations.

Table 4.2 - Patient parameters: Inflammatory Bowel Disease. IBD patient parameters and healthy controls (HC). Patients were categorised into the types of IBD, Crohn's disease or ulcerative colitis (UC) and diagnosed with inactive and active inflammatory flares based on clinical diagnoses, C-Reactive Protein (CRP) levels and endoscopy results. Results shown as mean with inter-quartile range (IQR).

Parameter	HC	All	Crohn's	UC
Number of patients	20	42	17	25
Age, mean (min-max)	28 (20-47)	38 (19-81)	34 (20-62)	40 (19-81)
Gender M:F	11:9	33:19	5:12	16:9
Inactive: Active	-	25:17	13:4	12:13
CRP Levels (mg/L):Mean (IQR)	-	8.9 (3.0-6.8)	5.7 (3.0-6.0)	11.0 (3-7.25)
Platelet count /x10^9/L : Mean (IQR)	-	279 (211-328)	299 (256-345)	265 (194-302)
Haemoglobin level g/L: Mean (IQR)	-	127 (113-145)	130 (116-144)	125 (103-146)
Ferritin ng/ml: Mean (IQR)	-	84.3 (10-113.3)	112.1 (10.0-119.3)	70.5 (8.5-111.3)

sGPVI correlations with other IBD clinical parameters were also investigated. There was no correlation between platelet count and sGPVI levels in any of the IBD patient groups (Figure 4.7B). When analysing the IBD patients as a whole cohort, C-reactive protein levels of the patients also did not correlate with sGPVI levels. There was also no significant correlation between age and sGPVI levels in the IBD patients (Figure 4.7B), which supports previous findings in other studies (Al-Tamimi et al., 2011a). Iron deficiency anaemia (IDA) is commonly associated with IBD cases, with around 17% of IBD patients having IDA, increasing in prevalence to around 60% when studying hospitalised IBD patients (Guagnozzi and Lucendo, 2014, Bergamaschi et al., 2010). Iron deficiency can affect disease severity in IBD patients and chronic gastrointestinal bleeding has been proposed as a cause. To establish if there are associations between platelet activation and iron deficiency in IBD patients, sGPVI correlations with haemoglobin (Hgb) levels and ferritin levels were studied. A weak correlation was seen with sGPVI and Hgb levels (Spearman's rank = -0.3; figure 4.7D) and a moderate correlation of sGPVI levels with ferritin levels of patients with a C-Reactive Protein level greater than 5 (Spearman's rank = -0.53). When separating IBD patients into groups of low Hgb levels (<120g/l) and high Hgb (>120/l) there was a significant difference, with patients with low Hgb have significantly higher levels of sGPVI compared to patients with higher Hgb levels and HCs (**$p<0.01$ ***$p<0.005$, figure 4.7C).

4.2.9 Soluble GPVI is detectable in patients with thermal injury and raised in patients that develop sepsis

sGPVI was measured in patients who have undergone thermal injury to establish sGPVI kinetics in an inflammatory condition over time. Burns patients were recruited as part of the Scientific Investigation of the Biological Pathways Following Thermal Injury in Adults (SIFTI) study, (Table 4.3; (Hampson et al., 2016)). This was a multi-centre prospective observational study which recruited patients with burns of various size from 1.5-95% total body surface area (TBSA). sGPVI was detected in 99 patients and were subdivided into non-septic and septic groups according to whether they met the American Burns Association (ABA) sepsis criteria (Greenhalgh et al., 2007) had a positive culture and/or an antibiotic response.

In this patient cohort sGPVI levels were measured at regular intervals from Day 1 (D1) to Month 12 (M12) in 99 burns patients. There was an increase in sGPVI levels from D1 until D14, where levels peaked in the majority of patients before declining back down to levels of HCs by M12 (Figure 4.8A and Table 4.4). With each time point there was a wide distribution of sGPVI levels, with some patients having significantly high levels than average (Figure 4.8A). However, statistical significance above healthy controls was only reached at D14 (***$p<0.005$; Figure 4.8A and Table 4.4). There was only weak correlation between sGPVI levels and total body surface area at D1 (Spearman's rank = 0.28, ***$p<0.005$).

Table 4.3. Patient parameters: thermal injury patients with and without sepsis. Patient parameters listed for thermal injury patients and healthy controls (HC). For patient recruitment details see Hampson *et al*. (2016). Sepsis diagnosis made when at least 3 of the criteria agreed in 2007 by the American Burn Association (ABA) were met along with either a positive bacterial culture or evidence of clinical antibiotic response. (Hampson et al., 2016, Greenhalgh et al., 2007). MOF represents Multiple Organ Failure based on a Denver Post-injury MOF score >3 on two consecutive days involving two organ systems (Kraft et al., 2014). %TBSA, percentage of total body surface area. IQR, inter-quartile range.

Parameter	HC	All	Septic	Non-septic
Number of patients	15	99	57	42
Age, mean (min-max)	29 (20-47)	49 (16-93)	49 (16-91)	49 (16-93)
Gender M:F	9:6	61:38	36:21	25:17
% TBSA: Mean (IQR)	-	24 (8-38)	34 (16-51)	12 (6-21)
Survival Y:N (%)	-	78:21 (79)	38:19 (67)	40:2 (95)
MOF Y:N (%)	-	25:71 (21)	23:32 (42)	2:39 (5)

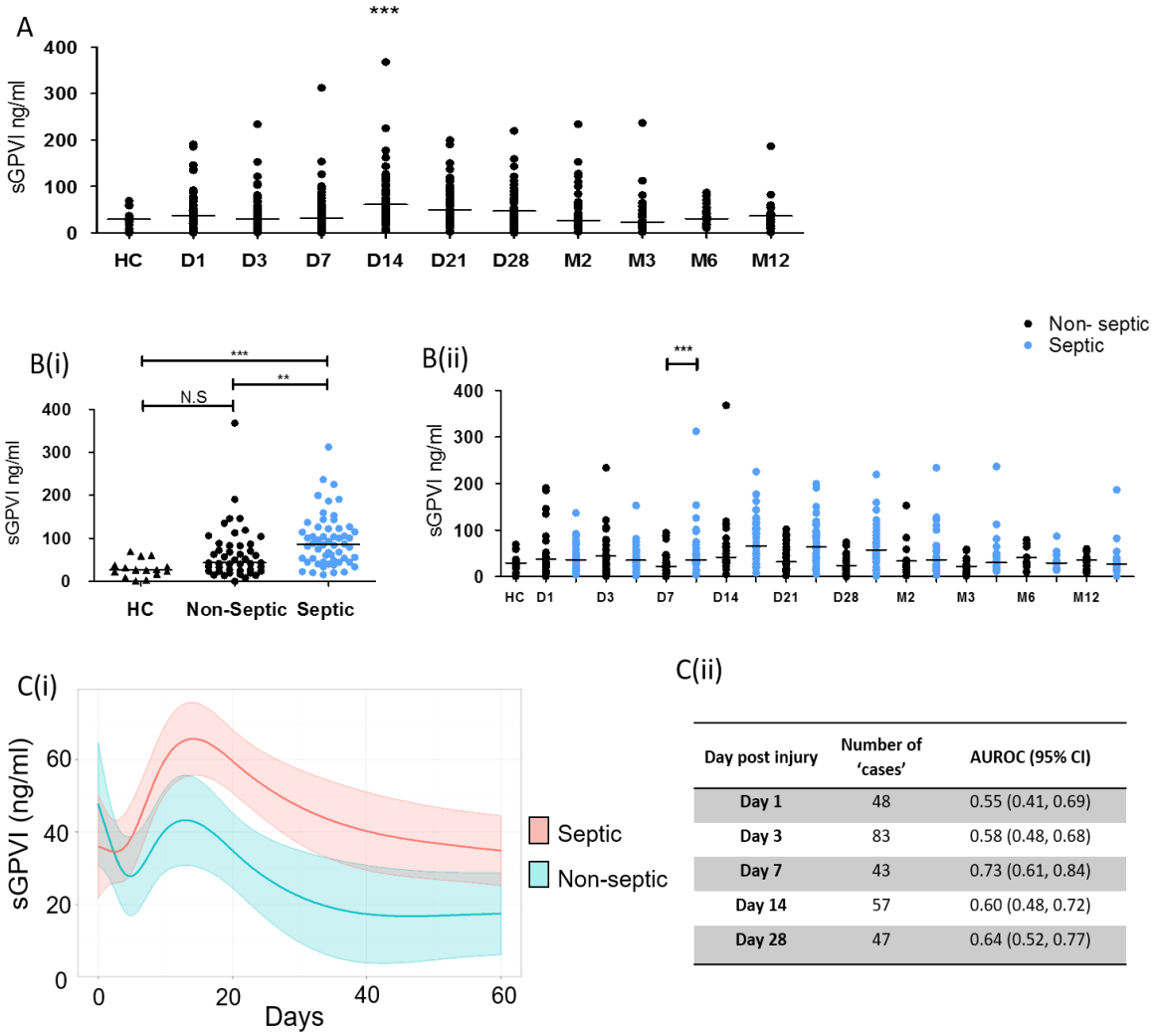

Day post injury	Number of 'cases'	AUROC (95% CI)
Day 1	48	0.55 (0.41, 0.69)
Day 3	83	0.58 (0.48, 0.68)
Day 7	43	0.73 (0.61, 0.84)
Day 14	57	0.60 (0.48, 0.72)
Day 28	47	0.64 (0.52, 0.77)

Figure 4.8 - sGPVI is detectable in patients with thermal injury and raised in patients who experience at least one episode of sepsis. A) sGPVI levels of patients with thermal injury (n=99) measured in samples taken from Day 1 (D1) to month (M12) compared to HCs (n=15). Mann-Whitney statistical test was performed to compare each patient time point to HC. ***p<0.005: median shown. B(i) Peak sGPVI levels in septic and non-septic patients with thermal injury and HCs. Sepsis diagnoses as meeting at least 3 of the American Burn Association (ABA) sepsis criteria and a positive culture. Mann-Whitney statistical test was performed to compare sGPVI levels of septic patients to non-septic patients and HCs, **p<0.01 ***p<0.005: median shown. B(ii)

Comparisons of sGPVI levels of septic patients compared to non-septic patients. Mann-Whitney statistical test was performed to compare sGPVI levels of septic and non-septic ***$p<0.005$: median shown. C(i) Longitudinal analysis using a linear mixed-effects model examining the relationship between sGPVI and time according to sepsis status. Line represents mean predicted effects and shaded area represents 95% confidence interval. B(ii) Table showing the discriminatory performance of GPVI for predicting sepsis on different sample days after logistic regression analysis. Discriminatory power represented as area under the receiver operator characteristic curve (AUROC) with a 95% confidence interval. A value of 0.9 represents a strong predictive value.

Sepsis was a common complication in thermal injury patients with a 56.7% incidence. Separating into septic and non-septic groups revealed a significant elevation in sGPVI levels at D7, which is associated with the time point were sepsis manifests in the patients (***p<0.005; Figure 4.8Bii). There is a limited time window in sGPVI elevation, which could reflect the different time course of sepsis onset. Peak levels of sGPVI were significantly higher in the septic patients compared to those non-septic patients and HCs (**p<0.01 ***p<0.005; Figure 4.8Bi).

To establish if sGPVI levels could be a potential diagnostic marker for sepsis progression, longitudinal statistical analysis and prediction models were performed, showing curves representing sGPVI levels of septic or non-septic patients over time (Figure 4.8C). The analysis shows crossovers of sGPVI levels and 95% confidence intervals of the septic and non-septic patients and a discriminatory predictive value (represented as an area under the receiver operating characteristic (AUROC) curve value) of 0.73 (0.61-0.84; 95% confidence interval), whereas a value of 0.9 is a strong predicator (Figure 4.8C), therefore suggesting sGPVI is not a good diagnostic predictor of sepsis progression.

sGPVI levels could be influenced by platelet count. Previous burn's studies have reported large drops in platelet counts at D3 post injury, which is followed by a rebound thrombocytosis phase (Marck et al., 2013). Figure 4.9A shows the platelet kinetics for non-septic and septic patients. The platelet counts reached a nadir at D3 and then rebounded to a peak between D14 for non-septic and D21 for septic patients (Figure 4.9 A&B). To establish there was no masking of low GPVI levels at the earlier time point by a low platelet count, sGPVI levels were normalised to platelet count (Figure 4.9C).

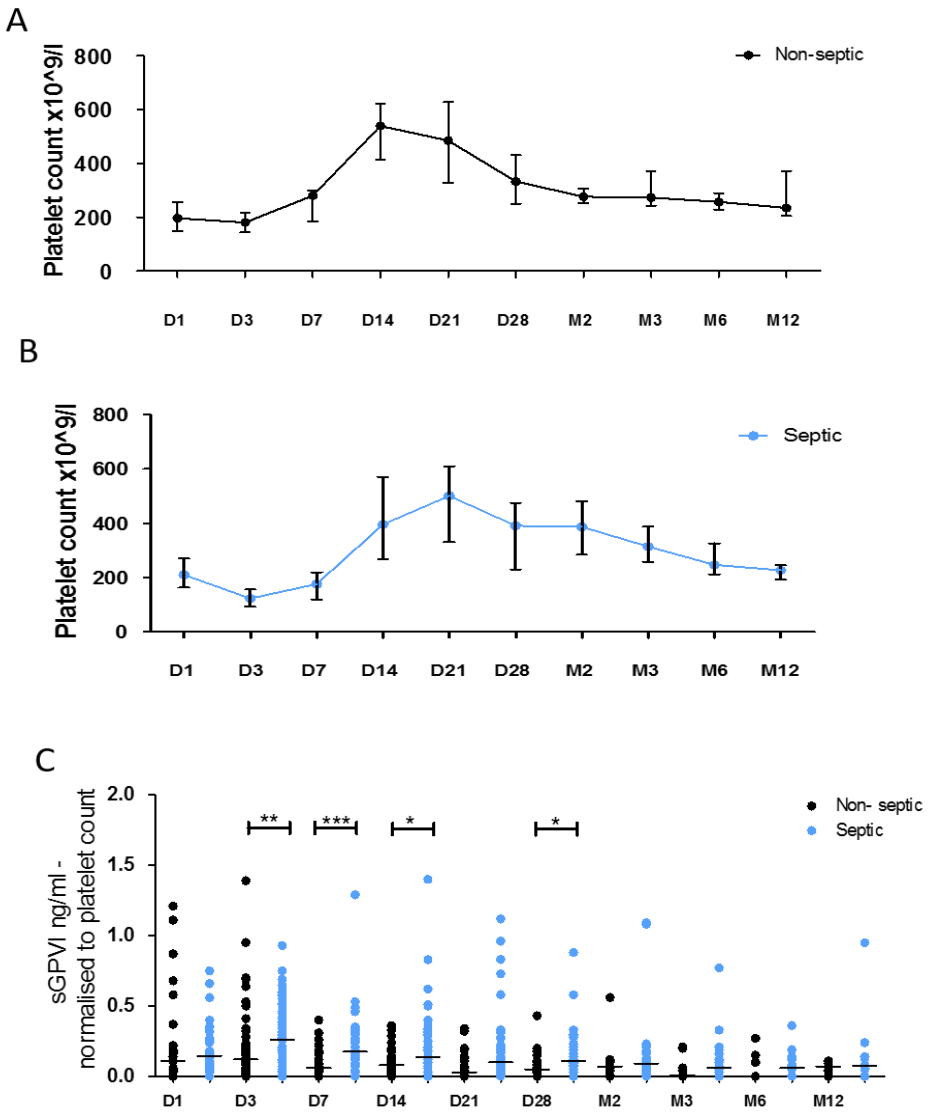

Figure 4.9 - sGPVI is elevated in patients with thermal injury who develop sepsis even when platelet count is taken into effect. Platelet counts of patients with thermal injury split into (A) non-septic and (B) septic groups, measured using the Sysmex XN-1000-Hematology Analyser, over the full time course, from Day 1 (D1) to month (M12): median shown with interquartile range. C) sGPVI levels normalised to platelet count of septic and non-septic thermal injury patients. Mann-Whitney statistical test was performed to compare sGPVI levels of septic patients and non-septic burns patients. *p<0.05, **p<0.01 ***p<0.005 and median shown.

Table 4.4–sGPVI levels and platelet count at the different time points of patients with thermal injury. Median, mean values (±standard error of mean) and inter-quartile (IQR) range of sGPVI levels (ng/ml) and platelet counts ($x10^9$/l) of patients at the different time points (Day 1- Month 12). HC=Healthy control.

Time point	sGPVI levels ng/ml					Platelet count $x10^9$/l				
	N number	Median	IQR	Mean ±SEM	Significance to HC	N number	Median	IQR	Mean ±SEM	Significance to M12
D1	71	37.6	22.3-52.4	47.7 (4.84)	0.109 N.S.	64	202	182-265	216 (10.4)	0.124 N.S.
D3	88	29.8	17.2-52.4	39.9 (3.79)	0.430 N.S.	79	137	99-203	149 (6.63)	<0.0001 ***p<0.005
D7	77	32.7	19.9-47.9	42.6 (4.83)	0.237 N.S.	68	202	151-281	223 (13.7)	0.13 N.S.
D14	74	61.3	34.6-102.7	71.3 (6.52)	0.0005 ***p<0.005	69	469	300-615	481 (27.5)	<0.0001 ***p<0.005
D21	61	50.1	29.0-85.9	60.9 (5.55)	0.0057 *p<0.05	57	501	330-600	507 (32.6)	<0.0001 ***p<0.005
D28	62	38.2	16.7-68.5	47.3 (5.30)	0.148 N.S.	55	367	237-467	366 (24.0)	0.0034 **p<0.005
M2	44	27.6	18.5-55.5	44.5 (6.90)	0.537 N.S.	35	333	256-424	359 (21.6)	0.0006 ***p<0.005
M3	34	23.6	12.9-43.9	35.9 (7.37)	0.770 N.S.	22	301	245-388	325 (19.9)	0.0018 **p<0.005
M6	27	30.8	19.4-45.7	36.4 (3.84)	0.294 N.S.	20	257	227-310	271 (15.6)	0.148 N.S.
M12	30	29.0	17.3-42.1	36.4 (6.05)	0.622 N.S.	19	228	198-259	251 (19.3)	- -
HC	15	27.2	17.5-37.1	23.0 (5.21)	- -	-	-	-	- -	- -

From this there were significantly elevated sGPVI levels in septic patients at D3, D7 and D14 compared to non-septic patients (**p<0.01, ***p<0.005 and *p<0.05 respectively: Figure 4.9C). D28 also showed significant elevation in sGPVI between the septic groups (*p<0.05).

4.2.10 Soluble GPVI measurements in patients with sepsis

sGPVI were elevated in thermal injury patients that developed sepsis. To further the study of platelet activation in sepsis, sGPVI was measured in different sepsis groups, including patients with sepsis, severe sepsis, and patients with acute respiratory distress syndrome (ARDS). These patient samples were kindly given by the Dr D. Thickett's respiratory group. Initially, there seemed to be elevated sGPVI levels in all septic groups to the level of the heparin-induced thrombocytopenia (HIT) patient sample, which was used as a positive control (Figure 4.10A). However, these patients did not show any significant elevation above HCs, which were also much higher than the usual sGPVI levels observed with the other HCs. This proposed questions as to why the patient groups and HC gave higher levels. It was eventually found that the sepsis patient sample preparation differed as different centrifugation speeds were used. Blood was then collected from more HCs and spun at the different centrifugation speeds to establish any differences. Samples spun at 560 g gave significantly higher levels than double spun samples at the usual 2500 g speed (**p<0.01: Figure 4.10B), suggesting there was an issue with sample preparation.

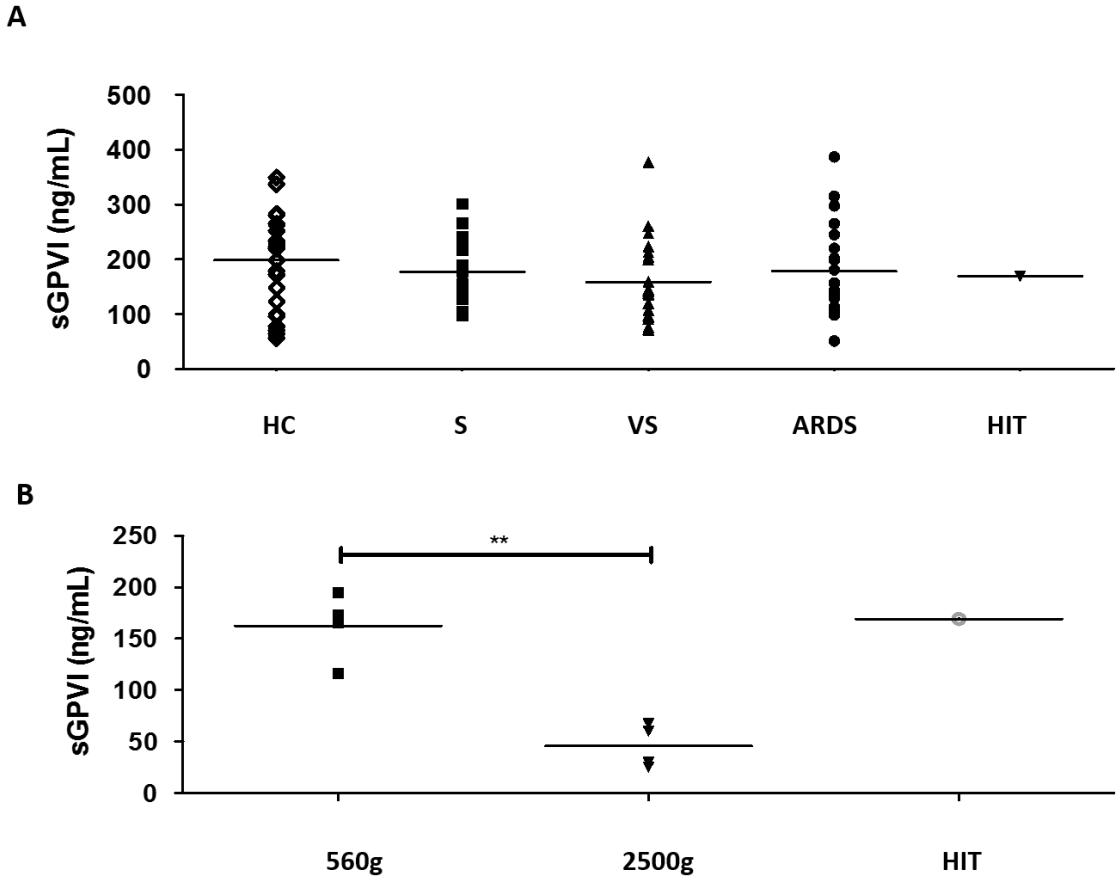

Figure 4.10 - sGPVI is not elevated in septic patients. A) sGPVI levels measured by sGPVI ELISA in septic patients; S=sepsis (n=20), VS= very septic (n=20) and ARDS= acute respiratory disease syndrome (n=22) and HCs (n=22). HIT= heparin-induced thrombocytopenia patient (n=1: positive control). Mann-Whitney statistical test was performed to compare sGPVI levels: median shown. B) sGPVI levels of HC samples spun at different centrifugation speeds (n=4). Unpaired T-test statistical test was performed to compare speeds, **p<0.01: median shown.

4.3 Discussion

The major platelet receptor for collagen, glycoprotein VI (GPVI) can undergo proteolytic cleavage after activation releasing a soluble GPVI fragment (55-kDa), known as sGPVI into the plasma (Gardiner et al., 2004). sGPVI is a recognised marker of platelet activation in thrombotic conditions (Al-Tamimi et al., 2011a, Wurster et al., 2013). Previous studies have shown ligand-mediated mechanisms behind GPVI shedding in response to platelet stimulation by known GPVI ligands, collagen and CRP (Gardiner et al., 2004, Bergmeier et al., 2004, Stephens et al., 2005). Moreover, activation of ITAM receptors FcγRIIa and the hemITAM receptor, CLEC-2, can also induce GPVI shedding (Gardiner et al., 2008b, Gitz et al., 2014). This study firstly wanted to confirm these findings and extend this to investigate if signalling through GPCRs also mediates GPVI shedding. GPVI ligands, collagen and CRP did mediate GPVI shedding, with increased shedding seen over time, reducing GPVI levels to less than half of GPVI in unstimulated samples. Signalling through GPCRs such as, $P2Y_1$ and PAR-1 did not induce GPVI shedding after platelet stimulation by ADP or PAR-1 peptide (SFLLRN). Using more GPCR ligands, such as PAR-4 peptide, arachidonic acid or U46619 to stimulate platelets would be required to further confirm that signalling through GPCRs do not induce GPVI signalling.

Thrombin was able to induce GPVI shedding to levels observed with the GPVI ligands, However, there was marked variation between donors in the thrombin-mediated shedding, with reduction in GPVI seen with some and appearance of the 10-17-kDa GPVI remnant observed in 50% of donors and others showing little shedding. This supports findings from previous studies where some showed thrombin inducing

shedding (Stephens et al., 2005) and others showed thrombin is a poor mediator of GPVI shedding (Gardiner et al., 2004). There are two potential explanations for the variation observed. Firstly, thrombin could directly cleave GPVI or there is wide variation in fibrinogen levels released from donor platelets after stimulation, which could lead to fibrin formation and shedding. Thrombin-mediated shedding did increase over time, suggesting more fibrinogen release and consequent shedding. As GPVI lacks of cleavage site for thrombin, which argues against direct cleavage by the protease. Overall thrombin-mediated shedding is not a result of signalling through PAR receptors and other mechanisms are involved.

Recent work from our lab (including work mentioned before; (Alshehri et al., 2015a) and from Jandrot-Perrus group (Mammadova-Bach et al., 2015) have discovered that fibrin is now GPVI ligand, which activates GPVI and contributes to thrombus stabilisation. It was previously unknown whether fibrin can also induce GPVI shedding. This part of the study demonstrated that polymerised fibrin, where platelets were stimulated with thrombin in the presence of fibrinogen induced GPVI shedding to a similar degree observed with the potent shedder, A23187 and other GPVI ligands. Fibrin-induced shedding was independent of the fibrinogen with integrin αIIbβ3 interaction with shedding still being observed in the presence of the integrin blocker eptifibatide.

The different mechanisms behind fibrin-induce shedding were then assessed. GPVI-shedding usually involves action of sheddases in the metalloendopeptidase family, a disintegrin and metalloproteinase (ADAMs) with shedding mediated by GPVI ligands

predominately being ADAM10 (Facey et al., 2016) dependent with a minor role for ADAM17 in mice (Bergmeier et al., 2004). Fibrin-induced shedding was shown to be dependent on multiple sheddases, presumably ADAM17 among others and not just through the activity of ADAM10, as ADAM10 inhibition only partially reduced shedding and a broad MMP inhibitor, GM6001 was needed for a greater reduction of GPVI shedding, suggesting other sheddases and potential other mechanisms are involved.

The conformational state of fibrin formed during stimulation seemed to have a major effect on GPVI shedding. The monomeric soluble form of fibrin, which is the predominant form when in the presence of GPRP, a peptide which inhibits polymerisation, only induced minimal GPVI shedding in comparisons with polymerised fibrin. Fibrin-induced shedding in suspension was observed with polymerised fibrin and not monomeric. Interestingly monomeric fibrin was shown to bind GPVI and induce activation when immobilised (Alshehri et al., 2015a). Fibrin fragments, such as D-dimers, released after fibrin degradation were also not able to induce GPVI shedding.

Ligand-mediated GPVI shedding by GPVI agonists has previously been shown to be dependent on receptor activation and signalling (Stephens et al., 2005).When inhibitors such as PP2 were added to inhibit signaling proteins downstream of GPVI, shedding was prevented. To establish if this was the case for fibrin-induced GPVI shedding, inhibitors for Src and Syk kinases were added before fibrinogen and thrombin stimulation. Fibrin-induced GPVI shedding was not reduced in the presence of src and Syk tyrosine kinases inhibitors suggesting that GPVI signaling is not required for

shedding to occur and fibrin-induced GPVI shedding is not ligand-mediated shedding. Moreover, the GPRP inhibition data showing that only polymeric fibrin induces shedding, suggests there is an alternative, yet undiscovered mechanism involved in fibrin-induced GPVI shedding, as observed during shear-induced or FXa-induced shedding (Al-Tamimi et al., 2011b, Al-Tamimi et al., 2012). Measuring GPVI shedding by fibrin under flow conditions at different shear rates and measuring GPVI shedding in the presence of Factor Xa inhibitors would give future directions to test whether shear and FXa has a role in fibrin-mediated GPVI shedding.

The findings that GPVI can be shed in response to fibrin stimulation of platelets as well as collagen provides an alternative physiological agonist that could cause sGPVI to be released into the plasma after GPVI shedding. sGPVI has previously been shown to be a platelet activation marker in thrombotic associated conditions (Yamashita et al., 2014a, Wurster et al., 2013, Al-Tamimi et al., 2011a). This study has extended this to show sGPVI can be a platelet activation marker in a range of different inflammatory conditions. sGPVI was detected in two chronic inflammatory conditions, rheumatoid arthritis (RA) and inflammatory bowel disease (IBD). Both these inflammatory conditions have episodes of flare ups followed by remission. sGPVI levels were elevated above healthy controls (HCs) in RA patients. As RA is associated with platelet activation (Del Rey et al., 2014, Boilard et al., 2010). sGPVI is therefore a potential platelet activation marker in patients with inflammatory flare ups. sGPVI levels were also elevated in patients with active ulcerative colitis (UC), but not Crohn's disease nor inactive UC patients. The majority of the Crohn's patients had lower C Reactive protein levels than active UC patients in this cohort, which could be a potential explanation for

the wider distribution of sGPVI levels observed and suggests the activate UC patients had more severe inflammation than the Crohn's patients.

sGPVI correlations with various clinical parameters of IBD patients were studied. There was no significant correlation with age and sGPVI, supporting findings of previous sGPVI studies (Al-Tamimi et al., 2011a) . Of the other parameters tested, haemoglobin levels and ferritin levels of patients with active inflammation gave the strongest correlations, with sGPVI levels being negatively correlated to both. These parameters suggest there is a potential link between platelet activation and iron deficiency. Patients with C-reactive protein levels greater than 5, had greater levels of inflammation, reduced ferritin levels and higher sGPVI, suggesting links between inflammatory status causing iron deficiency, which leads to increased platelet activation. Iron deficiency anaemia (IDA) is commonly associated with IBD cases, with around 17% of IBD patients developing IDA (Guagnozzi and Lucendo, 2014, Bergamaschi et al., 2010) and affects disease severity. Elevated sGPVI levels in iron-deficient patients may potentially arise from platelet activation during times of chronic gastrointestinal bleeding, where blood is lost from inflamed luminal surfaces leading to the development of IDA. GPVI plays a critical role in maintaining vascular integrity at sites of inflammation (Gros et al., 2015a) and could be cleaved once activated by fibrin at these inflamed areas, increasing sGPVI levels. sGPVI may therefore represent a novel marker to predict development of IDA in IBD patients. However, more patients with Crohn's disease and UC would need to be recruited and full medical history determined to confirm whether the higher sGPVI levels in these patients are a result of iron deficient and not other factors such as levels of inflammation, C reactive protein levels or medication taken.

The study also looked at sGPVI kinetics longitudinally in patients with thermal injury. sGPVI levels were measured in 99 patients from Day 1 post initial injury to Month 12. sGPVI was significantly elevated above HCs at Day 14. Surprisingly, sGPVI levels were not raised initially at early time points (Day 1-3) post injury, where it would be expected that with more tissue damage would occur and presumably more collagen exposure to allow platelet activation. This suggests that only a fraction of platelets were activated by collagen exposed after damage and other mechanism, potentially fibrin, was involved for the platelet activation observed at later time points.

An alternative explanation for low levels of sGPVI initially post injury is that elevations may be masked by the low platelet counts observed at Day 3. To address this, sGPVI levels were normalised to the platelet count. This then showed that sGPVI levels became elevated at Day 3 in septic patients, suggesting that some GPVI shedding is mediated through collagen exposed after damage. However, sGPVI levels remained elevated in the septic patients at Day 7 and 14. Collagen exposure at these time points would be minimal as the damaged area would undergo recovery. There was also only weak correlation between sGPVI levels and burn injury severity, suggesting sGPVI released at these time points was mediated through alternative mechanism associated with sepsis development. Overall sGPVI levels were significantly higher in those patients that developed sepsis. sGPVI did only have a moderate predictive value of 0.73 for predicting sepsis alone, where a strong predictive value would range between 0.9 and 1.0. The discriminatory power for predicting sepsis is likely to be increased when combined with other sepsis markers, such as cell-free DNA, neutrophil function or immature granulocytes, which have already been shown to be good prediction

markers of sepsis (Hampson et al., 2016). sGPVI elevations observed in the septic patients post injury is potentially due to platelet activation through alternative mechanisms. The main plausible explanation for elevation of sGPVI, where there is minimal activation of platelets by collagen, is that during disseminated intravascular coagulation (DIC) seen in sepsis (Semeraro et al., 2010a, Levi et al., 2003), platelets become activated by many DIC associated mechanisms, leading to the formation of thrombi encompassed by polymerised fibrin networks, which then induce GPVI shedding after activation. Correlating plasma fibrinogen levels or d-dimer levels (a breakdown product released after fibrinolysis), of patients with thermal injury and sepsis with sGPVI levels, would help provide support in the future as to if the elevations of sGPVI observed were mediated through fibrin-induced GPVI shedding. sGPVI measurements in a other patient cohorts, where increased fibrin formation is clinical characteristic such as patients with deep vein thrombosis (DVT), would be helpful in supporting the hypothesis that fibrin can mediate GPVI shedding, leading to increased sGPVI levels observed in these patients.

sGPVI levels were also measured in the plasma of patients with various forms of sepsis, including sepsis, severe sepsis, and acute respiratory distress syndrome (ARDS). No elevations were observed in the septic patients compared to HCs, although all samples had sGPVI levels raised above all the other samples in the other patient cohorts. Unfortunately, this resulted due to the different sample preparation as different centrifugation speeds were used. This affected the results as samples spun at 560 g gave significantly higher levels than the usual double spun samples at 2500 g when blood was collected and spun following this observation. This suggested an artefact produced

from the sample preparation, which caused the increase in sGPVI and not elevated levels due to sepsis. It would therefore be of great interest to repeat the sGPVI measurements in the various sepsis patient plasma cohorts to establish if sepsis development can cause platelet activation and elevated sGPVI levels.

Overall the findings in this chapter here provide more support for sGPVI as a platelet activation marker in certain inflammatory conditions, including RA, active UC patients and patients with thermal injury. sGPVI can be linked to some secondary complications such as iron deficiency in IBD patients and sepsis in certain patients following thermal injury. The mechanisms behind the GPVI cleavage resulting in the release of the soluble GPVI fragment into the plasma were extensively studied. Signalling through GPVI and other ITAM containing receptors, but not GPCR activation can induced GPVI shedding. Fibrin is a newly discovered GPVI agonist that can also induce GPVI shedding through multiple mechanisms, including the activity of multiple sheddases, including ADAM10 and ADAM17. Ligand-mediated mechanisms behind GPVI shedding by fibrin did not seem to have a predominant role, whereas fibrin conformational state having the most important role in mediating fibrin-induced GPVI shedding. Polymerised fibrin and not monomeric fibrin, or fibrin degradation productions can induce GPVI shedding. Fibrin along with collagen can mediate shedding and be physiological agonists involved in platelet activation in inflammatory conditions.

CHAPTER 5

PODOPLANIN UPREGULATION IN INFLAMMATORY SETTINGS

5.1 Introduction

The role of platelets is predominately in haemostasis and thrombosis, with emerging roles in development, angiogenesis, and maintaining vascular integrity (Bertozzi et al., 2010, Kisucka et al., 2006, Gros et al., 2015a). The roles of platelets in infection and inflammation are now also being extensively studied. This chapter will look at potential roles of platelets in inflammation through studying the podoplanin/ C-type lectin-like receptor 2 (CLEC-2) axis.

CLEC-2 is an important platelet-activating receptor involved in haemostasis and thrombosis (May et al., 2009). CLEC-2 is expressed on platelets with around 2000 copies per platelet and expressed on subset set of circulating inflammatory dendritic cells in mice (DCs; (Gitz et al., 2014, Lowe et al., 2015c)). CLEC-2 was thought to also be expressed on subsets of murine myeloid cells, including monocytes, in resting conditions, which increased in expression seen in response to inflammatory stimuli (Acton et al., 2012a, Mourao-Sa et al., 2011). However, recent studies have showed CLEC-2 with a more restricted expression profile to platelets and activated DCs in mice (Lowe et al., 2015c).

Podoplanin, a 36-43-kDa heavily glycosylated type-1 transmembrane sialoglycoprotein, is the only known endogenous CLEC-2 ligand. Podoplanin is expressed on kidney podocytes, alveolar type-1 epithelial cells lymphatic endothelial cells (LECs) and fibroblastic reticular cells (FRCs) from the T-cell zone of lymphoid cells (Breiteneder-Geleff et al., 1997, Astarita et al., 2015). In inflammatory settings, podoplanin

expression can be upregulated on T-helper 17 (T_H17 cells), tumour cells and inflammatory macrophages (Peters et al., 2015, Kato et al., 2003, Kerrigan et al., 2012). Podoplanin and CLEC-2 have important roles in several process including in development and maintenance of the lymphatic system. Deletions in podoplanin or CLEC-2 lead to similar blood lymphatic mixing, oedema and haemorrhaging observed during development, and are unable to properly inflate the lungs at birth, greatly effecting survival (Bertozzi et al., 2010, Finney et al., 2012, Turner et al., 1995, Schacht et al., 2003, Ramirez et al., 2003).

Podoplanin and CLEC-2 have roles in other processes beyond development. Podoplanin upregulation has been described in numerous inflammation settings, with CLEC-2 interactions also being implicated. Podoplanin upregulation has been observed on FRCs during inflammation and interactions with CLEC-2 affects FRC function. FRCs are mesenchymal cells found in lymph nodes, which form a dense reticular network, acting as a scaffold for lymph, T-cells and DCs to move along (Link et al., 2007, Astarita et al., 2015). In resting conditions, podoplanin regulates the contractility of actomyosin in FRCs to maintain FRC contraction and stability of the lymph node microarchitecture (Astarita et al., 2015). During inflammation, the contractility of FRCs is reduced due to CLEC-2 expressed on DCs interacting with podoplanin. This interaction leads to relaxation of FRCs, causing changes in FRC and T cell spacing and expansion of the FRC network, allowing greater movement of immune cells through the network (Acton et al., 2012a, Astarita et al., 2015). Platelet-CLEC-2 interactions with podoplanin expressing FRCs have also been shown to maintain the integrity of high-endothelial

venules within the lymph nodes, with blood-filled lymph nodes forming in the absence of CLEC-2 (Herzog et al., 2013).

Podoplanin upregulation in other inflammatory settings has also been described. Studies into multiple sclerosis (MS), an auto-immune inflammatory disorder, have shown that CLEC-2/podoplanin interactions improve the resolution of inflammation (Peters et al., 2015). Podoplanin expression is upregulated on T_H17 cells in inflamed central nervous system (CNS) tissue of mice in an autoimmune encephalomyelitis model (Miyamoto et al., 2013). Podoplanin on T_H17 cells acts to negatively regulate the persistence of T effector cells, with enhanced T-cell responses observed in podoplanin-deficient mice (Peters et al., 2015). In rheumatoid arthritis (RA), another chronic inflammatory disease, CLEC-2 and podoplanin were proposed to modulate the progression of the disease. Podoplanin and CLEC-2 expression have also been shown in tissue sections isolated from RA patients (Del Rey et al., 2014, Ekwall et al., 2011). Increased podoplanin expression was also detected in synovial arthroscopic biopsies from RA patients with lymphoid neogenesis and proposed as an early feature of RA (Del Rey et al., 2014). Overall, podoplanin upregulation is increased at sites of inflammation in RA, including areas where synovial fibroblast activation occurs (Miyamoto et al., 2013, Ekwall et al., 2011, Del Rey et al., 2014). In addition, platelet-CLEC-2 interactions with synovial fibroblasts through CLEC-2/podoplanin interactions could lead to release of pro-inflammatory cytokines (Del Rey et al., 2014).

Podoplanin upregulation also occurs on multiple tumour cells, including colorectal adenocarcinomas and CNS tumours (Kato et al., 2003, Shibahara et al., 2006b). Indeed,

tumour cells have been shown to upregulated podoplanin and induce platelet aggregation through podoplanin and platelet-CLEC-2 interactions after addition of tumour cells to platelets (Kato et al., 2003, Suzuki-Inoue et al., 2007, Kato et al., 2006). Some studies suggest podoplanin upregulation on cancer-associated fibroblasts (CAFs) in the stroma of areas near tumours can act as barriers to reduce tumour cell invasion (Yamanashi et al., 2009). However, other studies have suggested the formation of platelet/tumour aggregates protects the tumour from shear stress, helping with evasion of the immune system (Gay and Felding-Habermann, 2011, Jain et al., 2009). Targeting podoplanin with blocking antibodies has also been shown to reduce platelet aggregation and pulmonary metastasis (Takagi et al., 2013).

Podoplanin upregulation has been observed during inflammation in response to infection. Podoplanin expression has been described on fibroblastic macrophages (FN), a F4/80^{+} subtype macrophage found in the red pulp of the spleen, which is upregulated in response to zymosan induced peritonitis (Hou et al., 2010). Podoplanin upregulation has also been shown in response to bacterial infection. Hitchcock *et al*. showed that during inflammation of the liver after *Salmonella typhimurium* infection, podoplanin was upregulated on liver macrophages (F4/80+ cells) of infected mice (Hitchcock et al., 2015). This upregulated podoplanin was shown to trigger CLEC-2-mediated thrombosis in the liver (Hitchcock et al., 2015). The absence of platelet CLEC-2 reduced venous thrombosis, suggesting platelet CLEC-2/podoplanin interaction mediates the infection-driven thrombosis.

Podoplanin expressed on LECs has also been shown to induce platelet activation through interactions with CLEC-2. Studies have shown platelets form aggregates when blood is flowed over the surface of LECs; aggregation is CLEC-2 and SLP-76 dependent (Bertozzi et al., 2010, Pollitt et al., 2014). Platelet activation through podoplanin/CLEC-2 interactions has been shown following upregulation of podoplanin on RAW264.7 macrophages (a mouse macrophage cell line) following exposure to lipopolysaccharide (LPS; (Kerrigan et al., 2012)). However, this has not been described in macrophages in humans.

To mediate platelet activation, podoplanin interacts with CLEC-2 through its *O*-glycosylated platelet-aggregation stimulating domain (PLAG domain; (Suzuki-Inoue et al., 2007, Pollitt et al., 2014)). CLEC-2 binding to podoplanin shares a number of structural features with binding of CLEC-2 binding with rhodocytin (Nagae et al., 2014). Additionally, podoplanin can be cleaved at the *O*-glycosylated Thr52 site (Figure 5.1) from lymphatic endothelial cells (LECs) after treatment with proteases and sialidases (Pan et al., 2014). There is therefore the potential that upregulated podoplanin is released into the circulation although, as yet, the presence of podoplanin ectodomain in the plasma has not been reported.

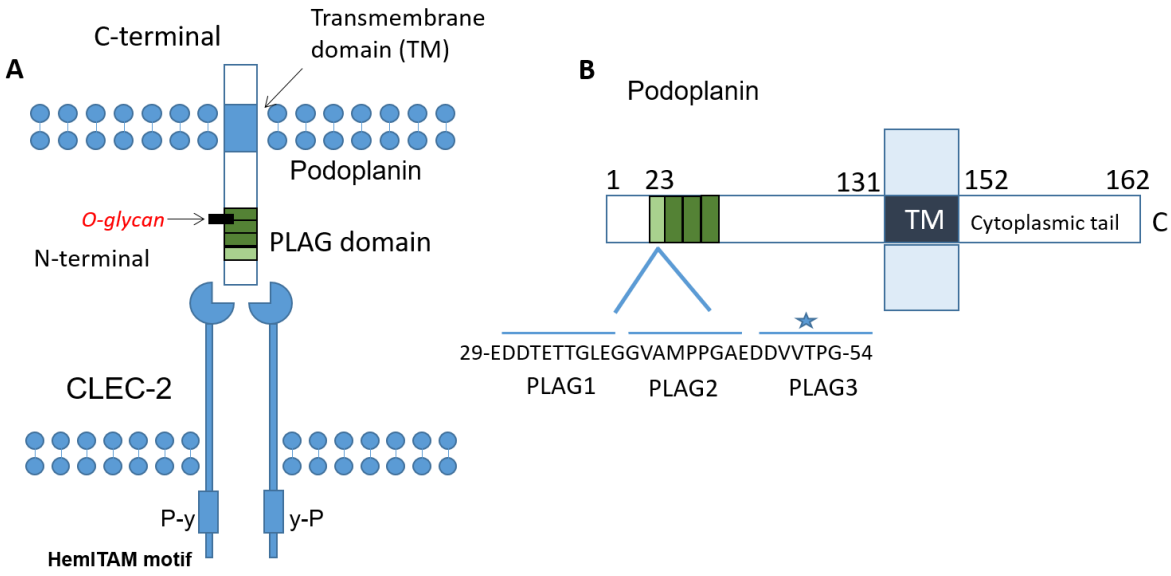

Figure 5.1 - Schematic of podoplanin. A) Podoplanin consists of a transmembrane domain and an O-glycosylated platelet-aggregation stimulating domain (PLAG domain), which interacts with the CLEC-2 receptor. B) Architecture of podoplanin. The amino acid sequences of the different PLAG domains (PLAG1-3) are listed. The star indicates the O-glycosylated Thr52. This area has the potential to undergo cleavage with treatment of proteases and sialidases (Pan et al., 2014, Nagae et al., 2014).

Podoplanin is upregulated on multiple cell types in several inflammatory settings and is therefore a potential biomarker of inflammation. The overall aim of this chapter is to determine which cell types in blood upregulate podoplanin when challenged with an inflammatory stimulus and to investigate if this upregulation is sufficient enough to induce platelet activation. Alongside this a series of pilot studies will be performed to measure podoplanin in plasma of patients with inflammatory conditions.

5.2 Results

5.2.1 Podoplanin upregulation on monocytes is not observed after LPS stimulation in whole blood

LPS is potent activator of monocytes and macrophages and a pro-inflammatory mediator (Meng and Lowell, 1997). Two serotypes of LPS (*E. coli* 0111: B4 and 055: B5) were added to stimulate monocytes in whole blood to assess if podoplanin could be upregulated by 4 and 24 h after stimulation (6 and 8 h were also tested, but didn't show much difference compared to 24h). Whole blood was stained with CD14, a monocyte marker, to allow gating for cell interactions and to determine podoplanin upregulation on monocytes. Co-staining with CD41, a platelet marker, was used to determine the percentages of monocyte/platelet complexes in the blood. In a single pilot experiment, there was an approximate 50% increase in levels of CD14+ and CD41+ platelet-leukocyte complexes after 4 h following stimulation with both types of LPS, which remained constant up to 24 h (Figure 5.2A). However, a similar increase in platelet/monocyte interactions was observed over time with unstimulated blood (Figure 5.2A). CD14+ cells were stained with CD69 or CD38 (monocyte activation markers), to follow their activation status. Limited activation of monocytes was observed in response to serotype 0111 (100 ng/ml) following stimulation after 4 h or 24 h (Figure 5.2B). To determine if podoplanin becomes upregulated on stimulated monocytes in whole blood, CD14+ cells were stained for podoplanin using the NZ-1.3 anti-podoplanin antibody and compared to isotype and unstimulated controls. Podoplanin upregulation was not observed after 4 or 24 h with or without LPS (0111) stimulation. (Figure 5.2C).

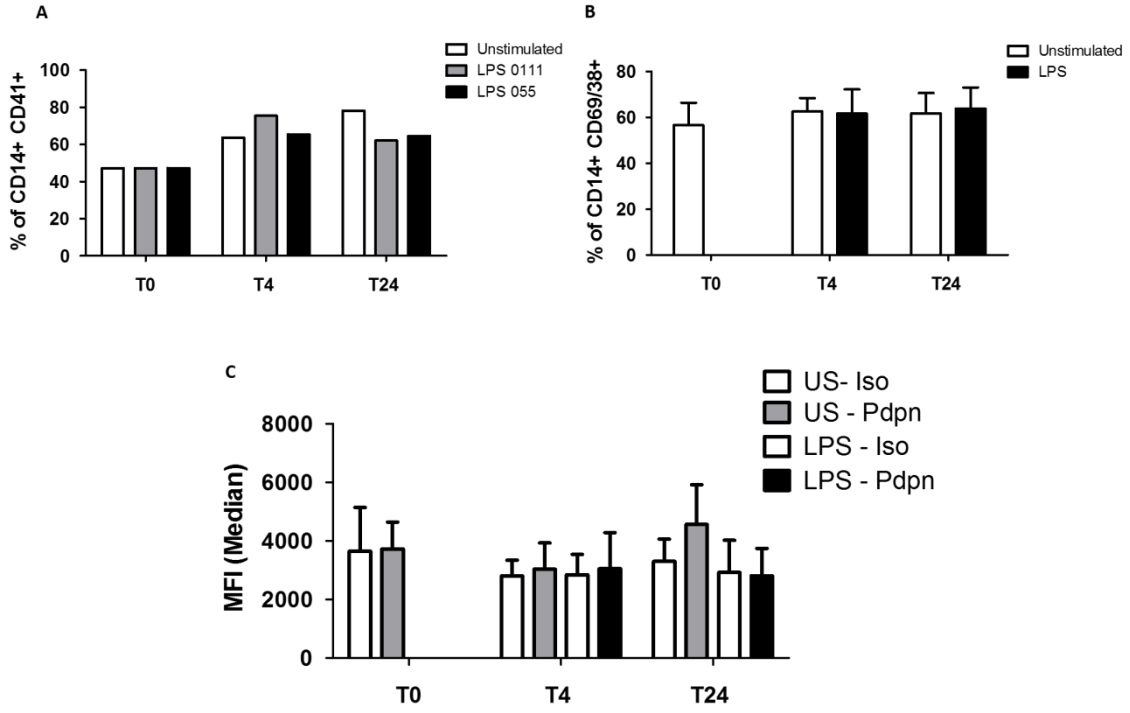

Figure 5.2 – Podoplanin is not upregulated on monocytes after LPS stimulation in whole blood. A) Whole blood was stimulated with two serotypes of LPS (*E. coli* 0111: B4 and 055: B5) in the presence of GPRP (10 µM) and integrilin (9 µM) for 4 h and 24 h at 37^{O}C on a shaker (low speed). Blood was stained for CD14 (monocyte marker) and CD41 (platelet marker). % of CD14+ CD41+ cells were measured by flow cytometry after LPS stimulation. N=1. B) % of cells stained for CD14 and monocyte activation markers CD69/38 after whole blood stimulation with LPS (0111; 100 ng/ml). Mean shown ±SEM, n=3. C) Median fluorescence Intensity (MFI) of podoplanin (Pdpn) staining of CD14+ cells after 4 h and 24 h LPS stimulation compared to unstimulated (US) blood and isotype (iso) control.

5.2.2 Podoplanin is not upregulated on THP-1 cells after LPS stimulation

THP-1 cells (a human acute monocytic leukaemia cell line (Auwerx, 1991) were also stimulated to test for podoplanin upregulation. Some studies have shown that podoplanin is upregulated on neuronal apoptotic cells after LPS injection (Song et al., 2014). Podoplanin upregulation on apoptotic THP-1 cells was also tested after cells were treated two agents that induce apoptosis, staurosporine (1 µM) and cycloheximide (25 µg/ml) which are a protein kinase inhibitor and protein synthesis inhibitor, respectively and stained with Annexin V (an apoptosis/activation marker). Annexins belong to a family of calcium-dependent phospholipid-binding proteins, which bind to cells exposing phosphatidylserine (PS). PS is exposed during cell activation and when cells are undergoing apoptosis. Cells stained with Annexin V were gated to determine whether podoplanin can be upregulated on Annexin V+ and Annexin V- THP-1 cells (Figure 5.3A). There was no podoplanin upregulation on Annexin V+ cells after stimulation with LPS or staurosporine and cycloheximide treatment compared to unstimulated cells (Figure 5.3Bi). Podoplanin upregulation was not observed in Annexin V- cells after stimulation with LPS or staurosporine and cycloheximide (Figure 5.3Bii). Moreover, no differences were seen in podoplanin upregulation in Annexin V+ or Annexin V- cells when podoplanin MFI (median) ratio over isotype was calculated (Figure 5.3C).

5.2.3 Podoplanin is not upregulated on isolated monocytes after stimulation

To confirm podoplanin was not upregulated on stimulated monocytes, monocytes were isolated from whole blood by negative selection of peripheral blood mononuclear cells

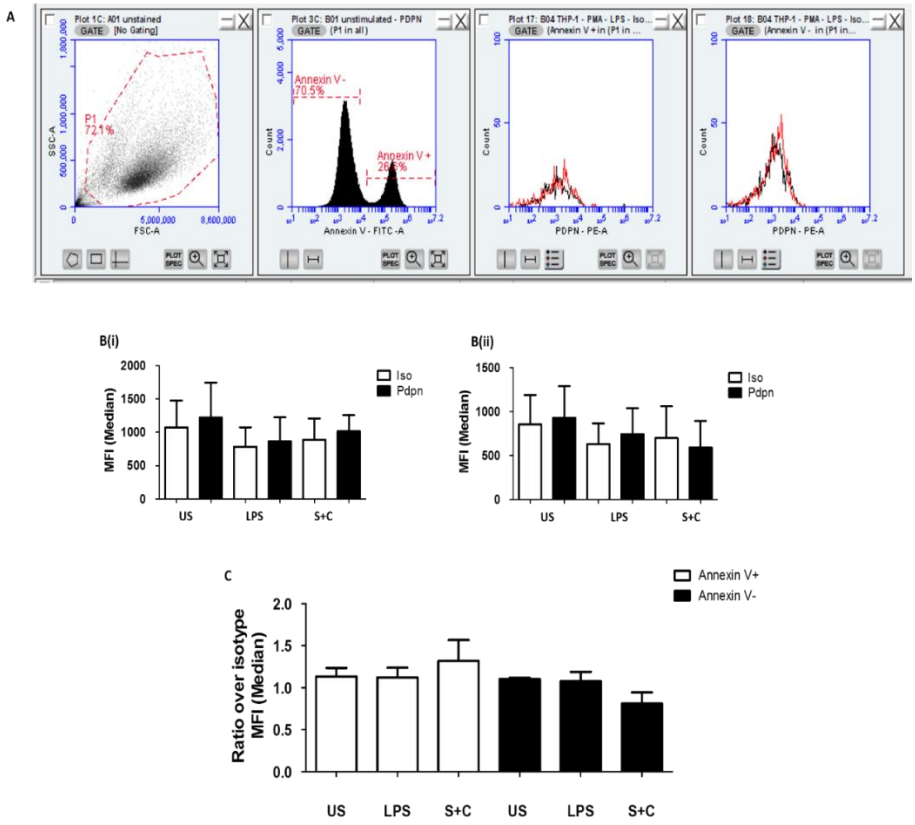

Figure 5.3 – Podoplanin is not upregulated on THP-1 cells after LPS stimulation. THP-1 cells (acute monocytic leukaemia cell line; $1x10^6$ cells/ml) were stimulated with LPS (100 ng/ml) for 24 h at 37°C followed by CD14, Annexin V and Pdpn staining. A) Gating strategy for determining Annexin V+ and Annexin V- cells that are Pdpn positive. Isotype in **black**, Pdpn in **red.** B(i) Median fluorescence Intensity (MFI) of podoplanin staining of Annexin V+ cells after LPS stimulation and treatment with staurosporine (1 µM) and cycloheximide (25 µg/ml) for 24 h compared to isotype controls. Mean shown ± SEM, n=4. B(ii) MFI (median) of podoplanin staining of Annexin V- cells after LPS stimulation and treatment with staurosporine (1 µM) and cycloheximide (25 µg/ml; S+C) for 24 h compared to isotype controls. Mean shown ± SEM, n=4. C) Ratio of podoplanin staining over isotype control of Annexin V+ and

Annexin V- THP-1 cells after stimulation. Mean shown ± SEM, n=4. One-way ANOVA performed with Bonferroni's post-hoc test. No significant difference observed.

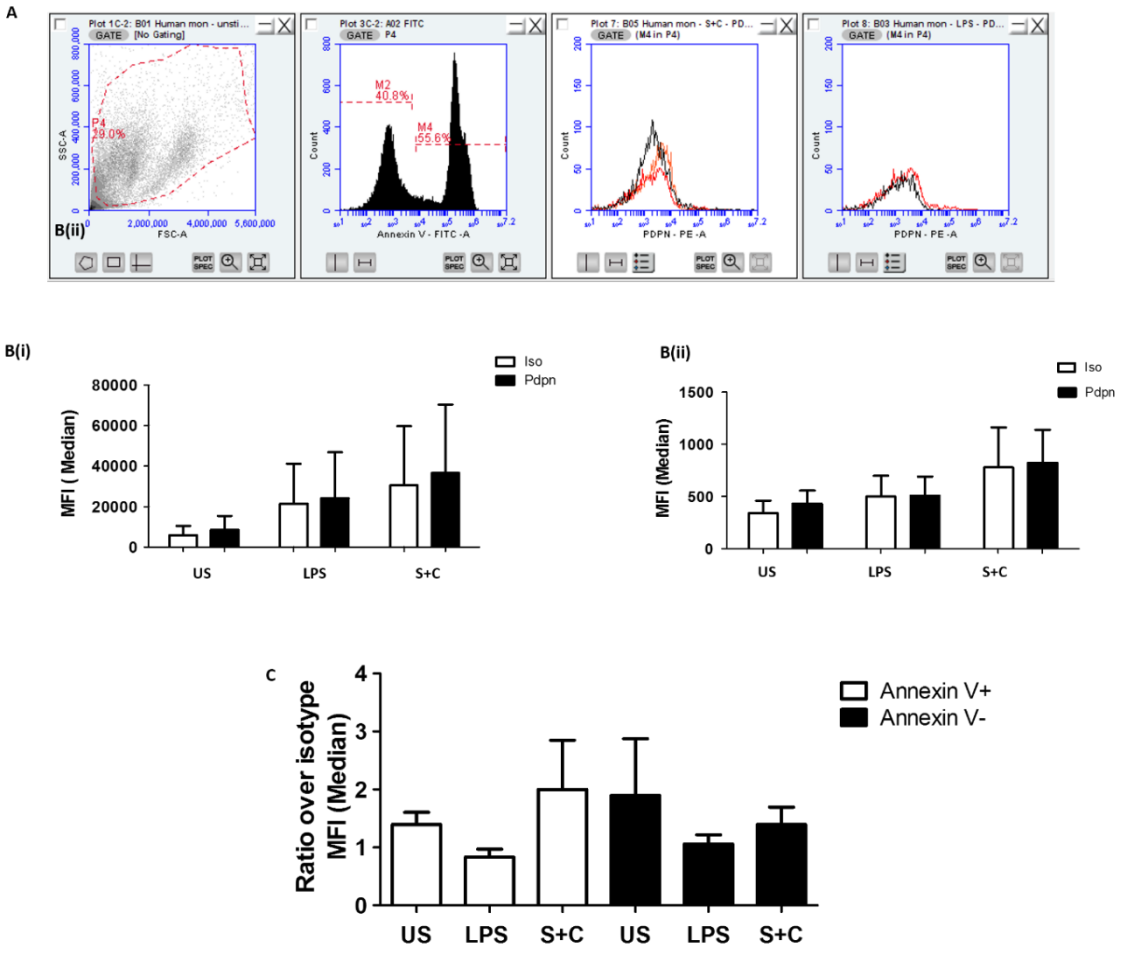

Figure 5.4 – Podoplanin is not upregulated on isolated monocytes after stimulation. Isolated monocytes (1x10^6 cells/ml) from donor blood were stimulated with LPS (100 ng/ml) or staurosporine (1 µM) and cycloheximide (25 µg/ml) for 24 h at 37^{o}C. A) Gating strategy for determining Annexin V+ and Annexin V- cells that are Pdpn positive. Isotype in **black,** Pdpn in **red.** B(i) Median fluorescence Intensity (MFI) of podoplanin staining of Annexin V+ cells after LPS stimulation and staurosporine (1 µM) and cycloheximide (25 µg/ml) treatment compared to isotype controls. Mean shown ± SEM, n=5. B(ii) MFI (median) of podoplanin staining of Annexin V- cells after stimulation compared to isotype controls. Results shown as mean ± SEM, n=5. C) Ratio of podoplanin staining over isotype control of Annexin V+ and Annexin V-

monocytes stimulated with LPS and staurosporine and cycloheximide. Mean shown ± SEM, n=5.

(PBMCs) and stained for CD14, podoplanin and Annexin V after LPS or staurosporine and cycloheximide stimulation (Figure 5.4A). There was no podoplanin upregulation on CD14+ and Annexin V+ cells after LPS stimulation and treatment with staurosporine and cycloheximide (added together; Figure 5.4Bi&C). There was also no upregulation seen with CD14+ and Annexin V- cells (Figure 5.4Bii&C).

5.2.4 Absence of upregulation of podoplanin after stimulation of PBMCs

In order to establish whether other blood cells can upregulate podoplanin following LPS stimulation, human PBMCs were isolated and stimulated with LPS. Citrated-human whole blood was collected from healthy donors, with no sign of infection or medication, and PBMCs were isolated using a ficoll-paque gradient using differential centrifugation. PBMCs were stimulated with LPS (100 ng/ml) or treated with staurosporine (1 µM) and cycloheximide (25 µg/ml) for 24 h followed by podoplanin and Annexin V staining and gated on size scatter and CD45 positivity. Podoplanin was measured on Annexin V+ cells and Annexin V- cells as before (Figure 5.5A). As expected, there was no upregulation of podoplanin was observed after LPS stimulation or staurosporine and cycloheximide treatment on Annexin V+ and Annexin V- cells (Figure 5.5B). There was no difference in the ratio of podoplanin staining over isotype with Annexin V+ and Annexin V- PBMCs after stimulation (Figure 5.5C).

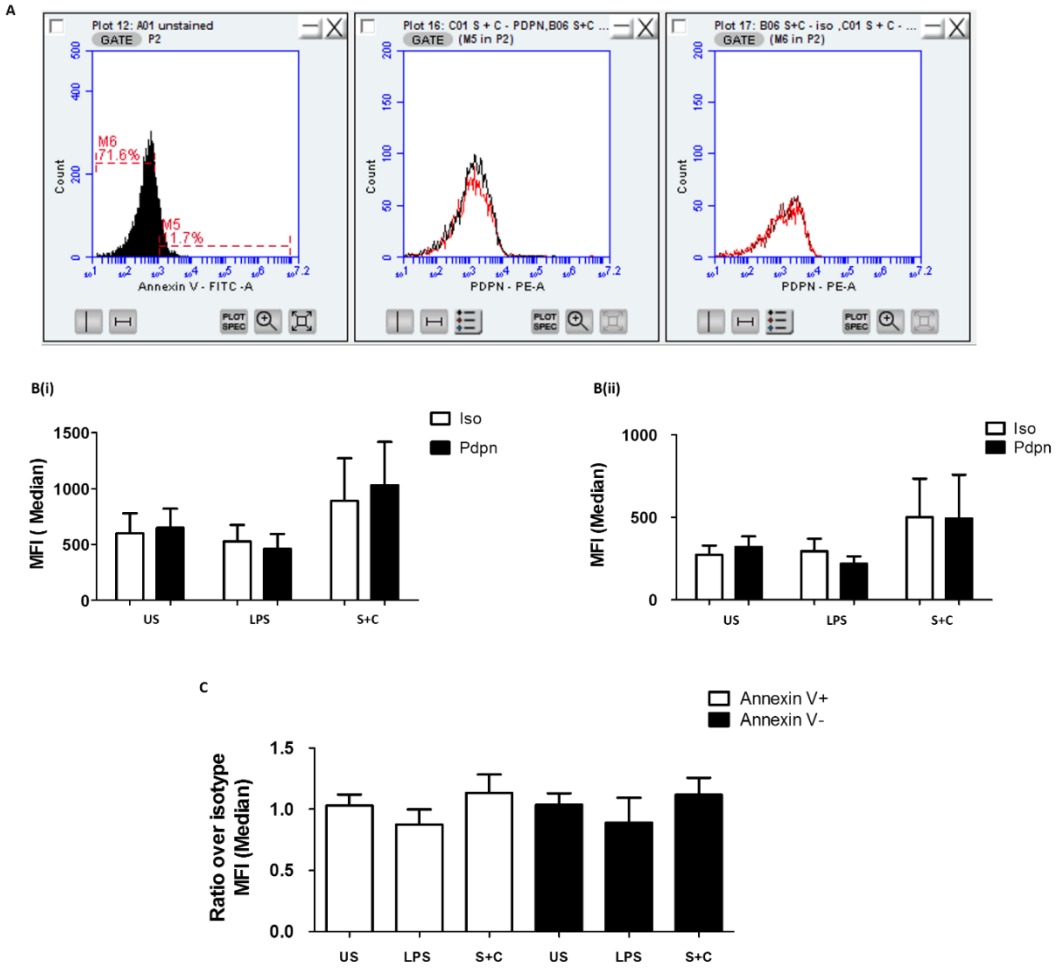

Figure 5.5 – Podoplanin is not upregulated after stimulation of PBMCs. Peripheral blood mononuclear cells (PBMCs; 1x10^6 cells/ml) were isolated from donor blood and stimulated with LPS (100 ng/ml) or staurosporine (1 µM) and cycloheximide (25 µg/ml) for 24 h at 37^{o}C. A) Gating strategy for determining Annexin V+ and Annexin V- cells that are Pdpn positive. Isotype in **black**, Pdpn in **red**. B(i) Median fluorescence Intensity (MFI) of podoplanin staining of Annexin V+ cells after stimulation compared to isotype controls. Mean shown ± SEM, n=5. B(ii) MFI (median) of podoplanin staining of Annexin V- cells after stimulation compared to isotype controls. Mean shown ± SEM, n=5. C) Ratio of podoplanin staining over isotype control of Annexin V+ and Annexin V- after stimulation of PBMCs. Mean shown ± SEM, n=5

5.2.5 Podoplanin is upregulated on M-CSF treated monocyte-derived macrophages but not GM-CSF treated cells after stimulation

Podoplanin was not upregulated on PBMCs or monocytes after LPS stimulation. Studies have shown that podoplanin can be upregulated on cultured RAW264.7 cells (inflammatory macrophages from a mouse cell line) after LPS stimulation (Kerrigan et al., 2012). To test whether this was the case for human macrophages, monocyte-derived macrophages were produced as an alternative, as macrophages are very difficult to isolate and there are very few reliable macrophage cell lines. Monocytes were isolated from the blood and treated with granulocyte-macrophage colony-stimulating factor (GM-CSF) or macrophage colony-stimulating factor (M-CSF) for 5-6 days to produce monocyte-derived macrophages, which were initially confirmed by CD68, CD14 (low), CD16 (high) expression by flow cytometry. Treatment with these cytokines was used to polarize monocyte into macrophage-like cells with 'M1 and M2' macrophage phenotype, respectively, resulting in profound differences in morphology (Figure 5.6). Untreated monocytes adhered to the plate wells and most cells had uniformed circular appearance after 6 days. GM-CSF treatment causes differentiation of monocytes into the 'M1' phenotype, which are cells with a pro-inflammatory phenotype and DC antigen-presenting properties (Masurier et al., 1999). M-CSF treatment of monocytes causes differentiation into the 'M2' macrophage phenotype with anti-inflammatory properties (Verreck et al., 2004, Lacey et al., 2012). Most cells had long thin extrusions when spreading on the plate well. M-CSF treatment cells had a different appearance with fewer extrusions. A CD206 marker was used initially to determine differences between M2 phenotype compared to M1 by flow cytometry, which then allowed consequent gating based on size and characteristics for future experiments.

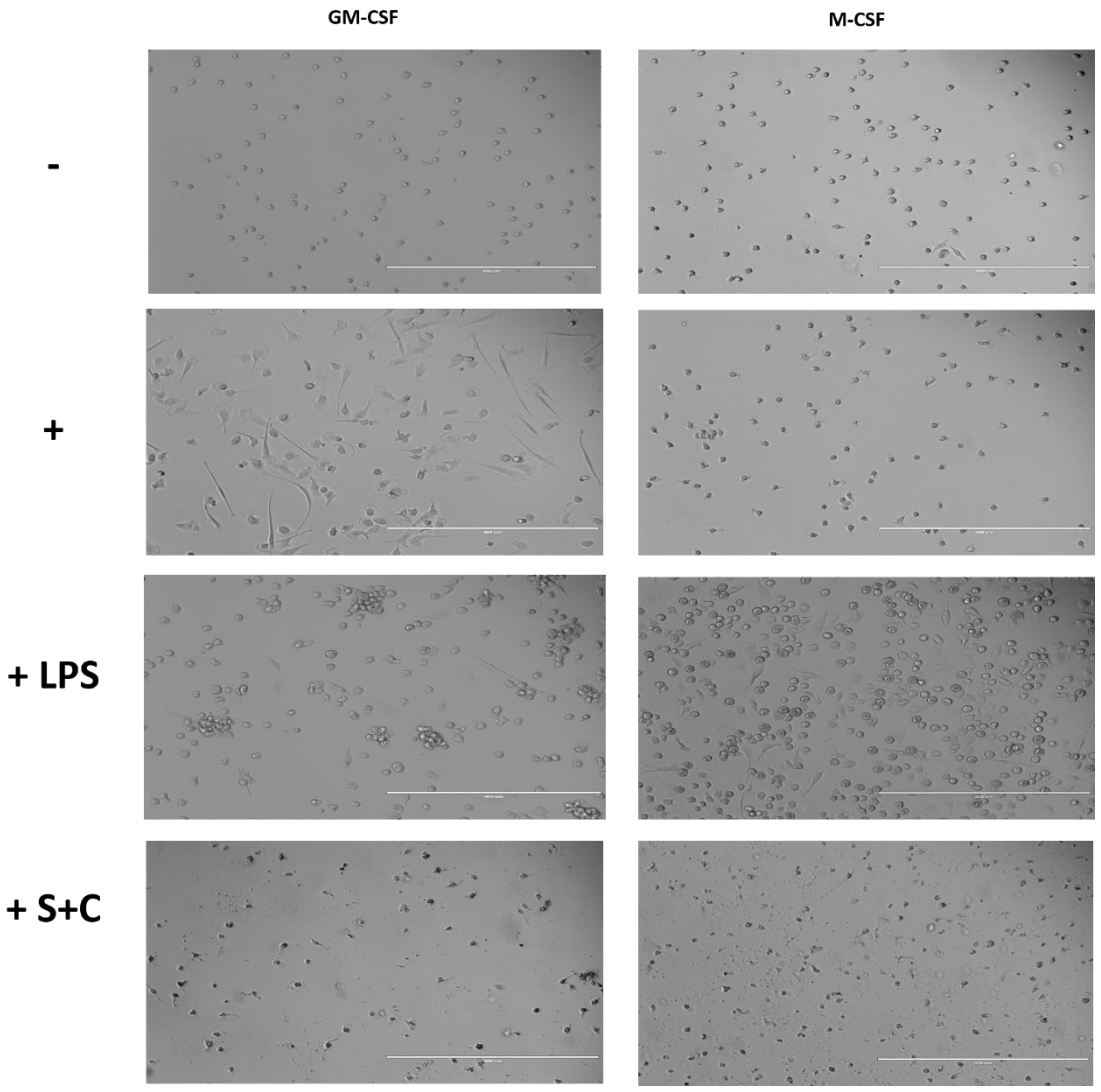

Figure 5.6 – Differentiation of monocyte-derived macrophages after GM-CSF and M-CSF treatment of isolated monocytes. Isolated monocytes ($1x10^6$ cells/ml) were incubated in a well of a 6-well plate added to wells and treated with GM-CSF (50 ng/ml) or M-CSF (100 ng/ml) to differentiate into 'M1' and 'M2' macrophages. For some conditions macrophages were treated with LPS (0111: B5 100 ng/ml) or staurosporine (1 µM) and cycloheximide (25 µg/ml). Brightfield images taken with the EVOS FL Cell imaging system. Scale bar represents 400 µm.

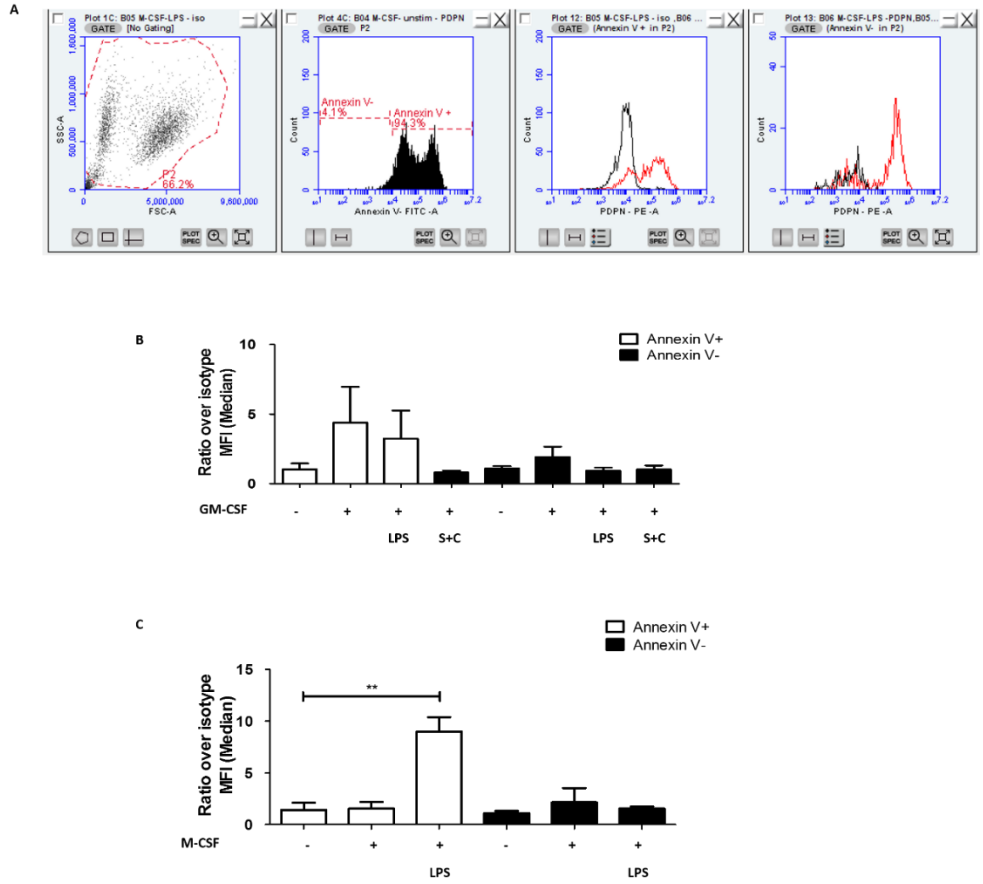

Figure 5.7 – Podoplanin is upregulated on LPS treated monocyte-derived macrophages treated with M-CSF. Isolated monocytes (1x10^6/ml) were treated with GM-CSF (50 ng/ml) or M-CSF (100 ng/ml) for 6 days to allow for macrophage differentiation. Cells were then stimulated with LPS (100 ng/ml) or staurosporine (1 µM) and cycloheximide (25 µg/ml) for a further 24 h. A) Gating strategy for determining Annexin V+ and Annexin V- cells that are Pdpn positive. Isotype in **black**, Pdpn in **red**. B) Ratio of podoplanin staining over isotype control of Annexin V+ and Annexin V- GM-CSF treated cells stimulated with LPS and staurosporine (1 µM) and cycloheximide (25 µg/ml). Mean shown ± SEM, n=5. C) Ratio of podoplanin staining over isotype control of Annexin V+ and Annexin V- M-CSF treated cells stimulated with LPS. Mean shown ± SEM, n=5. Unpaired T-test performed to determine difference between untreated cells, **p<0.0.1.

LPS (100 ng/ml) stimulation of both types of treated cells resulted in cell accumulation. Some extrusions were seen with the GM-CSF treated cells but not as many as with unstimulated GM-CSF treated cells. LPS stimulation of the M-CSF treated cells also lead to accumulation of cells, however, more extrusions were seen and some cells had expanded surface areas. The addition of staurosporine (1 µM) and cycloheximide (25 µg/ml) to both GM-CSF and M-CSF treated cells lead to cell disruption and apoptosis. (100 ng/ml) stimulation of both types of treated cells resulted in cell accumulation. Some extrusions were seen with the GM-CSF treated cells but not as many as with unstimulated GM-CSF treated cells. LPS stimulation of the M-CSF treated cells also lead to accumulation of cells, however, more extrusions were seen and some cells had expanded surface areas. The addition of staurosporine (1 µM) and cycloheximide (25 µg/ml) to both GM-CSF and M-CSF treated cells lead to cell disruption and apoptosis. GM-CSF and M-CSF treated monocytes were stimulated with LPS (100 ng/ml) and treated with staurosporine (1 µM) and cycloheximide (25 µg/m) for 24 h and then stained for podoplanin. Cells were gated on size and CD68 positivity (CD68 is a macrophage marker). Podoplanin upregulation was measured on Annexin V+ cells and Annexin V- cells (Figure 5.7A). There was a marginal increase in the MFI ratio of podoplanin staining over the isotype controls in Annexin V+ cells compared to untreated GM-CSF cells (Figure 5.7B) which however did not reach significance. There was no upregulation observed with GM-CSF treated cells which were stimulated with staurosporine and cycloheximide. There was no increase in podoplanin upregulation of GM-CSF treated cells that were Annexin V- (Figure 5.7B). Podoplanin was significantly upregulated on Annexin V+ M-CSF treated cells stimulated with LPS (Figure 5.7C). This suggests that only M2 macrophages have the capacity to upregulate

podoplanin once stimulated with LPS. M-CSF treated cells stimulated with staurosporine and cycloheximide did not show podoplanin upregulation. Podoplanin was not upregulated on Annexin V- M-CSF treated cells (Figure 5.7C).

5.2.6 Upregulated podoplanin on macrophages is unable to activate platelets

M-CSF treated monocytes (M2 macrophages) were the only blood cell type where podoplanin was upregulated after LPS stimulation. The ability of these macrophages to cause platelet activation was therefore studied. Monocytes were isolated from the blood, treated with M-CSF for 6 days before being stimulated with LPS for a further 24 h. These inflammatory macrophages were added to washed platelets from the same donor at 37^{o}C under stirring conditions (1200 rpm). Platelet interactions with macrophages were measured using anti-CD41 and -CD68 antibodies by flow cytometry. Activation of the platelets was measured by P-selectin expression, shown as increased MFI (median; Figure 5.8A). Positive CD68 and P-selectin staining represented the activated platelets on CD68 cells. P-selectin on CD68+ gated cells was measured in GM-CSF and M-CSF treated cells that were stimulated with LPS (Figure 5.8C). There were no increases in P-selectin expression on LPS treated monocyte-derived macrophages compared to unstimulated cells in the absence of platelets, suggesting the increases in P-selectin observed is through activation of the platelets. NZ-1.3 antibody was used to bind to and block podoplanin expressed on the macrophages, before the addition of macrophages to platelets, to investigate whether blocking podoplanin reduced any platelet-macrophage interactions. There were no increases in P-selectin expression on platelets added to the GM-CSF treated cells after stimulation (Figure 5.8Ci).

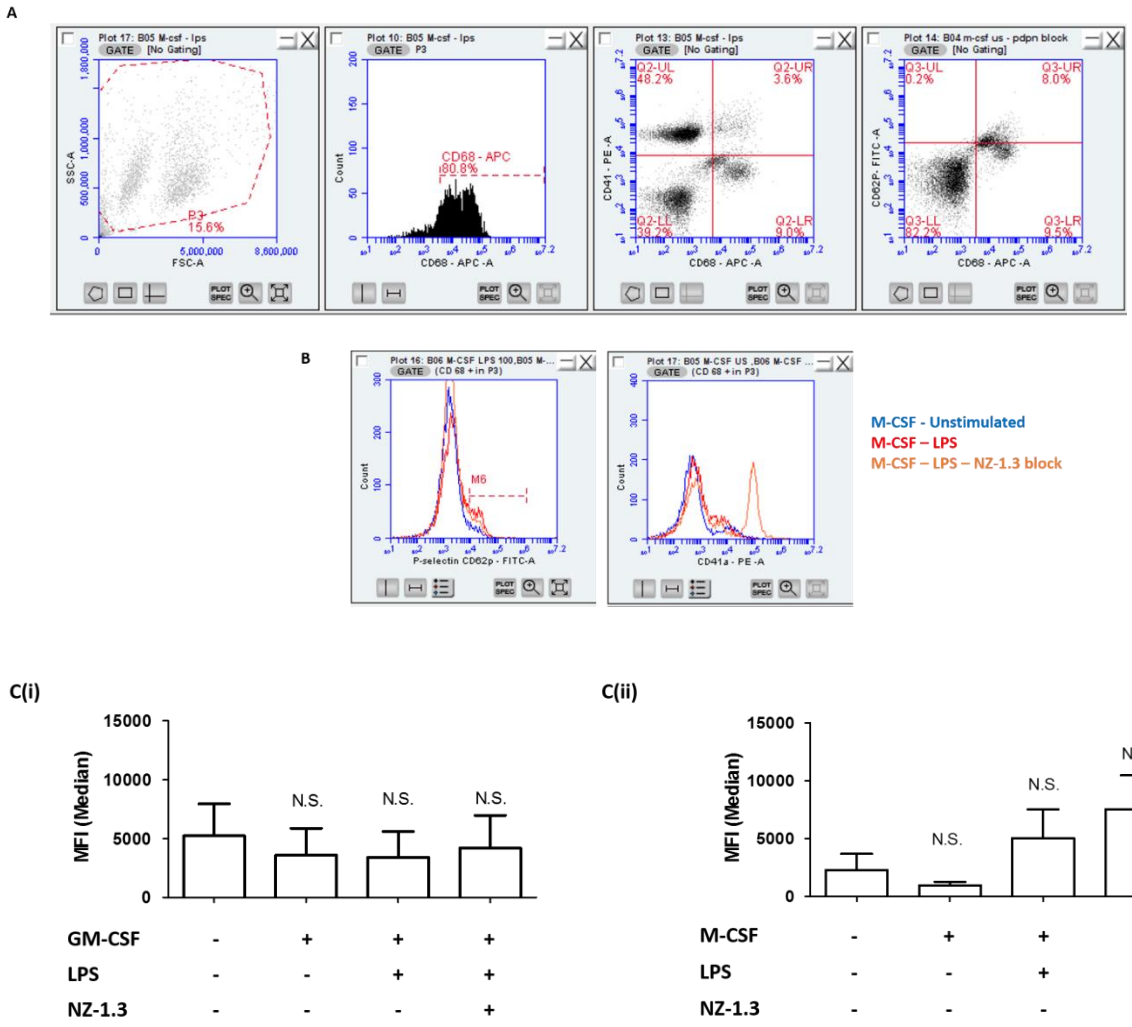

Figure 5.8 – Upregulated podoplanin on macrophages is not sufficient enough to induce platelet activation. GM-CSF (50 ng/ml) and M-CSF (100 ng/ml) treated cells were stimulated with LPS (0111; 100 ng/ml) for 24 h. Washed platelets ($2x10^7$ cells/ml) from same donor were mixed with macrophages ($0.3\ x10^6$ cells/ml) in the presence of integrilin (9 µM) under stirring conditions (1200 rpm) at 37°C for 10 min. Samples were then stained for CD68, CD41 and CD62P (P-selectin antibody) for 20 min before fluorescence signals were measured by flow cytometry. A) Gating strategy for determining CD68+ and CD62P+ cells. B) Shift of P-selectin on CD68+ cells after platelets were added to LPS stimulated M-CSF treated cells with and without NZ-1.3

antibody. C(i) MFI (median) of P-selectin staining of CD68+ cells (in M6) after platelets were mixed with unstimulated and LPS stimulated GM-CSF treated cells. NZ-1.3 antibody was added before mixing in some conditions. Mean shown ± SEM, n=6. One-way ANOVA performed with Bonferroni's post-hoc test; N.S: no significance shown. C(ii) MFI (median) of P-selectin staining of CD68+ cells (in M6) after platelets were mixed with unstimulated and LPS stimulated M-CSF treated cells were mixed. NZ-1.3 antibody was added before mixing in some conditions Mean shown ± SEM, n=5. One-way ANOVA performed with Bonferroni's post-hoc test; N.S: no significance shown.

There were no significant increases in P-selectin expression on platelets on M-CSF treated monocyte-derived macrophages stimulated with LPS (5042 ± 2492 MFI ± SEM, compared to 2294 ± 1383 MFI respectively; Figure 5.8B). There were also no significant increase when measuring the percentage of CD68+ CD62P+ cells (instead of MFI), with LPS stimulated monocyte-derived macrophages treated with M-CSF and GM-CSF. Unstimulated M-CSF cells and untreated cells also did not increase the P-selectin expression or induce platelet activation (Figure 5.8Cii). Interestingly, the addition of the anti-podoplanin antibody NZ1.3, previously shown to neutralise tumour-induced platelet aggregation (Kato et al., 2006), seemed to increase P-selectin expression on LPS-treated M-CSF differentiated cells following platelets addition (7529 ± 2925 MFI), but again this did not reach significance. It would be expected however that the NZ-1.3 antibody would reduce activation and P-selectin expression through blocking the podoplanin/CLEC-2 interactions, therefore the antibody might cause some off-target platelet activation, possibly through the low affinity FcγRIIA receptor.

5.2.7 Podoplanin is not upregulated on microvesicles of IBD or septic patients

Podoplanin is upregulated on a sub-set of human macrophages and on other cells in a range of inflammatory conditions, such as RA (Del Rey et al., 2014). Podoplanin has previously been shown in our lab to be upregulated on microvesicles derived from leukocytes in patients with RA (unpublished data). To further test this, podoplanin upregulation was measured on CD45+ microvesicles from two inflammatory cohorts, inflammatory bowel disease (IBD) and septic-patents. There was no difference in the number of microvesicles in IBD patients compared to healthy controls (HCs) and no podoplanin upregulation on CD45+ microvesicles (Figure 5.9A). There was only a

significant increase in the number of microvesicle compared to HCs in very septic patients (*p<0.05: Figure 5.9 Bi). However no significant podoplanin upregulation on the microvesicles in any patient group compared to HCs and isotype controls was observed (Figure 5.9 Bii).

5.2.8 Podoplanin detection by ELISA

Podoplanin has been shown to be cleaved after sialadase treatment (Pan et al., 2014). This study set out to confirm cleavage of podoplanin and to develop an ELISA for podoplanin detection in order to measure the cleaved form or microvesicle-associated form in patients with inflammatory conditions. Podoplanin cleavage and the use of suitable antibodies for detection were first established. Anti-human podoplanin antibodies, NZ-1.3 and 18H5 were tested. Both recognised podoplanin expression on human 293T cells, a cell line which constitutively expresses podoplanin, with the NZ-1.3 clone being preferred due to reduced background relative to the isotype control (Figure 5.10Ai). To test for cleavage of podoplanin, 293T cells were treated with trypsin (10%) for 15 min and 1 h. Podoplanin expression on cells and levels in the supernatant after centrifugation were then measured by flow cytometry (Figure 5.10Aii). Podoplanin expression on 293T cells decrease over following exposure to trypsin, with podoplanin levels in the supernatant increasing over time (74.3 ± 32.5% and 34.9 ± 17.1% of unstimulated MFI respectively, n=2; Figure 5.10B), suggesting cleavage; however, this could not be tested statistically due to the low n value. Podoplanin was also detected in the supernatant post trypsin treatment after western blotting using the anti-podoplanin (NZ1.3) antibody (Figure 5.10C).

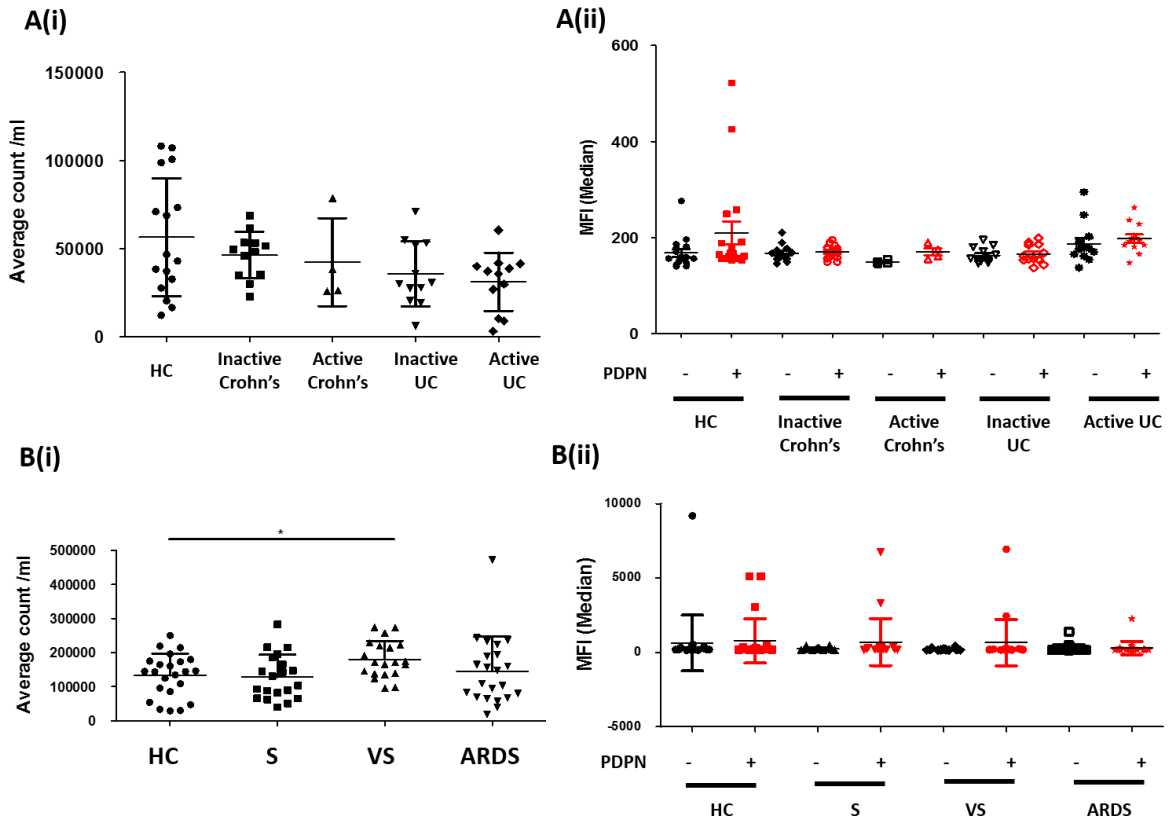

Figure 5.9 – Podoplanin is not upregulated on microvesicles in patients with IBD or in septic patients. A(i) average number of microvesicles counted/ml in plasma samples of IBD patients with inactive, active Crohn's disease (n=13, n=4), inactive and active UC (n=12, n=13), compared to HCs (n=20), Mean shown ±SD. A(ii) Median intensity fluorescence (MFI) of microvesicles gated on size and CD45+ of IBD patient groups and HCs. – and + represents presence of isotype or podoplanin (PDPN) antibody. Mean shown ±SD B(i) average number of microvesicles counted/ml in plasma samples of septic patient groups compared to HCs. Mean shown ±SD. Unpaired t-test was performed to compare microvesicle count between septic patients and HC. *$p<0.05$. B(ii) Median intensity fluorescence (MFI) of microvesicles gated on size and CD45+ of septic patient groups and HCs. – and + represents presence of isotype or PDPN antibody. Results are shown as mean shown ±SD.

The presence of podoplanin in the supernatant from trypsin-treated cells facilitated the development of the podoplanin ELISA. A sandwich ELISA, using the two anti-podoplanin antibodies (18H5 and NZ-1.3) as a capture and detection antibodies respectively was first tested (Figure 5.11A). Human recombinant podoplanin, with the Fc region attached, was used to generate a standard curve for extrapolation of test podoplanin concentrations (Figure 5.11Bi). The best standard curve generated using the recombinant podoplanin gave a R-square value of 0.747 (Figure 5.11Bi). The standard curve gave values in the µg/ml range, instead of the ng/ml range expected. There were also a number of inconsistencies using the sandwich ELISA method, with spiking of HC plasma samples with recombinant podoplanin reducing detection levels (Figure 5.11Bii).

Further assessment of podoplanin antibodies used revealed a potential overlap in binding sequences of the podoplanin epitopes. Therefore, a competitive podoplanin ELISA was developed, which used only the NZ-1.3 podoplanin antibody (Figure 5.12A). Varying amounts of recombinant podoplanin were pre-incubated with the NZ-1.3 antibody separately. Samples were incubated on a recombinant podoplanin (3 µg/ml) pre-coated plate to assess for antibody competition. With increased podoplanin in the samples, less antibody would be available to bind to recombinant podoplanin on the plate, giving a reduced signal (Figure 5.12B). The R-square value generated from the recombinant podoplanin standard curve was a respectable 0.96, in line with values observed with the sGPVI ELISA. The signal did decrease when the sample was spiked with recombinant podoplanin (3 µg/ml) as expected.

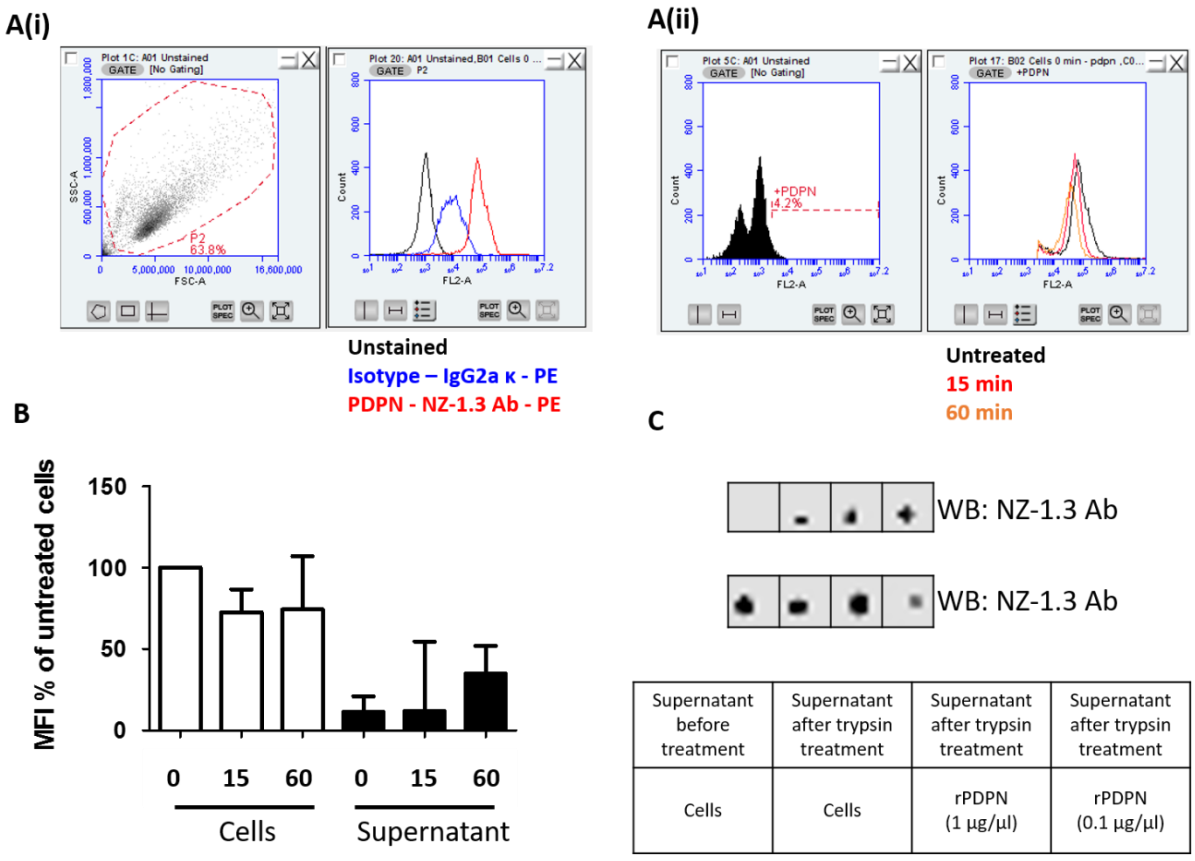

Figure 5.10– Podoplanin levels are reduced after trypsin treatment of 293T cells. A(i) Gating strategy for podoplanin staining of 293T cells by flow cytometry. Shift to right of unstained cells shows expression of podoplanin by the anti-podoplanin antibody (NZ-1.3). A(ii) Shifts of podoplanin expression of trypsin treated cells compare to unstimulated cells over time. B) Median intensity fluorescence (MFI) of cells and supernatant stained for podoplanin over various time points after trypsin treatment. Results are shown as mean shown ±SD. C) Detection of podoplanin in lysed 293T cells and in the supernatant post trypsin treatment using a dot plot with the NZ-1.3 antibody. Representative of 2 experiments.

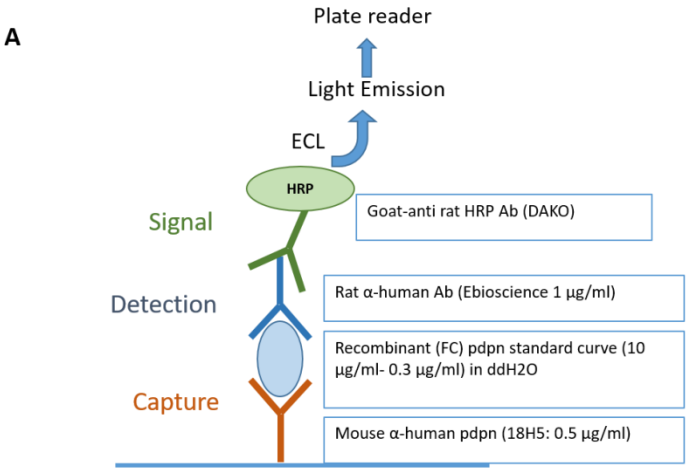

B(i)

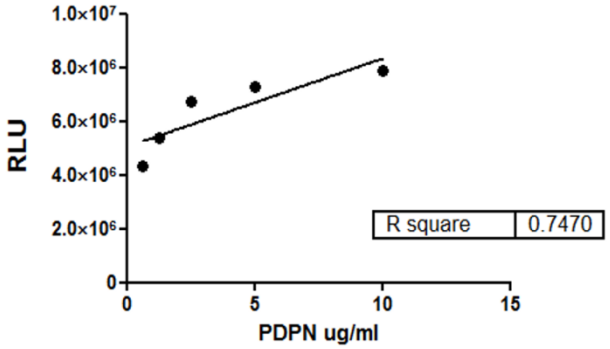

B(ii)

Condition	RLU values	Average pdpn (µg/ml)
Blank	3817243.33	-8.18
HC 1	7629609.50	15.68
HC 1 + pdpn	4127241.50	-5.66
HC 2	5064838.50	0.06
HC 2 + pdpn	4161686.00	-5.45
IBD - 1	4095176.00	-5.85

Figure 5.11 – Podoplanin sandwich ELISA development. A) Schematic of the podoplanin sandwich ELISA developed including capture, detection and signal antibody details. B(i) Best standard curve generated from measurements of a serial dilution of rPdpn containing FC region in ddH_2O. RLU represents relative luminescence units. B(ii) Podoplanin concentrations extrapolated from the standard curve in the difference conditions tested. Average values of 3 readings.

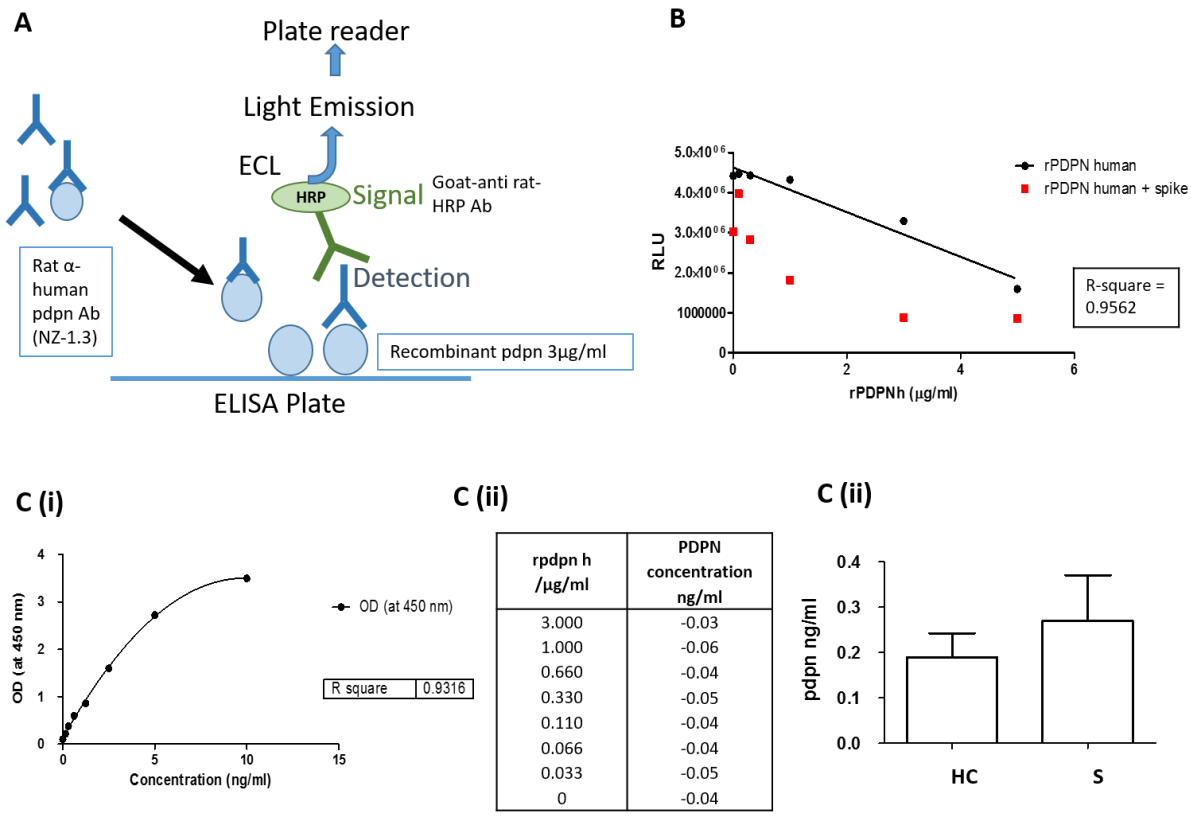

Figure 5.12 – Podoplanin competitive ELISA development and commercial podoplanin ELISA results. A) Schematic of the podoplanin competitive ELISA developed including capture, detection and signal antibody details. B) Standard curve generated from measurements of a serial dilution of rPdpn incubated with NZ-1.3 antibody added to a pre-coated rpdpn plate, with and without extra rPdpn spike. RLU represents relative luminescence units. C(i) Standard curve generated using the commercial podoplanin ELISA kit (Biomatik) showing optical density increases with increased podoplanin concentrations. C(ii) Podoplanin concentrations of the rPdpn serial dilution extrapolated from the standard curve. C(iii) Podoplanin concentrations detected by commercial ELISA in plasma samples of septic patients (n=4) and HCs (n=3). Results are shown as mean shown ±SD.

However, the generated standard curve was in the µg/ml range and the ELISA was not able to detect podoplanin in the plasma.

A commercial podoplanin ELISA (Biomatik) was the obtained and tested for podoplanin detection in patient samples. The standard curve generated using the manufacture's agonists, gave a reasonable R-square value of 0.93 (Figure 5.12Ci). However, the commercial podoplanin ELISA was unable to detect any human recombinant podoplanin (0-3 µg/ml; Figure 5.12Cii) thereby questioning its validity. When detecting podoplanin in the plasma samples of HCs and patients, no significant difference between podoplanin concentrations in the plasma of HCs compared to the septic patients was observed (very septic; Figure 5.12Cii).

5.3 Discussion

Podoplanin upregulation on different cells, including fibroblasts, LECs and a subset of liver macrophages has been described in several inflammatory settings (Astarita et al., 2015, Bertozzi et al., 2010, Hitchcock et al., 2015). Podoplanin upregulation has also been shown after LPS stimulation of mouse macrophages from the RAW264.7 cell line (Kerrigan et al., 2012). This chapter aimed to establish which cells, if any in human blood can upregulate podoplanin in response to inflammatory stimulus, in order to provide a route for podoplanin/CLEC-2 interactions, potentially leading to platelet activation.

LPS is potent pro-inflammatory mediator, used in many studies to induce inflammation. LPS stimulates myeloid cells, including monocytes and macrophages, triggering secretion of multiple cytokines including IL-1, IL-6 and TNF-α, leading to pro-inflammatory responses (Meng and Lowell, 1997). LPS is proposed to bind to TLR4 and CD14 to induce responses leading to the production and release of cytokines and chemokines (Tan and Kagan, 2014). Genomic analysis of LPS-mediated response has shown pro-inflammatory responses are similar across all myeloid cells after stimulation (Hutchins et al., 2015). In this study, LPS was used to stimulate a range of isolate blood cells to test for podoplanin upregulation in response to the inflammatory stimulus. Different serotypes of LPS (0111 and 055) were first tested to see which affect the cells the most. There was no difference observed with the LPS serotypes used. As LPS 0111 was used at lower concentrations to give the same potency of 055 serotype, this was used for further studies.

Stimulation of whole blood with LPS showed a small increase in CD14+ CD41+ complexes as measured by flow cytometry. This increase was also seen in the unstimulated blood samples, suggesting the blood incubation process could have affected the results, with platelets and monocytes forming more complexes over time. There was no significant increase in CD14+ CD69/38+ cells after time or with LPS stimulation, suggesting there was no activation of monocytes. The reduced monocyte activation may have potentially resulted from the 'resting' monocytes in the unstimulated samples being already slightly activated, so further increases in activity could not be detected. When staining CD14+ monocytes for podoplanin, there was no podoplanin upregulation observed after LPS stimulation for 4 h or 24 h after stimulation, suggesting monocytes do not express podoplanin. An alternative explanation is that the LPS stimulation of monocytes in whole blood is not sufficient enough to cause activation or podoplanin upregulation. To confirm there was no podoplanin upregulation on stimulated monocytes, both isolated monocytes from whole blood and THP-1 monocytes from the human acute monocytic leukaemia cell line (Auwerx, 1991), were stimulated with LPS for 24 h. THP-1 cells were used to give a good yield of monocytes to stimulate with LPS and look for podoplanin upregulation. The monocytes from the THP-1 cell line would give slightly different characteristics to isolated monocytes, however, with both types of monocytes, there was no podoplanin upregulation was observed after stimulation. Podoplanin upregulation on other blood cells, such as PBMCs and neutrophils were assessed after LPS stimulation for 24 h but again no podoplanin expression was seen.

Studies have shown upregulation of podoplanin on apoptotic cells. Podoplanin is upregulated on neuronal apoptotic cells after LPS infection into the CNS (Song et al., 2014). In this study, apoptosis was induced on monocytes, PMBCs and monocyte-derived macrophages after treatment with staurosporine and cycloheximide for 24 h, before being stained for Annexin and podoplanin. There was no increase in podoplanin upregulation of both apoptotic monocytes and PBMCs. Propidium iodide was also used to show cells were apoptotic, however, no podoplanin upregulation was seen either, confirming that both apoptotic and non-apoptotic monocytes and PBMCs do not upregulate podoplanin after LPS stimulation.

Podoplanin expression has previously been described on a subset of macrophages. Indeed, a population of macrophages F4/80+ in the red pulp of the spleen and in inflamed livers were shown to express podoplanin (Hou et al., 2010, Hitchcock et al., 2015). The macrophages found in the spleen have been termed as fibroblastic macrophages, which upregulate podoplanin in response to zymosan induced peritonitis (Hou et al., 2010). On the other hand, liver macrophages were shown upregulated podoplanin in response to *Salmonella typhimurium* driven inflammatory response to infection of mice. Podoplanin upregulation in response to an inflammatory stimulus has also previously been shown *in vitro* after LPS stimulation of mouse RAW264.7 cells (macrophage cell line; (Kerrigan et al., 2012). A main aim of this work is to study podoplanin upregulation in human macrophages in response to an inflammatory stimulus, such as LPS. To test these macrophages were derived from isolated monocytes with the addition of growth factors. These monocyte-derived macrophages will have some differences in characterises compared to isolated macrophages

(Ohradanova-Repic et al., 2016); however macrophage isolation is very difficult and there is a very limited availability of a reliable immortalised human macrophage cell line, therefore was the alternative option avaliable. THP-1 cells were also used for macrophage differentiation but did not produce a high yield of CD68+ macrophages. Therefore, monocytes isolated from human blood were differentiated into macrophages after GM-CSF and M-CSF treatment. GM-CSF addition leads to the formation of 'M1 macrophages' with a pro-inflammatory phenotype and DC antigen-presenting properties (Masurier et al., 1999). M-CSF addition leads to the formation of 'M2' macrophages with an anti-inflammatory phenotype (Verreck et al., 2004, Lacey et al., 2012). Macrophages have great heterogeneity during inflammation depending on the tissue in which they reside (Gordon and Taylor, 2005). Monocyte-derived macrophages were treated with GM-CSF or M-CSF for 5-6 days. This was a sufficient number of days to give reasonable yields of monocyte-derived macrophages, without increasing the levels of cell death. The GM-CSF and M-CSF treated monocyte-derived macrophages were both stimulated with LPS for 24 h before podoplanin expression was determined. It was initially expected that both types of monocyte-derived macrophages would be converted into an inflammatory macrophage after LPS stimulation. However, differences were seen between the two, both phenotypically and functionally. LPS stimulation lead to different morphological appearances. There was no major podoplanin upregulation with GM-CSF treated cells after LPS stimulation. M-CSF treated monocyte-derived macrophages did significantly upregulated podoplanin after LPS stimulation, which is interesting as M-CSF treatment is proposed to give a M2, anti-inflammatory phenotype. LPS stimulation is thought to switch the M2 phenotype to an M1 like, pro-inflammatory phenotype; however reasons why the LPS stimulated GM-CSF treated monocyte-

derived macrophages did not induce podoplanin upregulation are uncertain and suggests a preferential role for the M2 macrophages leading to the upregulation of podoplanin after an inflammatory stimulus. Interestingly however, podoplanin was upregulated in both bone-marrow derived macrophages and macrophages from the RAW 264.7 cell line, stimulated with LPS and when treated with staurosporine and cycloheximide to induce apoptosis (unpublished results in the laboratory; (Rayes et al., 2015)). Therefore, this suggests that the expression profile for podoplanin and upregulation in response to inflammatory stimulus is limited to inflammatory and apoptotic macrophages in mice and limited further to a few sub-types of inflammatory macrophages in humans.

Importantly in the context of platelets, podoplanin can interact with CLEC-2, leading to platelet activation. Platelet activation through CLEC-2 has been shown in response to up-regulation of podoplanin on inflammatory mouse macrophages (RAW264.7 cells), tumour cells and LECs (Kerrigan et al., 2012, Kato et al., 2003, Bertozzi et al., 2010). Podoplanin upregulation on liver macrophages in response to *Salmonella typhimurium* infection *in vivo* triggers a long-lasting, CLEC-2-dependent venous thrombosis in the liver (Hitchcock et al., 2015). My results show for the first time that a subset of human macrophages (monocyte-derived) upregulate podoplanin *in vitro* following LPS treatment. Podoplanin-upregulation on the M-CSF treated monocyte-derived macrophages was not sufficient to induce platelet activation, as measured by P-selectin expression on gated CD68+ cells. A small shift in P-selectin expression was seen with M-CSF derived macrophages stimulated with LPS, although this did not reach significance, which may have result from the cell ratio of platelets to macrophages. There was also no increase in P-selectin after platelets were added to GM-CSF treated

cells. The differentiation process of macrophages derived from treated monocytes only yielded a limit number of macrophages, therefore increased numbers may be required for significant platelet activation to occur. Therefore this part of the study was underpowered and would require increased sample size to conclude if the upregulated podoplanin can mediate platelet activation. *In vivo* studies may also be required to see if human macrophages can upregulate podoplanin in response to an inflammatory stimulus and if platelet activation consequently occurs.

In order to investigate whether blocking podoplanin could reduce the platelet activation by interactions with macrophages, the podoplanin antibody NZ-1.3 was added and platelet interaction with macrophages was assessed The anti-podoplanin antibody NZ-1.3 has previously been shown to neutralise and prevent tumour cell mediated platelet aggregation through blocking podoplanin (Kato et al., 2006). P-selectin expression, representing platelet activation, however did not decrease in the presence of NZ-1.3, possibly because of the limited (non-significant increase in expression). Surprisingly, the NZ-1.3 antibody caused a small increase in P-selectin expression and in the number of platelets in complex with macrophages. There are two possible explanations for these results; firstly, the anti-podoplanin antibody had some off target effects through FcγRIIA inducing platelet activation or secondly, the blocking podoplanin induces the expression of new receptors on macrophages and their interaction with another receptor on platelets leads to platelet activation. Using another podoplanin blocking antibody, or only using the fab fragment of a podoplanin antibody would establish if the antibody caused platelet activation. The NZ-1.3 anti-podoplanin antibody however, was the best anti-podoplanin antibody tested in these studies, with the least background given

compared to the isotype control. Therefore, a CLEC-2 blocking antibody in future studies would be more useful to establish if the platelet activation induced by inflammatory macrophages is mediated through podoplanin-CLEC-2 interactions.

Many studies showing podoplanin upregulation of fibroblasts and inflammatory macrophages in inflammatory settings have been limited to the study of mice. The results of this chapter have shown only a limited number of cells in the blood that have the capacity to upregulate podoplanin in response to an inflammatory stimulus. PBMCs and monocytes are unable to upregulate podoplanin after LPS stimulation. Monocyte-derived macrophages treated with M-CSF were the only cells able to sufficiently upregulated podoplanin in response to LPS stimulation, confirming findings that only a sub-set of inflammatory macrophages can upregulate podoplanin. However, monocyte-derived macrophages will have different morphology to human inflammatory macrophages and therefore further *in vivo* studies looking into podoplanin upregulation on macrophages after LPS stimulation would be required. Furthermore, the functional consequence of the finding that a subset of human macrophages can upregulate podoplanin and activate platelets in inflammatory setting remains to be determined.

Following a previous study in our laboratory of upregulation of podoplanin on CD45+ microvesicles, podoplanin has been proposed as potential candidate as an inflammatory marker. However, there was no significant upregulation of podoplanin on CD45+ microvesicles from IBD patients. Although some very septic patients had increased numbers of microvesicles compared to HCs, there was no increase in podoplanin on the

CD45+ microvesicles compared to HCs and isotype controls. Therefore, these results indicate that podoplanin is not upregulated on microvesicles in inflammatory settings.

Podoplanin has previously been shown to be cleaved after sialadase treatment (Pan et al., 2014). Podoplanin cleavage was also observed after 1 h trypsin treatment of 293T cells. Podoplanin could be detected in the cell supernatant by flow cytometry and by Western blotting. A podoplanin ELISA to measure microvesicle-bound podoplanin was developed. After various trials and development, it was found that a podoplanin sandwich ELISA could not be developed due to overlapping binding sequences of the podoplanin epitope in different podoplanin antibodies tested. Because of the lack of efficacy with the sandwich ELISA, a competitive ELISA was developed, using only the NZ-1.3 anti-podoplanin antibody. With the competitive ELISA, recombinant podoplanin was shown to generate a reasonable standard podoplanin curves although this fell in µg/ml range, reducing the sensitivity of the ELISA. This was unable to detect podoplanin in plasma of controls or patients. A similar sensitivity was seen with a commercial podoplanin ELISA. Further development is needed to increase the podoplanin ELISA sensitivity to establish if podoplanin is present in plasma at physiological levels.

Although podoplanin has been shown to be cleaved and can potentially be measured in the plasma of patients, its reliability as a marker of inflammation is of doubt. CLEC-2 has also been shown to be shed (Xie et al., 2008, Fei et al., 2012), making sCLEC-2 another potential marker for platelet activation in inflammation. However, other studies from our laboratory have shown that CLEC-2 does not undergo cleavage after activation

and is instead be internalised (Lorenz et al., 2015, Gitz et al., 2014). sCLEC-2 is also not yet a reputable marker for platelet activation in inflammation. The results of the studies showed that podoplanin can be upregulated on a subset of human macrophages in response to an inflammatory stimulus. Although this upregulation *in vitro* was not sufficient to mediate platelet activation, this may not be the case *in vivo*. Therefore further *in vivo* experiments exploring whether podoplanin upregulation in response to inflammatory stimuli can lead to platelet activation would be required to determine if the CLEC-2/podoplanin interaction between platelets and podoplanin expressing cells, could provide a potential therapeutic target for resolving excess inflammatory-driven disease.

CHAPTER 6

THE ROLE OF PLATELETS IN WOUND HEALING

6.1 Introduction

Wound healing is an important process in response to trauma, thermal injury and in the fight against infection. In a trauma context, where substantial tissue damage will occur including to the skin, there is the potential of chronic wound development, scarring, infection and mortality with impaired healing. Thermal injury can also result in significant damage of the skin at varying depths, depending on burn type and thickness, with full thickness burns disrupting all skin layers. Thermal injury can increase the risk of mortality, with around 265,000 deaths resulting from thermal injury per year according to the World Health Organisation (Mock et al., 2008). In addition, damage to the skin results in the loss of integrity of the protective barrier against the environment and infection (Singer and Clark, 1999). Cutaneous wound healing is therefore a vital process for repairing damaged tissue and maintaining the barrier against infection. Studying the roles of platelets in the process of cutaneous wound healing acts as a model for healing and gives further insight into the role of platelets in vascular integrity.

6.1.1 Structure of the skin

The skin is made up of different layers containing extracellular matrix proteins and various cell types. Figure 6.1 shows a schematic of mouse and human skin, illustrating the basic components of the two main skin layers, the epidermis and dermis of both mice and humans. In general, the epidermis is made up of several stratum layers and a uniform layer of basal keratinocytes attached to the basement membrane. Keratinocytes are specialised epithelial cells found abundantly in the epidermis, which can synthesise structural components of the epithelial barrier and can undergo differentiation-dependent structural changes when required (Eckert and Rorke, 1989). Basal

keratinocytes can process environmental signals, leading to the production of cytokines and chemokines to attract and recruit immune cells. Keratinocyte-intrinsic pathways are proposed to have a major role in the regulation of immune homeostasis and inflammation in the skin (Pasparakis et al., 2014). The dermis is beneath the epidermis and is the location of lymphatic vessels, immune cells, extracellular matrix proteins, including elastin and collagen, and fibroblasts. Fibroblasts are heterogeneous and dynamic stromal cells, with essential roles in skin maintenance (Sorrell and Caplan, 2004). Fibroblasts have several roles from synthesising granulation tissue and extracellular matrix components, such as collagen, to releasing cytokines in response to wound injury (Tracy et al., 2016). Fibroblasts are crucial at most stages of wound healing; they are attracted to the wound edge at initial stages of injury, involved in the deposition of extracellular matrices and differentiate into myofibroblasts during the latter remodelling stage (Li et al., 2007, Darby et al., 2014, Singer and Clark, 1999).

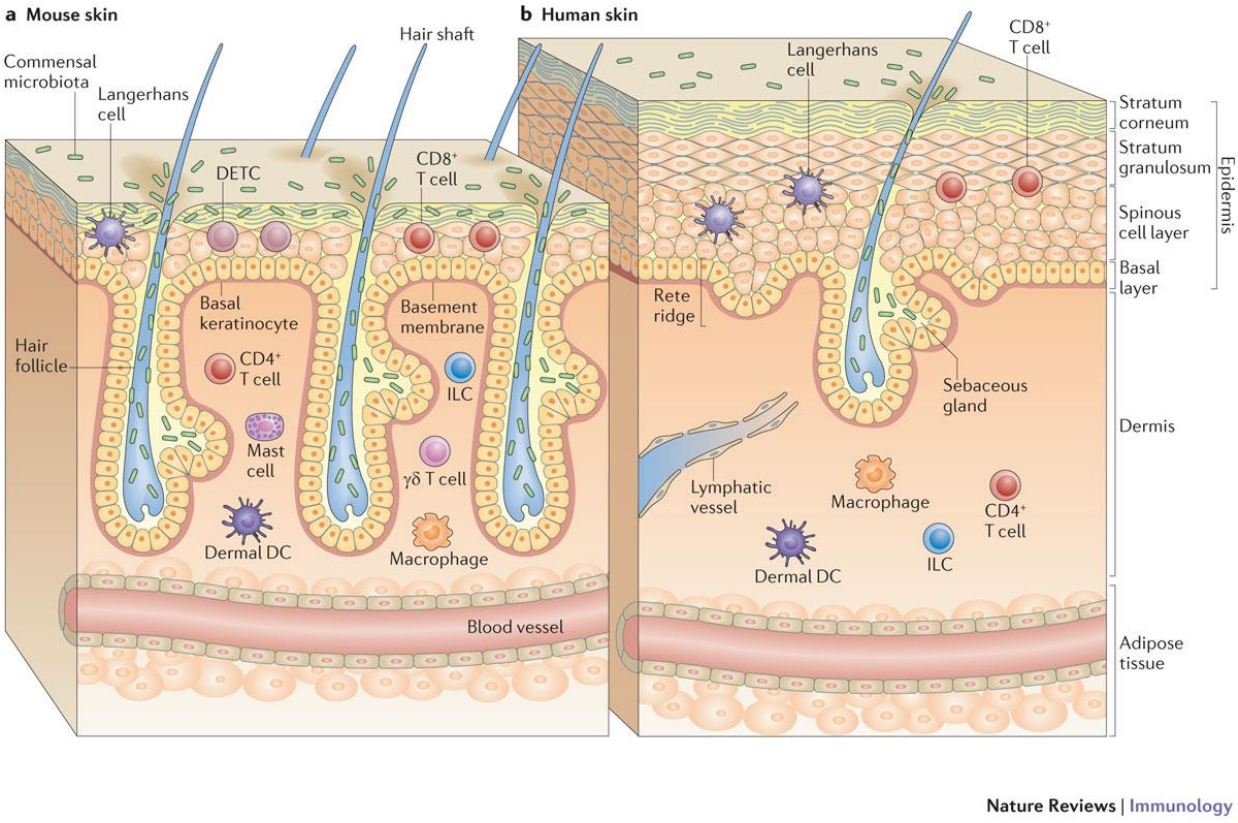

Figure 6.1 – Structure of skin in mice and humans taken from (Pasparakis et al., 2014). Structure of mouse and human skin and components of the epidermis and dermis. A) Model of mouse skin. A layer of basal keratinocytes lies above the basement membrane in the epidermis. Mouse skin contains densely packed hair follicles compared to human skin. Mouse epidermis contains Vγ5+ dendritic epidermal T cells (DETCs), which are not found in the epidermis of humans. Mouse dermis consists of macrophages, mast cells, conventional αβ T cells, innate lymphoid cells (ILCs) and dendritic cells (DCs) (Pasparakis et al., 2014). B) Model of human skin with less densely packed hair follicles and a thicker multi-layered epidermis. Human epidermis contains mainly Langerhans cells and CD8+ T cells in relation to other immune cells. Human dermis contains similar cells as mice dermis, however there is no major contribution of recruited γδ T cells, as seen with mouse skin (Pasparakis et al., 2014).

6.1.2 Process of wound healing

There are three main stages of wound healing which take place after injury; inflammatory, proliferation and remodelling. These phases do not occur in a linear fashion but overlap in time, with strong regulation in place by the release of multiple growth factors and cytokines (Li et al., 2007). Tissue injury can often result in damage of both the epidermis, the dermis and underlying blood vessels. In the initial stage after tissue damage, keratinocytes in the epidermis become activated and depending on the nature of the injury can become damaged, causing disruption to the basement membrane. Haemostasis will initially occur to prevent excess blood loss. Platelets will become activated and aggregate to form fibrin rich clots, sealing off the damaged areas. Granular contents from platelets will be released, including several chemokines and growth factors, such as platelet-derived growth factor (PDGF) for initiation of wound healing and immune cell and fibroblast recruitment (Singer and Clark, 1999, Werner and Grose, 2003).

Inflammatory phase

Circulating leukocytes, such as neutrophils, monocytes and macrophages, will be recruited to the damaged areas through chemokine gradients. These cells will release further chemokines and growth factors to enhance the immune response. Neutrophils and macrophages will kill and phagocytose infectious agents along with any cell damage debris (Li et al., 2007). Monocytes also infiltrate the wounded area and differentiate into macrophages, which go on to release PDGF and vascular endothelial growth factor (VEGF), leading to the formation of granulation tissue and the start of the proliferation stage (Singer and Clark, 1999). Granulation tissue formation involves fibroblast proliferation, deposition of extracellular matrix (ECM) proteins and the start

of the formation of new blood vessel (Li et al., 2007). Macrophages also promote keratinocyte migration and proliferation to reseal the epidermis and release mediators to promote dermal regeneration via activities of fibroblasts, including deposition of ECM proteins and myofibroblast differentiation (Shook et al., 2016, Lucas et al., 2010). This depletion of macrophages leads to defective wound repair through reducing granulation tissue and impaired re-epithelisation (Lucas et al., 2010, Singer and Clark, 1999). Resident cells, such as mast cells, located in the dermis, will also becoming activated post injury. This robust inflammatory response usually occurs around day 3 post wound injury in mice (Singer and Clark, 1999) and generally lasts for 24 to 48 hours. A similar time frame is observed in humans, however in some cases this stage can persist for up to 2 weeks (Li et al., 2007).

Proliferation phase

Recruited cells migrate to the wound edge, along with the basal keratinocytes to start rebuilding the disrupted epidermis. These will eventually cover the surface of the whole wound, a process termed re-epithelisation (Li et al., 2007). First, keratinocytes proliferate at the wound edge to ensure there are sufficient number of cells to fully cover the wound (Li et al., 2007, Singer and Clark, 1999). During this re-epithelialisation period, basement membrane proteins start to form a uniformed sequence (Singer and Clark, 1999) and fibroblasts from the dermis and monocyte-derived fibroblasts from the circulation move towards the wounded edge. At the same time in the dermis, fibroblasts differentiate into contractile myofibroblasts, characterised by large bundles of actin-containing microfilaments, which contract to reduced wound size (Tracy et al., 2016, Desmouliere et al., 2005).

Remodelling phase

The resolution and remodelling phase then follows to restore integrity of the wounded tissue. During this phase the epidermis thickens and the basement membrane is fully sealed. The dermal reconstruction occurs during this stage, which is characterised by granulation tissue formation and new blood vessel formation (Li et al., 2007). Blood vessels that have also undergone angiogenesis will mature to re-vascularise the damaged area. Fibroblasts, which have accumulated in the previous phases undergo proliferation and produce new collagen and extracellular matrix proteins (Li et al., 2007, Tracy et al., 2016). Wounds continue to undergo contraction mediated through myofibroblast activity (Young and McNaught, 2011, Desmouliere et al., 2005), and when near completion of the wound healing process, the immune cells recruited during the inflammatory phase and the contracted myofibroblasts will undergo apoptosis. This remodelling process and wound contraction by the myofibroblasts can last for around 2 weeks in mice, depending on size, depth and thickness of wound (Li et al., 2007). Remodelling in human wounds however can take much longer, up to two years. Scar tissue is formed if there is not a correct balance between synthesis and degradation of matrix proteins, such as collagen and fibronectin, deposited in the wound (Young and McNaught, 2011, Xue and Jackson, 2015).

6.1.3 Role of platelets in wound healing

Platelets have numerous roles at different stages of wound healing. The predominate role is during the immediate response after wound injury to maintain haemostasis by stopping blood loss. The clot formed to seal the wound also provides a matrix scaffold for recruited cells to infiltrate the damaged area (Li et al., 2007). Another important

function of platelets is in the release of chemoattractant and growth factors to recruit immune cells to initiate the healing process (Li et al., 2007). A range of pro-angiogenic and protein factors that promote differentiation, including, PDGF, transforming-growth factor-β (TGF-β), platelet factor 4 (PF4) are all released from platelets. These have all been implicated in wound healing, helping to increase the rate of granulation and promote tissue granulation formation (Ksander et al., 1990b, Li et al., 2007). Studies have looked into the roles of platelet releasate in the wound healing response; they show that platelet releasate, containing PDGF and TGF-β, can promote connective tissue deposition and improve wound healing in several animal models (Ksander et al., 1990b, Moulin et al., 1998, Margolis et al., 2001, Eppley et al., 2004). Furthermore, platelet releasate has been proposed to be an effective treatment in improving wound healing in large wounds caused by foot ulcers in diabetic neuropathic foot ulcers (Margolis et al., 2001). In similar studies, growth factors released from platelets have also been found in platelet-rich-plasma (PRP), which is used to prepare platelet gels and concentrates to also help improve wound healing. This has therefore been suggested to be a potential therapeutic treatment (Eppley et al., 2004, Crovetti et al., 2004). Indeed, a recent study reported that co-culture of PRP with keratinocytes and fibroblasts modulated wound healing by promoting remodelling and increasing collagen deposition (Xian et al., 2015). In addition, studies have proposed that platelets can modulate PBMCs directly to release growth factors and cytokines which help in wound healing when scratch wounds were performed (Nami et al., 2016).

There are limited studies to show the effects of wound healing after platelet depletion to confirm the role of platelets. This is presumably due to issues with the requirement of

haemostasis immediately after wound injury. However, a study has looked at the effects of platelets in acute immune complex–mediated inflammation in the mouse skin using the reverse passive Arthus (rpA) reaction model. These data suggest that there is a loss of vascular integrity with platelet depletion (using the JAQ1 anti-GPVI antibody). In addition, they show that the (hem)ITAM receptor CLEC-2 and GPVI are required for the maintenance of vascular integrity in the rpA model and at other sites of inflammation (Boulaftali et al., 2013). More recently, the platelet receptor CLEC-2 has been investigated in cutaneous wound healing; here it was shown that CLEC-2 on platelets regulate the migration of keratinocytes via interaction with podoplanin primarily on expressed keratinocytes (Asai et al., 2016). The contribution of podoplanin will be discussed further below.

6.1.4 Role of podoplanin in wound healing

Podoplanin, the only reported endogenous ligand for CLEC-2 has been shown to have multiple roles in wound healing, at different stages. Podoplanin signalling generally leads to effects on cell motility and migration (Astarita et al., 2012a, Baars et al., 2015). In the context of wound healing, it has been reported to promote the migration of fibroblasts to the disrupted epidermis. In addition, Baars *et al*., suggest that podoplanin is absent during normal epidermal homeostasis but is significantly upregulated to high levels on basal keratinocytes during wound healing (Baars et al., 2015). Other studies have assessed the timing of expression of podoplanin during wound healing; together these investigations show that upregulation starts at day 1 during the inflammatory phase, with high expression and upregulation being observed between day 3 and 7. Levels then decrease to nearly negligible levels at day 10 post injury, when the wound

is closed (Asai et al., 2016, Honma et al., 2012). As with fibroblasts, podoplanin upregulation is proposed to be important for keratinocyte migration as reductions in expression of podoplanin using siRNA in normal human epidermal keratinocytes (NHEKs) cause significant reductions in keratinocyte motility (Asai et al., 2016). Podoplanin is proposed to mediate keratinocyte motility through the RhoA signalling pathway, by downregulating E-cadherin, leading to the upregulation of N-cadherin which then promotes cell motility (Asai et al., 2016). Asai *et al*. hypothesise that platelets, via CLEC-2 interaction, downregulate podoplanin expression, leading to the reduction of keratinocyte motility once re-epithelisation has occurred (Asai et al., 2016). However, other studies using conditional genetic deletion of podoplanin in K14-basal keratinocytes have suggest there are no defects in wound healing (Baars et al., 2015). Therefore, the importance of podoplanin in wound healing has yet to be fully established.

In this chapter, a mouse model of wound healing will be used in conjunction with GPVI or platelet-specific CLEC-2 deficient mouse strains to determine the effects of ITAM receptors on wound healing. In addition, a haematopoietic-specific podoplanin-deficient strain will be used to assess the effects of podoplanin deficiency on wound healing. Together these mouse models will establish whether the platelet ITAM receptors contribute to wound healing, and/or whether podoplanin expressed on T cell and/or myeloid populations is required for appropriate wound closure.

6.2 Results

[redacted] *provided help in anaesthesia administration, mouse monitoring, mouse restraint for wound healing measurements and in the immunohistochemistry staining, in particular in the podoplanin staining as stated.*

6.2.1 Wounds of wild-type mice start to heal by day 5 post biopsy and are almost completely healed by day 10.

Wound closure kinetics in wild-type mice (WT) were assessed after 4 mm full thickness punch biopsies taken from the flanks of WT mice aged 8-10 weeks. The primary outcome measurement was to measure the extent of wound closure at different time points post biopsy. Images of the wound were taken daily, as well as measurements of the horizontal and vertical length of the wound to calculate wound area, giving an overall indication of wound size. There were no significant adverse effects to the mice post biopsy. A small drop in weight was observed initially post biopsy but increased to normal levels between day 2 and 3, remaining consistent through the rest of the time course. The wounds generally increased in diameter between 4 hours (h) and 2 days post biopsy, due to the initial movement of mice causing the wound to open up to some extent. From day 2 onwards the wound reduced in size, with a significant reduction from the original wound being observed at day 5 (Figure 6.2B). By day 9 post injury the wound was greatly reduced to fully healed levels (Figure 6.2A&B).

Platelet counts were measured in blood taken before mice were sacrificed for tissue extraction at day 10. There were no significant reductions in platelet counts between,

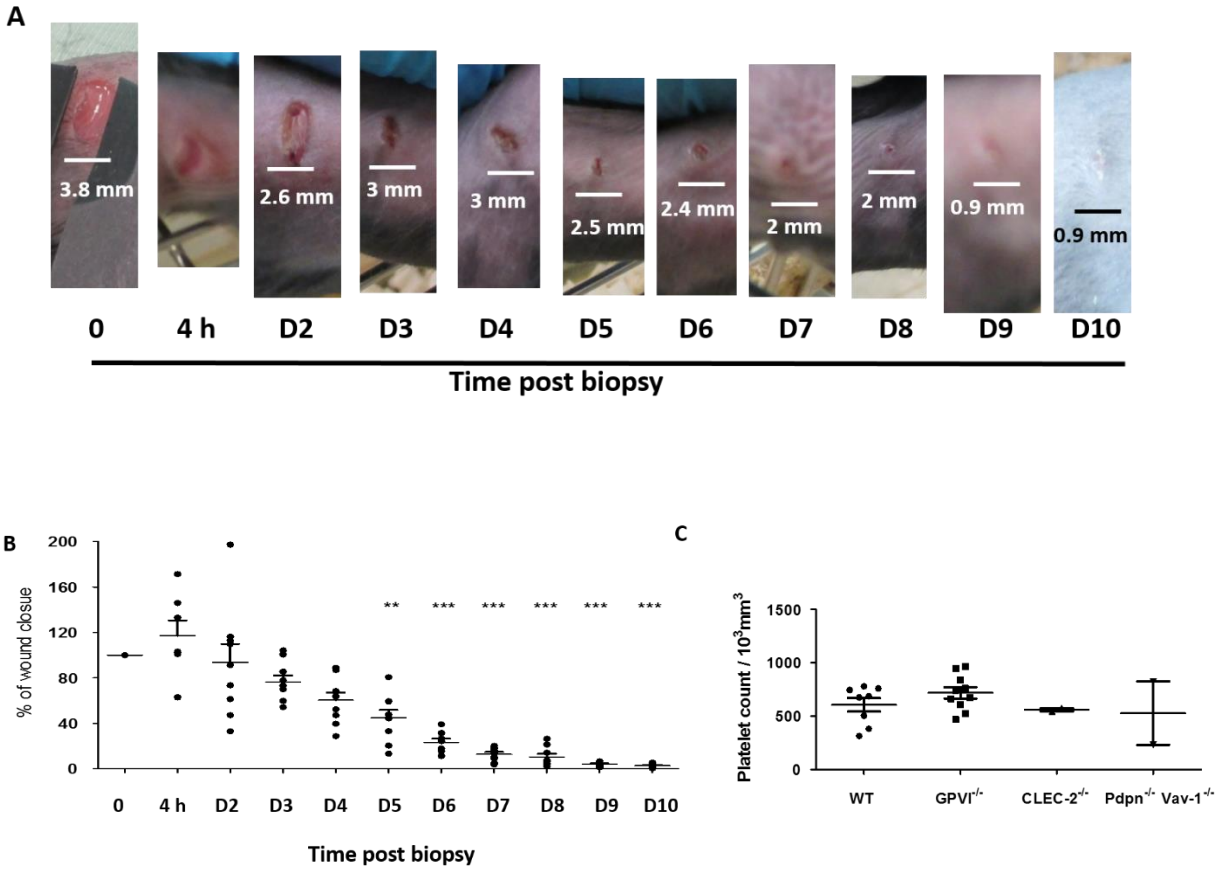

Figure 6.2 – Wound closure kinetics of wild-type (WT) mice. A) 4 mm punch biopsies were taken from the flank of WT mice. Wound diameters were imaged and measured daily for 10 Days to establish rate of wound closure, n=7. B) Percentage of wound closure was calculated compared to the original wound area at t=0. Mean shown ±SEM. Individual points represents one individual mouse. One-way ANOVA performed with Bonferroni post-test to test to compare % of wound closure at the different time points to original wound. **p<0.01. ***p<0.005. C) Platelet counts of mice at Day 10; individual points represent one mouse. Mean ±SEM shown.

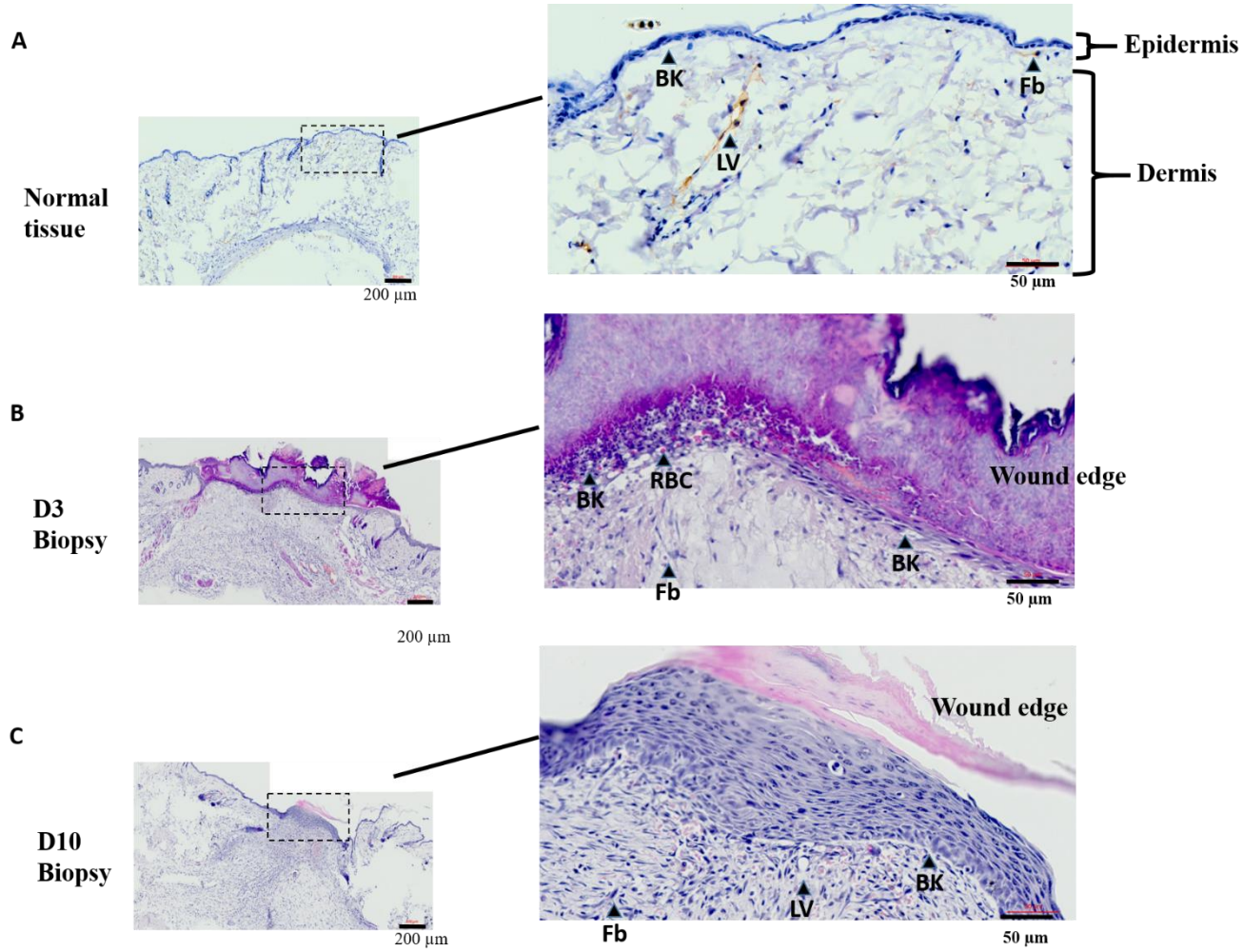

Figure 6.3 – Wound structure of WT mice during healing. Representative images of Haematoxylin and Eosin (H&E) staining of histology sections taken from WT mice at Day 3 (D3) and Day 10 (D10) post biopsy compared to skin tissue prior to biopsy. A) Normal undisrupted tissue showing the structure of the skin. Representative image of three wounds from three separate mice. B) Section of wounded area of skin from WT mice at Day 3. Representative wound image from seven separate mice C) Section of wounded area of skin at Day 10 post biopsy. Representative image of a wound from seven separate mice. *BK* = basal keratinocyte, Fb = fibroblast, LV = lymphatic vessel, V = blood vessel. Scale bar represents 200 µm and 50 µm, in small and large images, respectively.

GPVI$^{-/-}$ and CLEC-2$^{-/-}$ and WT mice, supporting the theory that it is the platelet receptors that potentially have a role in wound healing and not a result of reductions in overall platelet count (Figure 6.2C). Variations in platelet count were observed with the Pdpn$^{-/-}$ mice, with one mouse having a reduced platelet count compared to the other.

Wound structure of WT wounds were analysed after Haematoxylin and Eosin (H&E) staining of wound tissue extracted (Figure 6.3). At day 3 post biopsy, near the start of the proliferation phase and re-epithelialisation process, basal keratinocytes start to reform the epidermis layer and recruit other cells, including fibroblasts to the wound edge (Figure 6.3B). Red blood cells (RBCs) were observed at the wound edge, where bleeding potentially occurred in response to the punch biopsy. At day 10 post biopsy the re-epithelisation process had successfully sealed the wound, with the formation of granulation tissue and multiple layers of basal keratinocytes in the epidermis being observed (Figure 6.3C).

6.2.2 Wound closure did not vary between Pdpn$^{fl/fl}$ Vav-1-Cre and Clec1b$^{fl/fl}$ PF4-Cre mice compared to WT.

To establish if the podoplanin/CLEC-2 axis has a role in wound healing, punch biopsies were taken from Pdpn$^{fl/fl}$ Vav-1-Cre and Clec1b$^{fl/fl}$ PF4-Cre mice and wound closure compared to WT littermate controls. There were no significant differences in wound healing observed visually, including no signs of excess bleeding with the Pdpn$^{-/-}$ and CLEC-2$^{-/-}$ mice compared to WT controls (Figure 6.4A). Wound closure kinetics of the CLEC-2$^{-/-}$ mice were similar to those observed to WT, with an increase in size seen at 4 h to day 2 post biopsy (Figure 6.4B). A marginal increase in wound size compared to

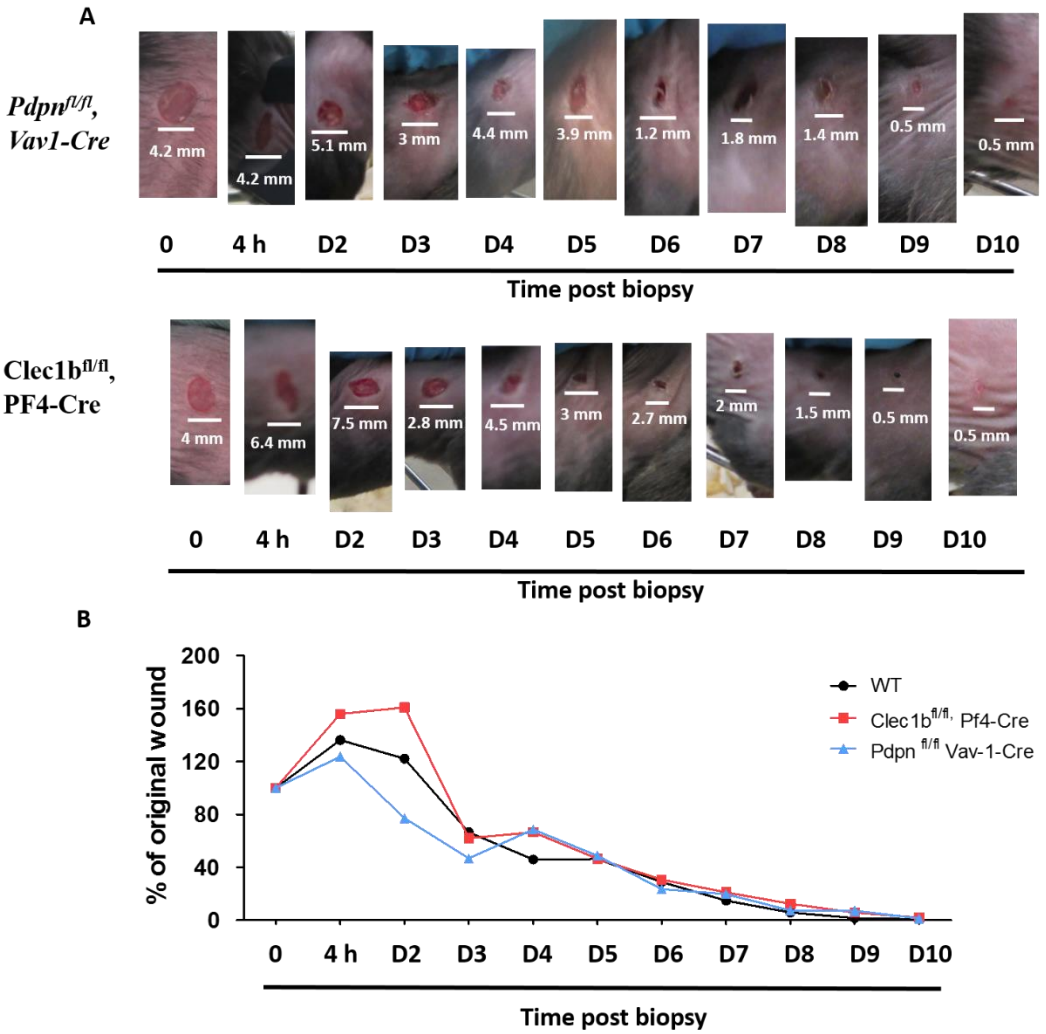

Figure 6.4 - No difference in wound closure kinetics with Pdpn$^{fl/fl}$ Vav-1^{-Cre}and CLEC-2$^{-/-}$ mice compared to WT. 4 mm punch biopsies were taken from the flank of Pdpn$^{fl/fl}$ Vav-1-Cre and Clec1b$^{fl/fl}$ PF4-Cre mice. A) Wound diameters were imaged and measured daily for 10 Days to establish rate of wound closure. Representative image of two separate mice per strain. B) Percentage (%) of wound closure calculated compared to the original wound area over time after biopsies were taken from Pdpn$^{fl/fl}$ Vav-1-Cre and Clec1b$^{fl/fl}$ PF4-Cre mice and compare to mice. (n=2 per strain).

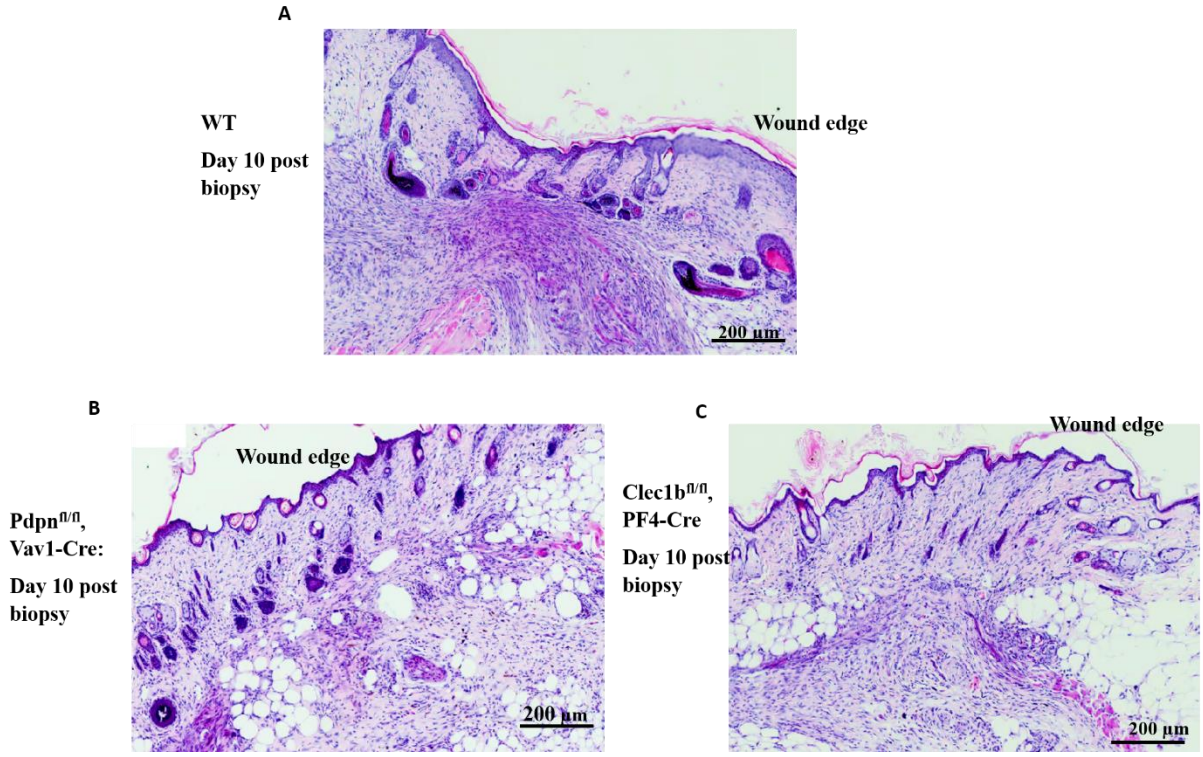

Figure 6.5 – No major structural difference with wounds taken from Pdpn$^{fl/fl}$ Vav-1-Cre and Clec1b$^{fl/fl}$ PF4-Cre mice compared to WT mice. Representative images of H&E staining of histology sections taken from WT, Pdpn$^{fl/fl}$ Vav-1-Cre and Clec1b$^{fl/fl}$ PF4-Cre mice 10 Days post biopsy. A) Section of wounded area of skin from WT mice Day 10 post biopsy. Representative image of a wound from seven separate mice. B) Section of wounded area of skin from Pdpn$^{fl/fl}$ Vav-1-Cre at Day 10. Representative image of two wounds C) Section of wounded area of skin at Day 10 post biopsy of Clec1b$^{fl/fl}$ PF4-Cre mice. Representative wound image from two separate mice. Scale bar represents 200 µm.

WT was observed at day 2, but did not reach significance and the overall rate of wound closure phenocopied WT from day 3 onwards (Figure 6.5 B). Moreover, Pdpn$^{fl/fl}$ Vav-1-Cre mice did not vary greatly in wound closure time of size compared to WT controls (Figure 6.4B). H&E staining of day 10 wound tissue to determine structural differences also showed no major differences, with the re-epithelisation process completed and intact epidermis observed in all wound sections from Pdpn$^{fl/fl}$ Vav-1-Cre Clec1b$^{fl/fl}$ PF4-Cre and WT mice (Figure 6.5).

6.2.3 Wound closure was slower with GPVI$^{-/-}$ mice compared to WT.

To assess whether GPVI, a major platelet receptor for collagen and fibrin, had a role in wound healing, wound closure was measured in GPVI$^{-/-}$ mice and compared to WT controls after punch biopsy. When assessing the wounds visually, GPVI$^{-/-}$ wounds seemed to be more pigmented and showed more signs of bleeding at early time points compared to WT controls (Figure 6.6). Furthermore, from observations only, the closed wound at day 10 in GPVI$^{-/-}$ mice was also more pigmented. Wounds in GPVI$^{-/-}$ mice did increase in size at 4 h post biopsy, as seen the WT controls. However, the wounds remained larger and took longer to reduce in size, as the percentage of original wound size remained higher in GPVI$^{-/-}$ until day 5 post biopsy (Figure 6.7A). Observationally, GPVI$^{-/-}$ wounds seemed to heal slower and the GPVI$^{-/-}$ wounds remained a similar size to the original wound at day 3 compared to WT wounds (95.4 ± 35.0% and 77.7 ± 16.5% of original wound respectively), however this did not reach significance (Figure 6.7B). Two populations of GPVI$^{-/-}$ mice also seemed to present, with one group having slower wound healing (Figure 6.7B).

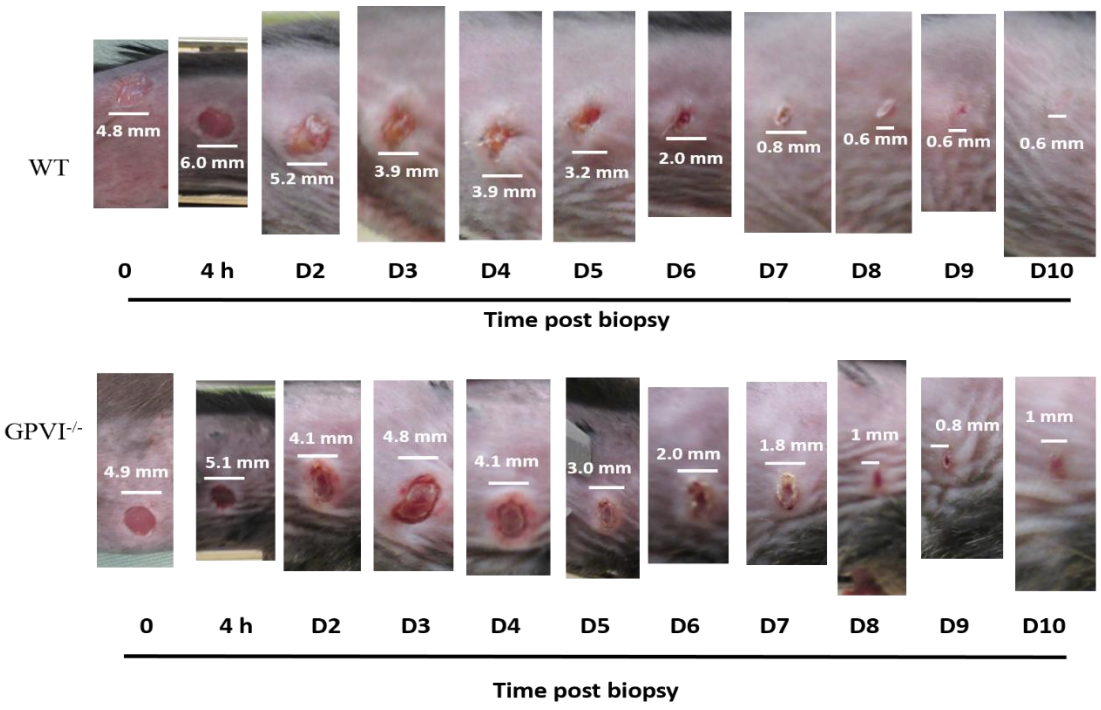

Figure 6.6 – Wound closure kinetics with GPVI$^{-/-}$ mice compared to WT. 4 mm punch biopsies were taken from the flank of WT and GPVI$^{-/-}$ mice. Wound diameters were imaged and measured daily up to 10 days post to establish rate of wound closure. Representative images of three nine separate mice**.**

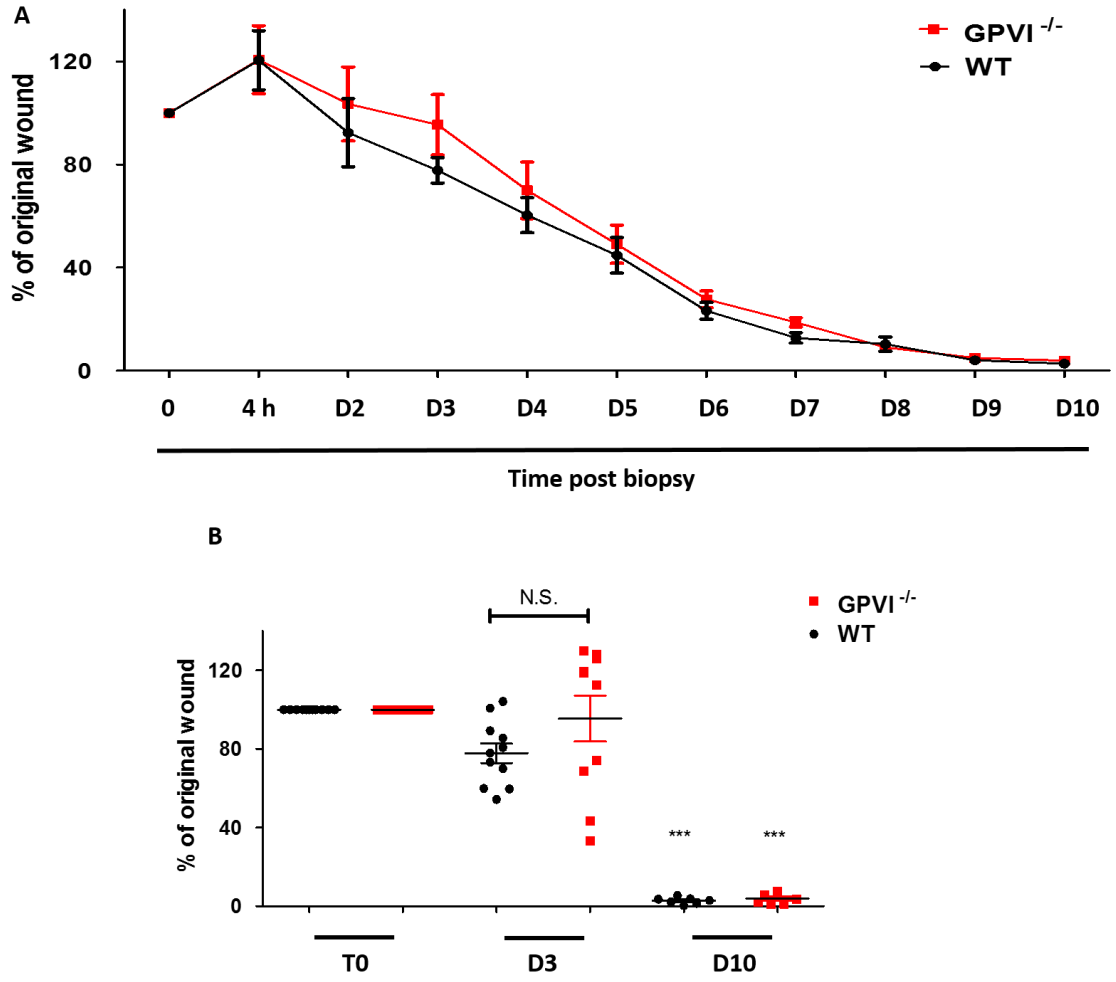

Figure 6.7 – Wound closure kinetics with GPVI$^{-/-}$ mice compared to WT. A) Percentage (%) of wound closure calculated compared to the original wound area over time after biopsies were taken from WT and GPVI$^{-/-}$ mice. Mean shown ±SEM. B) Percentage of original wound remaining with GPVI$^{-/-}$ and WT wounds at Day 3 and Day 10. Individual points represent individual mice. Mean ±SEM shown. One-way ANOVA performed with Bonferroni's post-hoc test to compare Day 3 and Day 10 wounds to original wound and to compare WT and GPVI$^{-/-}$ mice, ***p<0.005. N.S; not significant (n=9 (D0 and D3): n=7 (D10).

Wound structure after biopsy in WT and GPVI$^{-/-}$ mice were also examined on day 3, and at day 10, to see if absence of GPVI had an effect on healing of the wound and if any subtle differences in structure of the healing wound could be observed. The re-epithelisation process seemed delayed with GPVI$^{-/-}$ mice wounds compared to WT, with less granulation tissue formed (Figure 6.8A&B).

6.2.4 Podoplanin expression is normal in WT and GPVI$^{-/-}$ skin during wound healing

GPVI$^{-/-}$ and WT wound sections were assessed for podoplanin expression to establish any effects on podoplanin upregulation during wound healing. There was some difference in podoplanin staining of the wounds observed at day 3 and day 10 of GPVI$^{-/-}$ mice compared to WT mice, with podoplanin positive cells being located at the wound edge (keratinocytes) and in the dermis (primarily fibroblasts, but other immune cells cannot be ruled out; Figure 6.8A&B). Similar levels of podoplanin staining of the basal keratinocytes in the epidermis was observed near the wound edges in both GPVI$^{-/-}$ and WT mice (Figure 6.8A&B). However, podoplanin staining appeared more intense in the dermis of WT mice compared to GPVI$^{-/-}$ in day 3 tissue. This could represent more fibroblasts and immune cells being recruited and increased granulation tissue formation compared to GPVI$^{-/-}$ mice (Figure 6.8A&B). However, further staining of tissues from multiple wound sections from more mice are needed to confirm this. By day 10 the epidermal layer at the wound edge was sealed, with an intact layer of basal keratinocytes being present in both WT and GPVI$^{-/-}$ mice (Figure 6.8C&D). As expected, less podoplanin staining was observed in epidermal keratinocytes and dermal layers in day 10 wounds compared to day 3 wounds of both WT and GPVI$^{-/-}$.

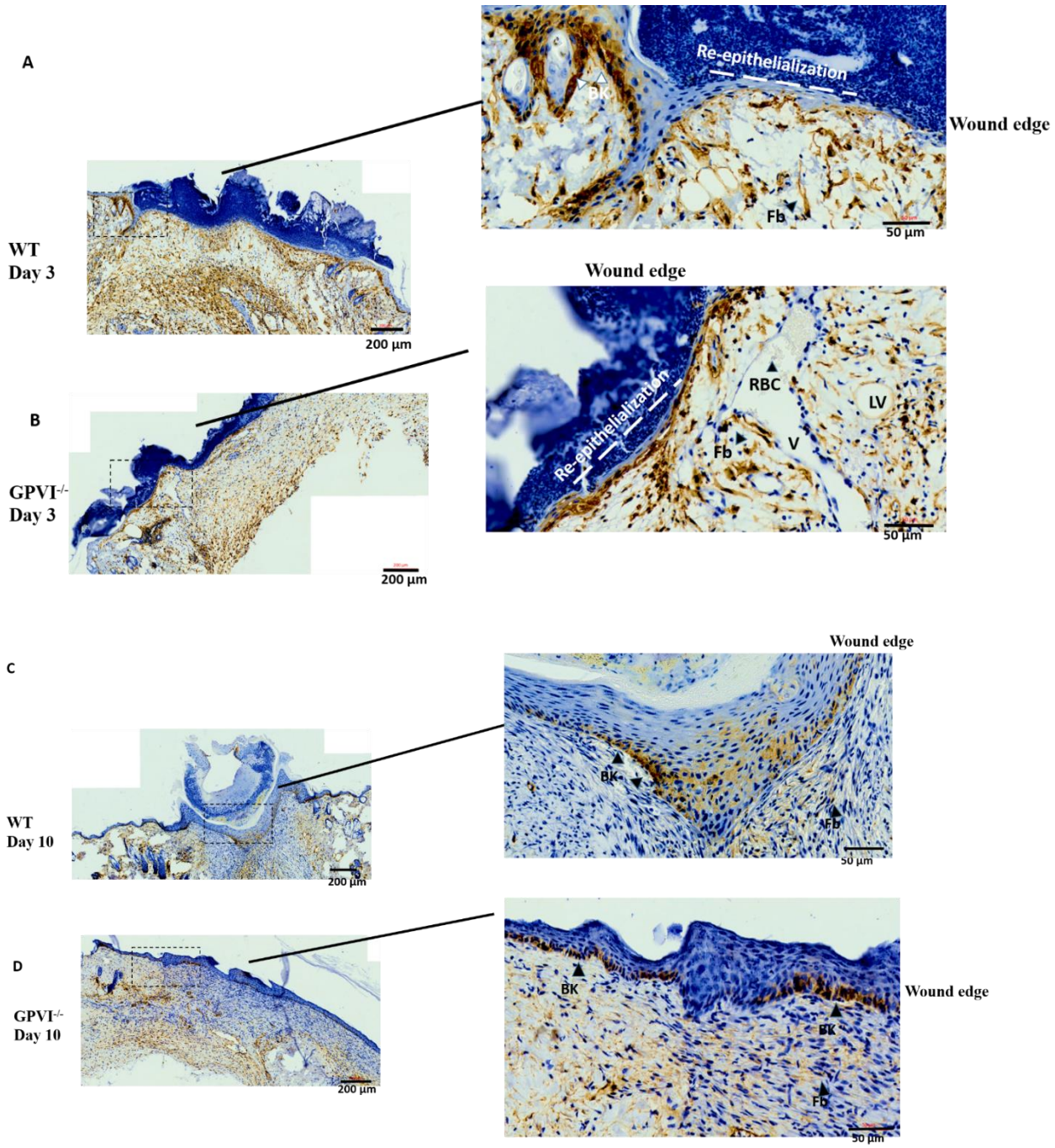

Figure 6.8 – Podoplanin staining and structure of wounds at Day 3 and Day 10 post biopsy of GPVI $^{-/-}$ mice compared to WT mice. Representative images of podoplanin (brown colour) staining of histology sections taken from WT and GPVI$^{-/-}$ mice at Day 3 and Day 10 post biopsy. A) Section of wounded area of skin from WT mice at Day 3. Representative wound image from three separate mice. B) Section of

wounded area of skin at Day 3 post biopsy of a GPVI$^{-/-}$ mouse. Representative wound image from three separate mice. C) Section of wounded area of skin from WT mice at Day 10. Representative wound image of three separate mice. D) Section of wounded area of skin of a GPVI$^{-/-}$ mouse at Day 10. Representative wound image from three separate mice. BK = basal keratinocyte, Fb = fibroblast, LV = lymphatic vessel, V = blood vessel. Scale bar represents 200 µm and 50 µm. All podoplanin staining was performed by [redacted].

6.3 Discussion

The main aim of this chapter was to establish whether the platelet ITAM receptors CLEC-2 or GPVI, and the endogenous CLEC-2 ligand podoplanin could affect wound healing. Wound biopsies were taken from mice deficient in GPVI or deficient in CLEC-2 or podoplanin from haematopoietic cells to determine if any differences in wound healing compared to WT mice.

The wound healing kinetics in WT mice were first established after punch biopsies taken, which showed wounds generally increased in size initially from 4 hours to day 2 after biopsy, potentially due to movement of the mice to some extent. Wounds started to decrease in size from day 2 post biopsy, with significant reductions in size being observed at day 5. The reduction in wound size at day 2 would correspond to the end of the inflammatory phase and start of the proliferation stage of wound healing (Li et al., 2007, Singer and Clark, 1999). When analysing wound structure by histology, at day 3 the epidermal layer of basal keratinocyte started to reform following the disruption caused from the punch biopsy, representing the start of re-epithelisation. Cells, including fibroblasts appeared to be recruited near to the wound edge. RBCs were observed in wound sections at day 3, presumably a result of initial bleeding occurring when punch biopsy was taken. Wound structure at day 10 showed that wounds were mostly healed with re-epithelisation process completed and fully intact epidermis being observed.

Platelet CLEC-2 and podoplanin have been shown to have crucial roles in migration and proliferation of keratinocytes and fibroblasts (Asai et al., 2016). To determine whether

there was a role for the CLEC-2/podoplanin axis in wound healing, biopsies were taken from Pdpn$^{fl/fl}$ Vav-1-Cre and Clec1b$^{fl/fl}$ PF4-Cre mice and compared to WT mice. Pdpn$^{fl/fl}$ Vav-1-Cre are mice with haematopoietic cells deficient in podoplanin, as global podoplanin knockouts die at birth (Schacht et al., 2003). Clec1b$^{fl/fl}$ PF4-Cre are mice with CLEC-2 knocked out of all CLEC-2 expressing cells, including platelets and dendritic cells. There were no structural differences in wounds of Pdpn$^{fl/fl}$ Vav-1-Cre and Clec1b$^{fl/fl}$ PF4-Cre mice, with wound closure similar to WT wounds for the full time course, and being healed between day 9 and 10. Overall this suggests that deficiencies in podoplanin or CLEC-2 have little effect on wound closure, supporting findings by Baars et al. (2015), who showed that podoplanin function was not rate-limiting in the re-epithelisation process in wound healing (Baars et al., 2015). However, to confirm this finding it would require increased sample number of mice to undergo biopsies. This study was a pilot study to give preliminary findings, as only two mice were used per condition, so therefore under-powered. The aim of the pilot study was to see which platelet receptors/ligands appeared to have roles in wound healing to pursuit further. The Pdpn$^{fl/fl}$ Vav-1-Cre mice seemed to have varying phenotypes as one had a lower platelet count than the other and bleeding in the guts, suggesting varying severity. Therefore, increasing the sample number would confirm if podoplanin deficiencies effected wound healing. Other strains of mice with deficiencies in podoplanin, such as an epithelial specific deletion of podoplanin or strains with fibroblasts deficient in podoplanin may be a useful to determine if podoplanin can modulate the wound healing response. CLEC-2 deficient mice also showed no signs of impaired healing. However, again only a small number of mice were used for the pilot study and using another CLEC-2 deficient mouse model such as the tamoxifen induced global CLEC-2

knockout model, where CLEC-2 is removed from all CLEC-2 expressing cells may help to confirm whether there is a role for CLEC-2 in wound healing.

GPVI and other ITAM receptors are important in maintain vascular integrity in the skin with acute immune complex–mediated inflammation (Boulaftali et al., 2013). Punch biopsies were taken from $GPVI^{-/-}$ mice in these preliminary studies to assess effects on cutaneous wound healing. $GPVI^{-/-}$ mice used were mice with GPVI knocked out from platelets and megakaryocytes (platelet precursor). Wounds from $GPVI^{-/-}$ mice did show visually differences in structure, size and composition at early time points (day 2 to day 5) compared to WT wounds, when looking visually at the wounds compared to WT. $GPVI^{-/-}$ mice tended to show more signs of bleeding, initially at the time of biopsy taken and through the ten-day time course. However, based on the wound healing measurements, the wound closure of $GPVI^{-/-}$ mice was not significantly different to WT at day 3. There was a split in the population of $GPVI^{-/-}$ mice on day 3 with some $GPVI^{-/-}$ mice having slower wound healing to the others. Explanations for this could be due to age of the mice, size of initial wound, sex or litter. However, most of the mice were aged between 8-10 weeks due to licence protocol and established methods, there was variation in the sex, with both males and females being used, which didn't associate with the split in the groups and the initial size of the wounds were similar. Mice used were also from different litters, but this can not be fully ruled out as a possible explanation as this study was only able to use a small number of $GPVI^{-/-}$ mice for this time point, therefore this could affect wound closure. Another limitation may arise due to the accuracy of the wound measurements. Due to animal licence restrictions and animal housing issues, only callipers were allowed for measuring the wounds whilst the

mice were awake, therefore potentially giving less accurate measurements. Future measurements could involve anaesthetising the mice to get exact wound measurements or using the appropriate cameras and software, which will accurately measure the wound lengths. Further exploration with the methods and increasing the number of mice undergoing the biopsy procedure could provide more information as to the reasons for the split population and also potentially increase the significance to show whether there is a delay in wound healing in GPVI$^{-/-}$ at day 3 post biopsy. By day 6 the wound healing processes of the GPVI$^{-/-}$ mice appeared to have reached the same levels of WT wound healing with the wounds being healed at day 10, suggesting that GPVI deficiency may delay wound healing but not prevent full wound closure. The re-epithelialisation process looked delayed when assessing wound structure using immunohistochemistry. There seemed to be less granulation tissue formed at day 3 in GPVI$^{-/-}$ mice wounds compared to WT. However, at day 10, there was a uniformed layer of basal keratinocytes and intact epidermis being present in both WT and GPVI$^{-/-}$ mice.

Wound sections were then co-stained for podoplanin to see if podoplanin staining could show more subtle differences in wound closure. Podoplanin upregulation during wound healing is regulated to modulate the migration of keratinocytes and fibroblasts at certain stages of healing (Asai et al., 2016). General podoplanin staining was similar at day 3 and day 10 in wounds of GPVI$^{-/-}$ and WT mice. Podoplanin positive cells were located at the wound edge, representing keratinocytes and the number of podoplanin positive cells, most likely fibroblasts, were located in the dermal layer at day 3, consistent with findings of previous studies (Asai et al., 2016). There was however denser podoplanin

staining observed in the dermis of WT mice compared to GPVI$^{-/-}$, which could represent less fibroblasts and keratinocytes being recruited and reduced granulation tissue formation at this stage in GPVI$^{-/-}$ mice, consistent with our findings that the proliferation phase may be delayed in these mice. More tissue sections would need to be performed to fully establish this, along with using other epithelialisation markers to stain sections to look for delayed wound healing and effects on re-epithelisation. The podoplanin positive cells are thought to be fibroblast however it would also be of use to stain for inflammatory macrophages (CD45^{+} or F4/80^{+} together) to confirm which cell type is present and expressing podoplanin. Co-staining with CD41 could also determine if are platelets are present at the different stages of wound healing. To determine whether there is a reduction in podoplanin positive cells in the dermis of GPVI$^{-/-}$ wounds at the earlier time points, flow cytometry, real-time QT-PCR and Western blots could all be used to measure podoplanin upregulation in cell suspensions from isolated dermis and epidermis of the wounds. Overall, further studies are needed to determine in GPVI has a role in cutaneous wound healing.

The findings of these preliminary wound healing experiments suggest that deficiencies of podoplanin in haematopoietic cells and CLEC-2 deficiencies do not affect wound healing, supporting findings of Baars et al. (2015), which showed podoplanin deletion in keratinocytes did not affect migration or ability of wounds to heal (Baars et al., 2015). Overall this suggests podoplanin mainly as an inflammatory maker or an alternative explanation is that there is a compensatory mechanism in place to maintain keratinocyte function in the absence of podoplanin (Baars et al., 2015). An important aim of this chapter was to establish if platelet ITAM receptors had any part in wound

healing. The results suggest that GPVI does not have a major role in wound healing, as the wounds did not significantly heal different in the GPVI$^{-/-}$ mice compared to WT. However, based on some of the observations, the wounds did seem more pigmented, suggest a slight healing impairment. Further studies looking at healing in GPVI$^{-/-}$ mice, including having more accurate ways of measuring wound closure, increasing the number of mice to increase power of the study and more H&E staining of the wounds to show subtle differences, will be required to confirm if there is a role for GPVI in wound healing.

The potential role of GPVI in wound healing could be due to delays in proliferation and re-epithelisation, which may result from immediate haemostasis that occurs post injury. It is at this stage that platelet GPVI activation may be important for aggregate formation and release of chemokines and growth factors for the initiation of the inflammation phase for wound healing. The absence of GPVI may result in delayed immune cell recruitment, which only then occurs once the neutrophils and monocytes infiltrate the wound to the release the important mediations and growth factors needed to drive the wound healing process. However, further studies are required to determine the full role of platelet GPVI in all the different stages of the wound healing process.

CHAPTER 7

GENERAL DISCUSSION

7.1 Summary of results

Platelets play critical roles in thrombosis, inflammation and wound healing, which are essential processes needed in the response to trauma and have been fundamental to the work performed in this thesis. The following have driven the work in this thesis; (i) identifying which of the endogenous mediators released following trauma and during inflammation induce platelet activation; (ii) the molecular basis of activation; (iii) the consequences of platelet activation in disease as indicated using molecular biomarkers; and (iv) investigating the role of platelets in wound healing.

7.1.1 Platelet activation in response to trauma and inflammation

I have assessed several different types of Alarmins and other endogenous mediators released after trauma and have shown histones to be one of the most potent Alarmins in mediating robust platelet activation both *in vitro* and *in vivo*. Histone-mediated platelet activation i*n vitro* was shown to be through the ITAM receptor, GPVI, providing an alternative mechanism to the toll-like receptor mechanism previously described (Semeraro et al., 2011, Fuchs et al., 2011a). However, histone-mediated platelet activation was shown to be independent of GPVI *in vivo* by measurement of thrombocytopenia after injection into mice, as this was not reduced in $GPVI^{-/-}$ mice (even in the presence of a direct thrombin inhibitor, hirudin), suggesting an alternative *in vivo* mechanism(s) for histone-mediated platelet activation, such as endothelial damage and release of mediators or through activation of multiple platelet receptors. Histones are highly positive charged proteins, which have multiple effects on several different cells, suggesting that targeting or neutralising histones directly, such as heparin treatment, may have the greatest potential for preventing their cytotoxic effects.

Other mechanisms for platelet activation as a result of inflammation were also studied. Podoplanin, the endogenous ligand for the hemITAM receptor, CLEC-2, has been shown to be upregulated on several cells under inflammatory conditions (Astarita et al., 2012b, Ekwall et al., 2011), including on inflammatory macrophages in mice (Mourao-Sa et al., 2011, Kerrigan et al., 2012). I extended this to show an important difference with podoplanin upregulation on human blood cells, with podoplanin only being upregulated on inflammatory macrophages (monocyte-derived macrophages) in response to the inflammatory stimulus LPS. Surprisingly, podoplanin upregulation was not sufficient to induce platelet activation. However, due to the low sample size for these sets of experiments, further studies looking to alter the platelet – macrophage ratio would be required to confirm whether the podoplanin upregulation can induce platelet activation. *In vivo* studies would also be beneficial to determine precisely which cells can upregulate podoplanin in response to an inflammatory challenge and establish if this would be sufficient to induce platelet activation.

7.1.2 Consequences of platelet activation

It is known that soluble GPVI (sGPVI) is released into the circulation after GPVI cleavage following activation of the predominate sheddase ADAM10, in response to numerous stimuli including collagen, other ITAM ligand, shear and FXa (Facey et al., 2016). In this study, I have confirmed that activation of GPCRs by ADP and PAR-1 did not induce GPVI shedding. Thrombin stimulation did however induce GPVI shedding in 50% of the donors, presumably as a result of fibrin formation. Fibrin-mediated GPVI shedding was found to be mainly dependent on the confirmation of fibrin, with only polymeric and not monomeric fibrin mediating shedding. There were limited roles for matrix metalloproteinases, including ADAM10 and ADAM17 in the fibrin-mediated

shedding. Fibrin-mediated shedding did not appear to dependent on GPVI signalling, as inhibitors to key signalling proteins Src and Syk did not reduce fibrin-induced GPVI shedding. This is in contrast to activation by GPVI and indicates that shedding may not be related to binding to GPVI, however this remains to be investigated. The ability of fibrin to induce GPVI shedding provides an alternative physiological agonist to collagen for mediating GPVI shedding *in vivo.*

sGPVI has been a recognised platelet activation marker in thrombo-inflammatory conditions, including stroke and microangiopathy (Wurster et al., 2013, Al-Tamimi et al., 2011a). This study extended this to show that sGPVI is a marker of platelet activation in patients with rheumatoid arthritis, inflammatory bowel disease (IBD) patients with active ulcerative colitis (UC) and patients with thermal injury (a model of trauma) who develop sepsis. The level of expression of sGPVI in these cohorts of patients allows correlations to be drawn with clinical outcomes, such as iron deficiency in the IBD patients and sepsis in the thermal injury patients. The elevation of sGPVI in the patients with thermal injury peaked around day 14 when minimal collagen exposure would be expected, suggesting another agonist or mechanism behind the shedding observed. sGPVI was shown not to correlate with age or platelet count suggesting alternative reasons for the elevations. This with the sGPVI elevations being significantly higher in septic patients, suggests a sepsis-driven response to cause platelet activation, and not due to initial size of injury. One potential explanation is that there is potentially increased disseminated intravascular coagulation (DIC) observed in sepsis (Semeraro et al., 2010b), whereby platelets could become further activated by polymerised fibrin networks associated with newly formed thrombi, inducing fibrin-

mediated GPVI shedding. In the future, it will be important to correlate sGPVI levels with markers of fibrin formation, such as D-dimer levels to strengthen the evidence that sGPVI elevation is a consequence of fibrin activation of platelets. Measurements of patients with high levels of fibrin formed, such as in patients with deep vein thrombosis (DVT), may also allow further conclusions to whether fibrin mediates the GPVI shedding.

Several attempts were made to measure soluble podoplanin and podoplanin-expressing microvesicles to establish if they present in inflammatory settings. Podoplanin has been previously shown to undergo cleavage after sialadase treatment *in vitro* (Pan et al., 2014) and therefore could be released and detected into the circulation. Microvesicles in the circulation could also potentially express podoplanin in inflammatory settings. However, there was no detection of podoplanin expression on microvesicles in patients with inflammatory bowel disease and sepsis when measuring by flow cytometry and the podoplanin ELISAs developed were not sensitive enough to detect either microvesicle bound or soluble podoplanin at physiological ranges. A more sensitive bioassay would need to be developed to rigorously test this although searching of available proteomic databases has also failed to find evidence of podoplanin in plasma in inflammatory conditions (Burkhart et al., 2014).

7.1.3. The role of platelets in wound healing

A cutaneous wound healing model was developed to assess the roles of platelets in wound healing, in particular studying if the ITAM receptors, GPVI and CLEC-2, along with podoplanin, are involved in wound healing. A series of preliminary experiments took wounds from mice deficient in these receptors and ligands were compared to wild-

type mice to assess differences in wound closure and in structures at certain time points post injury. Preliminary results suggest no differences in wound healing in mice with deficiencies of CLEC-2 or podoplanin. Preliminary data also showed mice deficient in GPVI did not impair wound healing compared to wild-type mice. However, due to the limited numbers of mice available at the time, further studies are required to fully establish if there is a role for GPVI in wound healing and the molecular basis of this role.

7.2 Final Conclusions

The overall findings of this thesis have added to the evidence that GPVI can serve as a marker of platelet activation in certain inflammatory conditions and in thermal injury patients who develop sepsis. After exploring the mechanisms behind a range of Alarmins, histones were the only Alarmins where GPVI had a role. Histone-mediated platelet activation *in vitro* was GPVI dependent; however, multiple mechanisms were involved *in vivo*. Proteolytic cleavage of CLEC-2 (data not shown) and podoplanin gave slightly disappoint results and did not show increased levels in the plasma in patients with inflammatory conditions. sGPVI, released after GPVI cleavage, was shown to be elevated in certain inflammatory disorders, notably in association with sepsis and with iron deficiency in inflammatory bowel disease patients, supporting the clinical relevance of sGPVI as a platelet activation marker. The finding that fibrin induces GPVI shedding further strengthens the evidence that fibrin is a physiological ligand of the immunoglobulin receptor and a future potential target for therapeutic intervention in inflammatory and thrombosis settings.

REFERENCES

ABRAMS, S. T., ZHANG, N., MANSON, J., LIU, T., DART, C., BALUWA, F., WANG, S. S., BROHI, K., KIPAR, A., YU, W., WANG, G. & TOH, C.-H. 2013. Circulating Histones Are Mediators of Trauma-associated Lung Injury. ***American Journal of Respiratory and Critical Care Medicine,*** **187, 160-169.**

ACTON, SOPHIE E., ASTARITA, JILLIAN L., MALHOTRA, D., LUKACS-KORNEK, V., FRANZ, B., HESS, PAUL R., JAKUS, Z., KULIGOWSKI, M., FLETCHER, ANNE L., ELPEK, KUTLU G., BELLEMARE-PELLETIER, A., SCEATS, L., REYNOSO, ERIKA D., GONZALEZ, SANTIAGO F., GRAHAM, DANIEL B., CHANG, J., PETERS, A., WOODRUFF, M., KIM, Y.-A., SWAT, W., MORITA, T., KUCHROO, V., CARROLL, MICHAEL C., KAHN, MARK L., WUCHERPFENNIG, KAI W. & TURLEY, SHANNON J. 2012a. Podoplanin-Rich Stromal Networks Induce Dendritic Cell Motility via Activation of the C-type Lectin Receptor CLEC-2. ***Immunity,*** **37, 276-289.**

ADAMS, M. N., RAMACHANDRAN, R., YAU, M. K., SUEN, J. Y., FAIRLIE, D. P., HOLLENBERG, M. D. & HOOPER, J. D. 2011. Structure, function and pathophysiology of protease activated receptors. ***Pharmacol Ther,*** **130, 248-82.**

ADHIKARI, N. K., FOWLER, R. A., BHAGWANJEE, S. & RUBENFELD, G. D. 2010. Critical care and the global burden of critical illness in adults. ***Lancet,*** **376, 1339-46.**

AL-TAMIMI, M., GARDINER, E. E., THOM, J. Y., SHEN, Y., COOPER, M. N., HANKEY, G. J., BERNDT, M. C., BAKER, R. I. & ANDREWS, R. K. 2011a. Soluble glycoprotein VI is raised in the plasma of patients with acute ischemic stroke. ***Stroke,*** **42, 498-500.**

AL-TAMIMI, M., GRIGORIADIS, G., TRAN, H., PAUL, E., SERVADEI, P., BERNDT, M. C., GARDINER, E. E. & ANDREWS, R. K. 2011b. Coagulation-induced shedding of platelet glycoprotein VI mediated by factor Xa. ***Blood,*** **117, 3912-20.**

AL-TAMIMI, M., MU, F. T., MOROI, M., GARDINER, E. E., BERNDT, M. C. & ANDREWS, R. K. 2009. Measuring soluble platelet glycoprotein VI in human plasma by ELISA. ***Platelets,*** **20, 143-9.**

AL-TAMIMI, M., TAN, C. W., QIAO, J., PENNINGS, G. J., JAVADZADEGAN, A., YONG, A. S., ARTHUR, J. F., DAVIS, A. K., JING, J., MU, F. T., HAMILTON, J. R., JACKSON, S. P., LUDWIG, A., BERNDT, M. C., WARD, C. M., KRITHARIDES, L., ANDREWS, R. K. & GARDINER, E. E. 2012. Pathologic shear triggers shedding of vascular receptors: a novel mechanism for down-regulation of platelet glycoprotein VI in stenosed coronary vessels. ***Blood,*** **119, 4311-20.**

ALSHEHRI, O. M., HUGHES, C. E., MONTAGUE, S., WATSON, S. K., FRAMPTON, J., BENDER, M. & WATSON, S. P. 2015a. Fibrin activates GPVI in human and mouse platelets. ***Blood,*** **126, 1601-8.**

ALSHEHRI, O. M., MONTAGUE, S., WATSON, S., CARTER, P., SARKER, N., MANNE, B. K., MILLER, J. L., HERR, A. B., POLLITT, A. Y., O'CALLAGHAN, C. A., KUNAPULI, S., ARMAN, M., HUGHES, C. E. & WATSON, S. P. 2015b. Activation of glycoprotein VI (GPVI) and C-type lectin-like receptor-2 (CLEC-2) underlies platelet activation by diesel exhaust particles and other charged/hydrophobic ligands. ***Biochem J,*** **468, 459-73.**

ANDREWS, R. K., KARUNAKARAN, D., GARDINER, E. E. & BERNDT, M. C. 2007. Platelet receptor proteolysis: a mechanism for downregulating platelet reactivity. ***Arterioscler Thromb Vasc Biol,*** **27, 1511-20.**

ANG, L., THANI, K. B., ILAPAKURTI, M., LEE, M. S., PALAKODETI, V. & MAHMUD, E. 2013. Elevated Plasma Fibrinogen Rather Than Residual Platelet Reactivity After Clopidogrel Pre-Treatment Is Associated With an Increased

Ischemic Risk During Elective Percutaneous Coronary Intervention. ***Journal of the American College of Cardiology,*** **61, 23-34.**

ANGUS, D. C. & VAN DER POLL, T. 2013. Severe sepsis and septic shock. ***N Engl J Med,*** **369, 840-51.**

ARIAS-SALGADO, E. G., LIZANO, S., SHATTIL, S. J. & GINSBERG, M. H. 2005. Specification of the direction of adhesive signaling by the integrin beta cytoplasmic domain. ***J Biol Chem,*** **280, 29699-707.**

ARMAN, M., KRAUEL, K., TILLEY, D. O., WEBER, C., COX, D., GREINACHER, A., KERRIGAN, S. W. & WATSON, S. P. 2014. Amplification of bacteria-induced platelet activation is triggered by FcγRIIA, integrin αIIbβ3, and platelet factor 4. ***Blood,*** **123, 3166-3174.**

ARNETT, F. C., EDWORTHY, S. M., BLOCH, D. A., MCSHANE, D. J., FRIES, J. F., COOPER, N. S., HEALEY, L. A., KAPLAN, S. R., LIANG, M. H., LUTHRA, H. S. & ET AL. 1988. The American Rheumatism Association 1987 revised criteria for the classification of rheumatoid arthritis. ***Arthritis Rheum,*** **31, 315-24.**

ARTHUR, J. F., DUNKLEY, S. & ANDREWS, R. K. 2007. Platelet glycoprotein VI-related clinical defects. ***Br J Haematol,*** **139, 363-72.**

ASAI, J., HIRAKAWA, S., SAKABE, J., KISHIDA, T., WADA, M., NAKAMURA, N., TAKENAKA, H., MAZDA, O., URANO, T., SUZUKI-INOUE, K., TOKURA, Y. & KATOH, N. 2016. Platelets Regulate the Migration of Keratinocytes via Podoplanin/CLEC-2 Signaling during Cutaneous Wound Healing in Mice. ***Am J Pathol,*** **186, 101-8.**

ASTARITA, J. L., ACTON, S. E. & TURLEY, S. J. 2012a. Podoplanin: emerging functions in development, the immune system, and cancer. ***Front Immunol,*** **3, 283.**

ASTARITA, J. L., ACTON, S. E. & TURLEY, S. J. 2012b. Podoplanin: emerging functions in development, the immune system, and cancer. ***Frontiers in Immunology,*** **3, 283.**

ASTARITA, J. L., CREMASCO, V., FU, J., DARNELL, M. C., PECK, J. R., NIEVES-BONILLA, J. M., SONG, K., KONDO, Y., WOODRUFF, M. C., GOGINENI, A., ONDER, L., LUDEWIG, B., WEIMER, R. M., CARROLL, M. C., MOONEY, D. J., XIA, L. & TURLEY, S. J. 2015. The CLEC-2-podoplanin axis controls the contractility of fibroblastic reticular cells and lymph node microarchitecture. ***Nat Immunol,*** **16, 75-84.**

AUWERX, J. 1991. The human leukemia cell line, THP-1: a multifacetted model for the study of monocyte-macrophage differentiation. ***Experientia,*** **47, 22-31.**

BAARS, S., BAUER, C., SZABOWSKI, S., HARTENSTEIN, B. & ANGEL, P. 2015. Epithelial deletion of podoplanin is dispensable for re-epithelialization of skin wounds. ***Exp Dermatol,*** **24, 785-7.**

BENDER, M., HOFMANN, S., STEGNER, D., CHALARIS, A., BOSL, M., BRAUN, A., SCHELLER, J., ROSE-JOHN, S. & NIESWANDT, B. 2010. Differentially regulated GPVI ectodomain shedding by multiple platelet-expressed proteinases. ***Blood,*** **116, 3347-55.**

BENDER, M., STEGNER, D. & NIESWANDT, B. 2016. Model systems for platelet receptor shedding. ***Platelets,*** **1-8.**

BENNETT, J. S. 2005. Structure and function of the platelet integrin alphaIIbbeta3. ***J Clin Invest,*** **115, 3363-9.**

BERGAMASCHI, G., DI SABATINO, A., ALBERTINI, R., ARDIZZONE, S., BIANCHERI, P., BONETTI, E., CASSINOTTI, A., CAZZOLA, P., MARKOPOULOS, K., MASSARI, A., ROSTI, V., PORRO, G. B. & CORAZZA, G. R. 2010. Prevalence and pathogenesis of anemia in inflammatory bowel disease. Influence of anti-tumor necrosis factor-alpha treatment. ***Haematologica,*** **95, 199-205.**

BERGMEIER, W., RABIE, T., STREHL, A., PIFFATH, C. L., PROSTREDNA, M., WAGNER, D. D. & NIESWANDT, B. 2004. GPVI down-regulation in murine platelets through metalloproteinase-dependent shedding. *Thromb Haemost,* 91, 951-8.

BERLANGA, O., BORI-SANZ, T., JAMES, J. R., FRAMPTON, J., DAVIS, S. J., TOMLINSON, M. G. & WATSON, S. P. 2007. Glycoprotein VI oligomerization in cell lines and platelets. *J Thromb Haemost,* 5, 1026-33.

BERTOZZI, C. C., SCHMAIER, A. A., MERICKO, P., HESS, P. R., ZOU, Z., CHEN, M., CHEN, C. Y., XU, B., LU, M. M., ZHOU, D., SEBZDA, E., SANTORE, M. T., MERIANOS, D. J., STADTFELD, M., FLAKE, A. W., GRAF, T., SKODA, R., MALTZMAN, J. S., KORETZKY, G. A. & KAHN, M. L. 2010. Platelets regulate lymphatic vascular development through CLEC-2-SLP-76 signaling. *Blood,* 116, 661-70.

BEST, D., SENIS, Y. A., JARVIS, G. E., EAGLETON, H. J., ROBERTS, D. J., SAITO, T., JUNG, S. M., MOROI, M., HARRISON, P., GREEN, F. R. & WATSON, S. P. 2003. GPVI levels in platelets: relationship to platelet function at high shear. *Blood,* 102, 2811-8.

BIANCHI, M. E. & MANFREDI, A. A. 2007. High-mobility group box 1 (HMGB1) protein at the crossroads between innate and adaptive immunity. *Immunol Rev,* 220, 35-46.

BIERHAUS, A. & NAWROTH, P. P. 2009. Multiple levels of regulation determine the role of the receptor for AGE (RAGE) as common soil in inflammation, immune responses and diabetes mellitus and its complications. *Diabetologia,* 52, 2251-2263.

BIERHAUS, A., SCHIEKOFER, S., SCHWANINGER, M., ANDRASSY, M., HUMPERT, P. M., CHEN, J., HONG, M., LUTHER, T., HENLE, T., KLOTING, I., MORCOS, M., HOFMANN, M., TRITSCHLER, H., WEIGLE, B., KASPER, M., SMITH, M., PERRY, G., SCHMIDT, A. M., STERN, D. M., HARING, H. U., SCHLEICHER, E. & NAWROTH, P. P. 2001. Diabetes-associated sustained activation of the transcription factor nuclear factor-kappaB. *Diabetes,* 50, 2792-808.

BLANN, A. D., FARAGHER, E. B. & MCCOLLUM, C. N. 1997. Increased soluble P-selectin following myocardial infarction: a new marker for the progression of atherosclerosis. *Blood Coagul Fibrinolysis,* 8, 383-90.

BOILARD, E., NIGROVIC, P. A., LARABEE, K., WATTS, G. F., COBLYN, J. S., WEINBLATT, M. E., MASSAROTTI, E. M., REMOLD-O'DONNELL, E., FARNDALE, R. W., WARE, J. & LEE, D. M. 2010. Platelets amplify inflammation in arthritis via collagen-dependent microparticle production. *Science,* 327, 580-3.

BOLTON-MAGGS, P. H., CHALMERS, E. A., COLLINS, P. W., HARRISON, P., KITCHEN, S., LIESNER, R. J., MINFORD, A., MUMFORD, A. D., PARAPIA, L. A., PERRY, D. J., WATSON, S. P., WILDE, J. T., WILLIAMS, M. D. & UKHCDO 2006. A review of inherited platelet disorders with guidelines for their management on behalf of the UKHCDO. *Br J Haematol,* 135, 603-33.

BOULAFTALI, Y., HESS, P. R., GETZ, T. M., CHOLKA, A., STOLLA, M., MACKMAN, N., OWENS, A. P., 3RD, WARE, J., KAHN, M. L. & BERGMEIER, W. 2013. Platelet ITAM signaling is critical for vascular integrity in inflammation. *J Clin Invest,* 123, 908-16.

BREITENEDER-GELEFF, S., MATSUI, K., SOLEIMAN, A., MERANER, P., POCZEWSKI, H., KALT, R., SCHAFFNER, G. & KERJASCHKI, D. 1997. Podoplanin, novel 43-kd membrane protein of glomerular epithelial cells, is down-regulated in puromycin nephrosis. *Am J Pathol,* 151, 1141-52.

BRILL, A., FUCHS, T. A., SAVCHENKO, A. S., THOMAS, G. M., MARTINOD, K., DE MEYER, S. F., BHANDARI, A. A. & WAGNER, D. D. 2012. Neutrophil

extracellular traps promote deep vein thrombosis in mice. *J Thromb Haemost,* 10, 136-44.

BRINKMANN, V., REICHARD, U., GOOSMANN, C., FAULER, B., UHLEMANN, Y., WEISS, D. S., WEINRAUCH, Y. & ZYCHLINSKY, A. 2004. Neutrophil extracellular traps kill bacteria. *Science,* 303, 1532-5.

BURKHART, J. M., GAMBARYAN, S., WATSON, S. P., JURK, K., WALTER, U., SICKMANN, A., HEEMSKERK, J. W. & ZAHEDI, R. P. 2014. What can proteomics tell us about platelets? *Circ Res,* 114, 1204-19.

BURKHART, J. M., VAUDEL, M., GAMBARYAN, S., RADAU, S., WALTER, U., MARTENS, L., GEIGER, J., SICKMANN, A. & ZAHEDI, R. P. 2012. The first comprehensive and quantitative analysis of human platelet protein composition allows the comparative analysis of structural and functional pathways. *Blood,* 120, e73-82.

CALAMINUS, S. D., THOMAS, S., MCCARTY, O. J., MACHESKY, L. M. & WATSON, S. P. 2008. Identification of a novel, actin-rich structure, the actin nodule, in the early stages of platelet spreading. *J Thromb Haemost,* 6, 1944-52.

CARLSSON, L. E., SANTOSO, S., BAURICHTER, G., KROLL, H., PAPENBERG, S., EICHLER, P., WESTERDAAL, N. A. C., KIEFEL, V., VAN DE WINKEL, J. G. J. & GREINACHER, A. 1998. Heparin-Induced Thrombocytopenia: New Insights Into the Impact of the FcγRIIa-R-H131 Polymorphism. *Blood,* 92, 1526-1531.

CHACKO, G. W., BRANDT, J. T., COGGESHALL, K. M. & ANDERSON, C. L. 1996. Phosphoinositide 3-kinase and p72syk noncovalently associate with the low affinity Fc gamma receptor on human platelets through an immunoreceptor tyrosine-based activation motif. Reconstitution with synthetic phosphopeptides. *J Biol Chem,* 271, 10775-81.

CHACKO, G. W., DUCHEMIN, A. M., COGGESHALL, K. M., OSBORNE, J. M., BRANDT, J. T. & ANDERSON, C. L. 1994. Clustering of the platelet Fc gamma receptor induces noncovalent association with the tyrosine kinase p72syk. *J Biol Chem,* 269, 32435-40.

CHAIPAN, C., SOILLEUX, E. J., SIMPSON, P., HOFMANN, H., GRAMBERG, T., MARZI, A., GEIER, M., STEWART, E. A., EISEMANN, J., STEINKASSERER, A., SUZUKI-INOUE, K., FULLER, G. L., PEARCE, A. C., WATSON, S. P., HOXIE, J. A., BARIBAUD, F. & POHLMANN, S. 2006. DC-SIGN and CLEC-2 mediate human immunodeficiency virus type 1 capture by platelets. *J Virol,* 80, 8951-60.

CHAN, J. K., ROTH, J., OPPENHEIM, J. J., TRACEY, K. J., VOGL, T., FELDMANN, M., HORWOOD, N. & NANCHAHAL, J. 2012. Alarmins: awaiting a clinical response. *The Journal of Clinical Investigation,* 122, 2711-2719.

CHAVAKIS, T., BIERHAUS, A. & NAWROTH, P. P. 2004. RAGE (receptor for advanced glycation end products): a central player in the inflammatory response. *Microbes Infect,* 6, 1219-25.

CHRISTOU, C. M., PEARCE, A. C., WATSON, A. A., MISTRY, A. R., POLLITT, A. Y., FENTON-MAY, A. E., JOHNSON, L. A., JACKSON, D. G., WATSON, S. P. & O'CALLAGHAN, C. A. 2008. Renal cells activate the platelet receptor CLEC-2 through podoplanin. *The Biochemical journal,* 411, 133-140.

CLARK, S. R., MA, A. C., TAVENER, S. A., MCDONALD, B., GOODARZI, Z., KELLY, M. M., PATEL, K. D., CHAKRABARTI, S., MCAVOY, E., SINCLAIR, G. D., KEYS, E. M., ALLEN-VERCOE, E., DEVINNEY, R., DOIG, C. J., GREEN, F. H. & KUBES, P. 2007. Platelet TLR4 activates neutrophil extracellular traps to ensnare bacteria in septic blood. *Nat Med,* 13, 463-9.

CLAUSHUIS, T. A. M., VAN VUGHT, L. A., SCICLUNA, B. P., WIEWEL, M. A., KLEIN KLOUWENBERG, P. M. C., HOOGENDIJK, A. J., ONG, D. S. Y., CREMER, O. L., HORN, J., FRANITZA, M., TOLIAT, M. R., NÜRNBERG, P.,

ZWINDERMAN, A. H., BONTEN, M. J., SCHULTZ, M. J. & VAN DER POLL, T. 2016. Thrombocytopenia is associated with a dysregulated host response in critically ill sepsis patients. *Blood,* 127, 3062-3072.

CLEMENTS, J. L., LEE, J. R., GROSS, B., YANG, B., OLSON, J. D., SANDRA, A., WATSON, S. P., LENTZ, S. R. & KORETZKY, G. A. 1999. Fetal hemorrhage and platelet dysfunction in SLP-76–deficient mice. *Journal of Clinical Investigation,* 103, 19-25.

CLEMETSON, J. M., POLGAR, J., MAGNENAT, E., WELLS, T. N. & CLEMETSON, K. J. 1999. The platelet collagen receptor glycoprotein VI is a member of the immunoglobulin superfamily closely related to FcalphaR and the natural killer receptors. *J Biol Chem,* 274, 29019-24.

COGNASSE, F., HAMZEH, H., CHAVARIN, P., ACQUART, S., GENIN, C. & GARRAUD, O. 2005. Evidence of Toll-like receptor molecules on human platelets. *Immunol Cell Biol,* 83, 196-8.

COHEN, M. J., CARLES, M., BROHI, K., CALFEE, C. S., RAHN, P., CALL, M. S., CHESEBRO, B. B., WEST, M. A. & PITTET, J. F. 2010. Early release of soluble receptor for advanced glycation endproducts after severe trauma in humans. *J Trauma,* 68, 1273-8.

COX, D., KERRIGAN, S. W. & WATSON, S. P. 2011. Platelets and the innate immune system: mechanisms of bacterial-induced platelet activation. *J Thromb Haemost,* 9, 1097-107.

CROVETTI, G., MARTINELLI, G., ISSI, M., BARONE, M., GUIZZARDI, M., CAMPANATI, B., MORONI, M. & CARABELLI, A. 2004. Platelet gel for healing cutaneous chronic wounds. *Transfus Apher Sci,* 30, 145-51.

DAERON, M. 1997. Fc receptor biology. *Annu Rev Immunol,* 15, 203-34.

DARBY, I. A., LAVERDET, B., BONTE, F. & DESMOULIERE, A. 2014. Fibroblasts and myofibroblasts in wound healing. *Clin Cosmet Investig Dermatol,* 7, 301-11.

DAWOOD, B. B., WILDE, J. & WATSON, S. P. 2007. Reference curves for aggregation and ATP secretion to aid diagnose of platelet-based bleeding disorders: effect of inhibition of ADP and thromboxane A(2) pathways. *Platelets,* 18, 329-45.

DE STOPPELAAR, S. F., VAN 'T VEER, C., CLAUSHUIS, T. A., ALBERSEN, B. J., ROELOFS, J. J. & VAN DER POLL, T. 2014. Thrombocytopenia impairs host defense in gram-negative pneumonia-derived sepsis in mice. *Blood,* 124, 3781-90.

DEL REY, M. J., FARE, R., IZQUIERDO, E., USATEGUI, A., RODRIGUEZ-FERNANDEZ, J. L., SUAREZ-FUEYO, A., CANETE, J. D. & PABLOS, J. L. 2014. Clinicopathological correlations of podoplanin (gp38) expression in rheumatoid synovium and its potential contribution to fibroblast platelet crosstalk. *PLoS One,* 9, e99607.

DEPPERMANN, C., CHERPOKOVA, D., NURDEN, P., SCHULZ, J. N., THIELMANN, I., KRAFT, P., VOGTLE, T., KLEINSCHNITZ, C., DUTTING, S., KROHNE, G., EMING, S. A., NURDEN, A. T., ECKES, B., STOLL, G., STEGNER, D. & NIESWANDT, B. 2013. Gray platelet syndrome and defective thrombo-inflammation in Nbeal2-deficient mice. *J Clin Invest.*

DESMOULIERE, A., CHAPONNIER, C. & GABBIANI, G. 2005. Tissue repair, contraction, and the myofibroblast. *Wound Repair Regen,* 13, 7-12.

DHANJAL, T. S., PENDARIES, C., ROSS, E. A., LARSON, M. K., PROTTY, M. B., BUCKLEY, C. D. & WATSON, S. P. 2007. A novel role for PECAM-1 in megakaryocytokinesis and recovery of platelet counts in thrombocytopenic mice. *Blood,* 109, 4237-44.

DOENECKE, D. & ALBIG, W. 2001. Histones. *eLS.* John Wiley & Sons, Ltd.

DRICKAMER, K. 1999. C-type lectin-like domains. *Curr Opin Struct Biol,* 9, 585-90.

DUBOIS, C., PANICOT-DUBOIS, L., GAINOR, J. F., FURIE, B. C. & FURIE, B. 2007. Thrombin-initiated platelet activation in vivo is vWF independent during thrombus formation in a laser injury model. ***J Clin Invest,*** **117, 953-60.**

ECKERT, R. L. & RORKE, E. A. 1989. Molecular biology of keratinocyte differentiation. ***Environ Health Perspect,*** **80, 109-16.**

EKWALL, A. K., EISLER, T., ANDERBERG, C., JIN, C., KARLSSON, N., BRISSLERT, M. & BOKAREWA, M. I. 2011. The tumour-associated glycoprotein podoplanin is expressed in fibroblast-like synoviocytes of the hyperplastic synovial lining layer in rheumatoid arthritis. ***Arthritis Res Ther,*** **13, R40.**

ENGELMANN, B. & MASSBERG, S. 2013. Thrombosis as an intravascular effector of innate immunity. ***Nat Rev Immunol,*** **13, 34-45.**

EPPLEY, B. L., WOODELL, J. E. & HIGGINS, J. 2004. Platelet quantification and growth factor analysis from platelet-rich plasma: implications for wound healing. ***Plast Reconstr Surg,*** **114, 1502-8.**

FACEY, A., PINAR, I., ARTHUR, J. F., QIAO, J., JING, J., MADO, B., CARBERRY, J., ANDREWS, R. K. & GARDINER, E. E. 2016. A-Disintegrin-And-Metalloproteinase (ADAM) 10 Activity on Resting and Activated Platelets. ***Biochemistry,*** **55, 1187-94.**

FANG, C., WEI, X. & WEI, Y. 2016. Mitochondrial DNA in the regulation of innate immune responses. ***Protein Cell,*** **7, 11-6.**

FEI, M., ZHOU, L., XIE, J., RUAN, Y., XU, J., HE, S., SHEN, H., HU, Y., REN, S. & RUAN, C. 2012. The production of soluble C-type lectin-like receptor 2 is a regulated process. ***Glycoconj J,*** **29, 315-21.**

FEIL, R., LOHMANN, S. M., DE JONGE, H., WALTER, U. & HOFMANN, F. 2003. Cyclic GMP-dependent protein kinases and the cardiovascular system: insights from genetically modified mice. ***Circ Res,*** **93, 907-16.**

FINNEY, B. A., SCHWEIGHOFFER, E., NAVARRO-NUNEZ, L., BENEZECH, C., BARONE, F., HUGHES, C. E., LANGAN, S. A., LOWE, K. L., POLLITT, A. Y., MOURAO-SA, D., SHEARDOWN, S., NASH, G. B., SMITHERS, N., REIS E SOUSA, C., TYBULEWICZ, V. L. & WATSON, S. P. 2012. CLEC-2 and Syk in the megakaryocytic/platelet lineage are essential for development. ***Blood,*** **119, 1747-56.**

FRANCIS, S. H., BUSCH, J. L., CORBIN, J. D. & SIBLEY, D. 2010. cGMP-dependent protein kinases and cGMP phosphodiesterases in nitric oxide and cGMP action. ***Pharmacol Rev,*** **62, 525-63.**

FRITZ, E., LUDWIG, H., SCHEITHAUER, W. & SINZINGER, H. 1986. Shortened platelet half-life in multiple myeloma. ***Blood,*** **68, 514-520.**

FUCHS, T. A., BHANDARI, A. A. & WAGNER, D. D. 2011a. Histones induce rapid and profound thrombocytopenia in mice. ***Blood,*** **118, 3708-3714.**

FUCHS, T. A., BRILL, A., DUERSCHMIED, D., SCHATZBERG, D., MONESTIER, M., MYERS, D. D., JR., WROBLESKI, S. K., WAKEFIELD, T. W., HARTWIG, J. H. & WAGNER, D. D. 2010. Extracellular DNA traps promote thrombosis. ***Proc Natl Acad Sci U S A,*** **107, 15880-5.**

FULLER, G. L., WILLIAMS, J. A., TOMLINSON, M. G., EBLE, J. A., HANNA, S. L., POHLMANN, S., SUZUKI-INOUE, K., OZAKI, Y., WATSON, S. P. & PEARCE, A. C. 2007. The C-type lectin receptors CLEC-2 and Dectin-1, but not DC-SIGN, signal via a novel YXXL-dependent signaling cascade. ***J Biol Chem,*** **282, 12397-409.**

GARDINER, E. E., AL-TAMIMI, M., MU, F. T., KARUNAKARAN, D., THOM, J. Y., MOROI, M., ANDREWS, R. K., BERNDT, M. C. & BAKER, R. I. 2008a. Compromised ITAM-based platelet receptor function in a patient with immune thrombocytopenic purpura. ***Journal of Thrombosis and Haemostasis,*** **6, 1175-1182.**

GARDINER, E. E., ARTHUR, J. F., KAHN, M. L., BERNDT, M. C. & ANDREWS, R. K. 2004. Regulation of platelet membrane levels of glycoprotein VI by a platelet-derived metalloproteinase. ***Blood,*** **104, 3611-7.**

GARDINER, E. E., KARUNAKARAN, D., ARTHUR, J. F., MU, F. T., POWELL, M. S., BAKER, R. I., HOGARTH, P. M., KAHN, M. L., ANDREWS, R. K. & BERNDT, M. C. 2008b. Dual ITAM-mediated proteolytic pathways for irreversible inactivation of platelet receptors: de-ITAM-izing FcgammaRIIa. ***Blood,*** **111, 165-74.**

GARDINER, E. E., KARUNAKARAN, D., SHEN, Y., ARTHUR, J. F., ANDREWS, R. K. & BERNDT, M. C. 2007. Controlled shedding of platelet glycoprotein (GP)VI and GPIb-IX-V by ADAM family metalloproteinases. ***J Thromb Haemost,*** **5, 1530-7.**

GARRAUD, O. & COGNASSE, F. 2010. Platelet Toll-like receptor expression: the link between "danger" ligands and inflammation. ***Inflamm Allergy Drug Targets,*** **9, 322-33.**

GAY, L. J. & FELDING-HABERMANN, B. 2011. Contribution of platelets to tumour metastasis. ***Nat Rev Cancer,*** **11, 123-34.**

GEIJTENBEEK, T. B., KWON, D. S., TORENSMA, R., VAN VLIET, S. J., VAN DUIJNHOVEN, G. C., MIDDEL, J., CORNELISSEN, I. L., NOTTET, H. S., KEWALRAMANI, V. N., LITTMAN, D. R., FIGDOR, C. G. & VAN KOOYK, Y. 2000. DC-SIGN, a dendritic cell-specific HIV-1-binding protein that enhances trans-infection of T cells. ***Cell,*** **100, 587-97.**

GHOSH, A., LI, W., FEBBRAIO, M., ESPINOLA, R. G., MCCRAE, K. R., COCKRELL, E. & SILVERSTEIN, R. L. 2008. Platelet CD36 mediates interactions with endothelial cell-derived microparticles and contributes to thrombosis in mice. ***J Clin Invest,*** **118, 1934-43.**

GHOSH, A., MURUGESAN, G., CHEN, K., ZHANG, L., WANG, Q., FEBBRAIO, M., ANSELMO, R. M., MARCHANT, K., BARNARD, J. & SILVERSTEIN, R. L. 2011. Platelet CD36 surface expression levels affect functional responses to oxidized LDL and are associated with inheritance of specific genetic polymorphisms. ***Blood,*** **117, 6355-66.**

GHOSHAL, K. & BHATTACHARYYA, M. 2014. Overview of platelet physiology: its hemostatic and nonhemostatic role in disease pathogenesis. ***ScientificWorldJournal,*** **2014, 781857.**

GIACCO, F. & BROWNLEE, M. 2010. Oxidative Stress and Diabetic Complications. ***Circulation Research,*** **107, 1058-1070.**

GIANNOTTA, M., TAPETE, G., EMMI, G., SILVESTRI, E. & MILLA, M. 2015. Thrombosis in inflammatory bowel diseases: what's the link? ***Thromb J,*** **13, 14.**

GIBBINS, J. M., OKUMA, M., FARNDALE, R., BARNES, M. & WATSON, S. P. 1997. Glycoprotein VI is the collagen receptor in platelets which underlies tyrosine phosphorylation of the Fc receptor γ-chain. ***FEBS Letters,*** **413, 255-259.**

GIESELER, F., UNGEFROREN, H., SETTMACHER, U., HOLLENBERG, M. D. & KAUFMANN, R. 2013. Proteinase-activated receptors (PARs) – focus on receptor-receptor-interactions and their physiological and pathophysiological impact. ***Cell Communication and Signaling : CCS,*** **11, 86-86.**

GITZ, E., POLLITT, A. Y., GITZ-FRANCOIS, J. J., ALSHEHRI, O., MORI, J., MONTAGUE, S., NASH, G. B., DOUGLAS, M. R., GARDINER, E. E., ANDREWS, R. K., BUCKLEY, C. D., HARRISON, P. & WATSON, S. P. 2014. CLEC-2 expression is maintained on activated platelets and on platelet microparticles. ***Blood,*** **124, 2262-70.**

GLENN, J. R., WHITE, A. E., JOHNSON, A. J., FOX, S. C., MYERS, B. & HEPTINSTALL, S. 2008. Raised levels of CD39 in leucocytosis result in marked inhibition of ADP-induced platelet aggregation via rapid ADP hydrolysis. ***Platelets,*** **19, 59-69.**

GOLDIN, A., BECKMAN, J. A., SCHMIDT, A. M. & CREAGER, M. A. 2006. Advanced glycation end products: sparking the development of diabetic vascular injury. ***Circulation,*** **114, 597-605.**

GORDON, S. & TAYLOR, P. R. 2005. Monocyte and macrophage heterogeneity. ***Nat Rev Immunol,*** **5, 953-64.**

GREENHALGH, D. G., SAFFLE, J. R., HOLMES, J. H. T., GAMELLI, R. L., PALMIERI, T. L., HORTON, J. W., TOMPKINS, R. G., TRABER, D. L., MOZINGO, D. W., DEITCH, E. A., GOODWIN, C. W., HERNDON, D. N., GALLAGHER, J. J., SANFORD, A. P., JENG, J. C., AHRENHOLZ, D. H., NEELY, A. N., O'MARA, M. S., WOLF, S. E., PURDUE, G. F., GARNER, W. L., YOWLER, C. J. & LATENSER, B. A. 2007. American Burn Association consensus conference to define sepsis and infection in burns. ***J Burn Care Res,*** **28, 776-90.**

GREENWOOD, H., PATEL, J., MAHIDA, R., WANG, Q., PAREKH, D., DANCER, R. C., KHIROYA, H., SAPEY, E. & THICKETT, D. R. 2014. Simvastatin to modify neutrophil function in older patients with septic pneumonia (SNOOPI): study protocol for a randomised placebo-controlled trial. ***Trials,*** **15, 1-6.**

GROS, A., OLLIVIER, V. & HO-TIN-NOE, B. 2014. Platelets in inflammation: regulation of leukocyte activities and vascular repair. ***Front Immunol,*** **5, 678.**

GROS, A., SYVANNARATH, V., LAMRANI, L., OLLIVIER, V., LOYAU, S., GOERGE, T., NIESWANDT, B., JANDROT-PERRUS, M. & HO-TIN-NOE, B. 2015a. Single platelets seal neutrophil-induced vascular breaches via GPVI during immune-complex-mediated inflammation in mice. ***Blood,*** **126, 1017-26.**

GUAGNOZZI, D. & LUCENDO, A. J. 2014. Anemia in inflammatory bowel disease: a neglected issue with relevant effects. ***World J Gastroenterol,*** **20, 3542-51.**

GURBEL, P. A., KEREIAKES, D. J., DALESANDRO, M. R., BAHR, R. D., O'CONNOR, C. M. & SEREBRUANY, V. L. 2000. Role of soluble and platelet-bound P-selectin in discriminating cardiac from noncardiac chest pain at presentation in the emergency department. ***American Heart Journal,*** **139, 320-328.**

GURNEY, D., LIP, G. Y. & BLANN, A. D. 2002. A reliable plasma marker of platelet activation: does it exist? ***Am J Hematol,*** **70, 139-44.**

HAMPSON, P., DINSDALE, R. J., WEARN, C. M., BAMFORD, A. L., BISHOP, J. R., HAZELDINE, J., MOIEMEN, N. S., HARRISON, P. & LORD, J. M. 2016. Neutrophil Dysfunction, Immature Granulocytes, and Cell-free DNA are Early Biomarkers of Sepsis in Burn-injured Patients: A Prospective Observational Cohort Study. ***Ann Surg*****.**

HARRIS, H. E. & RAUCCI, A. 2006. Alarmin(g) news about danger: workshop on innate danger signals and HMGB1. ***EMBO Rep,*** **7, 774-8.**

HARTWIG, J. H. 1992. Mechanisms of actin rearrangements mediating platelet activation. ***J Cell Biol,*** **118, 1421-42.**

HATAKEYAMA, K., KANEKO, M. K., KATO, Y., ISHIKAWA, T., NISHIHIRA, K., TSUJIMOTO, Y., SHIBATA, Y., OZAKI, Y. & ASADA, Y. 2012. Podoplanin expression in advanced atherosclerotic lesions of human aortas. ***Thromb Res,*** **129, e70-6.**

HAUSER, C. J., SURSAL, T., RODRIGUEZ, E. K., APPLETON, P. T., ZHANG, Q. & ITAGAKI, K. 2010. Mitochondrial damage associated molecular patterns from femoral reamings activate neutrophils through formyl peptide receptors and P44/42 MAP kinase. ***J Orthop Trauma,*** **24, 534-8.**

HERMANSKY, F. & PUDLAK, P. 1959. Albinism Associated with Hemorrhagic Diathesis and Unusual Pigmented Reticular Cells in the Bone Marrow: Report of Two Cases with Histochemical Studies. ***Blood,*** **14, 162-169.**

HERZOG, B. H., FU, J., WILSON, S. J., HESS, P. R., SEN, A., MCDANIEL, J. M., PAN, Y., SHENG, M., YAGO, T., SILASI-MANSAT, R., MCGEE, S., MAY, F.,

NIESWANDT, B., MORRIS, A. J., LUPU, F., COUGHLIN, S. R., MCEVER, R. P., CHEN, H., KAHN, M. L. & XIA, L. 2013. Podoplanin maintains high endothelial venule integrity by interacting with platelet CLEC-2. ***Nature,*** **502, 105-9.**

HIRSIGER, S., SIMMEN, H. P., WERNER, C. M., WANNER, G. A. & RITTIRSCH, D. 2012. Danger signals activating the immune response after trauma. ***Mediators Inflamm,*** **2012, 315941.**

HITCHCOCK, J. R., COOK, C. N., BOBAT, S., ROSS, E. A., FLORES-LANGARICA, A., LOWE, K. L., KHAN, M., DOMINGUEZ-MEDINA, C. C., LAX, S., CARVALHO-GASPAR, M., HUBSCHER, S., RAINGER, G. E., COBBOLD, M., BUCKLEY, C. D., MITCHELL, T. J., MITCHELL, A., JONES, N. D., VAN ROOIJEN, N., KIRCHHOFER, D., HENDERSON, I. R., ADAMS, D. H., WATSON, S. P. & CUNNINGHAM, A. F. 2015. Inflammation drives thrombosis after Salmonella infection via CLEC-2 on platelets. ***J Clin Invest,*** **125, 4429-46.**

HOGAN, M., CERAMI, A. & BUCALA, R. 1992. Advanced glycosylation endproducts block the antiproliferative effect of nitric oxide. Role in the vascular and renal complications of diabetes mellitus. ***J Clin Invest,*** **90, 1110-5.**

HONMA, M., MINAMI-HORI, M., TAKAHASHI, H. & IIZUKA, H. 2012. Podoplanin expression in wound and hyperproliferative psoriatic epidermis: regulation by TGF-beta and STAT-3 activating cytokines, IFN-gamma, IL-6, and IL-22. ***J Dermatol Sci,*** **65, 134-40.**

HOU, T. Z., BYSTROM, J., SHERLOCK, J. P., QURESHI, O., PARNELL, S. M., ANDERSON, G., GILROY, D. W. & BUCKLEY, C. D. 2010. A distinct subset of podoplanin (gp38) expressing F4/80+ macrophages mediate phagocytosis and are induced following zymosan peritonitis. ***FEBS Lett,*** **584, 3955-61.**

HRANJEC, T., SWENSON, B. R., DOSSETT, L. A., METZGER, R., FLOHR, T. R., POPOVSKY, K. A., BONATTI, H. J., MAY, A. K. & SAWYER, R. G. 2010. Diagnosis-dependent relationships between cytokine levels and survival in patients admitted for surgical critical care. ***J Am Coll Surg,*** **210, 833-44, 845-6.**

HUGHES, C. E., POLLITT, A. Y., MORI, J., EBLE, J. A., TOMLINSON, M. G., HARTWIG, J. H., O'CALLAGHAN, C. A., FÜTTERER, K. & WATSON, S. P. 2010. CLEC-2 activates Syk through dimerization. ***Blood,*** **115, 2947-2955.**

HUO, Y., SCHOBER, A., FORLOW, S. B., SMITH, D. F., HYMAN, M. C., JUNG, S., LITTMAN, D. R., WEBER, C. & LEY, K. 2003. Circulating activated platelets exacerbate atherosclerosis in mice deficient in apolipoprotein E. ***Nat Med,*** **9, 61-7.**

HUTCHINS, A. P., TAKAHASHI, Y. & MIRANDA-SAAVEDRA, D. 2015. Genomic analysis of LPS-stimulated myeloid cells identifies a common pro-inflammatory response but divergent IL-10 anti-inflammatory responses. ***Sci Rep,*** **5, 9100.**

IBA, T., HASHIGUCHI, N., NAGAOKA, I., TABE, Y., KADOTA, K. & SATO, K. 2015. Heparins attenuated histone-mediated cytotoxicity in vitro and improved the survival in a rat model of histone-induced organ dysfunction. ***Intensive Care Medicine Experimental,*** **3, 36.**

INOUE, O., SUZUKI-INOUE, K., MCCARTY, O. J., MOROI, M., RUGGERI, Z. M., KUNICKI, T. J., OZAKI, Y. & WATSON, S. P. 2006. Laminin stimulates spreading of platelets through integrin alpha6beta1-dependent activation of GPVI. ***Blood,*** **107, 1405-12.**

JACKSON, S. P. & CALKIN, A. C. 2007. The clot thickens[mdash]oxidized lipids and thrombosis. ***Nat Med,*** **13, 1015-1016.**

JAIN, S., RUSSELL, S. & WARE, J. 2009. Platelet glycoprotein VI facilitates experimental lung metastasis in syngenic mouse models. ***J Thromb Haemost,*** **7, 1713-7.**

JANDROT-PERRUS, M., LAGRUE, A. H., OKUMA, M. & BON, C. 1997. Adhesion and activation of human platelets induced by convulxin involve glycoprotein VI and integrin alpha2beta1. ***J Biol Chem,*** **272, 27035-41.**

JAREMO, P. & SANDBERG-GERTZEN, H. 1996. Platelet density and size in inflammatory bowel disease. ***Thromb Haemost,*** **75, 560-1.**

JASTROW, K. M., 3RD, GONZALEZ, E. A., MCGUIRE, M. F., SULIBURK, J. W., KOZAR, R. A., IYENGAR, S., MOTSCHALL, D. A., MCKINLEY, B. A., MOORE, F. A. & MERCER, D. W. 2009. Early cytokine production risk stratifies trauma patients for multiple organ failure. ***J Am Coll Surg,*** **209, 320-31.**

JOHNSON, B., FLETCHER, S. J. & MORGAN, N. V. 2016. Inherited thrombocytopenia: novel insights into megakaryocyte maturation, proplatelet formation and platelet lifespan. ***Platelets,*** **27, 519-25.**

JUNG, S. M., MOROI, M., SOEJIMA, K., NAKAGAKI, T., MIURA, Y., BERNDT, M. C., GARDINER, E. E., HOWES, J. M., PUGH, N., BIHAN, D., WATSON, S. P. & FARNDALE, R. W. 2012. Constitutive dimerization of glycoprotein VI (GPVI) in resting platelets is essential for binding to collagen and activation in flowing blood. ***J Biol Chem,*** **287, 30000-13.**

KATO, Y., FUJITA, N., KUNITA, A., SATO, S., KANEKO, M., OSAWA, M. & TSURUO, T. 2003. Molecular identification of Aggrus/T1alpha as a platelet aggregation-inducing factor expressed in colorectal tumors. ***J Biol Chem,*** **278, 51599-605.**

KATO, Y., KANEKO, M., SATA, M., FUJITA, N., TSURUO, T. & OSAWA, M. 2005. Enhanced expression of Aggrus (T1alpha/podoplanin), a platelet-aggregation-inducing factor in lung squamous cell carcinoma. ***Tumour Biol,*** **26, 195-200.**

KATO, Y., KANEKO, M. K., KUNO, A., UCHIYAMA, N., AMANO, K., CHIBA, Y., HASEGAWA, Y., HIRABAYASHI, J., NARIMATSU, H., MISHIMA, K. & OSAWA, M. 2006. Inhibition of tumor cell-induced platelet aggregation using a novel anti-podoplanin antibody reacting with its platelet-aggregation-stimulating domain. ***Biochemical and Biophysical Research Communications,*** **349, 1301-1307.**

KAUSHANSKY, K. 2005. The molecular mechanisms that control thrombopoiesis. ***The Journal of Clinical Investigation,*** **115, 3339-3347.**

KERRIGAN, A. M., DENNEHY, K. M., MOURAO-SA, D., FARO-TRINDADE, I., WILLMENT, J. A., TAYLOR, P. R., EBLE, J. A., REIS E SOUSA, C. & BROWN, G. D. 2009. CLEC-2 is a phagocytic activation receptor expressed on murine peripheral blood neutrophils. ***J Immunol,*** **182, 4150-7.**

KERRIGAN, A. M., NAVARRO-NUNEZ, L., PYZ, E., FINNEY, B. A., WILLMENT, J. A., WATSON, S. P. & BROWN, G. D. 2012. Podoplanin-expressing inflammatory macrophages activate murine platelets via CLEC-2. ***J Thromb Haemost,*** **10, 484-6.**

KISUCKA, J., BUTTERFIELD, C. E., DUDA, D. G., EICHENBERGER, S. C., SAFFARIPOUR, S., WARE, J., RUGGERI, Z. M., JAIN, R. K., FOLKMAN, J. & WAGNER, D. D. 2006. Platelets and platelet adhesion support angiogenesis while preventing excessive hemorrhage. ***Proc Natl Acad Sci U S A,*** **103, 855-60.**

KLUNE, J. R., DHUPAR, R., CARDINAL, J., BILLIAR, T. R. & TSUNG, A. 2008. HMGB1: endogenous danger signaling. ***Mol Med,*** **14, 476-84.**

KNIGHT, C. G., MORTON, L. F., ONLEY, D. J., PEACHEY, A. R., ICHINOHE, T., OKUMA, M., FARNDALE, R. W. & BARNES, M. J. 1999. Collagen-platelet interaction: Gly-Pro-Hyp is uniquely specific for platelet Gp VI and mediates platelet activation by collagen. ***Cardiovasc Res,*** **41, 450-7.**

KONDO, M., WAGERS, A. J., MANZ, M. G., PROHASKA, S. S., SCHERER, D. C., BEILHACK, G. F., SHIZURU, J. A. & WEISSMAN, I. L. 2003. Biology of hematopoietic stem cells and progenitors: implications for clinical application. ***Annu Rev Immunol,*** **21, 759-806.**

KONO, H. & ROCK, K. L. 2008. How dying cells alert the immune system to danger. ***Nat Rev Immunol,*** **8, 279-89.**

KRAFT, R., HERNDON, D. N., FINNERTY, C. C., SHAHROKHI, S. & JESCHKE, M. G. 2014. Occurrence of multiorgan dysfunction in pediatric burn patients: incidence and clinical outcome. ***Ann Surg,*** **259, 381-7.**

KSANDER, G. A., SAWAMURA, S. J., OGAWA, Y., SUNDSMO, J. & MCPHERSON, J. M. 1990a. The effect of platelet releasate on wound healing in animal models. ***Journal of the American Academy of Dermatology,*** **22, 781-791.**

LACEY, D. C., ACHUTHAN, A., FLEETWOOD, A. J., DINH, H., ROINIOTIS, J., SCHOLZ, G. M., CHANG, M. W., BECKMAN, S. K., COOK, A. D. & HAMILTON, J. A. 2012. Defining GM-CSF- and macrophage-CSF-dependent macrophage responses by in vitro models. ***J Immunol,*** **188, 5752-65.**

LAPOLLA, A., PIARULLI, F., SARTORE, G., CERIELLO, A., RAGAZZI, E., REITANO, R., BACCARIN, L., LAVERDA, B. & FEDELE, D. 2007. Advanced glycation end products and antioxidant status in type 2 diabetic patients with and without peripheral artery disease. ***Diabetes Care,*** **30, 670-6.**

LASKE, C., LEYHE, T., STRANSKY, E., ESCHWEILER, G. W., BUELTMANN, A., LANGER, H., STELLOS, K. & GAWAZ, M. 2008. Association of platelet-derived soluble glycoprotein VI in plasma with Alzheimer's disease. ***Journal of Psychiatric Research,*** **42, 746-751.**

LEE, S. H., LEE, J. G., KIM, J. R. & BAEK, S. H. 2007. Toll-like receptor 9-mediated cytosolic phospholipase A2 activation regulates expression of inducible nitric oxide synthase. ***Biochem Biophys Res Commun,*** **364, 996-1001.**

LEVI, M., DE JONGE, E. & VAN DER POLL, T. 2003. Sepsis and disseminated intravascular coagulation. ***J Thromb Thrombolysis,*** **16, 43-7.**

LEVY, M. M., FINK, M. P., MARSHALL, J. C., ABRAHAM, E., ANGUS, D., COOK, D., COHEN, J., OPAL, S. M., VINCENT, J. L. & RAMSAY, G. 2003. 2001 SCCM/ESICM/ACCP/ATS/SIS International Sepsis Definitions Conference. ***Intensive Care Med,*** **29, 530-8.**

LI, J., CHEN, J. & KIRSNER, R. 2007. Pathophysiology of acute wound healing. ***Clin Dermatol,*** **25, 9-18.**

LI, Z., DELANEY, M. K., O'BRIEN, K. A. & DU, X. 2010. Signaling during platelet adhesion and activation. ***Arterioscler Thromb Vasc Biol,*** **30, 2341-9.**

LINDEMANN, S., KRÄMER, B., SEIZER, P. & GAWAZ, M. 2007. Platelets, inflammation and atherosclerosis. ***Journal of Thrombosis and Haemostasis,*** **5, 203-211.**

LINK, A., VOGT, T. K., FAVRE, S., BRITSCHGI, M. R., ACHA-ORBEA, H., HINZ, B., CYSTER, J. G. & LUTHER, S. A. 2007. Fibroblastic reticular cells in lymph nodes regulate the homeostasis of naive T cells. ***Nat Immunol,*** **8, 1255-1265.**

LIU, W. H., YANG, C. H., YEH, K. H., CHANG, H. W., CHEN, Y. H., CHEN, S. M., CHENG, C. I., CHEN, C. J., YU, T. H., HUNG, W. C., HANG, C. L., WU, C. J. & YIP, H. K. 2005. Circulating levels of soluble P-selectin in patients in the early and recent phases of myocardial infarction. ***Chang Gung Med J,*** **28, 613-20.**

LO, Y. M. 2000. Fetal DNA in maternal plasma: biology and diagnostic applications. ***Clin Chem,*** **46, 1903-6.**

LORENZ, V., STEGNER, D., STRITT, S., VÖGTLE, T., KIEFER, F., WITKE, W., SCHYMEINSKY, J., WATSON, S. P., WALZOG, B. & NIESWANDT, B. 2015. Targeted downregulation of platelet CLEC-2 occurs through Syk-independent internalization. ***Blood,*** **125, 4069-4077.**

LOWE, K. L., FINNEY, B. A., DEPPERMANN, C., HAGERLING, R., GAZIT, S. L., FRAMPTON, J., BUCKLEY, C., CAMERER, E., NIESWANDT, B., KIEFER, F. & WATSON, S. P. 2015a. Podoplanin and CLEC-2 drive cerebrovascular patterning and integrity during development. ***Blood,*** **125, 3769-77.**

LOWE, K. L., NAVARRO-NUNEZ, L., BENEZECH, C., NAYAR, S., KINGSTON, B. L., NIESWANDT, B., BARONE, F., WATSON, S. P., BUCKLEY, C. D. & DESANTI, G. E. 2015b. The expression of mouse CLEC-2 on leucocyte subsets varies according to their anatomical location and inflammatory state. *Eur J Immunol,* 45, 2484-93.

LOWE, K. L., NAVARRO-NÚÑEZ, L., BÉNÉZECH, C., NAYAR, S., KINGSTON, B. L., NIESWANDT, B., BARONE, F., WATSON, S. P., BUCKLEY, C. D. & DESANTI, G. E. 2015c. The expression of mouse CLEC-2 on leucocyte subsets varies according to their anatomical location and inflammatory state. *European Journal of Immunology,* 45, 2484-2493.

LOYAU, S., DUMONT, B., OLLIVIER, V., BOULAFTALI, Y., FELDMAN, L., AJZENBERG, N. & JANDROT-PERRUS, M. 2012. Platelet glycoprotein VI dimerization, an active process inducing receptor competence, is an indicator of platelet reactivity. *Arterioscler Thromb Vasc Biol,* 32, 778-85.

LUCAS, T., WAISMAN, A., RANJAN, R., ROES, J., KRIEG, T., MULLER, W., ROERS, A. & EMING, S. A. 2010. Differential roles of macrophages in diverse phases of skin repair. *J Immunol,* 184, 3964-77.

MAMMADOVA-BACH, E., OLLIVIER, V., LOYAU, S., SCHAFF, M., DUMONT, B., FAVIER, R., FREYBURGER, G., LATGER-CANNARD, V., NIESWANDT, B., GACHET, C., MANGIN, P. H. & JANDROT-PERRUS, M. 2015. Platelet glycoprotein VI binds to polymerized fibrin and promotes thrombin generation. *Blood,* 126, 683-91.

MANN, E. A., BAUN, M. M., MEININGER, J. C. & WADE, C. E. 2012. Comparison of mortality associated with sepsis in the burn, trauma, and general intensive care unit patient: a systematic review of the literature. *Shock,* 37, 4-16.

MANNE, B. K., GETZ, T. M., HUGHES, C. E., ALSHEHRI, O., DANGELMAIER, C., NAIK, U. P., WATSON, S. P. & KUNAPULI, S. P. 2013. Fucoidan Is a Novel Platelet Agonist for the C-type Lectin-like Receptor 2 (CLEC-2). *The Journal of Biological Chemistry,* 288, 7717-7726.

MANSON, J., THIEMERMANN, C. & BROHI, K. 2012. Trauma alarmins as activators of damage-induced inflammation. *Br J Surg,* 99 Suppl 1, 12-20.

MARCK, R. E., MONTAGNE, H. L., TUINEBREIJER, W. E. & BREEDERVELD, R. S. 2013. Time course of thrombocytes in burn patients and its predictive value for outcome. *Burns,* 39, 714-22.

MARGOLIS, D. J., KANTOR, J., SANTANNA, J., STROM, B. L. & BERLIN, J. A. 2001. Effectiveness of platelet releasate for the treatment of diabetic neuropathic foot ulcers. *Diabetes Care,* 24, 483-8.

MARGRAF, S., LOGTERS, T., REIPEN, J., ALTRICHTER, J., SCHOLZ, M. & WINDOLF, J. 2008. Neutrophil-derived circulating free DNA (cf-DNA/NETs): a potential prognostic marker for posttraumatic development of inflammatory second hit and sepsis. *Shock,* 30, 352-8.

MARTIN-VILLAR, E., MEGIAS, D., CASTEL, S., YURRITA, M. M., VILARO, S. & QUINTANILLA, M. 2006. Podoplanin binds ERM proteins to activate RhoA and promote epithelial-mesenchymal transition. *J Cell Sci,* 119, 4541-53.

MASURIER, C., PIOCHE-DURIEU, C., COLOMBO, B. M., LACAVE, R., LEMOINE, F. M., KLATZMANN, D. & GUIGON, M. 1999. Immunophenotypical and functional heterogeneity of dendritic cells generated from murine bone marrow cultured with different cytokine combinations: implications for anti-tumoral cell therapy. *Immunology,* 96, 569-77.

MATSUURA, E., HUGHES, G. R. & KHAMASHTA, M. A. 2008. Oxidation of LDL and its clinical implication. *Autoimmun Rev,* 7, 558-66.

MATTHEWS, A. L., NOY, P. J., REYAT, J. S. & TOMLINSON, M. G. 2016. Regulation of A disintegrin and metalloproteinase (ADAM) family sheddases ADAM10 and ADAM17: The emerging role of tetraspanins and rhomboids. ***Platelets*****, 1-9.**

MATUS, V., VALENZUELA, G., SÁEZ, C. G., HIDALGO, P., LAGOS, M., ARANDA, E., PANES, O., PEREIRA, J., PILLOIS, X., NURDEN, A. T. & MEZZANO, D. 2013. An adenine insertion in exon 6 of human GP6 generates a truncated protein associated with a bleeding disorder in four Chilean families. ***Journal of Thrombosis and Haemostasis*****, 11, 1751-1759.**

MATZINGER, P. 1994. Tolerance, danger, and the extended family. ***Annu Rev Immunol*****, 12, 991-1045.**

MAY, F., HAGEDORN, I., PLEINES, I., BENDER, M., VOGTLE, T., EBLE, J., ELVERS, M. & NIESWANDT, B. 2009. CLEC-2 is an essential platelet-activating receptor in hemostasis and thrombosis. ***Blood*****, 114, 3464-72.**

MAZHARIAN, A., WANG, Y. J., MORI, J., BEM, D., FINNEY, B., HEISING, S., GISSEN, P., WHITE, J. G., BERNDT, M. C., GARDINER, E. E., NIESWANDT, B., DOUGLAS, M. R., CAMPBELL, R. D., WATSON, S. P. & SENIS, Y. A. 2012. Mice lacking the ITIM-containing receptor G6b-B exhibit macrothrombocytopenia and aberrant platelet function. ***Sci Signal*****, 5, ra78.**

MCCARTHY, C. G., WENCESLAU, C. F., GOULOPOULOU, S., OGBI, S., BABAN, B., SULLIVAN, J. C., MATSUMOTO, T. & WEBB, R. C. 2015. Circulating mitochondrial DNA and Toll-like receptor 9 are associated with vascular dysfunction in spontaneously hypertensive rats. ***Cardiovasc Res*****, 107, 119-30.**

MENG, F. & LOWELL, C. A. 1997. Lipopolysaccharide (LPS)-induced Macrophage Activation and Signal Transduction in the Absence of Src-Family Kinases Hck, Fgr, and Lyn. ***The Journal of Experimental Medicine*****, 185, 1661-1670.**

MIURA, Y., TAKAHASHI, T., JUNG, S. M. & MOROI, M. 2002. Analysis of the Interaction of Platelet Collagen Receptor Glycoprotein VI (GPVI) with Collagen: A DIMERIC FORM OF GPVI, BUT NOT THE MONOMERIC FORM, SHOWS AFFINITY TO FIBROUS COLLAGEN. ***Journal of Biological Chemistry*****, 277, 46197-46204.**

MIYAMOTO, Y., UGA, H., TANAKA, S., KADOWAKI, M., IKEDA, M., SAEGUSA, J., MORINOBU, A., KUMAGAI, S. & KURATA, H. 2013. Podoplanin is an inflammatory protein upregulated in Th17 cells in SKG arthritic joints. ***Mol Immunol*****, 54, 199-207.**

MOCK, C., PECK, M., PEDEN, M., KRUG, E., AHUJA, R., ALBERTYN, H., BODHA, W., CASSAN, P., GODAKUMBURA, W., LO, G., PARTRIDGE, J. & POTOKAR, T. 2008. A WHO plan for burn prevention and care. Geneva, Switzerland: The World Health Organization

MÓCSAI, A., RULAND, J. & TYBULEWICZ, V. L. J. 2010. The SYK tyrosine kinase: a crucial player in diverse biological functions. ***Nature reviews. Immunology*****, 10, 387-402.**

MORI, J., PEARCE, A. C., SPALTON, J. C., GRYGIELSKA, B., EBLE, J. A., TOMLINSON, M. G., SENIS, Y. A. & WATSON, S. P. 2008. G6b-B inhibits constitutive and agonist-induced signaling by glycoprotein VI and CLEC-2. ***J Biol Chem*****, 283, 35419-27.**

MORRELL, C. N., AGGREY, A. A., CHAPMAN, L. M. & MODJESKI, K. L. 2014. Emerging roles for platelets as immune and inflammatory cells. ***Blood*****, 123, 2759-2767.**

MOULIN, V., LAWNY, F., BARRITAULT, D. & CARUELLE, J. P. 1998. Platelet releasate treatment improves skin healing in diabetic rats through endogenous growth factor secretion. ***Cell Mol Biol (Noisy-le-grand)*****, 44, 961-71.**

MOURAO-SA, D., ROBINSON, M. J., ZELENAY, S., SANCHO, D., CHAKRAVARTY, P., LARSEN, R., PLANTINGA, M., VAN ROOIJEN, N., SOARES, M. P.,

LAMBRECHT, B. & REIS E SOUSA, C. 2011. CLEC-2 signaling via Syk in myeloid cells can regulate inflammatory responses. ***Eur J Immunol,*** **41, 3040-53.**

MURUGAPPA, S. & KUNAPULI, S. P. 2006. The role of ADP receptors in platelet function. ***Front Biosci,*** **11, 1977-86.**

NAGAE, M., MORITA-MATSUMOTO, K., KATO, M., KANEKO, M. K., KATO, Y. & YAMAGUCHI, Y. 2014. A platform of C-type lectin-like receptor CLEC-2 for binding O-glycosylated podoplanin and nonglycosylated rhodocytin. ***Structure,*** **22, 1711-21.**

NAITOH, K., HOSAKA, Y., HONDA, M., OGAWA, K., SHIRAKAWA, K. & FURUSAKO, S. 2015. Properties of soluble glycoprotein VI, a potential platelet activation biomarker. ***Platelets,*** **26, 745-50.**

NAMI, N., FECI, L., NAPOLIELLO, L., GIORDANO, A., LORENZINI, S., GALEAZZI, M., RUBEGNI, P. & FIMIANI, M. 2016. Crosstalk between platelets and PBMC: New evidence in wound healing. ***Platelets,*** **27, 143-148.**

NASEEM, K. M. & RIBA, R. 2008. Unresolved roles of platelet nitric oxide synthase. ***Journal of Thrombosis and Haemostasis,*** **6, 10-19.**

NCEPOD 2007. Trauma: who cares? . London: National Confidential Enquiry into Patient Outcome and Death.

NIESWANDT, B., AKTAS, B., MOERS, A. & SACHS, U. J. H. 2005. Platelets in atherothrombosis: lessons from mouse models. ***Journal of Thrombosis and Haemostasis,*** **3, 1725-1736.**

NIESWANDT, B., BRAKEBUSCH, C., BERGMEIER, W., SCHULTE, V., BOUVARD, D., MOKHTARI-NEJAD, R., LINDHOUT, T., HEEMSKERK, J. W. M., ZIRNGIBL, H. & FÄSSLER, R. 2001. Glycoprotein VI but not α2β1 integrin is essential for platelet interaction with collagen. ***The EMBO Journal,*** **20, 2120-2130.**

NIESWANDT, B. & WATSON, S. P. 2003. Platelet-collagen interaction: is GPVI the central receptor? ***Blood,*** **102, 449-61.**

NURDEN, A. T., NURDEN, P., SANCHEZ, M., ANDIA, I. & ANITUA, E. 2008. Platelets and wound healing. ***Front Biosci,*** **13, 3532-48.**

OFFERMANNS, S. 2006. Activation of platelet function through G protein-coupled receptors. ***Circ Res,*** **99, 1293-304.**

OHLMANN, P., FAURE, A., MOREL, O., PETIT, H., KABBAJ, H., MEYER, N., CHENEAU, E., JESEL, L., EPAILLY, E., DESPREZ, D., GRUNEBAUM, L., SCHNEIDER, F., ROUL, G., MAZZUCOTTELI, J. P., EISENMANN, B. & BAREISS, P. 2006. Diagnostic and prognostic value of circulating D-Dimers in patients with acute aortic dissection. ***Crit Care Med,*** **34, 1358-64.**

OHRADANOVA-REPIC, A., MACHACEK, C., FISCHER, M. B. & STOCKINGER, H. 2016. Differentiation of human monocytes and derived subsets of macrophages and dendritic cells by the HLDA10 monoclonal antibody panel. ***Clin Trans Immunol,*** **5, e55.**

ONO, Y., AOKI, S., OHNISHI, K., YASUDA, T., KAWANO, K. & TSUKADA, Y. 1998. Increased serum levels of advanced glycation end-products and diabetic complications. ***Diabetes Res Clin Pract,*** **41, 131-7.**

PACHER, P., BECKMAN, J. S. & LIAUDET, L. 2007. Nitric oxide and peroxynitrite in health and disease. ***Physiol Rev,*** **87, 315-424.**

PAN, Y., YAGO, T., FU, J., HERZOG, B., MCDANIEL, J. M., MEHTA-D'SOUZA, P., CAI, X., RUAN, C., MCEVER, R. P., WEST, C., DAI, K., CHEN, H. & XIA, L. 2014. Podoplanin requires sialylated O-glycans for stable expression on lymphatic endothelial cells and for interaction with platelets. ***Blood,*** **124, 3656-3665.**

PARK, J. S., SVETKAUSKAITE, D., HE, Q., KIM, J. Y., STRASSHEIM, D., ISHIZAKA, A. & ABRAHAM, E. 2004. Involvement of toll-like receptors 2 and 4 in cellular activation by high mobility group box 1 protein. ***J Biol Chem,*** **279, 7370-7.**

PASPARAKIS, M., HAASE, I. & NESTLE, F. O. 2014. Mechanisms regulating skin immunity and inflammation. *Nat Rev Immunol,* 14, 289-301.

PATEL, S. R., HARTWIG, J. H. & ITALIANO, J. E., JR. 2005. The biogenesis of platelets from megakaryocyte proplatelets. *J Clin Invest,* 115, 3348-54.

PEDERSEN, J., COSKUN, M., SOENDERGAARD, C., SALEM, M. & NIELSEN, O. H. 2014. Inflammatory pathways of importance for management of inflammatory bowel disease. *World J Gastroenterol,* 20, 64-77.

PELTZ, E. D., MOORE, E. E., ECKELS, P. C., DAMLE, S. S., TSURUTA, Y., JOHNSON, J. L., SAUAIA, A., SILLIMAN, C. C., BANERJEE, A. & ABRAHAM, E. 2009. HMGB1 is markedly elevated within 6 hours of mechanical trauma in humans. *Shock,* 32, 17-22.

PERKINS, G. D., MCAULEY, D. F., THICKETT, D. R. & GAO, F. 2006. The beta-agonist lung injury trial (BALTI): a randomized placebo-controlled clinical trial. *Am J Respir Crit Care Med,* 173, 281-7.

PETERS, A., BURKETT, P. R., SOBEL, R. A., BUCKLEY, C. D., WATSON, S. P., BETTELLI, E. & KUCHROO, V. K. 2015. Podoplanin negatively regulates CD4+ effector T cell responses. *J Clin Invest,* 125, 129-40.

PODREZ, E. A., BYZOVA, T. V., FEBBRAIO, M., SALOMON, R. G., MA, Y., VALIYAVEETTIL, M., POLIAKOV, E., SUN, M., FINTON, P. J., CURTIS, B. R., CHEN, J., ZHANG, R., SILVERSTEIN, R. L. & HAZEN, S. L. 2007. Platelet CD36 links hyperlipidemia, oxidant stress and a prothrombotic phenotype. *Nat Med,* 13, 1086-95.

POLGAR, J., MAGNENAT, E. M., PEITSCH, M. C., WELLS, T. N., SAQI, M. S. & CLEMETSON, K. J. 1997. Amino acid sequence of the alpha subunit and computer modelling of the alpha and beta subunits of echicetin from the venom of Echis carinatus (saw-scaled viper). *Biochem J,* 323 (Pt 2), 533-7.

POLLITT, A. Y., POULTER, N. S., GITZ, E., NAVARRO-NUÑEZ, L., WANG, Y.-J., HUGHES, C. E., THOMAS, S. G., NIESWANDT, B., DOUGLAS, M. R., OWEN, D. M., JACKSON, D. G., DUSTIN, M. L. & WATSON, S. P. 2014. Syk and Src Family Kinases Regulate C-type Lectin Receptor 2 (CLEC-2)-mediated Clustering of Podoplanin and Platelet Adhesion to Lymphatic Endothelial Cells. *The Journal of Biological Chemistry,* 289, 35695-35710.

PONDER, A. & LONG, M. D. 2013. A clinical review of recent findings in the epidemiology of inflammatory bowel disease. *Clin Epidemiol,* 5, 237-47.

POOLE, A., GIBBINS, J. M., TURNER, M., VAN VUGT, M. J., VAN DE WINKEL, J. G., SAITO, T., TYBULEWICZ, V. L. & WATSON, S. P. 1997. The Fc receptor gamma-chain and the tyrosine kinase Syk are essential for activation of mouse platelets by collagen. *Embo j,* 16, 2333-41.

PROUDFOOT, A. G. & SUMMERS, C. 2014. Killing without collateral damage: new hope for sepsis therapy. *Immunol Cell Biol,* 92, 739-40.

QIAO, J. L., SHEN, Y., GARDINER, E. E. & ANDREWS, R. K. 2010. Proteolysis of platelet receptors in humans and other species. *Biol Chem,* 391, 893-900.

RABIE, T., VARGA-SZABO, D., BENDER, M., POZGAJ, R., LANZA, F., SAITO, T., WATSON, S. P. & NIESWANDT, B. 2007. Diverging signaling events control the pathway of GPVI down-regulation in vivo. *Blood,* 110, 529-35.

RACCUGLIA, G. 1971. Gray platelet syndrome. A variety of qualitative platelet disorder. *Am J Med,* 51, 818-28.

RAMIREZ, M. I., MILLIEN, G., HINDS, A., CAO, Y., SELDIN, D. C. & WILLIAMS, M. C. 2003. T1α, a lung type I cell differentiation gene, is required for normal lung cell proliferation and alveolus formation at birth. *Developmental biology,* 256, 62-73.

RASLAN, Z. & NASEEM, K. M. 2015. Compartmentalisation of cAMP-dependent signalling in blood platelets: The role of lipid rafts and actin polymerisation. ***Platelets,*** **26, 349-57.**

RAYES, J., MONTAGUE, S., WATSON, S. & WATSON, S. P. 2015. Mouse macrophages upreuglate podoplanin under inflammmatory and apoptotic conditions. International Society on Thrombosis and Haemostatis 2015 Congress Toronoto.

RENNE, T., POZGAJOVA, M., GRUNER, S., SCHUH, K., PAUER, H. U., BURFEIND, P., GAILANI, D. & NIESWANDT, B. 2005. Defective thrombus formation in mice lacking coagulation factor XII. ***J Exp Med,*** **202, 271-81.**

RIDKER, P. M., BURING, J. E. & RIFAI, N. 2001. Soluble P-selectin and the risk of future cardiovascular events. ***Circulation,*** **103, 491-5.**

ROCK, K. L., HEARN, A., CHEN, C. J. & SHI, Y. 2005. Natural endogenous adjuvants. ***Springer Semin Immunopathol,*** **26, 231-46.**

SABOOR, M., AYUB, Q., ILYAS, S. & MOINUDDIN 2013. Platelet receptors: An instrumental of platelet physiology. ***Pakistan Journal of Medical Sciences,*** **29.**

SCHACHT, V., RAMIREZ, M. I., HONG, Y.-K., HIRAKAWA, S., FENG, D., HARVEY, N., WILLIAMS, M., DVORAK, A. M., DVORAK, H. F., OLIVER, G. & DETMAR, M. 2003. T1α/podoplanin deficiency disrupts normal lymphatic vasculature formation and causes lymphedema. ***The EMBO Journal,*** **22, 3546-3556.**

SCHIRALDI, M., RAUCCI, A., MUNOZ, L. M., LIVOTI, E., CELONA, B., VENEREAU, E., APUZZO, T., DE MARCHIS, F., PEDOTTI, M., BACHI, A., THELEN, M., VARANI, L., MELLADO, M., PROUDFOOT, A., BIANCHI, M. E. & UGUCCIONI, M. 2012. HMGB1 promotes recruitment of inflammatory cells to damaged tissues by forming a complex with CXCL12 and signaling via CXCR4. ***J Exp Med,*** **209, 551-63.**

SCHLOSSMANN, J., AMMENDOLA, A., ASHMAN, K., ZONG, X., HUBER, A., NEUBAUER, G., WANG, G. X., ALLESCHER, H. D., KORTH, M., WILM, M., HOFMANN, F. & RUTH, P. 2000. Regulation of intracellular calcium by a signalling complex of IRAG, IP3 receptor and cGMP kinase Ibeta. ***Nature,*** **404, 197-201.**

SCHNEIDER, E. M., VORLAENDER, K., MA, X., DU, W. & WEISS, M. 2006. Role of ATP in trauma-associated cytokine release and apoptosis by P2X7 ion channel stimulation. ***Ann N Y Acad Sci,*** **1090, 245-52.**

SEIZER, P., BORST, O., LANGER, H. F., BULTMANN, A., MUNCH, G., HEROUY, Y., STELLOS, K., KRAMER, B., BIGALKE, B., BUCHELE, B., BACHEM, M. G., VESTWEBER, D., SIMMET, T., GAWAZ, M. & MAY, A. E. 2009. EMMPRIN (CD147) is a novel receptor for platelet GPVI and mediates platelet rolling via GPVI-EMMPRIN interaction. ***Thromb Haemost,*** **101, 682-6.**

SEMERARO, F., AMMOLLO, C. T., MORRISSEY, J. H., DALE, G. L., FRIESE, P., ESMON, N. L. & ESMON, C. T. 2011. Extracellular histones promote thrombin generation through platelet-dependent mechanisms: involvement of platelet TLR2 and TLR4. ***Blood,*** **118, 1952-61.**

SEMERARO, N., AMMOLLO, C. T., SEMERARO, F. & COLUCCI, M. 2010a. Sepsis-Associated Disseminated Intravascular Coagulation and Thromboembolic Disease. ***Mediterranean Journal of Hematology and Infectious Diseases,*** **2, e2010024.**

SENIS, Y. A. 2013. Protein-tyrosine phosphatases: a new frontier in platelet signal transduction. ***J Thromb Haemost,*** **11, 1800-13.**

SENIS, Y. A., MAZHARIAN, A. & MORI, J. 2014. Src family kinases: at the forefront of platelet activation. ***Blood,*** **124, 2013-2024.**

SEVERIN, S., NASH, C. A., MORI, J., ZHAO, Y., ABRAM, C., LOWELL, C. A., SENIS, Y. A. & WATSON, S. P. 2012. Distinct and overlapping functional roles of Src family kinases in mouse platelets. ***J Thromb Haemost,*** **10, 1631-45.**

SEVERIN, S., POLLITT, A. Y., NAVARRO-NUNEZ, L., NASH, C. A., MOURAO-SA, D., EBLE, J. A., SENIS, Y. A. & WATSON, S. P. 2011. Syk-dependent phosphorylation of CLEC-2: a novel mechanism of hem-immunoreceptor tyrosine-based activation motif signaling. ***J Biol Chem,*** **286, 4107-16.**

SHAPIRO, V. S., TRUITT, K. E., IMBODEN, J. B. & WEISS, A. 1997. CD28 mediates transcriptional upregulation of the interleukin-2 (IL-2) promoter through a composite element containing the CD28RE and NF-IL-2B AP-1 sites. ***Mol Cell Biol,*** **17, 4051-8.**

SHARMA, B., SHARMA, M., MAJUMDER, M., STEIER, W., SANGAL, A. & KALAWAR, M. 2007. Thrombocytopenia in septic shock patients--a prospective observational study of incidence, risk factors and correlation with clinical outcome. ***Anaesth Intensive Care,*** **35, 874-80.**

SHI, Y., GALUSHA, S. A. & ROCK, K. L. 2006. Cutting edge: elimination of an endogenous adjuvant reduces the activation of CD8 T lymphocytes to transplanted cells and in an autoimmune diabetes model. ***J Immunol,*** **176, 3905-8.**

SHIBAHARA, J., KASHIMA, T., KIKUCHI, Y., KUNITA, A. & FUKAYAMA, M. 2006a. Podoplanin is expressed in subsets of tumors of the central nervous system. ***Virchows Arch,*** **448, 493-9.**

SHIBAHARA, J., KASHIMA, T., KIKUCHI, Y., KUNITA, A. & FUKAYAMA, M. 2006b. Podoplanin is expressed in subsets of tumors of the central nervous system. ***Virchows Archiv,*** **448, 493-499.**

SHIMOMURA, H., OGAWA, H., ARAI, H., MORIYAMA, Y., TAKAZOE, K., HIRAI, N., KAIKITA, K., HIRASHIMA, O., MISUMI, K. & SOEJIMA, H. 1998. Serial changes in plasma levels of soluble P-selectin in patients with acute myocardial infarction. ***The American journal of cardiology,*** **81, 397-400.**

SHOOK, B., XIAO, E., KUMAMOTO, Y., IWASAKI, A. & HORSLEY, V. 2016. CD301b+ Macrophages Are Essential for Effective Skin Wound Healing. ***J Invest Dermatol,*** **136, 1885-91.**

SIMS, G. P., ROWE, D. C., RIETDIJK, S. T., HERBST, R. & COYLE, A. J. 2010. HMGB1 and RAGE in inflammation and cancer. ***Annu Rev Immunol,*** **28, 367-88.**

SINGER, A. J. & CLARK, R. A. 1999. Cutaneous wound healing. ***N Engl J Med,*** **341, 738-46.**

SMETHURST, P. A., ONLEY, D. J., JARVIS, G. E., O'CONNOR, M. N., KNIGHT, C. G., HERR, A. B., OUWEHAND, W. H. & FARNDALE, R. W. 2007. Structural basis for the platelet-collagen interaction: the smallest motif within collagen that recognizes and activates platelet Glycoprotein VI contains two glycine-proline-hydroxyproline triplets. ***J Biol Chem,*** **282, 1296-304.**

SNELL, D. C., SCHULTE, V., JARVIS, G. E., ARASE, K., SAKURAI, D., SAITO, T., WATSON, S. P. & NIESWANDT, B. 2002. Differential effects of reduced glycoprotein VI levels on activation of murine platelets by glycoprotein VI ligands. ***Biochem J,*** **368, 293-300.**

SONG, Y., SHEN, J., LIN, Y., SHEN, J., WU, X., YAN, Y., ZHOU, L., ZHANG, H., ZHOU, Y., CAO, M. & LIU, Y. 2014. Up-regulation of podoplanin involves in neuronal apoptosis in LPS-induced neuroinflammation. ***Cell Mol Neurobiol,*** **34, 839-49.**

SORRELL, J. M. & CAPLAN, A. I. 2004. Fibroblast heterogeneity: more than skin deep. ***J Cell Sci,*** **117, 667-75.**

SPALTON, J. C., MORI, J., POLLITT, A. Y., HUGHES, C. E., EBLE, J. A. & WATSON, S. P. 2009. The novel Syk inhibitor R406 reveals mechanistic differences in the initiation of GPVI and CLEC-2 signaling in platelets. ***J Thromb Haemost,*** **7, 1192-9.**

SRIKRISHNA, G. & FREEZE, H. H. 2009. Endogenous Damage-Associated Molecular Pattern Molecules at the Crossroads of Inflammation and Cancer. ***Neoplasia (New York, N.Y.),*** **11, 615-628.**

STEPHENS, G., YAN, Y., JANDROT-PERRUS, M., VILLEVAL, J. L., CLEMETSON, K. J. & PHILLIPS, D. R. 2005. Platelet activation induces metalloproteinase-dependent GP VI cleavage to down-regulate platelet reactivity to collagen. ***Blood,*** **105, 186-91.**

STEWART, C. R., STUART, L. M., WILKINSON, K., VAN GILS, J. M., DENG, J., HALLE, A., RAYNER, K. J., BOYER, L., ZHONG, R., FRAZIER, W. A., LACY-HULBERT, A., EL KHOURY, J., GOLENBOCK, D. T. & MOORE, K. J. 2010. CD36 ligands promote sterile inflammation through assembly of a Toll-like receptor 4 and 6 heterodimer. ***Nat Immunol,*** **11, 155-61.**

STEWART, C. R., TSENG, A. A., MOK, Y. F., STAPLES, M. K., SCHIESSER, C. H., LAWRENCE, L. J., VARGHESE, J. N., MOORE, K. J. & HOWLETT, G. J. 2005. Oxidation of low-density lipoproteins induces amyloid-like structures that are recognized by macrophages. ***Biochemistry,*** **44, 9108-16.**

SU, X. & ABUMRAD, N. A. 2009. Cellular Fatty Acid Uptake: A Pathway Under Construction. ***Trends in endocrinology and metabolism: TEM,*** **20, 72-77.**

SUN, S., SURSAL, T., ADIBNIA, Y., ZHAO, C., ZHENG, Y., LI, H., OTTERBEIN, L. E., HAUSER, C. J. & ITAGAKI, K. 2013. Mitochondrial DAMPs increase endothelial permeability through neutrophil dependent and independent pathways. ***PLoS One,*** **8, e59989.**

SUZUKI-INOUE, K., FULLER, G. L., GARCIA, A., EBLE, J. A., POHLMANN, S., INOUE, O., GARTNER, T. K., HUGHAN, S. C., PEARCE, A. C., LAING, G. D., THEAKSTON, R. D., SCHWEIGHOFFER, E., ZITZMANN, N., MORITA, T., TYBULEWICZ, V. L., OZAKI, Y. & WATSON, S. P. 2006. A novel Syk-dependent mechanism of platelet activation by the C-type lectin receptor CLEC-2. ***Blood,*** **107, 542-9.**

SUZUKI-INOUE, K., KATO, Y., INOUE, O., KANEKO, M. K., MISHIMA, K., YATOMI, Y., YAMAZAKI, Y., NARIMATSU, H. & OZAKI, Y. 2007. Involvement of the snake toxin receptor CLEC-2, in podoplanin-mediated platelet activation, by cancer cells. ***J Biol Chem,*** **282, 25993-6001.**

SUZUKI-INOUE, K., TULASNE, D., SHEN, Y., BORI-SANZ, T., INOUE, O., JUNG, S. M., MOROI, M., ANDREWS, R. K., BERNDT, M. C. & WATSON, S. P. 2002. Association of Fyn and Lyn with the proline-rich domain of glycoprotein VI regulates intracellular signaling. ***J Biol Chem,*** **277, 21561-6.**

TADIE, J. M., BAE, H. B., JIANG, S., PARK, D. W., BELL, C. P., YANG, H., PITTET, J. F., TRACEY, K., THANNICKAL, V. J., ABRAHAM, E. & ZMIJEWSKI, J. W. 2013. HMGB1 promotes neutrophil extracellular trap formation through interactions with Toll-like receptor 4. ***Am J Physiol Lung Cell Mol Physiol,*** **304, L342-9.**

TAKAGI, S., SATO, S., OH-HARA, T., TAKAMI, M., KOIKE, S., MISHIMA, Y., HATAKE, K. & FUJITA, N. 2013. Platelets promote tumor growth and metastasis via direct interaction between Aggrus/podoplanin and CLEC-2. ***PLoS One,*** **8, e73609.**

TAKAYAMA, H., HOSAKA, Y., NAKAYAMA, K., SHIRAKAWA, K., NAITOH, K., MATSUSUE, T., SHINOZAKI, M., HONDA, M., YATAGAI, Y., KAWAHARA, T., HIROSE, J., YOKOYAMA, T., KURIHARA, M. & FURUSAKO, S. 2008. A novel antiplatelet antibody therapy that induces cAMP-dependent endocytosis of the GPVI/Fc receptor γ-chain complex. ***The Journal of Clinical Investigation,*** **118, 1785-1795.**

TAN, Y. & KAGAN, J. C. 2014. A cross-disciplinary perspective on the innate immune responses to bacterial lipopolysaccharide. ***Mol Cell,*** **54, 212-23.**

TOMLINSON, M. G., CALAMINUS, S. D., BERLANGA, O., AUGER, J. M., BORI-SANZ, T., MEYAARD, L. & WATSON, S. P. 2007. Collagen promotes sustained glycoprotein VI signaling in platelets and cell lines. ***J Thromb Haemost,*** **5, 2274-83.**

TRACY, L. E., MINASIAN, R. A. & CATERSON, E. J. 2016. Extracellular Matrix and Dermal Fibroblast Function in the Healing Wound. ***Adv Wound Care (New Rochelle),*** **5, 119-136.**

TURNER, M., MEE, P. J., COSTELLO, P. S., WILLIAMS, O., PRICE, A. A., DUDDY, L. P., FURLONG, M. T., GEAHLEN, R. L. & TYBULEWICZ, V. L. 1995. Perinatal lethality and blocked B-cell development in mice lacking the tyrosine kinase Syk. ***Nature,*** **378, 298-302.**

VERRECK, F. A., DE BOER, T., LANGENBERG, D. M., HOEVE, M. A., KRAMER, M., VAISBERG, E., KASTELEIN, R., KOLK, A., DE WAAL-MALEFYT, R. & OTTENHOFF, T. H. 2004. Human IL-23-producing type 1 macrophages promote but IL-10-producing type 2 macrophages subvert immunity to (myco)bacteria. ***Proc Natl Acad Sci U S A,*** **101, 4560-5.**

VOUDOUKIS, E., KARMIRIS, K. & KOUTROUBAKIS, I. E. 2014. Multipotent role of platelets in inflammatory bowel diseases: a clinical approach. ***World J Gastroenterol,*** **20, 3180-90.**

WASHINGTON, A. V., QUIGLEY, L. & MCVICAR, D. W. 2002. Initial characterization of TREM-like transcript (TLT)-1: a putative inhibitory receptor within the TREM cluster. ***Blood,*** **100, 3822-4.**

WATSON, C. N., KERRIGAN, S. W., COX, D., HENDERSON, I. R., WATSON, S. P. & ARMAN, M. 2016. Human platelet activation by Escherichia coli: roles for FcgammaRIIA and integrin alphaIIbbeta3. ***Platelets,*** **27, 535-40.**

WATSON, S. P. & HARRISON, P. 2007. The Vascular Function of Platelets. ***Postgraduate Haematology.*** **Blackwell Publishing Ltd.**

WEIS, W. I., TAYLOR, M. E. & DRICKAMER, K. 1998. The C-type lectin superfamily in the immune system. ***Immunol Rev,*** **163, 19-34.**

WENTWORTH, J. K., PULA, G. & POOLE, A. W. 2006. Vasodilator-stimulated phosphoprotein (VASP) is phosphorylated on Ser157 by protein kinase C-dependent and -independent mechanisms in thrombin-stimulated human platelets. ***Biochem J,*** **393, 555-64.**

WERNER, S. & GROSE, R. 2003. Regulation of wound healing by growth factors and cytokines. ***Physiol Rev,*** **83, 835-70.**

WETTERWALD, A., HOFFSTETTER, W., CECCHINI, M. G., LANSKE, B., WAGNER, C., FLEISCH, H. & ATKINSON, M. 1996. Characterization and cloning of the E11 antigen, a marker expressed by rat osteoblasts and osteocytes. ***Bone,*** **18, 125-32.**

WICKI, A. & CHRISTOFORI, G. 2006. The potential role of podoplanin in tumour invasion. ***Br J Cancer,*** **96, 1-5.**

WIJEYEWICKREMA, L. C., GARDINER, E. E., MOROI, M., BERNDT, M. C. & ANDREWS, R. K. 2007. Snake venom metalloproteinases, crotarhagin and alborhagin, induce ectodomain shedding of the platelet collagen receptor, glycoprotein VI. ***Thrombosis and Haemostasis*****.**

WILDHAGEN, K. C., GARCIA DE FRUTOS, P., REUTELINGSPERGER, C. P., SCHRIJVER, R., ARESTE, C., ORTEGA-GOMEZ, A., DECKERS, N. M., HEMKER, H. C., SOEHNLEIN, O. & NICOLAES, G. A. 2014. Nonanticoagulant heparin prevents histone-mediated cytotoxicity in vitro and improves survival in sepsis. ***Blood,*** **123, 1098-101.**

WONG, C., LIU, Y., YIP, J., CHAND, R., WEE, J. L., OATES, L., NIESWANDT, B., REHEMAN, A., NI, H., BEAUCHEMIN, N. & JACKSON, D. E. 2009. CEACAM1 negatively regulates platelet-collagen interactions and thrombus growth in vitro and in vivo. ***Blood,*** **113, 1818-28.**

WRAITH, K. S., MAGWENZI, S., ABURIMA, A., WEN, Y., LEAKE, D. & NASEEM, K. M. 2013. Oxidized low-density lipoproteins induce rapid platelet activation and shape change through tyrosine kinase and Rho kinase-signaling pathways. ***Blood,*** **122, 580-9.**

WURSTER, T., POETZ, O., STELLOS, K., KREMMER, E., MELMS, A., SCHUSTER, A., NAGEL, E., JOOS, T., GAWAZ, M. & BIGALKE, B. 2013. Plasma levels of soluble glycoprotein VI (sGPVI) are associated with ischemic stroke. ***Platelets,*** **24, 560-5.**

XIAN, L. J., CHOWDHURY, S. R., BIN SAIM, A. & IDRUS, R. B. 2015. Concentration-dependent effect of platelet-rich plasma on keratinocyte and fibroblast wound healing. ***Cytotherapy,*** **17, 293-300.**

XIE, J., WU, T., GUO, L., RUAN, Y., ZHOU, L., ZHU, H., YUN, X., HONG, Y., JIANG, J., WEN, Y. & GU, J. 2008. Molecular characterization of two novel isoforms and a soluble form of mouse CLEC-2. ***Biochem Biophys Res Commun,*** **371, 180-4.**

XU, J., ZHANG, X., MONESTIER, M., ESMON, N. L. & ESMON, C. T. 2011. Extracellular histones are mediators of death through TLR2 and TLR4 in mouse fatal liver injury. ***J Immunol,*** **187, 2626-31.**

XU, J., ZHANG, X., PELAYO, R., MONESTIER, M., AMMOLLO, C. T., SEMERARO, F., TAYLOR, F. B., ESMON, N. L., LUPU, F. & ESMON, C. T. 2009. Extracellular histones are major mediators of death in sepsis. ***Nat Med,*** **15, 1318-21.**

XUE, M. & JACKSON, C. J. 2015. Extracellular Matrix Reorganization During Wound Healing and Its Impact on Abnormal Scarring. ***Advances in Wound Care,*** **4, 119-136.**

YAMANASHI, T., NAKANISHI, Y., FUJII, G., AKISHIMA-FUKASAWA, Y., MORIYA, Y., KANAI, Y., WATANABE, M. & HIROHASHI, S. 2009. Podoplanin Expression Identified in Stromal Fibroblasts as a Favorable Prognostic Marker in Patients with Colorectal Carcinoma. ***Oncology,*** **77, 53-62.**

YAMASHITA, Y., NAITOH, K., WADA, H., IKEJIRI, M., MASTUMOTO, T., OHISHI, K., HOSAKA, Y., NISHIKAWA, M. & KATAYAMA, N. 2014a. Elevated plasma levels of soluble platelet glycoprotein VI (GPVI) in patients with thrombotic microangiopathy. ***Thromb Res,*** **133, 440-4.**

YAMASHITA, Y., NAITOH, K., WADA, H., IKEJIRI, M., MASTUMOTO, T., OHISHI, K., HOSAKA, Y., NISHIKAWA, M. & KATAYAMA, N. 2014b. Elevated plasma levels of soluble platelet glycoprotein VI (GPVI) in patients with thrombotic microangiopathy. ***Thrombosis research,*** **133, 440-444.**

YANG, X., WANG, H., ZHANG, M., LIU, J., LV, B. & CHEN, F. 2015. HMGB1: a novel protein that induced platelets active and aggregation via Toll-like receptor-4, NF-kappaB and cGMP dependent mechanisms. ***Diagn Pathol,*** **10, 134.**

YIPP, B. G., PETRI, B., SALINA, D., JENNE, C. N., SCOTT, B. N., ZBYTNUIK, L. D., PITTMAN, K., ASADUZZAMAN, M., WU, K., MEIJNDERT, H. C., MALAWISTA, S. E., DE BOISFLEURY CHEVANCE, A., ZHANG, K., CONLY, J. & KUBES, P. 2012. Infection-induced NETosis is a dynamic process involving neutrophil multitasking in vivo. ***Nat Med,*** **18, 1386-93.**

YOUNG, A. & MCNAUGHT, C.-E. 2011. The physiology of wound healing. ***Surgery - Oxford International Edition,*** **29, 475-479.**

ZEERLEDER, S., ZWART, B., WUILLEMIN, W. A., AARDEN, L. A., GROENEVELD, A. B., CALIEZI, C., VAN NIEUWENHUIJZE, A. E., VAN MIERLO, G. J., EERENBERG, A. J., LAMMLE, B. & HACK, C. E. 2003. Elevated nucleosome levels in systemic inflammation and sepsis. ***Crit Care Med,*** **31, 1947-51.**

ZHANG, Q., RAOOF, M., CHEN, Y., SUMI, Y., SURSAL, T., JUNGER, W., BROHI, K., ITAGAKI, K. & HAUSER, C. J. 2010. Circulating mitochondrial DAMPs cause inflammatory responses to injury. ***Nature,*** **464, 104-7.**

ZHI, H., RAUOVA, L., HAYES, V., GAO, C., BOYLAN, B., NEWMAN, D. K., MCKENZIE, S. E., COOLEY, B. C., PONCZ, M. & NEWMAN, P. J. 2013. Cooperative integrin/ITAM signaling in platelets enhances thrombus formation in vitro and in vivo. *Blood,* 121, 1858-67.

ZHU, W., LI, W. & SILVERSTEIN, R. L. 2012. Advanced glycation end products induce a prothrombotic phenotype in mice via interaction with platelet CD36. *Blood,* 119, 6136-44.